# DESIGN OF SURFACE ACOUSTIC WAVE FILTERS AND APPLICATIONS IN FUTURE COMMUNICATION SYSTEMS

A thesis submitted to the Faculty of Science of the University of Edinburgh, for the degree of Doctor of Philosophy

by

P M GRANT, B.Sc., C.ENG., M.I.E.E.

DEPARTMENT OF ELECTRICAL ENGINEERING

March 1975

# ABSTRACT

DESIGN OF SURFACE ACOUSTIC WAVE FILTERS AND APPLICATIONS IN FUTURE COMMUNICATION SYSTEMS

The design, development and evaluation of Surface Acoustic Wave (SAW) Electronically Programmable Analogue Matched Filters (PAMF's) is examined. Potential applications for these and other SAW devices are identified in Civil Radio Relay, Military Spread Spectrum, Communication and Air Traffic Control (ATC) systems.

First, the development of Surface Acoustic Wave technology is surveyed in Chapter 1, highlighting its attractive features. SAW devices are shown to be capable of performing many familiar electronic signal processing functions, such as stable signal generation and bandpass filtering. Chapter 2 investigates the potential applications of frequency filters, oscillators, delay lines and code generators in analogue and digital civil communication equipments.

Next, the principle of Spread Spectrum communication is introduced in Chapter 3, emphasising the continuous mode, direct sequence system. Chapter 4 reviews the current status of fixed coded SAW AMF's, noting the requirements for, and development of, sophisticated reflection suppression design techniques.

This leads to the design and development of SAW PAMF's, incorporating external programming switches in Chapters 5 and 6. An analysis is developed to compare several distinct PAMF switch designs and fabrication technologies. Hybrid construction, employing beam lead PIN diodes and thin film nichrome resistors,

is finally selected. Thirty one tap prototype devices demonstrated the high performance fidelity predicted by theory.

The hybrid PAMF is incorporated into a sophisticated Spread Spectrum receiver, Chapter 7, which employs a Serial Parallel signal processing technique. This extends the basic SAW PAMF capabilities permitting signals with longer time bandwidth products to be processed. The receiver is demonstrated detecting a 100 MHz carrier signal Phase Shift Keyed at a 5 MHz rate by a 2047 chip Pseudo Noise sequence.

Concluding studies in Chapter 8 investigate the potential impact of these matched filters and other SAW components on ATC systems. Following a survey of existing procedures and equipments, several new proposals are briefly reviewed and the likely incorporation of SAW AMF's is discussed.

It is considered that the *original work* of this thesis comprises Chapters 5, 6 and 7 which detail theoretical and practical studies on the design and construction of SAW PAMF's. Chapter 7 also reports the construction and operation of a Spread Spectrum receiver, incorporating one of these PAMF's, to illustrate how the devices are likely to be used in systems. In addition to this device oriented work, Chapters 2 and 8 summarise the results of *original investigations* by the author, to assess the likely impact of SAW devices on existing and proposed Communication and ATC systems. The scope of the author's studies can be appreciated by the fifteen published references, detailed in Appendix C, which have arisen directly from the work. The remainder of the thesis material is included for continuity purposes.

# DECLARATION OF ORIGINALITY

This thesis reports the section of a programme of work, undertaken in the Department of Electrical Engineering for the Science Research Council on their contract no B/SR/8696, which was conducted exclusively by myself. The thesis only includes my studies and it was composed entirely by myself.

signed

PETER M GRANT

# ACKNOWLEDGEMENTS

The author would like to express his gratitude to Professor J H Collins for his supervision and provision of the research grant which permitted these studies to be undertaken. Also to Professor W E J Farvis for his continuing interest in the work.

I would like to express my appreciation to various members of staff, particularly Dr B J Darby for helpfull discussions, Mr R D Lambert and Mr R R Halstead for fabrication of the SAW devices and Mr H McKeating and Mr A A Folkarde for the construction of the code selector. Thanks are also due to other colleagues, Dr D P Morgan and Mr J M Hannah and to Mr D Stewart and Miss J Brown for their relevant undergraduate project studies. I must also thank Mr M J Moran and Mr J N Johnson for the interest they have shown throughout this project.

I would like to thank the Science Research Council for permitting me to present the results of my researches in this thesis and sincere thanks are due to Miss L J Murray for her special care in typing this manuscript. I would finally like to thank my wife, Marjory, for her constructive comments on the final manuscript.

# CONTENTS

page no

*Please note that the Tables and Figures are included at the end of each Chapter.*

page no

page no

# GLOSSARY OF ABBREVIATIONS AND TERMINOLOGY

| | |
|---|---|
| A/D | Analogue to Digital Converter |
| AEROSAT | North Atlantic Aeronautical Satellite System |
| AGARD | Advisory Group for Aerospace Research and Development |
| AGC | Automatic Gain Control |
| AMF | Analogue Matched Filter |
| ATC | Air Traffic Control |
| BIT | Information Data |
| BPO | British Post Office |
| CAD | Computer Aided Design |
| CAS | Collision Avoidance Surveillance |
| CCD | Charge Coupled Device |
| CD | Code Division |
| CHIP | Spread Spectrum Data |
| CMOS | Complimentary Metal Oxide Silicon Transistor |
| CSK | Code Shift Keyed |
| DABS | Direct Address Beacon SSR |
| DFT | Discrete Fourier Transform |
| DIL | Dual In Line |
| DME | Distance Measuring Equipment |
| DMF | Digital Matched Filter |
| DPDT | Double Pole Double Throw |
| DPSK | Differential Phase Shift Keyed |
| DSSS | Direct Sequence Spread Spectrum |
| ECL | Emitter Coupled Logic |
| ECM | Electronic Counter Measures |
| ESRO | European Space Research Organisation |
| FDM | Frequency Division Multiplex |

GLOSSARY OF ABBREVIATIONS AND TERMINOLOGY (continued)

| | |
|---|---|
| FDMA | Frequency Division Multiple Access |
| FET | Field Effect Transistor |
| FFT | Fast Fourier Transform |
| FH | Frequency Hopped |
| FM | Frequency Modulation |
| FSK | Frequency Shift Keyed |
| HF | High Frequency |
| IC | Integrated Circuit |
| ICNI | Integrated Communication Navigation and Identification |
| IDT | Inter Digital Transducer |
| IF | Intermediate Frequency |
| IFF | Interrogate Friend or Foe |
| ILS | Instrument Landing System |
| LO | Local Oscillator |
| LOS | Line of Sight |
| LSI | Large Scale Integration |
| MFSK | Multiple Frequency Shift Keyed |
| MOSFET | Metal Oxide Silicon Field Effect Transistor |
| MSL | Microwave Landing Systems |
| MSI | Medium Scale Integration |
| MSC | Multi Strip Coupler |
| MTBF | Mean Time Between Failures |
| PAMF | Programmable Analogue Matched Filter |
| PCB | Printed Circuit Board |
| PCM | Pulse Code Modulation |
| PIN | P Doped-Intrinsic-N Doped Semiconductor Diode |
| PN | Pseudo Noise |
| PPM | Pulse Position Modulation |

GLOSSARY OF ABBREVIATIONS AND TERMINOLOGY (continued)

| | |
|---|---|
| PRBS | Pseudo Random Bit Sequence |
| PRP | Pulse Repetition Period |
| PSK | Phase Shift Keyed |
| RADA | Random Access Discrete Address |
| RF | Radio Frequency |
| SAW | Surface Acoustic Wave |
| SNR | Signal to Noise Ratio |
| SOS | Silicon on Sapphire |
| SPDT | Single Pole Double Throw |
| SRC | Science Research Council |
| SS | Spread Spectrum |
| SSB | Single Side Band |
| SSR | Secondary Surveillance Radar |
| TACAN | Tactical Air Navigation System |
| TB | Time Bandwidth (product) |
| TDMA | Time Division Multiple Access |
| TH | Time Hopped |
| TTL | Transistor Transistor Logic |
| TWT | Travelling Wave Tube |
| TX/RX | Transmit - Receive |
| UHF | Ultra High Frequency |
| USB | Upper Side Band |
| VCO | Voltage Controlled Oscillator |
| VCXO | Voltage Controlled Crystal Oscillator |
| VHF | Very High Frequency |
| VOR | VHF OMNI Ranging |
| VSWR | Voltage Standing Wave Ratio |
| XTAL | Crystal |

# 1. INTRODUCTION TO SURFACE ACOUSTIC WAVES

## 1.1 SURFACE ACOUSTIC WAVES ON SOLIDS

### 1.1.1 INTRODUCTION

Acoustic waves in solids have been known and understood for a considerable period of time. They propagate with a velocity approximately five orders of magnitude slower than electromagnetic waves and for crystalline materials it is possible to achieve low attenuation propagation up to UHF. Devices utilising bulk wave propagation are in everyday use in many electronic systems. For example, the conventional quartz crystal oscillator uses a high Q acoustic resonance to generate stable frequencies, and acoustic delay lines provide compactly the signal delays required in the domestic television (TV) receiver.

The revived interest in Surface Acoustic Waves (SAW) which stems from original research by Lord Raleigh[1] arises predominantly for two reasons. One is the development, within the last decade, of the highly efficient interdigital electrode transducer (IDT)[2] for operation on low loss, non-dispersive cuts of piezoelectric substrate materials[3,4]. The other is the slow propagation velocity which permits a 3 μsec signal, occupying 1 km as an electromagnetic wave, to be compressed into 1 cm on the solid. Although this is initially attractive for information storage the potential to arbitrarily sample and modify a wave propagating along the surface opens up many new possibilities for realising signal processing functions. These have been extensively reviewed by several authors[5,6,7,8].

### 1.1.2 THE INTERDIGITAL ELECTRODE TRANSDUCER

The IDT[2], which is basic to all SAW devices, consists of a set of interleaved metal electrodes, fabricated[10] in a deposited metal film. In the simplest form the overlap and spacing of electrodes is equal and uniform throughout the pattern, as shown in Figure 1.1. Electrical excitation of the transducer produces, through the piezoelectric effect, a strain pattern of periodicity, p, the periodicity of the structure. If the excitation frequency is such that p approximates to the wavelength of the surface wave there is strong coupling and two surface acoustic wave beams of aperture, W , are produced which propagate normal to the IDT electrodes. With suitable choice of substrate and orientation, Table 1.1, it is possible to minimise the attenuation and diffraction of the SAW. Peak output occurs at the synchronous frequency, $f_o$ , where

$$f_o = v/\lambda \qquad 1.1$$

when $v$ = SAW velocity

$\lambda$ = SAW wavelength ie, IDT periodicity, p

For ST-X quartz substrate material v = 3158 m/sec, hence at 100 MHz $\lambda$ = 31.6 μm. Thus, the width of the IDT electrode fingers is ~8 μm. At acoustic synchronism the stress contributions of the E electrodes add in phase, analogous to an end fire array[9].

$$\text{ie, Stress output} \propto E \frac{\text{Sin } E\ \pi(f-f_o)}{E\ \pi(f-f_o)} \qquad 1.2$$

which illustrates the frequency selective property of the IDT.

Delay lines are fabricated with two transducers, as shown in Figure 1.1, with the undesired signals terminated in acoustic absorbers.

The ability to arbitrarily place the IDT electrodes along the SAW propagation path results in these delay lines belonging to the general class of transversal filters[11] in which the output is formed by weighting and summing the contributions from each electrode of the IDT. The output signal from such a filter is the convolution of the input signal with the device impulse response. Thus, electrically impulsing the constant overlap and spacing IDT shown in Figure 1.1, generates a square pulse of acoustic energy whose frequency is defined by the electrode spacing. Examination in the frequency domain shows the Fourier Transform with the characteristic $\frac{\text{Sin } x}{x}$ envelope (Equation 1.2) where the 3 dB bandwidth is determined by pulse length (no of electrodes). If conversely the IDT electrodes had incorporated amplitude weighting (variation of W) and phase weighting (in the p dimension) to generate in the time domain a $\frac{\text{Sin } x}{x}$ impulse response, then the frequency domain characteristic would ideally exhibit a square response with a flat passband, sharp skirts and good suppression at all other frequencies. It is this characteristic of the IDT which forms the basis of the synthesis of SAW frequency filters.

This introduction has attempted to explain the broad principles of IDT operation. The structure and behaviour of the anisotropic piezoelectric substrate results in the theoretical analysis becoming very complex. The design of sophisticated devices requires a detailed knowledge of the physics (ie, modes of propagation , beam

steering and diffraction of the SAW) and of the deleterious second order effects (bulk wave generation and reflection at finger edges) before high performance can be guaranteed. However simplified IDT theories have developed[9], which give close agreement with practice. SAW IDT theory is discussed further in Chapter 4.

The attractiveness of SAW devices result predominantly from the ability to realise, with sophisticated computer aided design (CAD) routines[12], complex device responses. The compatibility of fabrication with existing microelectronic techniques is also an important advantage. SAW device fabrication which is detailed later in Section 4.2.1, involves the evaporation onto a polished piezoelectric substrate of a thin metal film. This is subsequently coated with photoresist, exposed through the chromium mask, developed and etched to yield the IDT pattern. The single mask required for the IDT structure can often be generated directly from the CAD output tapes using standard photoreduction techniques.

### 1.1.3 PIEZOELECTRIC SUBSTRATE MATERIALS

Device performance is always constrained by the parameters of the selected piezoelectric substrate material. Table 1.1 summarises the relevant SAW parameters of several preferred substrate materials[3,4]. The factors of strong piezoelectric coupling, $k^2$, which permit high percentage bandwidth, low acoustic propagation loss for efficient operation, and low acoustic velocity for large signal time delay, all require to be evaluated in the context of specific device applications. E opt refers to the number of electrode periods required with single inductor tuning of the IDT interelectrode capacity to ensure maximum bandwidth for minimum insertion loss at the device centre frequency.

W opt denotes the IDT aperture (W, Figure 1.1) in wavelengths which gives a 50 Ω radiation resistance.

The commonly used ST-X cut of quartz has a very low temperature coefficient of delay (~ 3 ppm/$^{o}$C), but weak electromagnetic coupling ($k^2$) limits available bandwidths to 5-10%. Consequent delay line insertion loss is typically 10 dB. 6 dB arises directly from the bidirectional nature of the two IDT's. The high $k^2$, closely coupled, lithium niobate permits the fabrication of delay lines with 8 dB insertion loss and 40% bandwidth. However, for large structures second order effects, such as bulk wave generation, limit the fidelity of device operation. Both these materials can comfortably handle VHF/UHF signals between 10 and 700 MHz. The cheap PZT (ceramic) substrates are favoured for low frequency operation (< 50 MHz) where attenuation is not a severe problem. The low acoustic velocity of bismuth germanium oxide, whose piezoelectric properties are similar to bismuth silicon oxide, makes them attractive for applications requiring long delays. Conversely aluminium nitride achieves high operating frequency and hence increased bandwidth without placing heavy demands on photolithography.

The acoustic velocity of approximately 3 km per second achieved on easily prepared quartz and lithium niobate materials permits up to 50 μsec total delay to be accommodated within a 6" substrate. Minimum delay is limited by difficulties in isolating input and output matching networks to typically 100-500 nsec. The maximum frequency, 700 MHz, is currently limited by the resolution of photolithographically controlled etching using flexible mask and lift off techniques[10] to about 1 μm. This can be overcome by alternative

masking techniques such as electron beam fabrication, or by operating at harmonics of the IDT. However, for operation above L Band the high propagation loss results in low delay line efficiencies and limits the available Q's of filters. Low frequency operation is limited to approximately 10 MHz by acoustic diffraction and the substrate width required to achieve the necessary aperture, W opt, for satisfactory transducer design.

From these discussions it is obvious that SAW devices are destined to be used predominantly as IF signal processors. The maximum bandwidth is limited by the coupling coefficient, $k^2$, to values of <40%. The minimum device bandwidth is limited to >¼% by the physical size of substrate materials and deleterious second order effects, which are discussed later in Chapter 4.

## 1.2 DEVICES AND APPLICATIONS

### 1.2.1 DEVICE CLASSIFICATION

Table 1.2 gives a brief survey of the basic SAW devices and simple derivatives which result when two or more SAW devices are combined together, or simple electronic components such as amplifiers and detectors incorporated with the basic device. The table also indicates the major areas where these devices are currently expected to find applications. Space precludes a detailed discussion of Table 1.2 but most of the devices are reported in Reference 8. References *13* through *19* have been selected as accurate, up to date, survey papers on the devices and derivatives of Table 1.2 which are not adequately discussed in Reference 8.

It is considered relevant in this introduction to review a few of the SAW devices discussed in this thesis. The sophisticated performance of SAW frequency filters and oscillators are detailed to illustrate the key features which make them applicable to the radio relay communications equipments reported in the next Chapter.

### 1.2.2 FREQUENCY FILTERS

The inherent flexibility of design obtainable with SAW IDT's permits the construction of delay lines whose frequency response can be tailored to *almost* any desired bandpass filter characteristic. SAW filters can be designed to operate at centre frequencies from 10 MHz to 700 MHz but the highest Q factors (100) are obtained around 200 MHz[5].

SAW frequency filter designs have developed predominantly from the simple relationship which exists between the time domain impulse response and the frequency response of the IDT[12]. Computation of the inverse Fourier Transform of the desired filter frequency response provides directly the spatial image of the IDT electrodes which can be implemented by finger break weighting (apodisation). This has the advantage of relative insensitivity to fabrication errors, but it results in a non-uniform surface wave necessitating a wideband output IDT. These filters have been reported to give relatively high insertion loss (~ 20 dB tuned, ~40 dB untuned) and poor stop band rejection (~ -40 dB). Figure 1.2 shows the response of such a filter designed to meet the requirements of the IF stage of a Colour TV receiver[12].

Tancrell[24] has recently reported performance improvements by

incorporating a multi-strip coupler (MSC) between two identical apodised transducers. This converts the generated SAW into a spatially uniform wave before it is received by the second transducer. In addition the track change in the MSC gives improved rejection of bulk acoustic waves. An alternative design by Hartmann[8,25] avoids the spatial non-uniformity by weighting, with selective withdrawal, the electrodes of two constant overlap IDT's arranged in a non-dispersive combination. When combined with the phase weighting of a graded periodicity IDT, the passband width can be optimally traded off against insertion loss. Both these developments have reduced insertion loss and improved stop band rejection by a further 20 dB.

Hartmann[7] is also studying methods of reducing the filter bidirectionality loss, by incorporating dual output IDT's. Current minimum loss is 6 dB, comprising a 3 dB reflection at the output transducer with the additional 3 dB degradation caused by propagation and resistive loss in the IDT's and matching networks. In addition to these developments, contiguous frequency filter banks are under design, see Melngailis[26], using reflective array device design techniques. Effort is also being directed towards the development of programmable frequency filters[25,26], in which the centre frequency can be electronically selected with microelectronic switches similar to those discussed in Chapters 5 and 6.

SAW frequency filters have made tremendous advances in performance, reliability and cost over the last five years and they are now very competitive for high volume intermediate Q (10-100) designs in the UHF band. Investigations of bulk mode generation, electrical breakthrough and electroacoustic regeneration at the IDT electrodes are predicted to give yet further improvements in SAW filter performance.

### 1.2.3 OSCILLATORS

Two classes of oscillators are in common use : the quartz crystal bulk acoustic wave oscillator, and the LC or cavity oscillator. The former is of a high stability ($Q > 10^4$) but suffers from a number of disadvantages including mechanical fragility, low fundamental frequency operation (< 20 MHz), and limited frequency modulation (FM) capability (500 ppm). Harmonic operation permits extension to 100 MHz necessitating further multiplication to achieve UHF or microwave frequencies. On the other hand LC or cavity oscillators have an increased operating range and improved FM performance but their stability is considerably inferior to bulk quartz oscillators (typical Q = 100). Lewis[8,27] has reported the design of a SAW oscillator which possesses the intermediate stability and modulation capability as detailed in Table 1.3.

The SAW oscillator comprises a frequency selective delay line in which the output is fed back to the input with sufficient gain to overcome the loss in the acoustic line, Figure 1.3. Oscillation will occur at any frequency, $f$ , which satisfies the phase condition

$$\phi_{el} + \frac{2\pi f_n \ell}{v} = 2\pi n \qquad 1.3$$

(n integer)

where $\ell$ is the acoustic path length, $f_n$ , the frequency of the $n^{th}$ mode, and $\phi_{el}$ the phase shift through the feedback loop and the reactive part of the IDT's. Multimode operation can be overcome by suitable design of the IDT geometry and the sensitivity of the generated frequency to the external circuit is dependent upon the relative size of $2\pi f_n \ell/v$ and $\phi_{el}$. It is this property which permits the design trade-off between stability and modulation capability.

The attraction of the SAW oscillator increases with frequency since the basic device can be designed to work *fundamentally* at frequencies above 10 MHz. The relatively simple IDT geometry permits the frequency to be extended into L Band before photolithographic resolution limits the device yield. The operating frequency of the SAW oscillator is determined by the transducer pattern and *not* by a dimension of the quartz crystal as in the bulk oscillator. Hence, the crystal can be firmly bonded to the header to form a rugged oscillator. Good thermal contact enables the loop to oscillate up to 1 watt power levels. Other significant performance figures[27] reported for the SAW oscillator are : frequency deviation up to 1%; short term stability of < 1 in $10^9$ for 1 second; medium term stability of 100 ppm for temperature excursion of $\pm 40^{o}C$; and single sideband FM noise <-150 dB per Hz, has been measured 10 kHz away from carrier in a 10 mW saturated output device. Limits to the long term stability still need establishing but one part in $10^5$ over one year is readily achievable. These results, which have been achieved with the initial designs already look attractive when compared to bulk oscillator performance.

When operated at UHF frequencies SAW oscillators replace an expensive assembly (~$300) of overtone bulk oscillator, multiplier chain and output filter; with a simple delay line and amplifier, offering a tenfold reduction in size, weight and power consumption. This suggest that these devices will have considerable impact on communications and radar equipment design over the next decade.

## 1.3 LAYOUT OF THESIS

Although many SAW devices exist, at the present time the only serious applications have occurred in radar systems[28]. SAW dispersers have

proved invaluable for the generation and reception of wideband chirp signals in airborne radar equipment. The high performance obtained and reduced equipment complexity arising directly from the incorporation of the SAW devices is now persuading the systems designers to give serious consideration to using other SAW components such as frequency filters and oscillators in the next generation of radar equipments.

This thesis acknowledges these developments and addresses the question - Are there similar SAW device applications in communication systems? Studies of this nature comprise the basic theme of the three-year Science Research Council (SRC) Contract B/SR/8696 entitled "Acoustoelectronic Materials, Devices and Subsystems"[29], which was awarded to the University of Edinburgh in August 1971. Studies conducted under this contract on detailed design of *fixed coded* SAW Analogue Matched Filters (AMF) incorporating novel reflection suppression tap geometries were recently reported in B J Darby's thesis[30]. This development, which overcomes the deleterious second order effects experienced with the multiple tapping electrodes which are employed in AMF mask designs, is summarised *here* in Chapter 4. In addition, Darby discussed the application of these devices to *burst* mode spread spectrum communications, highlighting the simplicity of equipment hardware and high performance achieved when SAW AMF's are used to generate and detect the coded signal formats.

This thesis reports *complementary* studies, based predominantly at the applications and systems level, which have also been carried out on this SRC contract. Specifically, Chapter 2 reports an investigation of the potential applications of SAW frequency filters, oscillators and several other devices highlighted in Table 1.2, to civil radio relay communication systems.

As an introduction to the requirements for the SAW Programmable AMF's detailed in Chapters 5 and 6, the concepts of digital spread spectrum communication systems are summarised in Chapter 3. Chapter 4 reviews the current status of SAW fixed coded AMF development prior to reporting in Chapters 5 and 6 original work at the device level on the design, development, construction and performance of several Electronically Programmable SAW AMF's. These devices were designed using a hybrid fabrication technique, interfacing diode switches between the taps and output sum bus of simple, first order, fixed coded AMF designs. Chapter 7 details the design and performance of a novel, programmable SAW matched filter modem which employs serial-parallel signal processing techniques and incorporates one of the programmable AMF's described in Chapter 6. The development of this modem now permits continuous coherent processing of long Pseudo Noise (PN) Phase Shift Keyed (PSK) sequences. Chapter 8 concludes by briefly reporting likely applications of SAW devices in Air Traffic Control (ATC) systems. Detailed are possible improvements in the processing of Secondary Surveillance Radar (SSR) returns and many new navigation and surveillance system concepts. These new systems, which seem likely to be implemented towards the end of this decade, are based on spread spectrum subscriber accessing techniques. Chapter 9 summarises the thesis indicating the future prospects for Surface Acoustic Wave technology. The Figures and Tables in this thesis are included at the end of each Chapter.

| MATERIAL | CRYSTAL CUT AND ORIENTATION | VELOCITY (km/sec) | $K^2$(%) | $E_{opt}$ | $W_{opt}$ (in wavelengths) | OPTIMUM BANDWIDTH (%) | TEMP COEFFT OF DELAY (ppm/$^oC$) | ATTENUATION at 1 GHz (dB/μsec) |
|---|---|---|---|---|---|---|---|---|
| $LiNbO_3$ | Y-Z | 3.485 | 4.30 | 4 | 108 | 22 | 85 | 1.6 |
| Quartz | Y-X | 3.159 | 0.22 | 19 | 53 | 5.5 | -24 | 2.2 |
| Quartz | ST-X | 3.158 | 0.17 | 21 | 28 | 4.5 | < 3 | --- |
| $Bi_{12}GeO_{20}$ | (100)(011) | 1.681 | 1.40 | 8 | 26 | 14 | - 122 | 1.5 |
| PZT | POLED DIRECTION | 2.200 | 2.40 | 6 | -- | 23 | -- | 6.0 † |
| $LiTaO_3$ | Z-Y | 3.329 | 1.00 | 13 | 31 | 8 | 67 | --- |
| $AlN/Al_2O_3$ | X-Z | 6.120 | 0.63 | 11 | 60 | 10 | 44 | 1.7 * |

† at 37 MHz

* at 200 MHz

TABLE 1.1 SAW PARAMETERS OF COMMONLY USED PIEZOELECTRIC MATERIALS

| SAW DEVICE | | POTENTIAL AREAS OF APPLICATION |
|---|---|---|
| BASIC | DERIVATIVES | |
| INTERDIGITAL TRANSDUCER | FREQUENCY FILTER | Color TV; Integrated IF's; satellite multiplexers; ECM |
| | INVERSE FILTER | Clutter dominated radar |
| | DISCRIMINATOR | Analog FM demodulator |
| | OSCILLATOR | Stable sources VHF to microwave; specialised comms; frequency synthesiser |
| DELAY LINE | | Altimetry, analog MTI radar; comms path length equaliser; time ordering |
| | TAPPED | Radar clutter reference; ECM; SSR |
| | BIT MATCHED FILTER | Digital comms PSK demodulator[20] |
| | ACOUSTIC AMPLIFIER | Long delay[21] for TV frame storage |
| | PSK MATCHED FILTER | Spread spectrum comms; IFF; ICNI |
| | PN PSK GENERATOR | Link analysis; spread spectrum comms |
| | DIGITAL | Recirculating memory[22]; data and bandwidth compression[23]; sonar |
| | TOUCH SENSITIVE | Man-machine interface; glass intrusion |
| MULTI-STRIP COUPLER | IMPROVED DEVICES | Signal routing |
| DISPERSER | | High resolution radar; navigation; group delay equalisers |
| | COMPRESSIVE RECEIVER | Spectral analysis |
| | VARIABLE DELAY LINE | Range calibration; target simulation; electronic timing; ECM |
| NON-LINEAR | CONVOLVER | Spread spectrum comms; radio astronomy; FFT processor |
| | ACOUSTIC IMAGING | Non-destructive testing |
| | ACOUSTO-OPTIC | Displays, cameras |
| WAVEGUIDE | ACOUSTIC IC's | Subminiature signal processing and routing sub-systems |

TABLE 1.2 SAW DEVICES AND POTENTIAL AREAS OF APPLICATION

| OSCILLATOR | APPROXIMATE FREQUENCY RANGE | EFFECTIVE LOADED Q | MAXIMUM FREQUENCY DEVIATION PPM | TEMPERATURE COEFF IN PPM/°C (-30°C TO +70°C) |
|---|---|---|---|---|
| CONVENTIONAL QUARTZ XTAL | $<10^8$ Hz | $5000\text{-}2.10^6$ | $\simeq 500$ | $<1$ PPM/°C |
| LC (INCLUDING CAVITY OSCILLATORS) | $10^3\text{-}10^{11}$ Hz | TYPICALLY $10\text{-}10^4$ | AS LARGE AS REQUIRED | TYPICALLY 10 PPM/°C |
| SAW | $10^7\text{-}2.10^9$ Hz | $200\text{-}10^4$ BY CHOICE OF $\ell$ | $10^2\text{-}10^4$ BY CHOICE OF $\ell$ | AVERAGE VALUE $\simeq 1$ PPM/°C |

TABLE 1.3 COMPARISON OF PROPERTIES OF VARIOUS OSCILLATORS

(COURTESY M LEWIS, RRE)

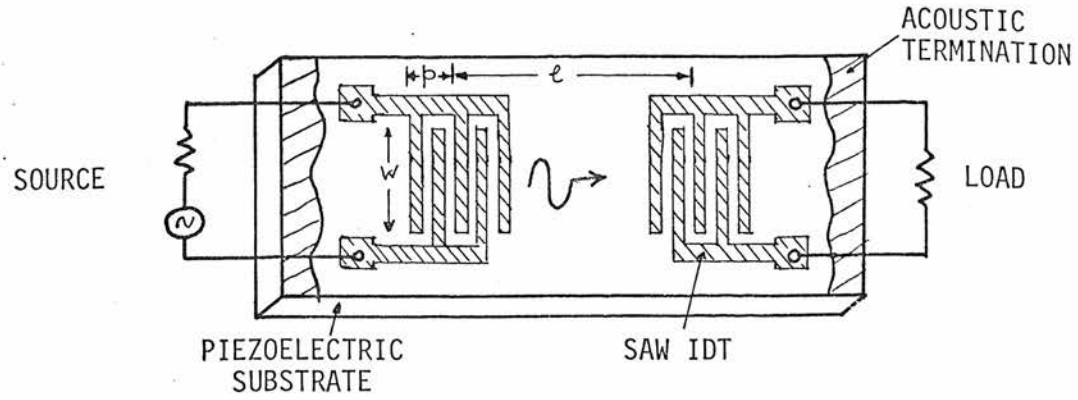


FIGURE 1.1 SAW DELAY LINE SCHEMATIC

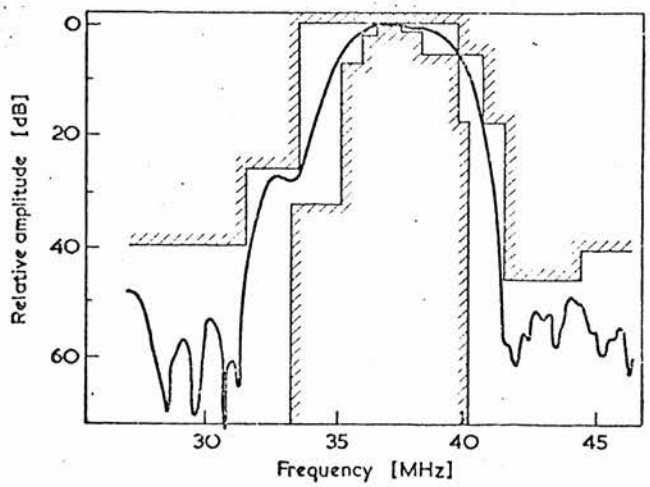


FIGURE 1.2 BRITISH COLOUR TV SAW IF FILTER AND ASSOCIATED SPECIFICATION (COURTESY R MITCHELL, MULLARD)

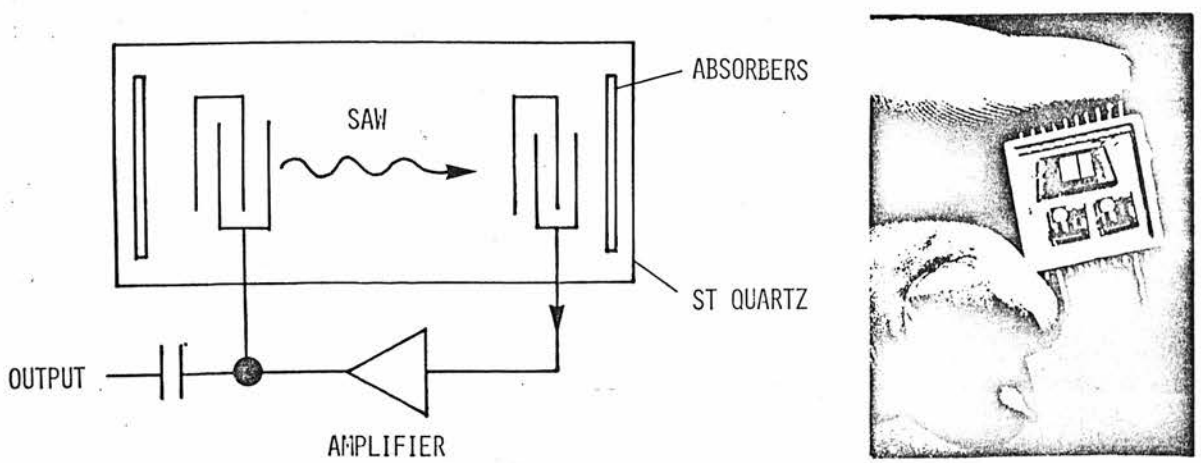


FIGURE 1.3 SCHEMATIC AND PHOTOGRAPH OF A 200 MHz SAW OSCILLATOR (COURTESY M LEWIS, RRE)

# 2. CIVIL RADIO RELAY COMMUNICATION SYSTEMS

## 2.1 INTRODUCTION

It is seen from Chapter 1 that the flexibility of SAW technology permits, with a detailed understanding of the device physics, the realisation of a multitude of different electronic components. This Chapter reviews potential SAW component applications in civil communication systems, summarising and updating previously published studies by the author[28, 31, 32].

Following an examination of the hardware currently used in Line of Sight (LOS) radio relay systems, the specifications of component parts of terminal and repeater equipment are detailed prior to comparison against the near term projected performance of relevant SAW devices. In this manner it is intended to assess realistically the retrofit potential of SAW filters, discriminators and oscillators in analogue communication systems.

In addition to the expansion of these systems to handle increased traffic, there is pressure on the telecommunications service[33] for increased conference and colour TV, new data and fascimile transmission facilities. These are likely to use flexible, digital signalling techniques which offer the opportunity to incorporate SAW components in prototype equipments.

## 2.2 EQUIPMENT DESIGNS

### 2.2.1 SIGNAL FORMATS

Analogue and digital communication systems[34] employ quite distinct multiplexing and modulation techniques. In *analogue* communications 60 Hz to 3.4 kHz individual telephone channels are Frequency Division Multiplexed (FDM) into a hypergroup of 960 subscriber

channels occupying a 60 kHz to 4.028 MHz band. Extensions of the system are now available to accommodate in Frequency Division Multiple Access (FDMA) format two or more hypergroups, ie, 1800 channels and 2700 channels. The requirement for increased capacity transmission systems has resulted in higher carrier frequencies at 6 GHz and above using *digital* Pulse Code Modulation (PCM) techniques. Here signals undergo analogue to digital conversion prior to Phase Shift Keying (PSK) the carrier oscillator. This enables subscribers to be accommodated in a Time Division Multiple Access (TDMA) format with low mutual interference.

### 2.2.2 FIXED TERRESTRIAL MICROWAVE ANALOGUE RADIO RELAY

Both intermediate frequency (IF) heterodyne and remodulation analogue FM repeaters are employed in terrestrial microwave radio relay equipments. Figure 2.1(a) shows a typical *remodulating* repeater for the 2-11 GHz range where the baseband (FDM) traffic is frequency modulated (FM) on to a 70 MHz IF carrier (140 MHz in 2700 channel systems). Following IF amplification, a local oscillator (LO) translates the signal to the required microwave radio channel. After upper sideband (USB) filtering and level adjustment, the signal is amplified for transmission. The four or eight transmitter radio channels, are combined in a circulator-filter bank into the characteristic FDM/FM/FDMA assemblage. Conversely the receiver employs a channel dropping network, down conversion to IF and discrimination to the baseband FDM traffic. These remodulating repeaters are favoured for short haul and spur routes where they offer the flexibility to drop and insert channels at each repeater. IF *heterodyne* repeaters which do not incorporate the discrimination and IF remodulation, are preferred for multi-repeater long haul or

backbone systems which carry high capacity telephone and television traffic.

The useful output power (5 watt at 4 GHz) and exceptional reliability (500,000 hours MTBF) of microwave transistors has resulted in all-solid-state equipments for 960 channel operation. 1800 channel telephony long hop systems demand high transmitter power, often requiring TWT output amplifiers. The typical output power for a UK long haul 6.175 GHz repeater is +40 dBm, permitting 50-80 Km hop lengths with receiver sensitivities of -70 dBm. There are 2 blocks of 8 radio channels, each 26 MHz wide, spaced 29.65 MHz apart, which is adequate to accommodate a single colour television signal or 1800 channel telephony signals within each radio channel.

### 2.2.3 TERRESTRIAL DIGITAL RADIO RELAY

Digital microwave communication systems are evolving due to the requirement for higher carrier frequencies where increased spectrum is available to accommodate the traffic growth. Regenerative repeaters are almost exclusively used as they permit series operation without loss of quality, and facilitate insertion and dropping of channels. Research is being carried out by the British Post Office (BPO) on both long and short haul, all-solid-state, systems. Low capacity links, such as spur routes, will use LOS propagating in the 11 and 20 GHz band[35]. Limitations on spectral width and hence data bandwidth in LOS propagation is resulting in the development of guided wave propagation, such as the 50 mm diameter $TE_{01}$ overmoded circular waveguide[33] and W40G[36], for trunk route traffic in the 1980's.

The digital communication repeater, detailed in Figure 2.1(b) uses a receiver whose microwave front end is identical to the analogue system of Figure 2.1(a). In the Differential Phase Shift Keyed (DPSK) demodulator[37] a power splitter separates the signal into two channels and a one bit delay is inserted into the reference channel. A phase sensitive detector performs the IF to baseband conversion. In the transmitter phase modulation (usually four-level) of the carrier can be obtained by several distinct methods. Direct phase modulation of the carrier with a PIN diode switch is commonly used.

The BPO digital poleline system[35] operates between 17.7 and 19.7 GHz, with a 1.2 GHz IF, and incorporates 8 transmit and 8 receive channels each 4 phase modulated at a 132 megabaud data rate. Digital phase modulation can be detected at much lower receiver SNR than analogue FM permitting solid state Impatt amplifiers (100-200 mW output) to be used in the system. However, power budgeting is still very critical under high precipitation conditions, necessitating either short, 4 km, spacings between repeaters, or use of dual transmission paths where a heavy rainstorm affects only one path, permitting more liberal spacing, 12 km, between repeaters.

### 2.2.4 SATELLITE COMMUNICATIONS

Transponders operating in the space environment must be designed to stringent volume, weight and primary power specifications and incorporate inbuilt redundancy for contingency against component failure . Synchronous satellite to ground link budgets are very critical due to the path attenuation of approximately 200 dB. Latest design of spin stabilised, Intelsat III and IV satellites

incorporate antennae which are accurately oriented towards the earth. Signal formats are mainly FDM/FM/FDMA assemblages similar to those used in analogue terrestrial communications. However, the repeater differs by employing a broadband front end prior to frequency translation and separate channel amplification. No demodulation or signal processing is performed at the satellite, see Figure 2.1(c).

The Intelsat IV[38] repeater employs low noise tunnel diode amplifiers (TDA's) at the inputs which ensures linear operation over 500 MHz bandwidth. The microwave multiplexer, consisting of filters, isolators and group delay equalisers, separates the signal into two banks of six channels, each 36 MHz wide. Individual channel amplification follows in one of two redundant high level TWT's. The channels are then recombined and routed in the output multiplexer for feeding the transmit antennae. This channel separation increases the system flexibility and spectral utilisation, enabling FM telephone or television, and multiphase PSK carriers, to be accommodated simultaneously with minimum interaction between channels.

### 2.2.5 VHF AND UHF MOBILE RADIO

In addition to the large numbers of fixed common carrier communications equipment, there is an ever increasing demand from the police, public service and other users for a flexible mobile radio service[39]. These currently use FDMA techniques with 50 kHz wide channels within allocated bands at VHF. Increased numbers of subscribers and improvements in oscillator stability are resulting both in a reduction of channel spacings to 25 and 12½ kHz, and use of UHF frequencies. Large area coverage systems, which employ several

transmitters, experience problems with signal interference and fading at the mobile receiver. New proposals for dynamic frequency assignment based on a cellular approach[40,41] aim to overcome this problem and provide additional system capacity.

Voice traffic in mobile systems is accommodated by frequency modulation and SSB filtering. The digital systems used for radio paging and control of remote equipment use multiple tone or Frequency Shift Keyed (FSK) signalling. Simple superhet mobile receivers with two IF stages are widely used to achieve the required selectivity and sensitivity. Tone detection is accomplished with active filters. The high dynamic range required by mobile equipment is obtained with sophisticated AGC control circuitry.

Mobile equipment generally uses well understood design principles, and development has concentrated on reducing the size and weight and improving the reliability of equipments. In particular the circuitry is optimised to operate with low power consumption giving long periods of operating between battery changes.

## 2.3 APPLICATIONS OF FREQUENCY FILTERS

### 2.3.1 IF FILTERS

SAW IF filters[25] are applicable in both analogue and digital terrestrial communication systems and in multiplexers for the analogue hypergroups of FDM signal assemblages. Harmonic operation also opens the possibility of lightweight channel multiplexing filters for satellite applications. As stated in Chapter 1, SAW bandpass filters have been designed with 0.25% to 40% passbands, and IF filters have

already been produced for the passband and sound traps required in domestic colour television receivers as shown in Figure 1.2.

The essential requirements of 140 MHz IF filters[42] for 2700 channel analogue repeaters are delineated in Table 2.1(a). SAW technology can readily achieve the bandwidth, with the specified ripple and out of band rejection at the expense of a higher insertion loss (15 dB typical). These links are specified for low AM/PM conversion[43] permitting only 10 nsec group delay variation over a 5 repeater hop, requiring each IF amplifier to possess <3 nsec variation over a 50 dB AGC range. Conventional realisation necessitates the design and cascading of a series of low pass and high pass filter stages with additional elements for group delay equalisation resulting in a network with 10 to 20 adjustments. By possessing the flexibility to incorporate most group delay variations, SAW designs remove the necessity for external equilisation networks.

SAW frequency filters are also applicable to digital communication systems. For example, a Gaussian response IF filter for a 32-channel PCM system operates at 70 MHz centre frequency with $\pm 2\frac{1}{2}$ MHz 3 dB bandwidth and stop bands 35 dB down at $\pm 7\frac{1}{2}$ MHz. A group delay variation over the 3 MHz centre of band must be maintained within 3 nsec. It is an anticipated that a SAW design can meet this specification.

In addition to these applications there are also requirements for IF filters in mobile communications. Most of the high volume production VHF and UHF equipments will soon use 25 kHz channel spacings, which requires good selectivity in the IF stages. For this reason the high Q crystal and ceramic filters are unlikely to be replaced by existing SAW devices. However, the explosive growth of UHF mobile

communications results in the necessity to allocate adjacent channels for transmitters situated in close geographical proximity. Receivers must therefore incorporate stable band-stop filters to suppress the undesired channel. SAW technology can realise these filters. Operation has been demonstrated[44] with a Lithium Niobate line at 430 MHz exhibiting a nominal 10 dB insertion loss with 22 kHz wide 10 dB stopbands. The requirement of UHF mobile equipments demands 20 dB stopbands each 5 kHz wide necessitating the temperature stable, ST-X cut quartz substrate.

### 2.3.2 SIGNAL MULTIPLEXERS

With the development of 60 MHz wide 10,800 channel, analogue telephony systems[36] potential applications exist for SAW multiplexers to separate and route the telephone traffic. Studies are being conducted by the French Post Office to separate a 50 MHz wide hypergroup FDM assemblage with a bank of 10 SAW filters. Individual filters are designed to select 4 MHz wide channels with ideally 20 dB loss and 80 dB out of band rejection. This is to be achieved with two SAW filters in series. Recent developments of signal multiplexers by Solie[26] based on the MSC look attractive for efficient seperation and combination of multiple signals.

Turning to SAW frequency filters in the context of satellite communication systems, the current Intelsat IV repeaters[38], (Figure 2.1(c),) employ input and output multiplexers incorporating 6 to 10 section Tchebycheff waveguide filters. Current lightweight invar multiplexers, which weigh several kg, often comprise 40% of the satellite payload. The likelihood of future satellites having more transponders has focussed attention on lightweight methods of

realising these filters.[45] Current photolithography limits the upper frequency of specialised SAW filters to about 700 MHz. However, harmonic operation has been demonstrated at 3 GHz, and in addition electron beam and X-ray lithography techniques are now available. The modest (1%) bandwidth requirement of Intelsat IV, Table 2.1(b), is met easily with SAW technology. The use of 10% guard bands between channels requires a sharp skirt selectivity with 40 dB/3 dB shape factor of 1.5:1. This, combined with the insertion loss requirement, constitutes a formidable goal for further design studies and fabrication procedures of SAW filters at microwave frequencies.

These examples of bandpass and bandstop filters, designed to meet comprehensive specifications, illustrate the seriousness which system designers are placing on the potential of SAW technology for communications equipment component design. However, the economics remain to be established particularly since only small numbers of devices (several hundred) at a time are required for most applications.

### 2.3.2 FREQUENCY DISCRIMINATORS

Analogue communication systems currently demodulate IF signals in a triple tuned circuit FM discriminator, to convert back to the baseband traffic. IF discrimination can be achieved with both bulk and SAW devices as described by Hartemann[8]. One approach uses two SAW filters operating at slightly different centre frequencies with each output individually rectified, prior to voltage sub traction. This provides a linear relationship between input frequency and output voltage over a frequency band defined by the difference between the two transducer frequencies. Currently, better than 1 mV/kHz sensitivity is obtained with 2% linearity over 10% bandwidth for devices

which operate above 20 MHz. They use quartz substrates to obtain < 1 ppm/$^{o}$C temperature sensitivity, which is far better than the 100 ppm/$^{o}$C temperature of tuned circuit discriminators.

The SAW analogue FM discriminator is potentially attractive for radio relay equipments where only a small improvement to 1% linearity is required. However, its fractional bandwidth is inadequate. Narrow bandwidth, high linearity (eg, 0.1%) devices also have potential application in microwave link analysis equipments. The strongest factor in favour of the SAW discriminator is its capability to operate up to L Band frequencies, and this is predicted to offer applications in high capacity analogue communication systems. Quartz substrate phase discriminators with high stability zero crossover may also find application in locking unstabilised high power local oscillators to a bulk quartz or SAW reference oscillator.

## 2.4 OSCILLATORS

Stable local oscillators are required extensively for frequency translation in communications equipment. The SAW oscillator, described in Chapter 1, possesses attractive electrical and mechanical properties for the design of a space qualified local oscillator drive module, whose typical requirements are outlined in Table 2.1(c). Short term stabilities (< 1 second) of 1 part in $10^{10}$ are required while SAW oscillators are achieving 1 part in $10^{9}$. Long term ageing of one ppm per month has been achieved, but is still inferior to the requirements which can only be met with bulk quartz oscillator performance. Improvements in preparation of the quartz surfaces and device packaging seem destined to alleviate this shortcoming.

The good FM capability of these oscillators permits consideration of an all SAW IF analogue communications modem incorporating an oscillator-discriminator pair. With voltage excitation of a varactor diode across an IDT the SAW modem generates and detects modulation depths of 1% which represents a significant advance over the 0.1% achievable with bulk quartz oscillators. However, the percentage modulation available from the oscillator is small compared with the requirements of the analogue remodulating repeater. The SAW devices appear at first sight to be more suited to mobile equipments. Here the close channel spacings, see section 2.2.5, necessitates high source stability and high Q discrimination to avoid cross talk between adjacent channels. In addition city wide radio pagers are designed for low power consumption, 4 mA at 1.5 volt, requiring low quiescent current (eg, 1 mA) single transistor stage oscillators. If a SAW oscillator were designed using this technique it is anticipated that external phase changes with battery voltage would degrade its already marginal frequency stability. Thus, immediate SAW oscillator applications in this area are unlikely. However, the recent development of the high Q SAW resonator[26] is attractive for future applications.

Increasing congestion in mobile systems has forced the FCC to reallocate a 115 MHz wide UHF band above 806 MHz for land mobile use[40]. To conserve spectrum the Bell Hi-Cap system, described by Fluhr[39], proposes to subdivide high density urban area into groups of cells each using a low power transmitter. A control computer automatically instructs mobiles to select the required channel. Such techniques require microminiature, low power consumption, frequency synthesisers[46], where the efficient SAW oscillator is attractive.

UHF synthesis employing straight division from an 806 MHz VCO requires expensive high power ECL circuitry. Figure 2.2 shows an alternative design approach based on the Wadley loop in which the output VCO is mixed with a stable SAW UHF local oscillator and the difference signal used to drive the control loop. The corresponding frequency reduction permits the maximum use of low power consuming CMOS circuitry. The wide tuning (<1%) of the SAW oscillator, which is stable enough to dispense with external frequency control, additionally permits the LO to be quickly offset (~100 μsec) by the IF frequency without additional digital circuitry complexity. A 2.5 kHz comparison frequency provides a fast settling time (~100 msec) for TX/RX operation. Wideband loops (1 MHz), which will necessitate faster variable divider circuits, are attractive especially to clean up the low Q VCO SSB noise performance to a standard compatible with the SAW oscillator. The arrangement shown in Figure 2.2 has 1,000 channels with 40 kHz channel spacing. It is designed to operate with 12 kHz FM deviation consuming ½-1 watt in the control loop. Naturally this concept can be applied to synthesis for the existing 450-470 MHz land mobile UHF band. Direct synthesis of the complete 2-30 MHz HF band can also be achieved by generation at UHF as shown in Figure 2.2 with an additional mixer and SAW LO down converting the output to HF.

## 2.5 COMPONENTS FOR DIGITAL COMMUNICATION SYSTEMS

### 2.5.1 IF DELAY LINES

Space diversity communication systems, such as the British Post Office 20 GHz poleline system[35], discussed in Section 2.2.3, are likely to employ two or more geographically separated transmission routes with wide repeater spacings as shown in Figure 2.3. Terminal receiver

path switching is employed to overcome the narrow fade margins, selecting the route which offers the lowest error rate under high precipitation conditions. Data must not be lost during switching. One approach is to use a compensating IF delay line to synchronise the signal from both paths.

A typical link of 100 km length employing 7 repeaters can be expected to exhibit a path length difference of 3 to 4 km owing to geographical repeater siting problems. It is anticipated that path length equalisation may be approximated at IF with fixed delay lines, to accommodate 2, 1, $\frac{1}{2}$, $\frac{1}{4}$ km differential spacings having 8, 4, 2 and 1 μs delays realised on YZ lithium niobate at 1.2 GHz centre frequency and 132 MHz, 3 dB bandwidth. Device insertion loss of <20 dB and group delay variations of approximately 2 ns would be required. However, route switching without loss of data requires synchronisation to within half a bit necessitating a variable delay line of 1 μs maximum delay and 4 ns setting accuracy. This can be achieved with a pair of dispersive SAW filters[16] or more efficiently with a magnetic bias field adjustable magnetostatic wave device[32].

### 2.5.2 DATA DEMODULATORS

Regenerative digital communications repeaters such as those shown in Figure 2.1(b) employ a demodulator to convert the received signal from PSK IF to baseband. Optimisation of the signal to noise ratio can be performed with a *bit matched filter* which permits the best decision to be made as to the relative phase of the received signal[37]. SAW technology can be used to decode PCM, PPM, MFSK, PSK or DPSK signals. Experiments conducted by Lever[8] with simple uncoded SAW

bit matched filters for use in a MFSK system showed receiver performance within 1 dB of theoretical, equivalent to that achieved with conventional quenched resonator devices. However, in most systems, the SAW devices can be implemented directly at VHF/UHF frequencies precluding the necessity for IF processing. A 4-phase SAW DPSK Gray demodulator has been constructed and its error rate performance evaluated[20] at the Norwegian Technical Institute. This decoder was designed for a 11 GHz link with a 280 MHz IF differentially phase modulated at 192 Megabaud. Similar SAW devices have also been constructed and evaluated in the DABS SSR System.

### 2.5.3 LINK DIAGNOSIS

Evaluation of a communications system is normally accomplished by a performance measurement simulating the traffic carried in the system[43]. Digital systems can be tested by modulation of the IF signal with a long Pseudo-Noise (PN) sequence, and comparing the received signal against an identical code generator. Bit and block error rate, skew and jitter measurements give an assessment of the quality of transmission and operation of terminal equipment. This performance measurement is similar to the white noise test on a FDMA system. It is not a diagnostic procedure like the transmission test, which measures the AM/PM conversion, gain and phase linearity and other factors which are degrading the link performance.

Conventional code generators employ microelectronic shift registers with logical feedback. However, when registers exceeding 20 stages at clock rates over 100 MHz are produced, factors such as propagation delays, clock synchronisation and power dissipation problems

become acute. SAW technology offers a solution by producing a PN-PSK modulated IF signal output without any mixer and oscillator. In the Pseudo-Noise generator, first demonstrated by Morgan[7], the microelectronic shift register was replaced by a SAW delay line incorporating one input transducer and two feedback taps. The tap outputs are amplified and summed, prior to gating positive or negative impulses on to the input transducer as shown in Figure 2.4. Crisp[26] has also reported a SAW generator equivalent to a 100 stage shift register with a 100 MHz IF output, PSK modulated at 60 Megabaud. Current fabrication techniques promise the possibility of extension to 300 stage registers at 150 Megabaud, for minimal increase in power consumption. Such a device, whose construction is not trivial, should consume typically 15 mW/bit, to give an order of magnitude improvement over standard ECL techniques.

## 2.6 SUMMARY

Table 2.2 summarises the potential applications of the SAW devices discussed in this Chapter in civil communication systems, outlining their particular strengths and weaknesses. This brief survey has not included detailed comparisons or accurate cost analysis with other technological implementations of equivalent functions. However, it can be stated that SAW devices are capable of meeting most of the component specifications. SAW technology also promises additional features, such as the flexibility to incorporate the required group delay equilisation into an IF filter.

To date, the technology has not received serious consideration in the context of component devices for communications systems. This requires the economics to be carefully established between SAW

and conventional approaches. The small numbers of microwave common carrier equipments results in high SAW component costs. Here the high capital cost £1,000 of designing the SAW structure with a computer model, and producing the chrome mask required for device fabrication, cannot be amortised over a large run of production devices. VHF and UHF mobile equipments are produced in larger volume but unfortunately the narrow channel spacings do not offer easily identified applications for SAW components. It must be stressed that this is not so in the case of the oscillator which has a promising future in frequency synthesis and as a local oscillator at UHF for mobile radio.

The desire to conserve energy resources is hastening the demand for more efficient communications employing extended confravision and new viewphone facilities. These are in turn generating the requirement for the higher capacity, more flexible, digital data transmission systems. Digital systems will provide in the future additional applications for new components where SAW devices can be competitively evaluated during the trials of prototype equipment. It must also be noted that communications growth naturally results in higher IF's and carrier frequencies which in the future must favour SAW components against current lumped element technology.

This Chapter has completed the introduction to SAW device applications in conventional communication systems. Prior to discussing the theoretical and practical studies of SAW programmable filter design it is first necessary to introduce another type of communications system, the Spread Spectrum system.

| | |
|---|---|
| CENTRE FREQUENCY | 140 MHz |
| INSERTION LOSS | < 8 dB |
| PASSBAND WIDTH | ±15 MHz (-1 dB)<br>±25 MHz (-3 dB) |
| PASSBAND RIPPLE | < 0.1 dB (±15 MHz) |
| STOPBAND ATTENUATION | > 50 dB (@ ±40, ± 80 MHz) |
| GROUP DELAY VARIATION | 0.1 nS (±15 MHz) |

TABLE 2.1(A) SAW ESSENTIALS OF IF FILTER SPECIFICATION FOR 2700 CHANNEL ANALOGUE REPEATER

| | |
|---|---|
| CENTRE FREQUENCY ($f_c$) | 4 GHz |
| INSERTION LOSS | < 15 dB |
| PASSBAND WIDTH | ±20 MHz |
| PASSBAND RIPPLE | < 0.22 dB |
| STOPBAND ATTENUATION (between 30 + 550 MHz from $f_c$) | > 40 dB |
| GROUP DELAY VARIATION | 6 nS (±16 MHz) |

TABLE 2.1(B) TYPICAL INTELSAT 4 SATELLITE CHANNEL MULTIPLEXING FILTER SPECIFICATION

| | |
|---|---|
| FREQUENCY | 500 MHz |
| SHORT TERM STABILITY (over ¼ second) | 1 in $10^{10}$ |
| LONG TERM STABILITY (over 3 years) | 1 in $10^6$ |
| TEMPERATURE STABILITY (over -10°C to +50°C) | 1 in $10^6$ |
| OUTPUT POWER | 5 mW |
| OVERALL EFFICIENCY | > 1% |

TABLE 2.1(C) SPACE QUALIFIED LOCAL OSCILLATOR DRIVE SPECIFICATION

| SAW DEVICE | APPLICATIONS AREA | ADVANTAGES | DISADVANTAGES |
|---|---|---|---|
| FREQUENCY (FUNDAMENTAL<br>(<br>(<br>FILTERS (HARMONIC | I.F. FILTERS<br><br>SATELLITE CHANNEL MULTIPLEXING FILTERS | NO ADJUSTMENTS<br>LIGHT WEIGHT<br>DESIGN OUT GROUP DELAY VARIATIONS | HIGH INSERTION LOSS |
| DISCRIMINATOR | ANALOGUE COMMUNICATIONS DEMODULATOR | HIGH OPERATING IF | MODERATE OPERATING BANDWIDTH<br>LINEARITY UNPROVEN |
| OSCILLATOR | SPACE QUALIFIED LOCAL OSCILLATOR DRIVE AND ANALOGUE COMMUNICATIONS MODULATOR | HIGH OPERATING IF<br>EASY HARMONIC SELECTION | POOR LONG TERM STABILITY |
| | FREQUENCY SYNTHESIS | WIDE PULL RANGE | |
| DELAY LINES | DELAY EQUALISATION FOR DIGITAL LINKS EMPLOYING SPACE DIVERSITY | STABLE AND ACCURATE DELAY | MARGINAL BANDWIDTH ON TEMPERATURE STABLE SUBSTRATES |
| D.P.S.K.<br>BIT MATCHED FILTER | DIGITAL IF TO BASEBAND DECODER | OPTIMISES SNR | DIFFICULT TO ACHIEVE HIGH DATA RATES |
| PSEUDO NOISE GENERATOR | ACCEPTANCE TESTING OF DIGITAL LINKS | DIRECT IF MODULATION | FIXED, LOW DATA RATE |

TABLE 2.2 SUMMARY OF SAW DEVICE APPLICATIONS RELEVANT TO CIVIL COMMUNICATIONS

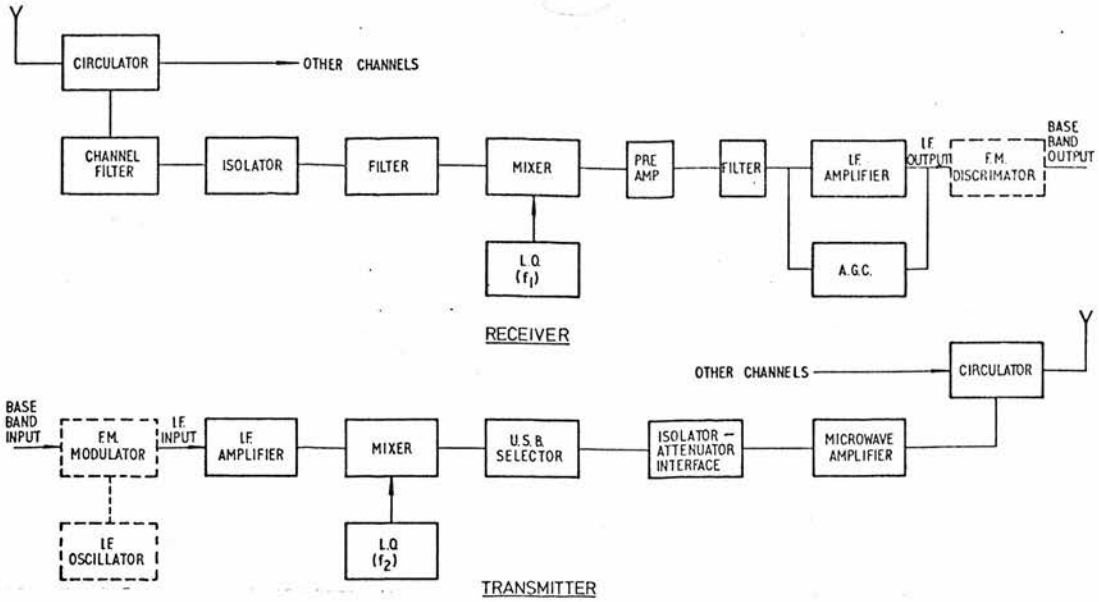


FIG 2.1(a) ANALOGUE COMMUNICATIONS REPEATER

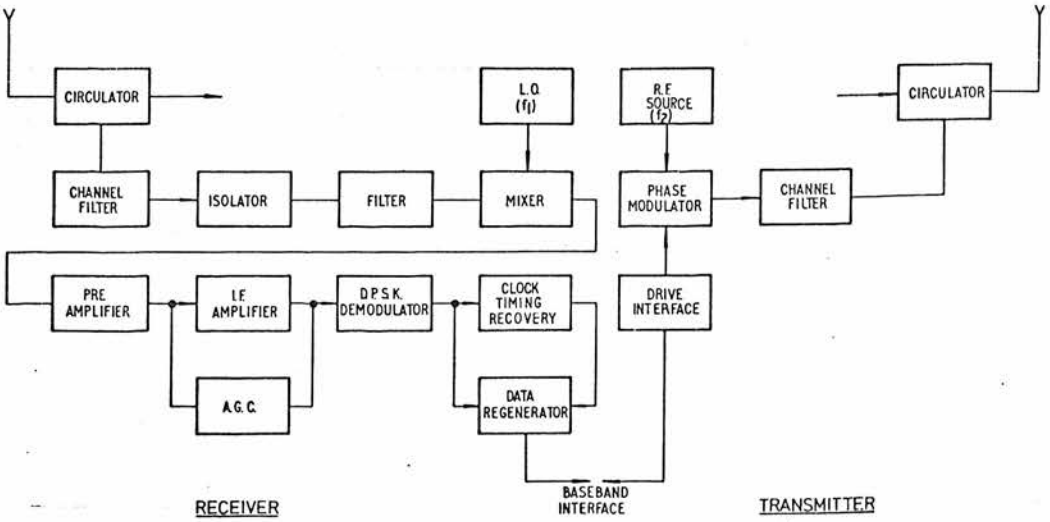


FIG 2.1(b) DIGITAL COMMUNICATIONS REGENERATIVE REPEATER

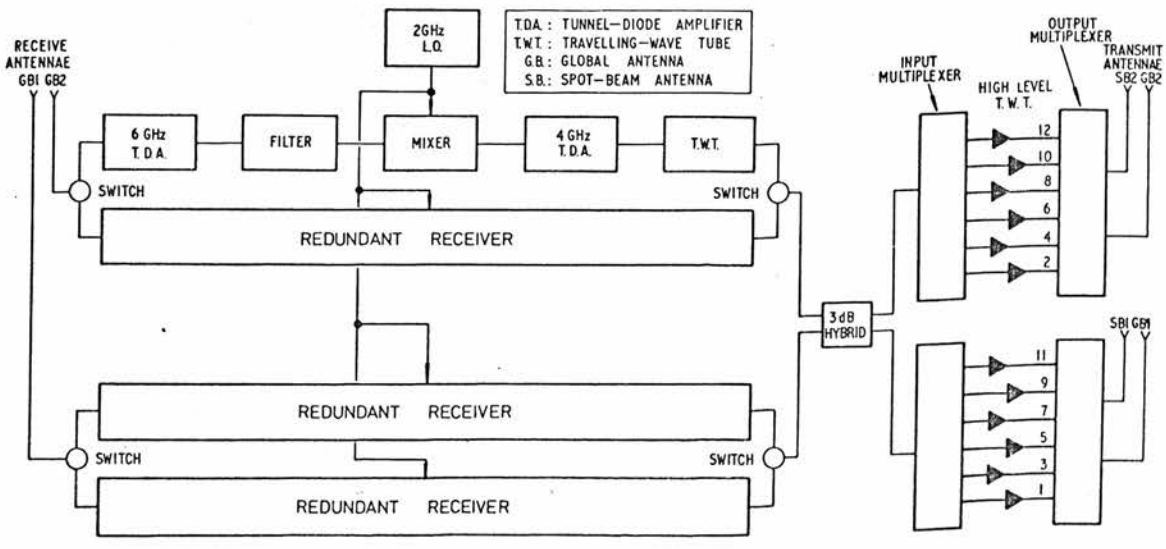


FIG 2.1(c) INTELSAT IV SATELLITE REPEATER

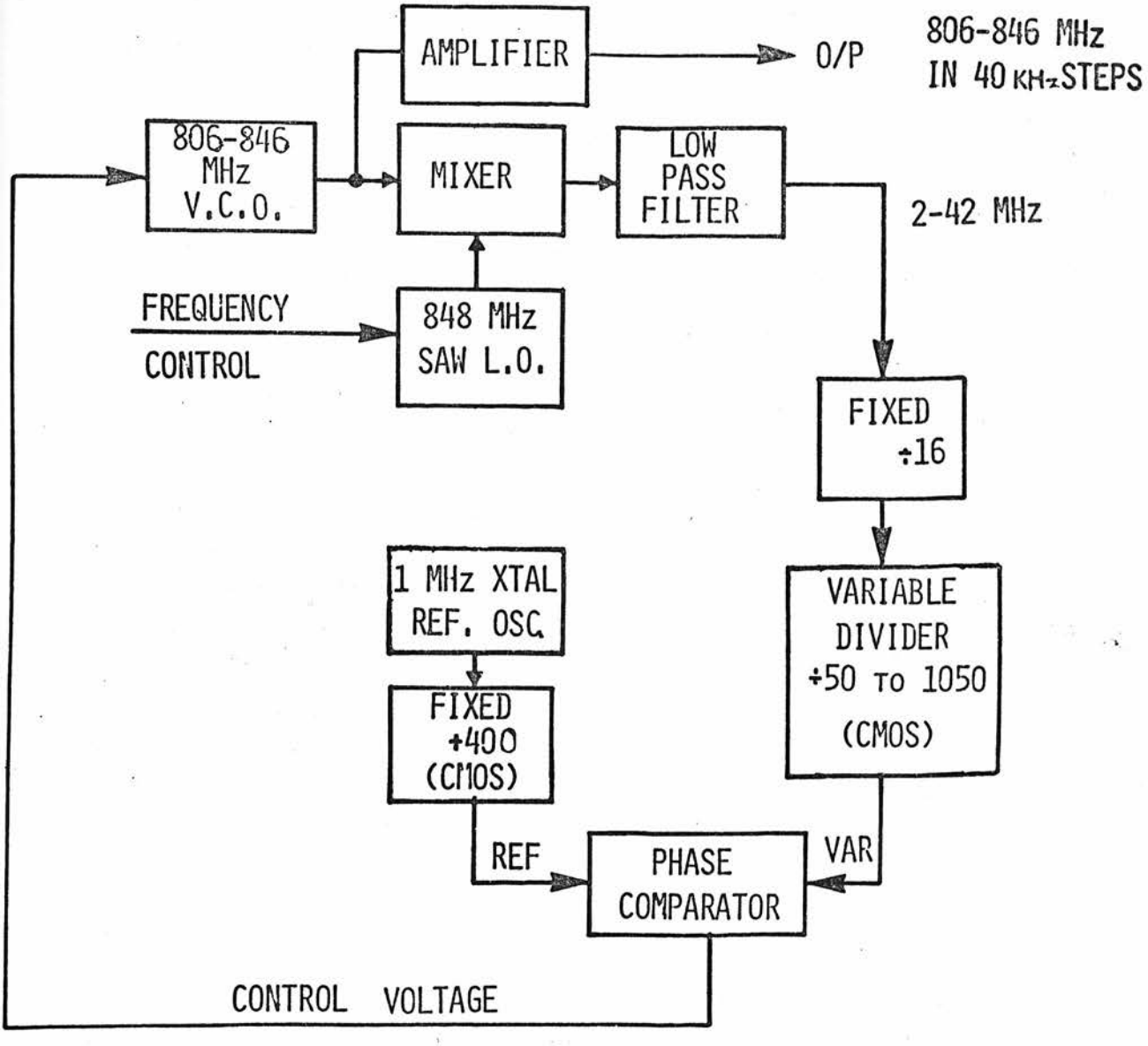


FIGURE 2.2 FREQUENCY SYNTHESISER FOR UHF MOBILE RADIO EMBODYING A SAW OSCILLATOR

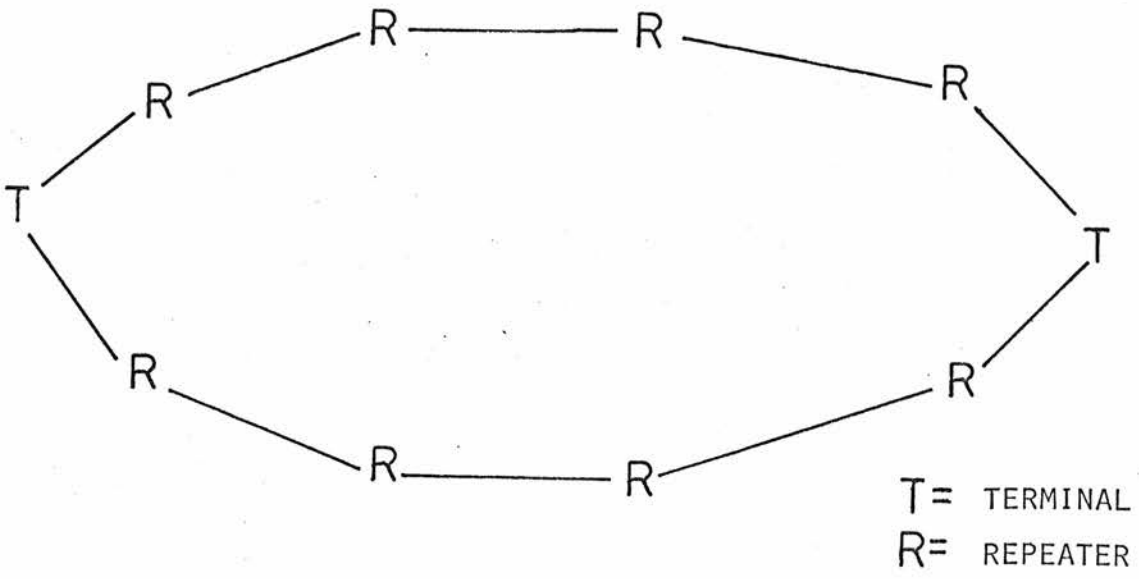


PROBLEM - EQUALISE DELAY BETWEEN TERMINAL STATIONS OVER TWO SEPARATE TRANSMISSION PATHS

FIGURE 2.3 B.P.O. 20 GHz POLELINE DIGITAL COMMUNICATIONS SYSTEM

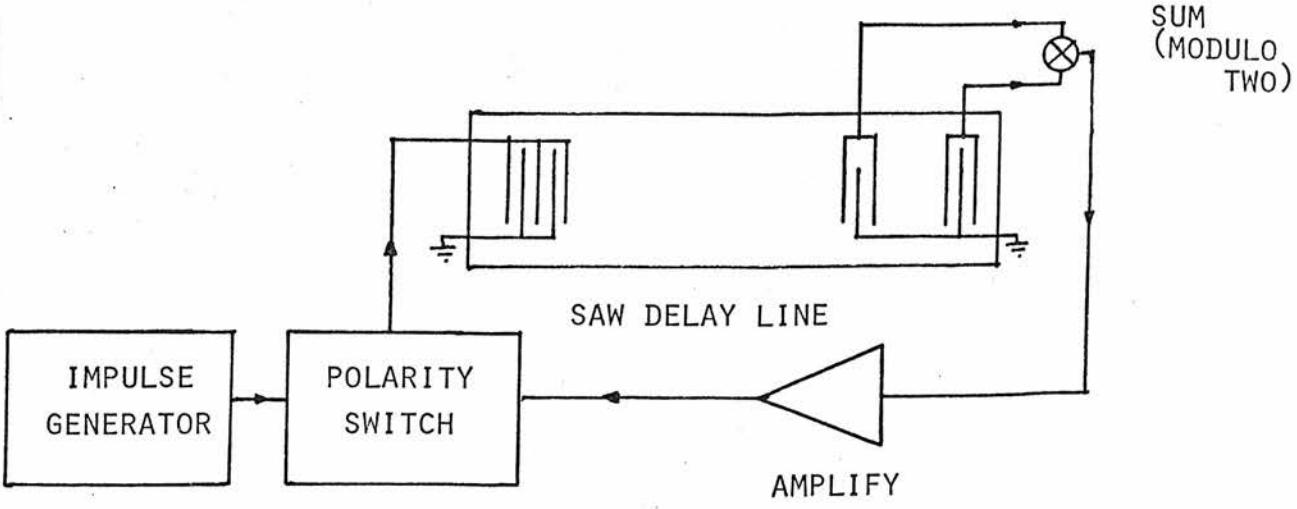


FIGURE 2.4 SAW PSEUDO-NOISE CODE GENERATOR

# 3. SPREAD SPECTRUM COMMUNICATIONS

## 3.1 INTRODUCTION

One multiple access technique widely adopted in civil communication systems allocates to each subscriber a narrow frequency slot within the available channel, ie, FDMA. An alternative system,discussed under the digital communication systems in Section 2.2.3,allocated the entire channel bandwidth to a subscriber but constrained him to transmit only regular short bursts of wideband signal (TDMA). Both these accessing techniques are well established for long haul terrestial and satellite communications as they offer very good utilisation of the available bandwidth.

In mobile applications such as Air Traffic Control, and Military and Police communications, where there are a large number of physically separated subscribers, the FDMA and TDMA channel accessing techniques are both restrictive and time consuming especially when the number of subscribers exceeds the number of available channels. In these low activity factor applications the messages are short and intermittent and housekeeping time is often longer than the message duration. In addition non-linear satellite repeaters are attractive for wide area coverage mobile systems as they offer good conversion efficiency and hence high microwave powers. However, Harris[47] has shown that they introduce degrading intermodulation products between channels making it impossible to use an FDMA system.

These de ficiencies in conventional accessing techniques have resulted in the development of new systems based on the spread spectrum (SS)[47] concept. In these systems the bits of slow speed data traffic from each subscriber, which may be either burst or continuous signal transmissions, are multiplied by a high chip rate spreading code, forcing the narrowband signal to fill the complete channel bandwidth. Spreading ratios, ie, transmitted (chip) bandwidth to data (bit) bandwidth are typically between 100 and 10,000. Many subscribers can be accessed by allocating a unique spreading code to each subscriber. The signals may be summed in a repeater to give a flat noise-like spectrum where each individual transmission is hidden in the multiple access interference.

In the receiver, detection of the desired signal is achieved by correlation against a local reference code which is identical to the particular spread spectrum encoding employed prior to transmission. Correlation detection gives a processing gain or signal to noise improvement equal to the spreading ratio.

$$\text{Processing Gain} = 10 \log_{10}\left[\frac{\text{Transmitted signal bandwidth}}{\text{Original data bandwidth}}\right] \text{dB} \quad 3.1$$

With suitable choice of the correlation properties of the spread spectrum codes selected for the different subscribers, the receiver will discriminate against multiple access interference. The effectiveness of wide or narrow band interference (ie, intentional jamming) is reduced by a factor equal to the receiver processing gain hence the system will operate in hostile environments. Multipath rejection can also be obtained if the differential propagation delay exceeds the chip time of the spreading code. The multipath appears

either as a separately resolved time shifted output or it will be summed with the multiple access interference, dependent on the particular spread spectrum coding system employed. New techniques are currently under development to use quasi-static multipath to constructively improve the receiver output SNR[48].

## 3.2 SPREAD SPECTRUM SYSTEMS

### 3.2.1 CLASSIFICATION

Spread spectrum systems have been previously classified[28] under four basic headings, to clarify the many variants which have developed from the basic concept. Table 3.1 shows this classification which initially separates the systems into the two main categories of *burst* or *continuous* signal transmissions. It must be noted that, with the exception of the M-ary coded systems[49], the British Skynet Communication System[47] is the only spread spectrum system in operation today. Most of the other systems listed in Table 3.1 are only proposals.

The signalling technique used to transmit the data is separately identified as a : phase shift keyed (PSK), pulse position modulated (PPM), code shift keyed (CSK), on-off keyed (OOK) or frequency shift keyed (FSK) transmission. Orthogonality between subscribers is obtained either by channel addressing with FDMA or TDMA or by spread spectrum addressing of the message with a unique or hybrid combination of code division (CD), frequency hopping (FH) and time hopping (TH) techniques. The spread spectrum signature selected is usually Pseudo-Noise (PN) coded PSK or FSK. When M-ary coding is employed a simple continuous wave signal can be used as the spectral bandwidth is automatically spread during encoding.

A brief examination of Table 3.1 reveals that there are a myriad of schemes which can be implemented for spread spectrum communications, and it must be appreciated that several of these proposals are dependent on SAW techniques to generate and detect the complex coded waveforms. Since many of the systems use the correlation properties of PN codes to differentiate between the subscriber signatures, it is now relevant to briefly review the correlation properties of the codes regularly employed in spread spectrum transmissions.

### 3.2.2 CORRELATION PROPERTIES OF PN CODES

The linear maximal sequence which can be generated in any n-stage shift register[58] with linear feedback is a Pseudo-Noise (PN) binary sequence. The period L of the sequence is given by

$$L = 2^n - 1 \qquad 3.2$$

Typical code lengths are therefore, 3, 7, 15, 31, 63, etc and there are usually more than one distinct sequence for the longer code lengths. Periodic linear maximal sequences have the property that the finite autocorrelation function is two valued and may be written :

$$C(K) = \sum_{n=1}^{L} a_n \cdot a_{n+k} = L \text{ if } k = 0, \pm L \pm 2L, \text{ etc}$$
$$= -1 \text{ otherwise} \qquad 3.3$$

*Continuous* transmission systems, such as the Direct Sequence Spread Spectrum (DSSS) system described by Harris[47] use a long fast spreading code of this type added, modulo two, with the traffic data. The code repeat time is usually considerably longer than the data bit

interval thus the receiver only correlates an N chip segment of the code. This results in an increase in the time sidelobes to approximately $2\sqrt{N}$[59]. Suitable codes for other subscribers, which possess cross-correlation products of $\leq 2\sqrt{N}$, are obtained by selecting other codes of the same length or by deriving the codes from the outputs of two separate generators as described by Cahn[47].

In *burst* transmission systems, such as the ranging system of Otten[52], which is detailed later in Chapter 8 and the random access discrete address (RADA) system reported by Darby[30], the receiver requires to recognise and time a short burst of coded sequence. It must therefore exclusively detect the distinct sequence and not false alarm on one of the other sequences being transmitted. The selected sequences are required therefore, over the complete time frame, to possess small autocorrelation and cross-correlation time sidelobes. Gold[59] has selected aperiodic disjoint subsequences from a very long maximal sequence to obtain a set of codes with acceptable properties. Sixteen sequences of length N = 511 are known which closely approximate to the minimum realisable cross-correlation products of $1.6\sqrt{N}$.

Other codes of interest are the Barker codes which exhibit good aperiodic autocorrelation properties. They are attractive for synchronisation applications, but no codes have been found for sequence lengths of greater than 13. A set of L orthogonal codes also exist for any sequence length L

$$\text{where } L = 2^m \quad (m \text{ integer}) \qquad 3.4$$

However, the large auto and cross-correlation time sidelobes[60] require

an accurate timing gate in the receiver to unambiguously detect the received code making them unsuitable for asynchronous access communication systems. Linear FM (chirp) signatures, although used extensively in radar, do not find many applications in communications primarily because they do not possess the natural code division capability of PN sequences.

### 3.2.3 SPREAD SPECTRUM SIGNAL DETECTION

Signal detection in the receiver can be achieved using several different methods. Unkauf[61] has reported these basic systems, the post detection Digital Matched Filter (DMF), the predetection serial correlator and the Surface Acoustic Wave Analogue Matched Filter (AMF).

The DMF performs wideband detection on the received noise corrupted signal. This requires a fast and expensive analogue to digital converter (A/D) which samples at half chip intervals and quantises into a multi-level digital signal. Comparison against the stored reference code is then performed in a single, high speed, adder accumulator. A microelectronic LSI DMF signal processor can be designed with 100 MHz bandwidth and a time bandwidth (TB) product of 1,000 to provide instantaneous synchronisation to the received signal. The recent development of analogue shift registers in Charge Coupled Device (CCD) technology[62] now permits direct implementation of an analogue equivalent of the DMF dispensing with the A/D conversion. Although attractive, this microelectronic technique is currently limited to smaller signal bandwidths by the maximum clock rate (~10 MHz) of the tapped CCD shift registers.

Another implementation of the spread spectrum receiver serially multiplies the received signal with a local reference code to "despread" the signal. This reconstitutes the original data for detection with a conventional narrowband filter and phase demodulator. The predetection serial correlator can accommodate almost an infinite length of code at very high chip rates (~1 GHz). However,accurate synchronisation to within ± one half a chip period is required between the received signal and local reference code before detection can commence. The receiver is capable therefore of receiving only the continuous mode transmissions outlined in Table 3.1. Synchronisation is achieved with serial search routines but they increase the acquisition time by a factor proportional to the receiver processing gain when compared with matched filter detection.

The recent development of SAW AMF's[63] has generated interest in these devices for use as high performance,cost effective,matched filter receivers. Their carrier phase and chip asynchronous capabilities make them especially attractive as the microelectronic DMF requires an expensive duplication of hardware to achieve asynchronous operation. SAW technology is predicted to achieve fixed coded filters with 100 MHz bandwidth and TB's of 1000 in the near term. These properties are attractive for burst mode systems but most continuous transmission systems employ a long code requiring an adaptive matched filter. The development of SAW Programmable AMF's, described in Chapters 5 and 6, looks attractive for overcoming this limitation but they are unlikely to achieve either the bandwidth or TB predicted for fixed coded AMF's. Adaptive matched filtering can also be achieved with the SAW non-linear convolver[64] which presently offers TB's in excess of fixed coded AMF's. The device

does require additional hardware for active reference code generation, and to obtain a real time output[64].

Following a review of the current thinking on receiver design it is interesting to note the recent development of sophisticated new concepts based on SAW and CCD signal processing techniques. Whitehouse[8], who has previously demonstrated that fast Fourier Transform processors based on the chirp Z transform algorithm can be constructed with SAW devices, is now studying the design of a two dimensional Discrete Fourier Transform (DFT) processor using CCD and SAW devices. It exploits the long delays achieved in CCD devices with the fast signal processing capabilities of SAW technology to construct a DFT processor with a TB of $10^6$. This is attractive for the design of a novel receiver where the signal is first transformed to the frequency domain, then multiplied by the appropriate reference signal before inverse transformation back into the time domain. In addition to performing matched filtering these sophisticated techniques permit narrowband interferance signals to be detected and tracked at the frequency domain interface for suppression with an adaptive notch filter.

This introduction to spread spectrum receiver design has attempted to outline the available techniques. Darby[30] has reviewed the current and future performance capabilities of matched filters fabricated both with microelectronic and surface acoustic wave techniques. It is impossible here to indicate which particular device gives the best performance as each system application requires an accurate trade-off between cost and required component performance.

## 3.3 SYSTEMS IMPLEMENTATION WITH SAW AMF's

Following the introduction to the concepts of spread spectrum communication systems it is interesting to investigate where SAW AMF's are likely to find applications in these systems.

### 3.3.1 SYSTEMS EMPLOYING BURST TRANSMISSION MODE

As truly asynchronous, passive matched filters SAW fixed coded AMF's are attractive for rapid generation and detection of short (<100 μsec) burst signals encoded in both time and frequency domain. Darby[8] and Setrin[55], see Table 3.1, have both exploited this unique feature to obtain a large number of coded signatures for use as an address alphabet in uncoordinated multiple access systems[65]. The Random Access Discrete Address (RADA) system allocates one address from the available alphabet to each subscriber wishing to use the system. Address preambles are not employed, instead the address is impressed as a spread spectrum modulation on top of the data. In other words,pulse position modulation or PCM traffic data is further modulated bit by bit with the spread spectrum address to route the transmission to the intended receiver. The concept is designed for systems,such as ATC,where there are low activity factor subscribers who only actively use the system for a short time. This gives a receiver performance which is dependant on the number of active subscribers rather than the total number of subscribers. These systems offer immediate reply, low signal detectability and low standby power,factors of considerable significance in mobile communications. Darby[8] has described the design of these systems and illustrated the simplicity of terminal hardware when SAW fixed coded AMF's are employed to generate and detect the complicated

frequency-time coded pulse patterns. A simple prototype system has been constructed and demonstrated giving close to theoretical error rate performance under conditions of bandlimited noise at the receiver input.

### 3.3.2 CONTINUOUS TRANSMISSION MODE SYSTEMS

In addition to the burst mode systems continuous signal transmission is equally popular for spread spectrum systems. Two important systems are included in Table 3.1. Hunsinger[54] has reported a coherent frequency synthesiser based on SAW devices and Harris[47] has described the Direct Sequence Spread Spectrum accessing technique which is the basis of an existing system.

The DSSS system, which is shown diagramatically in Figure 3.1, is used in the Skynet[66] ship and shore military communication system. In the transmitter the SS IF (70 MHz) modulator generates a continuous (repetitive) phase modulated PN-PSK code, the transmitter *signature*, at a 5 MHz rate which is many thousand chips long. This output is modulated further in the mixer by the encoded input data (typically 2.4 kbits/sec), and upconverted to an 8 GHz carrier, prior to transmission. After relay through a satellite, which is shared by many subscribers on a code division basis, the characteristic signal, now corrupted by other user interference and multipath, arrives at the receiving station. The intended receiver comprises a SS IF demodulator, similar to the modulator employed in the transmitter, a mixer, an integrator and a synchroniser. To detect the received data the demodulator provides an output identical to that emitted from the transmitter modulator and synchronised to include a delay equal to the propagation time. This demodulator output is

multiplied with the incoming corrupted characteristic signal removing the PN coding to leave a carrier modulated only by data. Integration over the bit period, eg ~½ msec, then determines whether an encoded data bit '1' or '0' was transmitted. These predetection serial correlation processors currently achieve processing gains in excess of 30 dB with ease.

The DSSS system provides anti-jam capability through processing gain; multipath rejection, by the delay and add property of PN sequences; low detectability by the code division accessing and low input SNR; and optimum channel utilisation through control of uplink powers to overcome the 'near-far' problem. The PN SS modulation is chosen purely for accessing the subscribers through the hard limited satellite repeater and *not* for military security. This is achieved separately by the cryptographic coding in the baseband encoder and decoder.

The predetection serial correlation receiver requires precise synchronisation, to within ±½ the chip period (100 nsec at 5 MHz), to establish the correct phase of the SS IF demodulator before data can be decoded. As a trial integration over the bit period is necessary before any receiver output is obtained, the acquisition time is equal to the time uncertainty multiplied by the processing gain. The serial search rate of the SS IF demodulator must therefore be slower than the baseband data rate often resulting in acquisition times of one minute.

Matched filters are under consideration for synchronisation as they offer an immediate improvement in acquisition time proportional to their TB. The passive SAW AMF's discussed in Chapter 4 are

attractive as their chip rates and centre frequencies fit the Skynet system. However, the maximum available TB of 511 falls short, by a factor of 4, of the requirements of current receivers. In addition the devices do not possess the programmability that is necessary to retrofit the existing system. The more applicable programmable AMF possesses a further reduction of at least 2 in processing gain as devices are most unlikely to be fabricated with greater than a 250 tap structure. Therefore the devices appear at first sight not to be directly applicable to the Skynet system.

However the recent development of serial parallel signal processing techniques[54] permits the TB of SAW AMF's to be extended considerably. Chapter 7 details the design of a Serial Parallel Receiver (SPR) employing a high speed reprogrammable AMF followed by coherent summation within a unity gain recirculating integrator. This permits Programmable PSK matched filters to be realised with TB of $> 10^3$ meeting the requirements of the DSSS synchroniser. A timing advantage accrues as the PN-PSK code vector set on the programmable AMF can be in error by $\pm \frac{1}{2}$ T, where T is the PAMF propagation delay, and coherent build-up of correlation peaks will still be achieved. This synchroniser provides an improvement in acquisition time equal to the TB of the programmable AMF when compared with the existing serial correlator. It also offers the added advantage of replacing the serial correlator for data demodulation.

## 3.4 CONCLUSIONS

This brief review has attempted to show that spread spectrum systems provide a flexible multiple access capability which is

better suited than existing FDMA and TDMA techniques for certain applications. The complex coded waveforms required to implement the systems can in many cases be conveniently generated at intermediate frequencies in SAW devices. The simplicity of construction and asynchronous properties of the SAW AMF are especially attractive for the reception of these coded signals when compared with a microelectronic signal processor. The importance of SAW AMF's can only be appreciated when it is noted that a number of the system proposals included in Table 3.1 are dependent on SAW techniques to generate and detect the complex F/TH-CD coded waveforms.

The following chapters of this thesis review the current status of SAW fixed coded AMF prior to detailing the development of high performance electronically programmable AMF's. Chapter 7 concludes the practical studies by describing the performance and limitations of a SAW serial parallel matched filter receiver when compared against the requirement of a synchroniser for the Direct Sequence Spread Spectrum communication system.

| *REFERENCE* | *TRANSMISSION MODE* | *DIGITAL SIGNALING TECHNIQUE* | *MULTIPLE ACCESS MODE* | *SPREAD SPECTRUM SIGNATURE* | *SYSTEM APPLICATION* |
|---|---|---|---|---|---|
| Piccolo[49] | CW | M-ary FSK | FD | CW | HF Diplomatic comms |
| Harris[47] | CW | CPSK | CD | PN-PSK | Milsatcom |
| Parker[50] | BURST | M-ary FSK | FD | CW | VHF high integrity data data link for mobiles |
| Lever[8] | CW | M-ary FSK | FD | CW | Narrow bandwidth milsatcom |
| Ellingson[51] | BURST | PSK | TD | PN-PSK | ICNI |
| Otten[52] | BURST | PPM | CD | PN-PSK | CAS |
| Burnsweig[53] | BURST | PSK | TD | CHIRP | RANGING |
| Hunsinger[54] | CW | PSK | FH-CD | PN-PSK | SATCOM |
| Setrin[55] | BURST | CSK | TD | PN-PSK | IFF |
| Bush[56] | BURST | OOK | FH | CHIRP | RPV |
| Reed-Blasbalg[57] | BURST | M-ary | TD | PN-FSK | Overcomes multipath |
| Darby[30] | BURST | OOK | F/TH-CD | PN-PSK | UHF mobile |

TABLE 3.1 CERTAIN REPORTED SPREAD SPECTRUM SYSTEMS

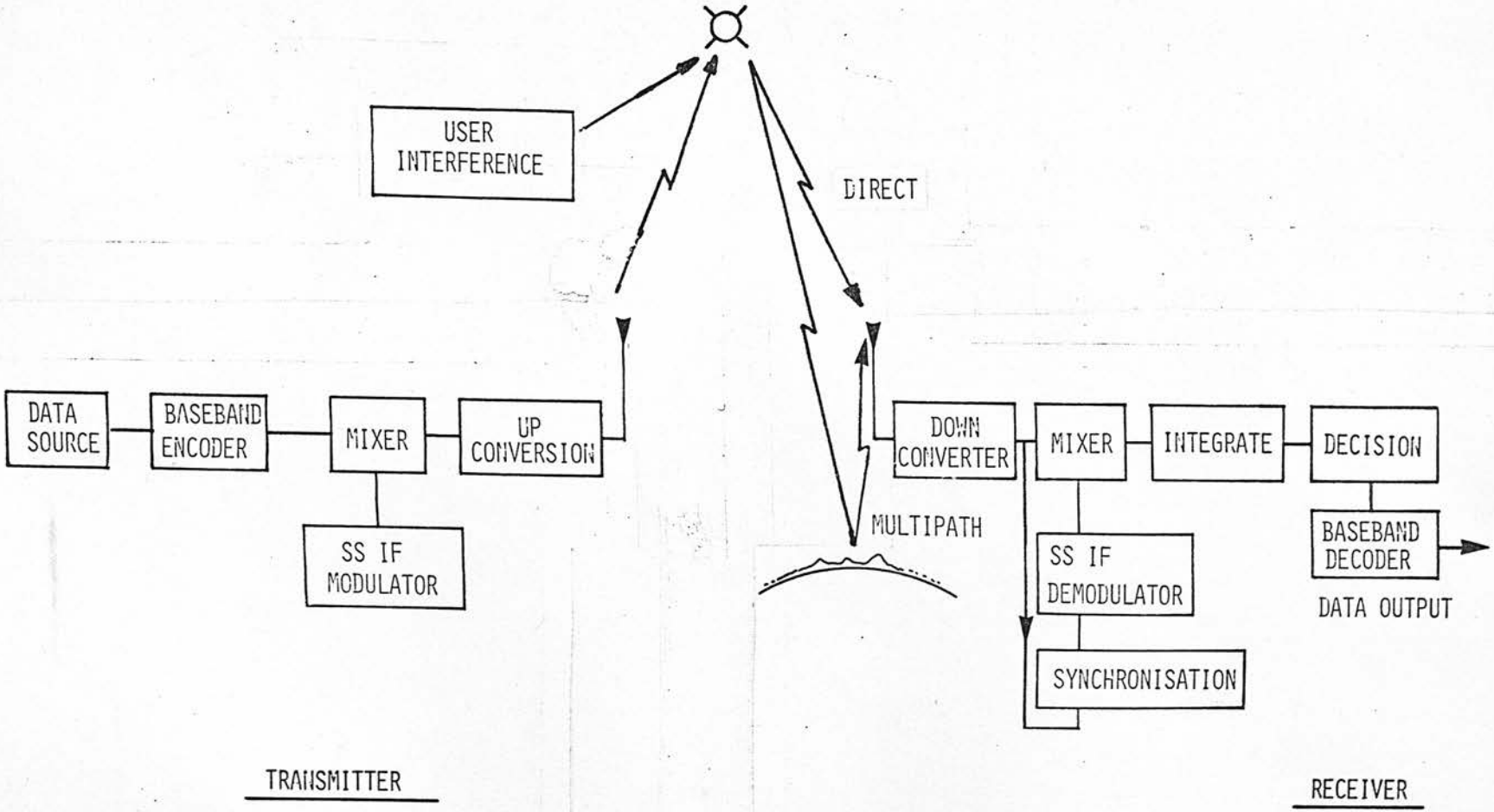


FIGURE 3.1 DIRECT SEQUENCE SPREAD SPECTRUM COMMUNICATION SYSTEM

# 4. DESIGN AND PERFORMANCE OF FIXED CODED ANALOGUE MATCHED FILTERS

## 4.1 THE ANALOGUE MATCHED FILTER

To perform the optimum predetection processing of a signal, s(t), corrupted by gaussian white noise the receiver must incorporate a filter which is *matched* precisely to the transmitted signal waveform. The matched filter processor gives the greatest possible improvement in receiver signal to noise ratio (SNR).

By definition[67], the matched filter must include a frequency filter to remove noise and interference outwith the passband of the transmitted signal. In addition it must possess an impulse response which is the time reverse on the transmitted waveform. These properties can be conveniently achieved with a linear transversal filter. For a Phase Shift Keyed IF signal the matched filter can be closely approximated with a lossless, non-dispersive, Surface Acoustic Wave Tapped Delay Line (TDL).

The preferred design[29,63] uses a narrow band input IDT to generate the Surface Acoustic Wave. Detection of the SAW is accomplished with an array of wideband, weakly coupled, tapping IDT's. Matching to a biphase coded signal requires each tap to be spaced apart by a delay, T, equal to the PRP of the transmitter chip clock. The $0^{o}$ or $180^{o}$ phase weighting is achieved by adjusting the interconnection polarity between the individual taps and the sum bus as shown diagramatically in Figure 4.1(a).

Matched filters can be used either for data encoding or decoding. In the SAW TDL code generation (expansion) is accomplished by impulsing

the input IDT to generate a packet of acoustic energy. As the wave propagates under the large tapping electrode, each individual tap samples the acoustic wave packet. The output signal is given by the convolution of the acoustic signal with the impulse response of the tap array. Hence, if the input IDT length equals the tap to tap spacing then the impulse response gives a constant amplitude electrical signal whose length equals the propagation delay from first to last tap. If, in addition, the tap interconnections are coded in a PN sequence then the impulse response is the characteristic PN-PSK IF sequence shown in Figure 4.1(b).

To detect a PSK sequence the taps must be coded to recognise the transmitted signal. An acoustic wave, containing the received signal coding, is generated at the input IDT and allowed to propagate under the tapping electrode. The output then gives the cross correlation function of the received signal with the tap coding. If the taps are encoded with the time reverse of the transmitted signal, then the output displays the codes autocorrelation function. When the acoustic wave is exactly registered below the tapping electrode, the voltage from each individual tap will add in phase to give a sharp correlation peak. This coherent addition of signal voltage compared to incoherent addition of the random noise voltages gives rise, at the instant of correlation, in a suitably coded AMF to a

$$\text{Processing Gain} = 10 \log_{10}[N] \text{ dB} \qquad 4.1$$

where N is the number of taps in the AMF, which normally equals the Time Bandwidth (TB) product of the coded signal.

This improvement in SNR across the matched filter gives a consequent reduction in received symbol error rate[68].

## 4.2 SURFACE ACOUSTIC WAVE ANALOGUE MATCHED FILTERS

### 4.2.1 DEVICE FABRICATION

Figure 4.2 shows a photograph detailing part of the EA 4 AMF structure. The SAW device was constructed by vacuum coating a polished cut quartz substrate with 1000$^{o}$A of aluminium and then defining the interdigital input transducer and taps using a positive resist system. The substrates used were 63 x 8 x 2.5 mm polished bars of ST cut quartz with the X axis oriented along the length. The electrodes on each tap have a length of 3.1 mm and a linewidth of 7.75 μm with 1:1 mark to space ratio. Care was necessary to reproduce these long narrow lines over the large area of the device (28 x 3.1 mm) without any open or short circuits. Standard semiconductor photomasking techniques were used with special emphasis on tap placement. It is vital to the device performance that the placement of each tap should have an accuracy of at least ± 0.25 μm without any accumulative error along the 35 tap array. This necessitated the use of step and repeat photography to fabricate the tap array. Less accurate placement would cause a phase shift in the sampled signal degrading the coherence of signal summation. Chrome on glass photomasks were used to define the SAW structure and the accuracy necessary is close to state of the art for these masks. Finally a pulsed thermocompression ball bonding system was used to attach 1½ thou diameter gold wires to the bonding pads to permit the AMF to be mounted in the box and electrically connected to the matching networks, input and output connectors.

4.2.2 FIRST ORDER AMF DESIGNS

The SAW AMF structure shown in Figure 4.2 is a simple first order design, similar to that used to demonstrate SAW AMF operation[63]. The EA 4 AMF design parameters are detailed in Table 4.1 along with the other AMF's which are discussed later in this thesis. The EA 4 was designed to operate at 100 MHz with a 5 MHz chip rate signal. The constant aperture, constant periodicity, input IDT incorporates 20 finger pairs ($E_I = 20$) to achieve a 5% fractional bandwidth. An IDT aperture, W in Figure 1.1, of 50 $\lambda$ was selected to give a radiation resistance, $R_a$, of 50 $\Omega$ at synchronism. Smith[9] has derived

$$R_a = \frac{4 \cdot k^2}{\pi \cdot C_{so} \cdot W \cdot \omega_o} \qquad 4.2$$

$$= \frac{2 \cdot k^2}{\pi^2 \cdot C_{so} \cdot W \cdot f_o} \qquad 4.3$$

where $k^2$ = piezoelectric coupling coefficient

$C_{so}$ = electrode capacitance per unit length

$f_o$ = synchronous frequency

When combined with single inductor tuning to resonate with the IDT interelectrode capacitance, $C_T$,

$$C_T = N \cdot C_{so} \cdot W \qquad 4.4$$

a close match can be obtained between the input electrical signal and acoustic wave (IDT conversion loss $\rho_{13} \sim -3$ dB, Appendix A).

Frequency domain measurements on the EA 4 AMF, Section 6.2, indicated that the IDT resistance was ~35 Ω. This required a recalculation of $W_{opt}$, with an updated value of $k^2$, as 28 λ (Table 1.1) to give 50 Ω radiation resistance in later AMF designs.

The tapping IDT's were designed with a larger, 100 λ , aperture to compensate for any beam steering due to misalignment with the crystal axis. A three finger pair design, $E_T$ = 3, was employed to extract only a small sample of the propagating wave as electrical energy at the output port ($\rho_{31}$ ~ -40 dB). This permits the AMF to be designed with a simple colinear tap structure with uniform weighting. Typical device pulse response insertion loss is 45 - 50 dB. Taps may be individually bonded to the sum bus giving the flexibility to fabricate any desired code. However, the mask precoding illustrated in Figure 4.2 is attractive for higher yield and reliability, reduced stray capacity and hence improved performance.

Figure 4.3 shows insertion loss predictions, for the AMF shown in Figure 4.2, which were derived from the computer analysis included in Appendix B. It applies the IDT acoustic to electric conversion loss, $\rho_{31}$, derived in Appendix A to a single AMF tap to illustrate the dependence of insertion loss on the number of taps. The upper solid curve plots the loss to the correlation peak (compression) when the AMF is detecting its uniquely coded sequence. The dotted curve is included to show the magnitude of the electro-acoustic reflection, $\rho_{11}$, at each tap with respect to the incident acoustic wave.

Figure 4.4(a) illustrates the performance achieved when a 35 tap AMF of the EA 4 series is precoded with a 31 chip PN sequence. The first trace shows the impulse response and the second trace the correlation response for an aperiodic input signal. Close

examination of the impulse response reveals spurious signals following the PN-PSK coded signal with an amplitude ~ -20 dB relative to the coded output. These spurious signals degrade the correlation response, giving only 14 ± 0.2 dB peak to sidelobe ratio (theoretical 15.8 dB), and destroy the theoretical mirror symmetry of the sidelobes.

Further investigation of these performance irregularities was performed by Darby[30] who examined the frequency domain transfer function, $h(\omega)$, and compared it against a theoretical analysis based on the delta function theory of Tancrell and Holland[69]. These measurements also highlighted degradations, as the practical measurement did not follow the fine structure predicted by theory.

The desire to fabricate high performance 127 tap SAW AMF's with minimal insertion loss (~ 40 dB) dictated that the deleterious second order effects evident in Figure 4.4(a) must be investigated and compensated for in an improved AMF design. Researches initiated by Carr[70] resulted subsequently in both Bristol[71] and Darby[30] identifying the cause as an *acoustic* reflection at the tapping electrodes. The following section discusses the multiple reflections which occur within the tapping electrodes of SAW AMF's.

### 4.2.3 DELETERIOUS SECOND ORDER EFFECTS

During code generation in the AMF, an acoustic impulse is generated at the input IDT and allowed to propagate below the tapping electrode. At each tap position part of the energy is extracted from the incident wave to form a small reflected wave packet. These primary reflected signals propagate in the reverse direction back

towards the input transducer. Figure 4.5 shows the reflections diagramatically. At time t = 0 the impulse is positioned below the first tap and after delay T it propagates to the second tap of the array. (Primary reflected signals, PR1 PR2 etc, are shown with negative amplitude to indicate the reverse direction of travel.) Due to the contra-directed nature of the incident and reflected surface waves, the primary reflected signals from adjacent taps have a spacing of twice T, the tap-to-tap propagation delay, as shown in Figure 4.5. As each tap has an identical load, the primary reflections comprise a train of equal amplitude pulses all possessing the same relative phase.

Further interaction of the primary reflected signals PR1, PR2, etc with the other taps gives rise to secondary reflections, SR1, SR2, etc. As the impulse propagates forwards the primary reflections at an arbitrary tap F and consequent secondary reflections at tap F-1 will sum across the N taps of the array to give a reflected acoustic pulse which follows the impulse with a delay equal to twice the tap-to-tap propagation delay. The amplitude of this pulse, SR1, is equal to twice the reflection coefficient, enhanced by a factor proportional to summation at each tap in the array. Similarly the second pulse, SR2, caused by primary reflection at tap F and secondary reflection at tap F-2 also sums at each tap in the array, giving a train of secondary acoustic pulses, which again possess the same relative phase. As a small quantity of energy is continuously being removed from the impulse at each tap position the pulse train gradually decreases in amplitude.

The reflections detailed here are all acoustic effects. However, when impulsing an AMF these spurious acoustic signals will

sum across the encoded tap array to give the degrading spurious electrical output shown in Figure 4.4(a). The dependence of the level of electrical spurious signals at the AMF output, on device coding, is discussed later in Section 6.5.6.

Acoustic reflections are caused by two separate mechanisms, electro-acoustic regeneration and acoustic wave impedance mismatch. The first effect is caused by reflection from the electrical tap load while the second effect results from an electrical shorting and mass loading of the piezoelectric substrate. Figure 4.3 predicted the level of regeneration as -85 dB for AMF's with <50 taps, indicating that these effects were of too small a magnitude to give the measured -20 dB impulse response spurious in a 31 tap structure.

Darby[30] has derived the acoustic reflection coefficient ($S_{11}$) for electrical shorting at an electrode finger edge as :

$$S_{11} \cong \frac{k^2}{4} \qquad 4.5$$

For a 3 finger pair tap on a ST-X quartz substrate this gives an acoustic reflection of -45 dB relative to the input acoustic signal which is considerably larger than the -85 dB regenerated signal. Bristol[8] has investigated mass loading and predicted a similar magnitude for this reflected signal. Practical measurements on the acoustic signal reflected from a tap array and analysis of the impulse response of a Programmable AMF, Section 6.5.6, indicate that primary acoustic reflection levels of -35 dB are typical in EA 4 AMF's. After allowing for variations in fabrication parameters, these measurements are in reasonable agreement with the -45 dB predicted theoretically.

4.2.4 REFLECTION COMPENSATED AMF DESIGNS

These deleterious second order effects have been minimised by incorporating a $\frac{\lambda}{4}$ differential phase shift between electrode edges to cancel reflected acoustic signals. Darby reports a dual tap AMF[72] with a main tap array similar to that shown in Figure 4.2 plus an identical dummy array which is interleaved with but spaced from the main array by an odd number of quarter wavelengths. When incorporated into the EA 5 AMF design[29] this dual tap structure gave in excess of 7 dB improvement in the impulse response spurious signals as shown in the first trace of Figure 4.4(b). It also restored the theoretical mirror symmetry to the autocorrelation function as shown in the second trace. The performance improvement is seen by comparing these results with the uncompensated AMF performance shown in the upper photographs of Figure 4.4. Table 4.2 summarises the main performance differences of 31 tap first order and reflection compensated SAW AMF structures.

Bristol[8,71] obtained similar improvements by splitting the $\frac{\lambda}{4}$ wide tap finger into two $\frac{\lambda}{8}$ wide electrodes. He also reported an electrically grounded fill in array of $\frac{\lambda}{8}$ electrodes between taps which gave further performance improvements.

SAW AMF structures incorporating up to 127 taps have been designed and critically evaluated using both these reflection suppression techniques. The results are presented in both the final contract report[29] and Darby's thesis[30] making it relevant only to summarise the conclusions here :

1. The dual tap geometry[72] permits the co-linear AMF design to be extended to longer codes while still giving acceptable performance without additional insertion loss. (The alternative inclined AMF structure[73]

also reduces interactions but incurs heavy additional loss penalties.) Dual taps suppress spurious arising both from acoustic wave impedance mismatch and electro-acoustic regeneration but scattering to bulk modes is increased giving a taper on the impulse response. Scattering can be reduced with multi-layer metalisation or the taper can be overcome with tap apodisation.

2. The split electrode geometry[71] gives a flatter response but it does not suppress electro-acoustic regenerated spurious. This is *not* a severe disadvantage as later results will show that the enhanced electro-acoustic reflection levels present in SAW PAMF's are still considerably smaller than acoustic wave impedance reflections. This geometry is therefore equally effective for improving AMF performance.

3. It must be noted that split electrodes impose further limitations on linewidth reducing,by a factor of two, the maximum frequency and hence AMF bandwidth for a given photolithographic resolution. However, Darby reports[29,30] replacement of the single inductor input IDT matching with a two stage network which increases the fractional bandwidth on ST-X quartz substrates from 4.5% to 8.5% with only 3 dB additional insertion loss.

## 4.3 SUMMARY

This Chapter has briefly reported developments in SAW IDT geometries to reduce the degradations in SAW AMF's arising from

acoustic reflections. It must be noted that other authors have performed detailed analysis of the performance degradations arising from : tap placement accuracy[74]; substrate mis-orientation[75]; IDT bandlimiting[30]; temperature sensitivity[75,76]; diffraction[55]; beam steering[55]; dispersion[26] and propagation loss[8]. Space limitations have precluded a discussion of the relative importance of these effects.

Therefore, it can be concluded that the design of high performance SAW AMF's is well understood. Although only 31 tap devices have been reported here, acceptable performance has been obtained with 127 tap AMF's and a device with 1000 taps has been designed using wrap around techniques[77]. However, Bell[7] predicts that SAW AMF's are unlikely to be extended beyond 511 taps in production quantities.

The choice between a Quartz or Lithium Niobate substrate for AMF fabrication is difficult. The high $k^2$, Table 1.1, of Lithium Niobate is attractive for high bandwidth, eg, 50 MHz, but it often necessitates tap apodisation[29] or an inclined structure[73] to reduce interactions. Most application require temperature stable operation resulting in our exclusive selection of ST-X quartz substrates for AMF fabrication. However, the wide fractional bandwidth of Lithium Niobate permits the design of AMF's with fewer cycles of RF signal per code chip, drastically reducing the AMF sensitivity to substrate thermal expansion coefficient.

With close to theoretical performance achieved in the aperiodic correlation performance of second generation AMF's their development would appear to be complete. However, the fixed coded AMF is only capable of recognising a single coded sequence. The following two chapters detail a study conducted to design, construct and evaluate several SAW Programmable Analogue Matched Filters (PAMF). These devices possess the added capability to generate or detect *any* desired PSK coded sequence. The goal in the study was to develop a SAW PAMF with a signal processing performance which was indistinguishable from similar fixed coded AMF's.

| MASK NO | INPUT IDT | | | | TAPPING IDT | | | | | REMARKS |
|---|---|---|---|---|---|---|---|---|---|---|
| | $\lambda_o$ (μm) | $f_o$ (MHz) | $E_I$ | $W_I$ | N | d (μm) | $W_T$ | $E_T$ | $B_s$ (MHz) | |
| EA3 | 15.5 | 200 | 20 | $50\lambda_o$ | 128 | 310 | $100\lambda_o$ | 3 | 10 | simple tap geometry , no reflection compensation-fixed coded AMF design |
| EA4 | 31.0 | 100 | 20 | $50\lambda_o$ | 35 | 620 | $100\lambda_o$ | 3 | 5 | simple tap geometry-fixed coded, precoded and programmable AMF's |
| EA6 | 26.0 | 120 | 12 | $115\lambda_o$ | 128 | 310 | $2 \times 38\lambda_o$ | 3 | 10 | dual phase tap structure - PAMF design |
| EA9 | 51.7 | 60 | 11 | $82\lambda_o$ | 64 | 620 | $2 \times 47\lambda_o$ | 3 | 5 | reflection compensated ,dual phase tap structure - PAMF design |

TABLE 4.1 PARAMETERS OF ST-X QUARTZ SUBSTRATE SAW AMF MASKS DESIGNED BY THE AUTHOR

| TEST | | SIMPLE FIRST ORDER AMF DESIGN | DUAL TAP REFLECTION COMPENSATED AMF TAP DESIGN |
|---|---|---|---|
| IMPULSE RESPONSE | INSERTION LOSS (dB) | 50 ± 0.5 | 50 ± 0.5 |
| | SPURIOUS LEVEL (dB) | -20 | < -27 |
| APERIODIC CORRELATION RESPONSE | PEAK TO SIDELOBE RATIO (dB) [theoretical 15.8 dB] | 14 ± 0.2 | 15 ± 0.2 |
| | SPURIOUS LEVEL (dB) | -25 | < -32 |
| PERIODIC CORRELATION RESPONSE | PEAK TO SIDELOBE RATIO (dB) [theoretical 30 dB] | 21 ± 0.2 | 24 ± 0.2 |

TABLE 4.2 PERFORMANCE COMPARISON OF SIMPLE FIRST ORDER AND REFLECTION COMPENSATED SAW 31 TAP FIXED CODED AMF'S

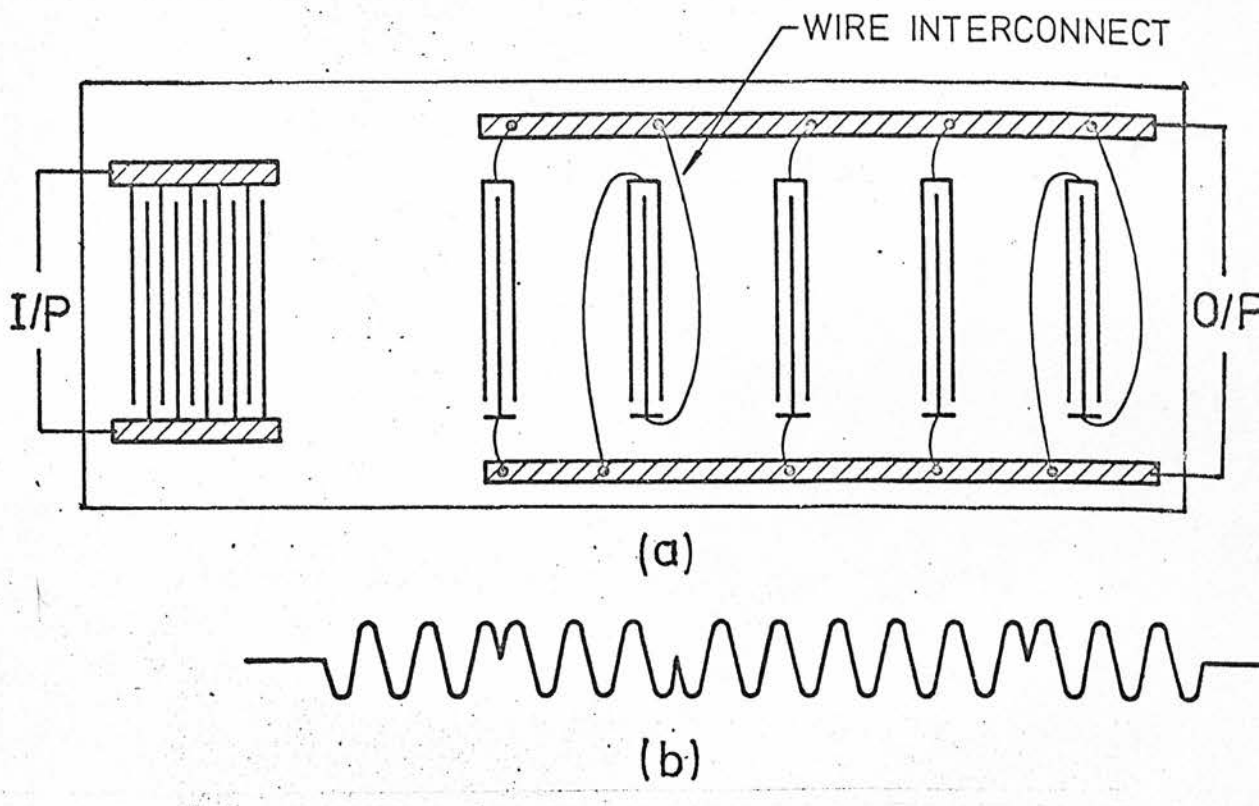


FIGURE 4.1 SAW FIXED CODED ANALOGUE MATCHED FILTER SCHEMATIC AND IMPULSE RESPONSE

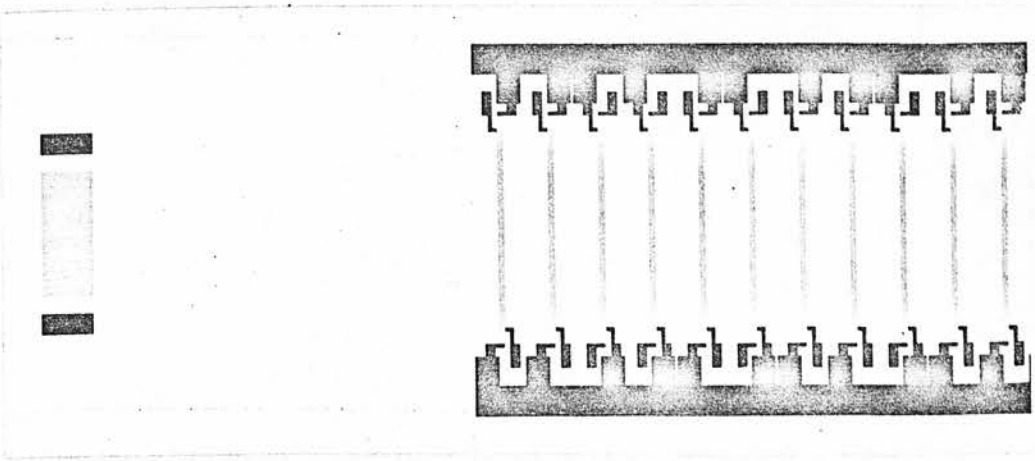

FIGURE 4.2 PART OF AN EA 4 SAW PRECODED AMF STRUCTURE DETAILING INPUT IDT, TAPS AND INTERCONNECTIONS

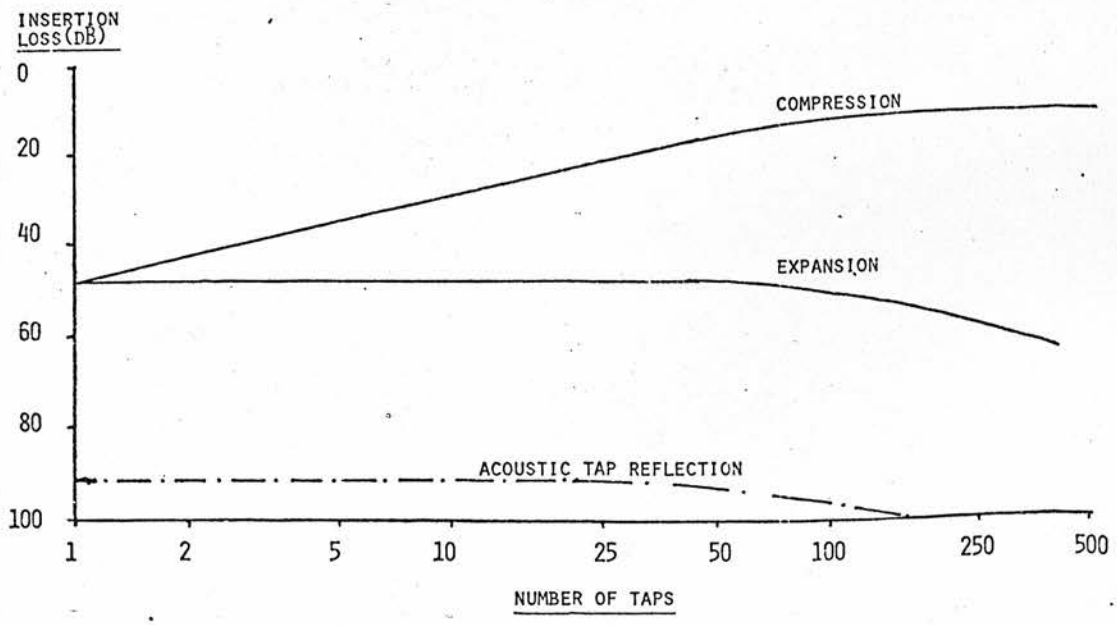


FIGURE 4.3 COMPUTER PERFORMANCE PREDICTIONS FOR SAW FIXED CODED AMF'S

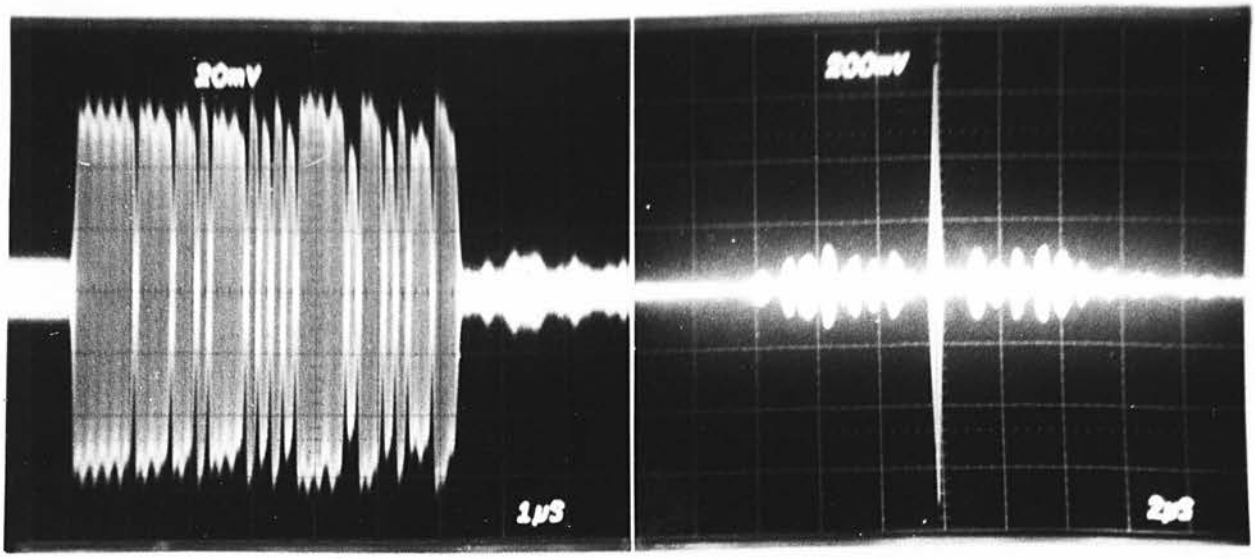


(a)

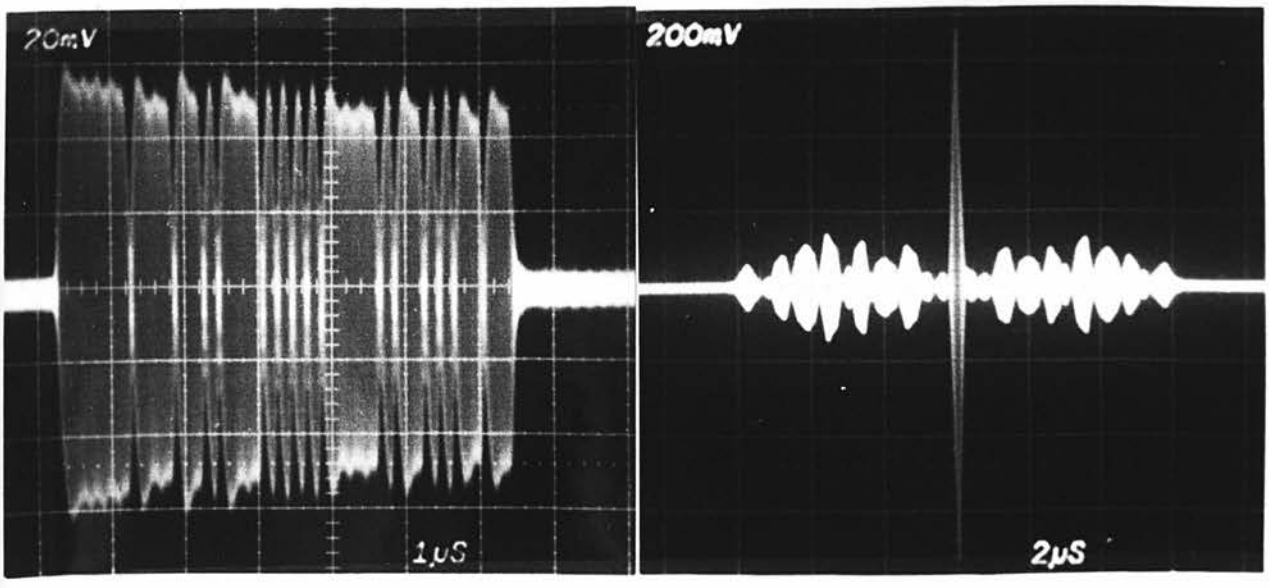


(b)

FIGURE 4.4 COMPARISON OF THE IMPULSE AND APERIODIC AUTOCORRELATION RESPONSES OF A SIMPLE FIRST ORDER EA 4 SAW 31 TAP AMF WITH THE DUAL TAP REFLECTION COMPENSATED EA 5 AMF DESIGN

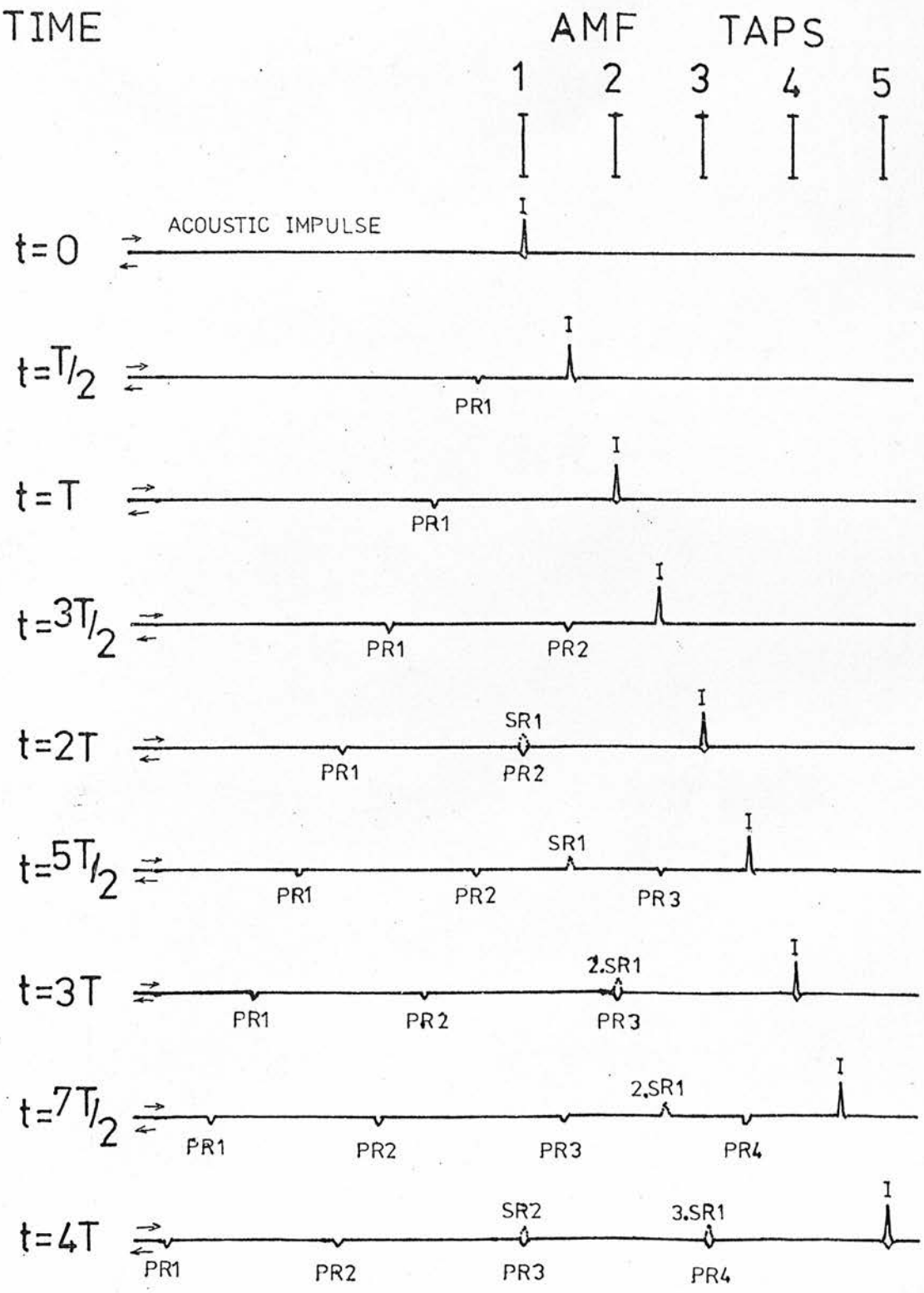


FIGURE 4.5 GENERATION AND SUMMATION OF ACOUSTIC SPURIOUS SIGNALS BELOW THE SAW AMF TAPPING ELECTRODE

# 5. DESIGN OF SURFACE ACOUSTIC WAVE PROGRAMMABLE ANALOGUE MATCHED FILTERS

## 5.1 INTRODUCTION

Chapter 4 has summarised the status of fixed coded AMF development, illustrating the high performance that has been achieved with the latest reflection compensated device designs[30]. These devices are however relatively inflexible of signal format as their coding is fixed during fabrication. A Programmable Analogue Matched Filter (PAMF) is attractive for several of the Spread Spectrum (SS) system applications discussed in Chapter 3. The inbuilt flexibility of device coding can be used to overcome variable interference, to add a level of security or to provide a selective address and multiple access capability. These factors can all be achieved by modulating the data prior to transmission by a unique wideband spread spectrum code which is demodulated in the receiver with a time synchronised replica of the transmitted code. In many systems, where the code requires to be infinitely variable, both the encoding and decoding functions can be performed in a programmable matched filter. Table 5.1 summarises some of the more important potential applications for programmable AMF's. This classification defines the many distinct signal processing functions that can be performed with a variety of transmitted signals. It is noted that a PAMF, as opposed to a fixed coded AMF, often gives an added flexibility permitting a single transceiver to interrogate and communicate with any of the other system users.

This chapter reviews the many designs that have been adopted for the realisation of SAW PAMF's and develops a circuit analysis to

permit a computer aided performance simulation of several device designs. The simulations are reported in Chapter 6 where the trade-offs between circuit designs and fabrication techniques are compared and evaluated. This permits realistic predictions to be made as to the maximum chip rate and time bandwidth product that is likely to be obtained in the future with these devices. Chapter 6 also includes practical measurements on simple 7 and 8 tap manually programmable AMF designs operating at 100 MHz with a $2\frac{1}{2}$ MHz chip rate. These results, which are based on a switching circuit fabricated with discrete components on a printed circuit board, serve to illustrate the feasibility of device design. Later measurements on more sophisticated devices show the performance that can be achieved with 31 tap fully electronically programmable AMF's which perform signal processing on the same bandwidth (5 MHz) phase shift keyed signals as the fixed coded AMF designs described in Chapter 4. These latter devices employ a hybrid construction, with thin film resistor and beam level diode switches, which were fabricated entirely within the clean room facilities in the Department of Electrical Engineering, University of Edinburgh.

## 5.2 THE PROGRAMMABLE ANALOGUE MATCHED FILTER

### 5.2.1 DEVICE DESCRIPTION

The block diagram of a fully functional electronically programmable AMF is shown in Figure 5.1. This device is designed to generate or detect a N chip bi-phase coded IF signal where N equals the number of taps in the AMF. To achieve programmability in an AMF, which uses the conventional SAW tapped delay line structure, an electronic switch is connected between each tap and the sum bus. They can then be externally programmed to provide either

the direct or inverted polarity of interconnection.

Conventional microelectronic integrated circuits are particularly suitable for selection and storage of the programming codes. Figure 5.1 shows the code selection in a Read-only-Memory (ROM) or switch bank, prior to reading into the serial register associated with the device. When the code is correctly located in this register the individual data bits are parallel loaded into the transfer store which holds the required code in the switch drive circuitry. This permits fast reprogramming, within the propagation time of the transfer store, provided the next code has been previously located in the serial register.

The goal in SAW AMF development is to design programmable devices which possess minimal degradations in signal processing performance when compared with similar fixed coded AMF designs. This dictates that the switches must achieve high on-to-off and tap-to-tap isolation to prevent loss and leakage of signal. Adverse loading of the tapped delay line must also be avoided to reduce undesirable electro-acoustic reflections. In addition most applications require low additional switch insertion loss (eg, 3-5 dB) and minimal power consumption (eg, 1 mW per tap). This latter constraint is of vital importance if the SAW PAMF is to be competitive against other microelectronic techniques such as the Digital Matched Filter (DMF) and Charge Coupled Devices (CCD). Studies have shown[30] that the large dynamic range (30-50 dB typical) of the programmable AMF is attractive when compared to DMF's, which require analogue to digital (A/D) conversion with multi-level quantisation to achieve high dynamic range. (5 level for 30 dB). However, the fixed SAW

propagation velocity and hence fixed AMF chip rate constitutes a severe limitation when compared with the almost infinitely variable clock rates that are achievable with DMF's and CCD's.

### 5.2.2 REVIEW OF SAW PAMF DESIGNS

It will be appreciated that microelectronics permits many different SAW PAMF's designs, see Staples[7]. One popular approach, outlined in Figure 5.1, uses a conventional SAW Tapped Delay Line (TDL) structure combined with simple electronic polarity switches and code store as a hybrid assembly. MOS transistors, bipolar transistors and diodes are all possible devices for realisation of the switching function.

In addition, many different techniques are available for switch fabrication. Printed circuit construction can be employed with discrete component switches. Hybrid switch construction with thin film passive components and discrete semiconductor chips is attractive for small physical size. The more expensive monolithic process, with all the switch components integrated on a common substrate, is also applicable to fabrication of these devices.

The code storage and selection circuits can be fabricated in MOS, TTL, ECL or any suitable microelectronic logic family. They may be encapsulated in seperate packages for mounting on a PCB prior to interconnection with the switches. Beam lead, wire bond or flip chip assembly of individual semiconductor chips onto a thick or thin film interconnection substrate can also be used. However, if integrated circuit switch fabrication techniques are employed, then the code store and switches may be combined to form a custom designed

LSI circuit element. This approach also offers the possibility of designing a sophisticated, fully integrated, monolithic programmable AMF. Either the SAW propagation medium, eg, an Aluminium Nitride film, can be accommodated beside a silicon layer containing the switches and code store on a common sapphire substrate, or SAW propagation can be performed within a semiconductor film which incorporates active MOSFET detectors[79].

Reliability is a *primary* parameter which must be carefully considered when choosing a suitable approach for device design. It is attractive to maintain the graceful degradation characteristic exhibited by the fixed coded AMF. This can be accomplished by selecting a proven IC technology for code storage and selection circuits with individually packaged M.SI devices. This gives a reliable code store which can be optimised for speed, power consumption and the necessary interference voltages for any particular switch design.

A major problem in switch design is minimisation of the stray loading when interfacing low capacity taps with microelectronic switches. For example, three finger pair AMF taps,designed for use in the EA4 Quartz substrate AMF's, Table 4.1, possess typically 1/3 pF capacity. It is easily seen therefore that high capacity 1-2 pF MOS switches are unsuitable for these applications.

However, MOS technology has been used for tap switching in monolithic devices employing SAW propagation on the silicon substrate. These devices use three terminal active solid state detectors based on the piezoresistive effect which is present in silicon MOSFET inversion layers. The early work of Claiborne[79] and later studies

by Defranould[80] both realised simple PAMF's using wedge input transducers to generate bulk acoustic waves which are subsequently mode converted into surface acoustic waves. This overcomes the difficulty of generating surface waves in a non-piezoelectric substrate. SAW detection is performed with silicon MOSFET taps. O'Clock[81] and Hickernell[82] have also reported similar tapping techniques, but they utilise an input transducer constructed with planar techniques. Here a conventional IDT electrode structure is overlaid by a spluttered polycrystalline,piezoelectric, zinc oxide (ZnO) film.

The prime characteristics of both p and n channel MOSFET detectors have been reviewed by Staples[7] for several crystal orientations. He showed that detection efficiency (tap insertion loss) when feeding an unmatched 50 Ω load, is typically -50 dB to -70 dB with a 50 mA bias current. Insertion loss, which is a function of both acoustic and electronic properties, can with a passive matching network, be reduced to -35 dB for a single tap. Typical figures for a MOSFET tapped delay line are -45 dB when a transimpedance amplifier (used to eliminate shunting reactances) is combined with a Q = 10 passive matching network. These theoretical predictions agree well with practical results on a 15 tap four phase PAMF[82]. The measured -80 dB CW device insertion loss comprised a -15 dB overlay input transducer tuned conversion loss and -65 dB broadband tuned p-channel MOSFET conversion efficiency. This device exhibited a spurious free impulse response at the expense of a 10 mA drain current per MOSFET resulting in a total power consumption of ~3 watts for the 15 tap PAMF.

In addition to the integrated programmable AMF hardware demonstrated with piezoresistive MOSFET detectors, gallium arsenide

piezoelectric FET's which promise to provide lower insertion loss per tap than piezoresistive devices, have recently been reported[83] for the detection of surface acoustic waves. They have exhibited tuned conversion losses as low as -26 dB when the signal was extracted from the drain electrode. Another type of FET employing a piezoelectric ZnO gate oxide[84] allows seperate optimisation of free carrier transport and piezoelectric properties. However, neither of these devices has as yet been used to switch more than one tap.

In addition to active MOSFET detectors, high speed bipolar transistors have also been used to switch conventional metal electrode taps. The problems of equalising the gain and accurately controlling the phase shift over an array of 128 switches was overcome with careful layout of grounded base amplifiers[85]. Discrete transistor encapsulation is undesirable due to the high header capacitances ($\frac{1}{2}$-1 pF) and difficulties of interfacing switches with the close tap-to-tap spacing of the SAW device. (310 μm for 10 MHz chip rate on quartz substrate). A thick film hybrid construction was chosen[85] to interconnect the components for a 127 tap programmable AMF. Switches were fabricated with matched transistor pair semiconductor chips and thin film bias resistors. Code selection was performed in 8 bit TTL serial shift register chips. The large number of bonds required in the complete device (>1500) caused severe reliability problems necessitating fabrication of 32 tap sub-assemblies for testing prior to final assembly. Although representing a comprehensive electronic subsystem, this device did not possess the fully electronic, fast reprogramme, capability of the programmable AMF shown in Figure 5.1.

Another possible approach to PAMF fabrication is to use diode switches. PIN and Silicon-on-sapphire (SOS) diodes are both

available with reverse biased junction capacitances considerably smaller than the $\frac{1}{3}$ pF tap interelectrode capacity. Unencapsulated SOS devices have been reported with values as low as 1/50 pF[86]. The extensive application of PIN diodes as low impedance microwave switches makes them attractive for PAMF tap switching applications. Diode switches, which will be analysed in more detail later in this Chapter, have been adopted by Hagon[7] for the design of high performance programmable AMF's. He has selected the exceptionally low capacity SOS diode for tap switching in a monolithic programmable AMF. SAW propagation is performed in a single crystal, piezolectric, aluminium nitride film grown by chemical vapour deposition on a sapphire substrate, while the switches and code store are fabricated in an epitaxial silicon film mounted side by side with the SAW delay line on a common sapphire substrate.

Integrated or thin film hybrid construction is unavoidable if the pitch of the switching circuit is to equal the device tap-to-tap spacing and avoid layout fan out. Fan out at IF is undesirable as differential phase shift can easily be introduced along the AMF length preventing coherent summation of the tap outputs. It is also difficult to achieve good isolation to prevent breakthrough between input and output circuits. Fan out of the DC control potentials which code the switches can however be employed to simplify device design without severely degrading the performance. Although the integrated approach is more technically elegant and reliable, there are severe problems in obtaining a good processing yield with a semiconductor chip whose length equals that of the SAW tap structure (1.3" for 128 taps at 10 MHz chip rate on ST-X Quartz). It is often considered expedient initially to segment switching and code storage

circuits into blocks of 16 or 32 taps to obtain an easily fabricated PAMF which will offer the flexibility for both pre and post-assembly testing and repair.

### 5.2.3 SELECTION OF A PROGRAMMING SWITCH

When selecting suitable switches for practical evaluation of PAMF design, monolithic MOSFET devices were rejected due to the requirement for an expensive, advanced fabrication technology. Their low, relatively uncontrolled, tapping efficiency and high power consumption were also considered to be a severe disadvantage. Bipolar transistor switches were not favoured due to the difficulties of matching the gain and phase shift over a large switch array. It was considered that this could severely degrade the coherent signal summation but subsequent results with grounded base transistor amplifier stages[85] have shown that this is not a problem.

This led naturally to an investigation of diodes for PAMF tap switching. Several measurements were first performed to determine the small signal characteristics of a selection of diodes and this information was then used to assess the likely performance of a variety of different programmable AMF switch configurations.

## 5.3 TAP SWITCHING EMPLOYING DIODES

### 5.3.1 VHF SMALL SIGNAL DIODE CHARACTERISTICS

For low additional insertion loss over a hard wired device it is necessary to use a diode switch which possesses a low, ideally zero, forward biased impedance, for minimal series loss, and small reverse bias capacity. A high on-to-off switch impedance ratio

results in an efficient switch with good isolation properties. In addition low switch capacity prevents excessive signal loss due to shunt loading. The curves of Figure 5.2 show the forward and reverse biased characteristics of several selected diodes. Low capacity germanium point contact diode - Radio Spares 1 GP5; high speed silicon computer switching diode - Texas Instruments IN914; Silicon ultra low leakage - Siliconix PAD5; axial lead glass encapsulated PIN - Hewlett Packard 5082-3039; and beam lead encapsulated PIN - Alpha D 5840 devices are all shown.

The small signal forward biased characteristics were measured at 100 MHz with signal power varied between -10 dBm and -30 dBm for several bias currents. These were obtained by mounting the diode between the centre pin and ground of a Conhex subminiature chassis connector 51-043-0000. Diode forward impedance measurements were made by monitoring direct and reflected signal (S11) within a Hewlett Packard type 8745 S parameter test set on the Smith chart display (8414) of a Hewlett Packard 8410 A Network Analyser. Figure 5.2(a) shows the comparison between the low impedance silicon planar diodes and relatively high impedance of germanium point contact devices. The 5082-3039 PIN is designed for low forward impedance whereas the D5840 PIN fabrication is optimised to provide a low reverse capacity and hence its smaller junction area results in a higher forward biased impedance. The 5082-3039 and PAD 5 both achieve lower than 50 Ω switch impedance at approximately ½ mA bias current. The IN914 and D5840 require three to four times this bias current to achieve the same impedance. In all these measurements the impedance was predominantly resistive and independent of signal level when a drive of <-20 dBm was employed. The results of

Stewart[87] show that most diodes possessed arguments of $<10^{o}$ at 50 Ω impedance. Practical measurements were not available for SOS diodes but the researches of Hagon[8] indicate that 10Ω impedance is typical with 0.1 mA bias current.

Reverse bias characteristics were measured on the same equipment by connecting the diode under test between the two arms of the S parameter test set to determine the transmission coefficient (S12). Impedance was measured as an attenuation on the gain and phase magnitude display. Figure 5.3 shows an electrical equivalent circuit. The display measured directly the ratio of Vout to Vin :

$$\text{Attenuation} = 20 \text{ Log}_{10}(\frac{\text{Vout}}{\text{Vin}}) \text{ dB} \qquad 5.1$$

Simple analysis shows that the device impedance ZD is given by :

$$ZD = ZL(\frac{\text{Vin}}{\text{Vout}} - 1) \qquad 5.2$$

where ZL = 50 Ω.

Figure 5.2(b) shows the diode characteristics under reverse bias conditions. The $90^{o}$ shift in displayed phase when compared with a standard resistive attenuator pad indicated that these impedances were capacitance. These curves agree well with the manufacturers' data sheets, which show silicon planar diodes with $\frac{3}{4}$ - 1 pF capacity. The germanium point contact diodes exhibit lowest capacity but the PIN devices both gave 1/3 pF showing a notable improvement over bulk silicon devices. The 5082-3039 PIN diodes are specified at 1/3 pF and D5840 as 1/20 pF. The similarity in practical measurement must result from the stray capacity introduced

by the bonding of the beam lead device onto a gold interconnection pattern and glass substrate prior to interconnection with wire bonds into the test jig. These curves are almost independent of bias voltage indicating that PAMF operation with only one Vbe of reverse bias will not degrade switch performance. Several measurements were also made of these devices at 100 MHz on a Hewlett Packard 250B RX meter, which does not incorporate a DC bias facility. This latter test verified the validity of the Network Analyser results.

When selecting diodes for programmable AMF assembly, component cost is of fundamental importance. The low price (<1p each) of the IN914 makes them ideal for discrete component applications where large numbers of diodes, eg, 16, are required in each switch. Other lower component count switches can be evaluated with glass encapsulated PINs but the high component cost, £3 each, prohibits construction of more than 8 tap arrays. The Alpha D5840, which is the cheapest member of a family of PIN diodes, is the *only* beam lead device which is readily available for hybrid device manufacture. Although its switch characteristics are not optimal when considering the bias current required to achieve a low impedance, it is the only component whose overall size permits switch design to be achieved in a physical area compatible with device tap-to-tap spacing.

### 5.3.2 PAMF TAP SWITCHING CIRCUITS

Diodes, which offer the possibility of high fidelity switch fabrication, have been reported in several designs of programmable AMF switches. The author favours the design of Double Pole Double Throw (DPDT) switches which can simply achieve the direct or inverted polarity interconnection of a tap onto the output sum and ground buses.

Figure 5.4(a) shows one design of such a switching circuit[60]. Four rings, each with four diodes, were employed with bias applied through series resistors. The diodes in each ring are connected to ensure that two rings are always forward biased and two reversed biased. With the supply polarity as shown in Figure 5.4(a), rings 1 and 3 are forward biased to provide low impedance switches which connect the transducer across the ground and sum buses while rings 2 and 4 are reverse biased to act as high impedance off switches. Interchanging the positive and negative supply connections forward biases the other rings to provide the opposite polarity of interconnection between tap and output buses.

Figure 5.4(b) shows an alternative circuit adopted by Hunsinger[88] to demonstrate coded signal generation in a simple AMF. This circuit employs a single diode in place of each of 4 diode rings used in (a). Bias is applied through six resistors, and capacitors are employed to isolate the individual switching elements. Recent studies have shown that if a radio frequency choke (RFC) can be accommodated across the output terminals of the device, then the circuit can be simplified to that shown in Figure 5.4(c). Figure 5.4(d) shows a further modification using a control input biased about ground, which enables the switches to be programmed from logic registers which possess only Q outputs. (Few MSI logic elements have both Q and $\overline{Q}$ outputs available.)

The proliferation of circuit ideas based on the DPDT switch merits careful performance evaluation for PAMF design. The following section therefore develops a theoretical analysis for the electrical performance of devices based on the DPDT switch.

## 5.4 THEORETICAL ANALYSIS OF PROGRAMMABLE AMF OPERATION

The computer aided analysis of programmable AMF performance is based on the scattering parameters for an interdigital transducer derived in Appendix A. The analysis applies these parameters to a single tap of an N tap PAMF, where N can be varied at will, to calculate the device electrical insertion loss in expansion and compression and also the electro-acoustic reflection signals from each tap. In addition, the effect of summing these reflections across an encoded tap array is investigated to assess the magnitude of electrical spurious signals. The development of this analysis into a computer programme permits a wide variety of different switching circuit configurations and active switch components to be quickly assessed. In addition, any SAW AMF design parameters can be accommodated to indicate the expected device performance for any desired number of taps. This permits a multitude of PAMF designs to be theoretically assessed for accurate performance trade-off. The results can also be compared both theoretically and practically with the existing fixed coded device designs reported in Chapter 4. The circuit analysis is based on the 4 ring DPDT switch of Figure 5.4(a), which was the only available circuit offering the possibility of fabrication as an integrated device, when the project was commenced. However, the analysis has subsequently been modified to accommodate the design of the DPDT switch shown in Figure 5.4(d).

Two separate effects have been shown to contribute to the insertion loss of the programmable AMF. The first is a loss in the series resistance of the forward biased switch associated with a tap, and the second a shunting of the output by all the switching

diodes and bias resistors. Staples[7] has analysed these effects in terms of the impedance ratio $\rho$. He defined tap degradation as :

$$20 \log[\, 1 + \rho] \ \text{dB} \qquad 5.3$$

where for series loss

$$\rho = \frac{R_s}{|Z_T|} \qquad 5.4$$

and shunt loss

$$\rho = \frac{R_L}{|Z_s|} \qquad 5.5$$

when $R_s$ = series resistance

$Z_T$ = transducer impedance

$R_L$ = load resistance (usually 50 Ω)

$Z_s$ = shunt impedance

For 100 MHz AMF's fabricated on quartz substrates, typical tap capacitances of $\frac{1}{3}$ pF result in $Z_T$ of approximately 5 KΩ. The diodes analysed in Figure 5.2 all give $R_s << |Z_T|$ resulting in low series loss. The shunt loss is considerable and this predominates in most designs of devices with large numbers of taps. However, these first order approximations are not sufficiently accurate to evaluate the optimum design of PAMF switch. Although the simple analysis has been shown to agree with practical results obtained on a 32 tap programmable AMF fabricated on a Lithium Niobate substrate[7] it is necessary in the ensuing studies of PAMF design to establish what limits of maximum number of taps that can be accommodated within a

programmable device. Hence, it is necessary to project performance up to 1000 tap devices, where the large output shunt capacity drastically reduces the effective load impedance, ie, $|Z_s| \ll R_L$. This makes separate analysis of series and shunt losses invalid as both are dependant on the effective shunt capacity.

In a PAMF, the insertion loss to one tap in expansion (generation of coded sequence) can be conveniently calculated in two parts. Firstly network analysis is required to determine the total equivalent electrical load at a single AMF tap arising from all the other taps, switching circuits and external load. This permits direct application of the scattering parameters defined in Appendix A to one of the AMF taps, to calculate the acoustic to electrical conversion loss $\rho_{31}$. Secondly a further analysis is required to determine the proportion of the electrical power which is delivered into the external load as useful output power.

Summation of these two conversion losses with the loss in the closely coupled input transducer will then give the insertion loss in expansion, of the complete device. Calculation of the compression gain which results when a correctly coded PSK sequence is fed into the device, also permits the insertion loss to the correlation peak (compression) to be determined. With an expression available for equivalent electrical load at each tap, it is a relatively simple matter to apply the scattering parameters again to yield the electro-acoustic reflected signal from each tap to give the level of electro-acoustic regenerated signals.

In the four ring circuit shown in Figure 5.4(a) it is first necessary to determine the equivalent series and shunt impedance of

both the forward and reverse biased switches. Consider the general case of Figure 5.5 where by symmetry it can be assumed that each diode possesses the same impedance, ZD, and the bias resistors an impedance, ZR. If the bias resistors are driven from a low impedance source then the DC control inputs ($\pm V$) can be considered as ground potential for AC analysis. Simple star-delta impedance transformation on the upper and lower three components gives an equivalent circuit for the complete ring as shown in Figure 5.6

where

$$ZA = ZD + \frac{(ZD)^2}{2 \cdot ZR} \qquad 5.6$$

$$ZB = ZR + \frac{ZD}{2} \qquad 5.7$$

For the forward biased ring where ZR >> ZD

$$ZA \triangleq ZD \qquad 5.8$$

$$ZB \triangleq ZR \qquad 5.9$$

hence the switch series impedance equals the forward biased impedance of a single diode. The equivalent impedances of the reverse biased ring are more complicated as $|ZD|$ is often of the same magnitude as $|ZR|$.

Figure 5.7 now represents the equivalent circuit of a single tap and its associated switching circuit in which the component numbers 1 through 4 correspond to the four rings of Figure 5.4(a). The tap is shown as a generator of admittance $\hat{G}a$ and susceptance Ba with two capacitors of impedance ZB = -jXc representing the parasitic shunt

loading of the bonding leads. This circuit may be represented in the simplified form of Figure 5.8 when

$$Z1 = ZA1 \qquad 5.10$$

$$Z2 = \frac{\frac{ZA2.ZB1}{ZA2+ZB1} \cdot \frac{ZB2.ZB}{ZB2+ZB}}{\frac{ZA2.ZB1}{ZA2+ZB1} + \frac{ZB2.ZB}{ZB2+ZB}} \qquad 5.11$$

$$Z3 = ZA3 \qquad 5.12$$

$$Z4 = \frac{\frac{ZA4.ZB4}{ZA4+ZB4} \cdot \frac{ZB3.ZB}{ZB3+ZB}}{\frac{ZA4.ZB4}{ZA4+ZB4} + \frac{ZB3.ZB}{ZB3+ZB}} \qquad 5.13$$

$$Z_T = \frac{1}{\hat{G}_a + jB_a} \qquad 5.14$$

$$Z25 = \frac{ZB1.ZB3}{ZB1+ZB3} \qquad 5.15$$

Network analysis again gives a single impedance Z15 equivalent to all the impedances of Figure 5.8 which represents the electrical load present on the sum bus due to a single tap and its associated switching circuit

where $$Z15 = \frac{Z12.Z25}{Z12+Z25} \qquad 5.16$$

and

$$Z12 = \frac{\left[\frac{Z1.ZT}{Z1+Z3+ZT} + Z2\right].\left[\frac{Z3.ZT}{Z1+Z3+ZT} + Z4\right]}{\left[\frac{Z1.ZT}{Z1+Z3+ZT} + Z2\right]+\left[\frac{Z3.ZT}{Z1+Z3+ZT} + Z4\right]} + \frac{Z1.Z3}{Z1+Z3+ZT} \qquad 5.17$$

Therefore, when considering one tap of an N tap AMF, the total electrical load on the sum bus comprises :

external load resistor RL

combined impedance of N-1 taps and switching circuits components and stray capacity $C_s$, associated with the thin film fabrication of the N switching circuits,

which is shown diagrammatically in Figure 5.9.

The equivalent impedance Z45 is given by

$$Z45 = \frac{\frac{Z15}{N-1} \cdot Z1}{\frac{Z15}{N-1} + Z1} \qquad 5.18$$

where

$$Z1 = \frac{1}{\frac{1}{RL} + jB_s} \qquad 5.19$$

and

$$B_s = 2\pi f C_s \qquad 5.20$$

Figure 5.10 now shows the single tap under analysis complete with its switching circuit and the two output buses with all other associated circuitry represented by the equivalent impedance Z45. The impedances Z1, Z2, Z3, Z4 and Z25 are identical to those calculated in equations 5.10, 5.11, 5.12, 5.13 and 5.15. An

analysis, similar to that described in equation 5.17, can now be performed with Z2 and Z3 interchanged and $\frac{Z45 \cdot Z25}{Z45 + Z25}$ substituted for ZT to yield a single equivalent electrical load Z12 on each tap of the AMF. Following conversion of Z12 to an admittance, $G_{12}$, and susceptance, $B_{12}$, it is possible to directly apply the scattering parameters calculated in Appendix A, to give the acoustic to electrical tap conversion loss ($\rho_{31}$) and electro-acoustic reflection signal from each tap ($\rho_{11}$).

$$\rho_{31} = 10 \text{ Log}_{10} \left[ \frac{2b}{(1+b)^2 + a^2} \right] \text{ dB} \qquad 5.21$$

$$\rho_{11} = 10 \text{ Log}_{10} \left[ \frac{1}{(1+b)^2 + a^2} \right] \text{ dB} \qquad 5.22$$

where
$$a = \frac{(B_{12} + B_a)}{\hat{G}_a} \qquad 5.23$$

and
$$b = \frac{G_{12}}{\hat{G}_a} \qquad 5.24$$

To obtain the programmable AMF insertion loss it is next necessary to determine the series and shunt losses arising during the transfer of electrical energy from the tap through the programming switches to the external load (RL). Series losses are conveniently calculated by using an analysis which replaces the load impedance Z12 by the composite electrical load on the sum bus Z45 in series with an equivalent switch impedance ZSW as shown in Figure 5.11.

If $$Z12 = R12 - jX12 \quad (5.25)$$

$$ZSW = RSW - jXSW \quad (5.26)$$

$$Z45 = R45 - jX45 \quad (5.27)$$

and the tap is considered as a generator of current I.

The voltage across the sum bus is given by

$$V_{BUS} = I \cdot Z45 \quad (5.28)$$

$$\text{Total tap output power} = |I|^2 \cdot R12 \quad (5.29)$$

$$\text{power delivered into sum bus} = |I|^2 \cdot R45 \quad (5.30)$$

Therefore, the series loss is given by :

$$\frac{\text{power into bus}}{\text{tap output power}} = \frac{R45}{R12} = \frac{R45}{R45 + RSW} \quad (5.31)$$

However, as shown earlier in Figure 5.9, Z45 is a combination of the external load resistor RL shunted by fabrication capacitance, $C_s$, and the impedance of all other taps and switching circuit elements, $\frac{Z15}{N-1}$. If the impedance of the other taps and switches is represented by a parallel combination of a resistor RXO and capacitor CXO

where $$RXO = \text{Real } \frac{N-1}{Z15} \quad (5.32)$$

& $$CXO = \frac{\text{Imaginary } \frac{N-1}{Z45}}{2\pi f} \quad (5.33)$$

and the voltage on the sum bus is given in equation 5.28 then the 'usable' output power

$$= |V_{BUS}|^2 \cdot \frac{1}{RL} \qquad 5.34$$

and power into bus $$= |V_{BUS}|^2 \cdot \frac{RXO + RLO}{RXO \cdot RLO} \qquad 5.35$$

Shunt losses can therefore be summarised as :

$$\frac{\text{usable output power}}{\text{power into bus}} = \frac{RXO}{(RXO + RLO)} \qquad 5.36$$

series and shunt electrical losses can now be summed by multiplying equations 5.31 and 5.36 to give

$$\frac{\text{usable output power}}{\text{tap output power}} = \frac{R45}{R12} \cdot \frac{RXO}{(RXO + RLO)} \qquad 5.37$$

Hence tap to load electrical conversion loss is given by

$$10 \text{ Log}_{10} \left[\frac{R45 \cdot RXO}{R12(RXO + RLO)}\right] \text{ dB} \qquad 5.38$$

When allowance is made for the conversion loss of the narrowband, closely coupled, input transducer the summation of this with equations 5.21 and 5.38 yields the Programmable AMF impulse insertion loss when generating a coded sequence.

For an N tap AMF

. Compression Gain $= 20 \text{ Log}_{10} [N] \text{ dB} \qquad 5.39$

can now be added to give the insertion loss to the correlation peak.

Appendix B includes a flow chart of these calculations and a printout of Programme 1, developed directly from this theory to analyse the projected performance of a programmable AMF employing the 4 ring switching circuit of Figure 5.4(a). For a given set of input data it computes insertion loss to the correlation peak, insertion loss to 1 tap and electro-acoustic reflection from each tap for a 1, 7, 15, 31, 63, 127, 255, 511 and 1023 tap AMF. The second computer printout gives the resulting performance data for both mask precoded, fixed coded and several programmable AMF's. This specific data shown was computed for the EA4 100 MHz centre frequency AMF design which utilises a 20 finger pair input IDT of 50 $\lambda$ aperture with 3 finger pair 80 $\lambda$ aperture taps. Tap to tap spacing is 620 $\mu$m permitting processing of 5 MHz rate PSK sequences, for details see Table 4.1. The output data shown, was used to derive the curves of Figures 4.3, 6.3 and 6.5.

Also included in Appendix B is Programme 2, which was developed from Programme 1, specifically for the switching circuit of Figure 5.4(d). This was used to give the output data for the performance of thin film resistor, beam lead diode hybrid PAMF's based on the lower component count switching circuit. Both programmes make extensive use of complex algebra to transform and manipulate the transducer and switch impedances and admittances.

Following this detailed examination of SAW PAMF switch operation it is now relevant to report the practical results which were obtained from several different prototype device designs. The experimental data will then be critically compared with the computer aided analysis included in Appendix B.

| TRANSMITTED SIGNAL | PROCESSING FUNCTION | SYSTEM APPLICATION |
|---|---|---|
| CONTINUOUS LONG PN SEQUENCE | SYNCHRONISATION ACQUISITION | DIRECT SEQUENCE SPREAD SPECTRUM[47] |
| RANDOMLY SELECTED APERIODIC CODED SUBSEQUENCES | TIMING INFORMATION | SATELLITE RANGING[53]<br>ACTIVE NAVIGATION[78] |
| PREVIOUSLY SELECTED APERIODIC CODED SUBSEQUENCES | ADDRESS IDENTIFICATION | RANDOM ACCESS[65]<br>DISCRETE ADDRESS |
| | TIMING INFORMATION | SONAR BUOY SURVEILLANCE<br>VEHICLE LOCATION<br>ATC COLLISION AVOIDANCE[52] |

TABLE 5.1 POTENTIAL PROGRAMMABLE AMF APPLICATIONS

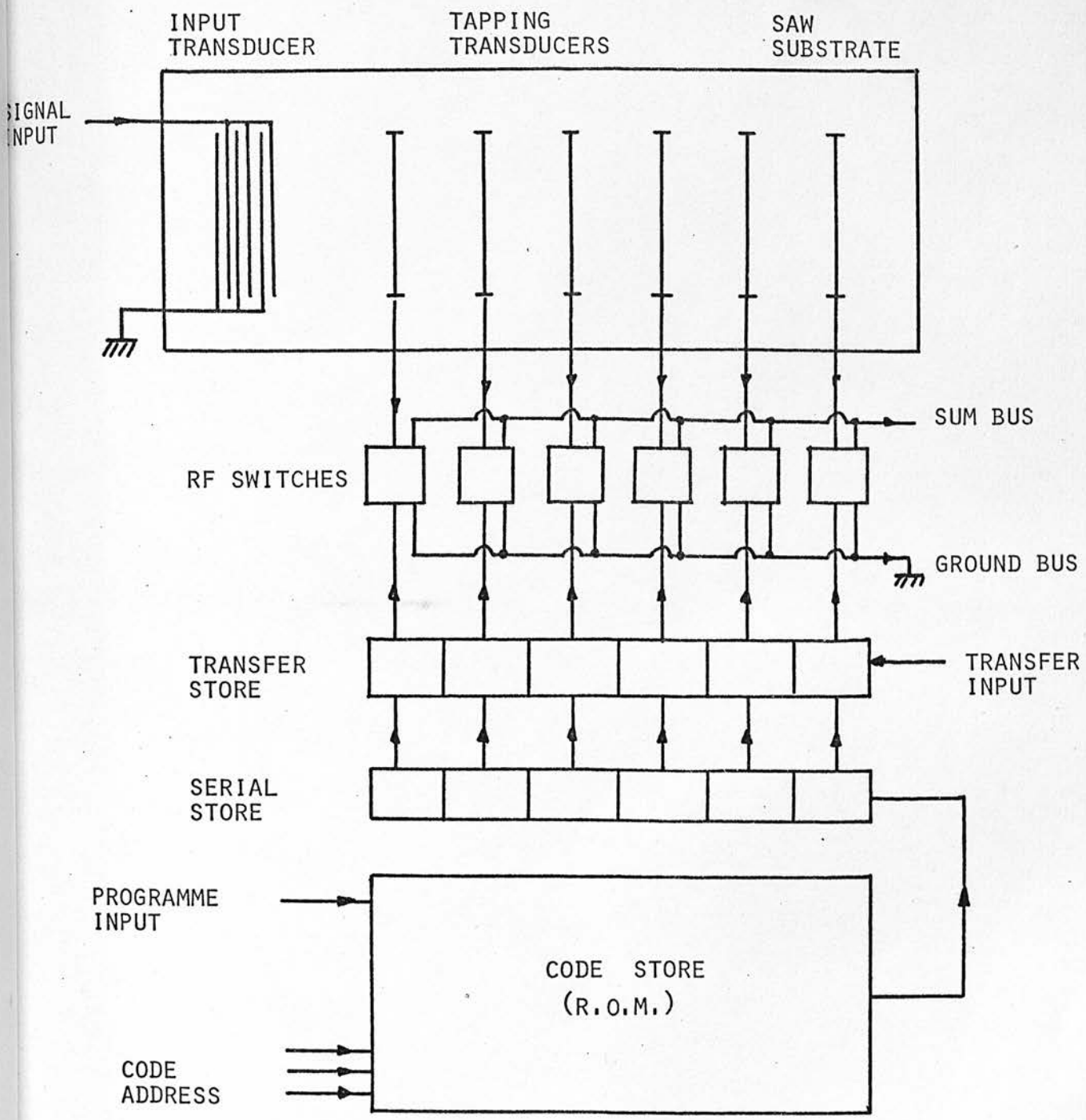


FULLY ELECTRONICALLY PROGRAMMABLE A.M.F.

FIGURE 5.1

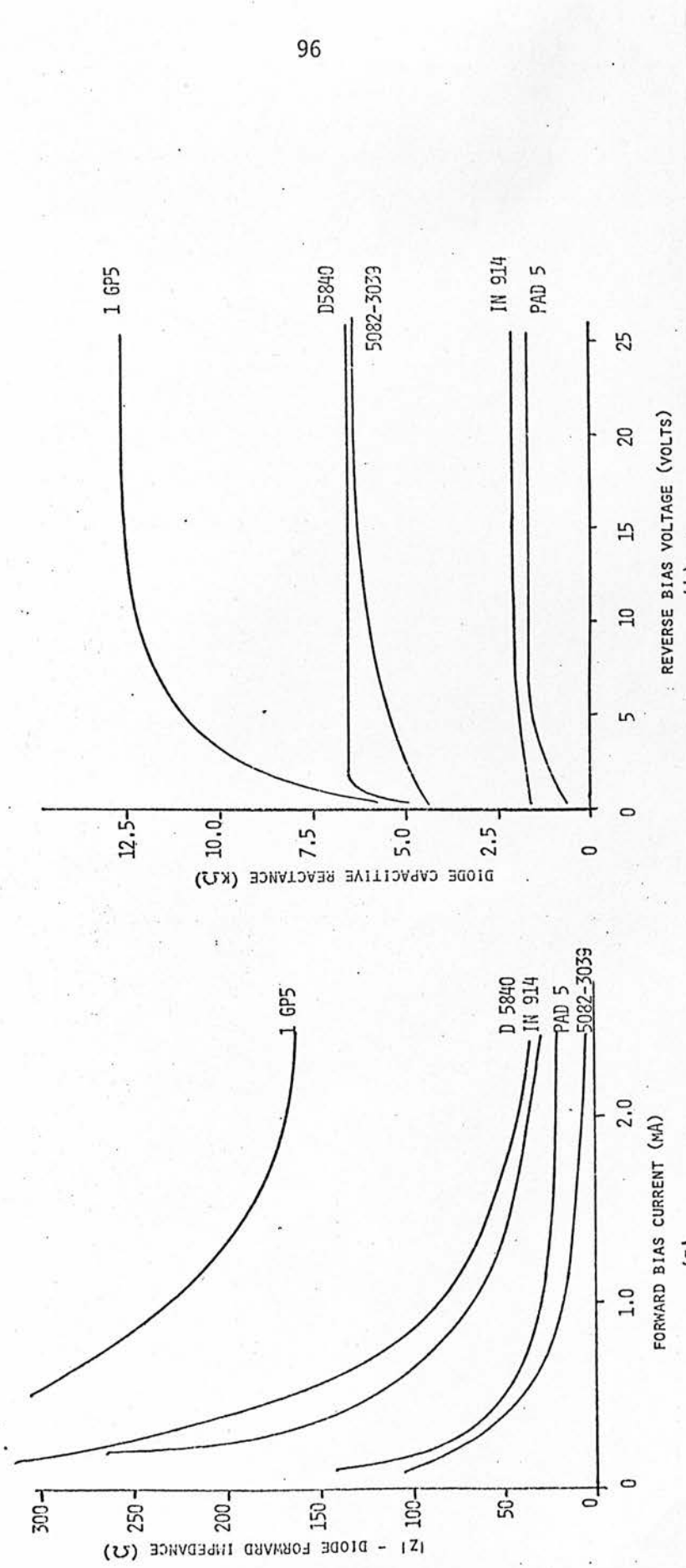


FIGURE 5.2 FORWARD AND REVERSE BIAS DIODE CHARACTERISTICS

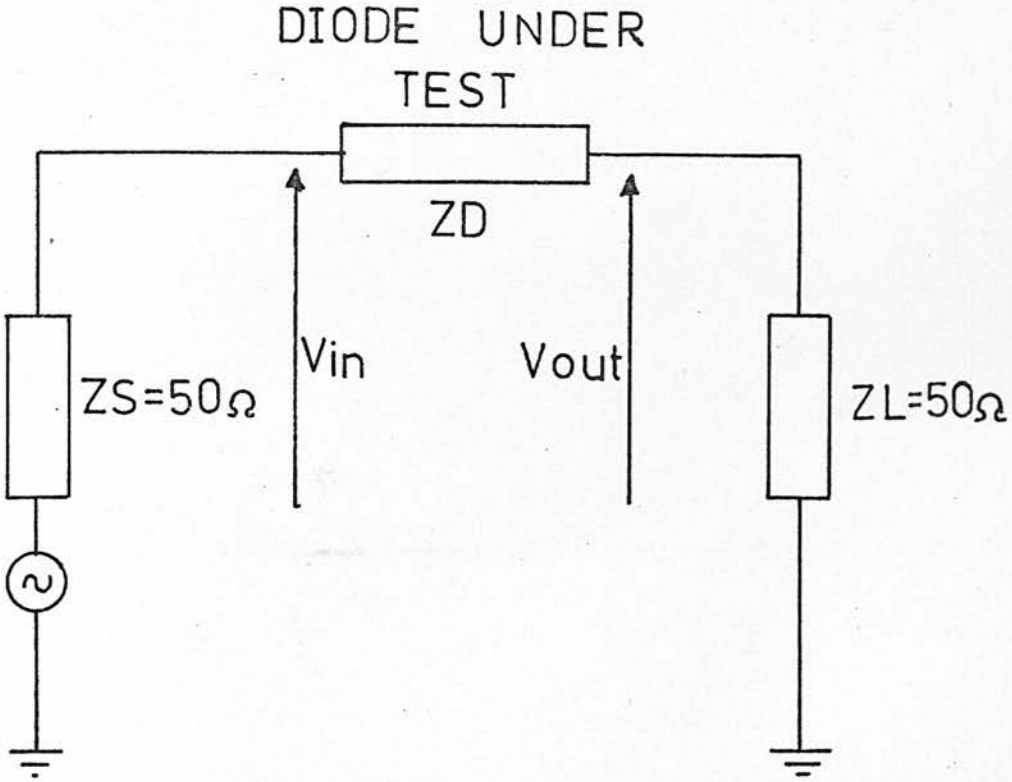


FIGURE 5.3 MEASUREMENT OF DIODE CHARACTERISTIC

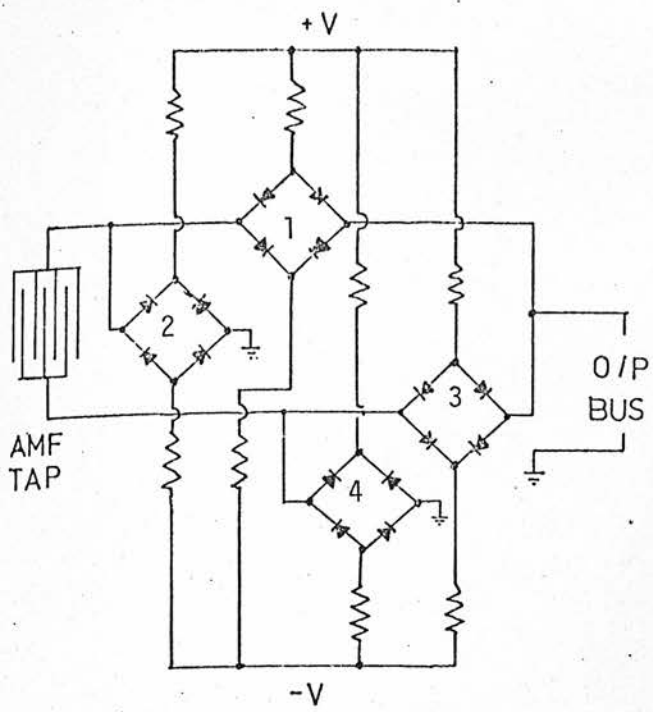


(a)

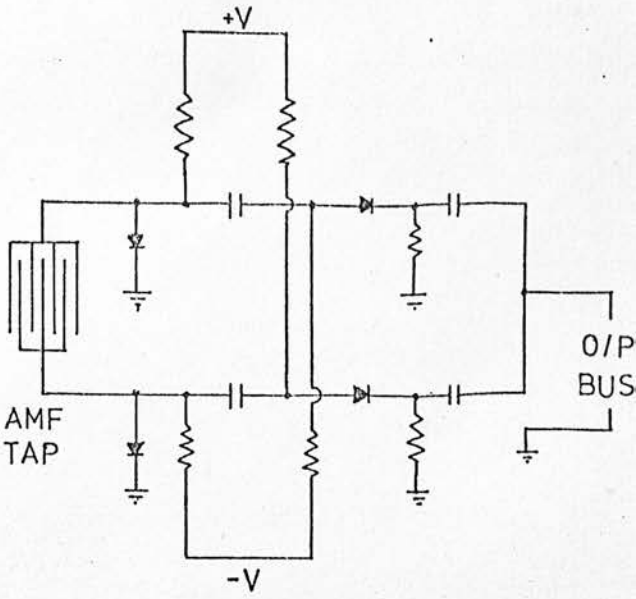


(b)

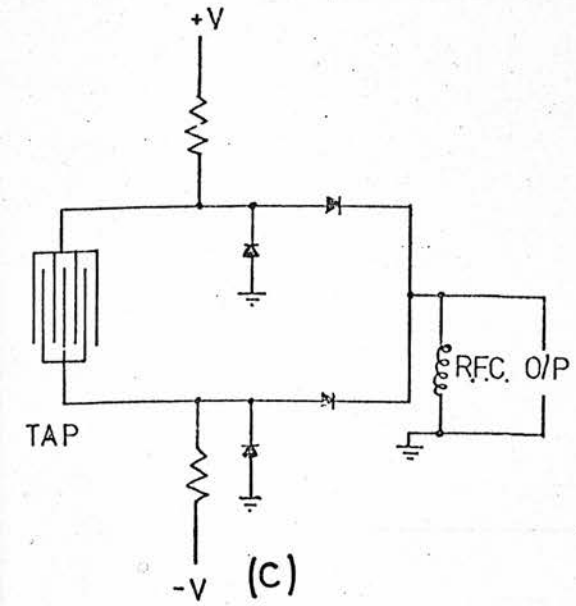


(c)

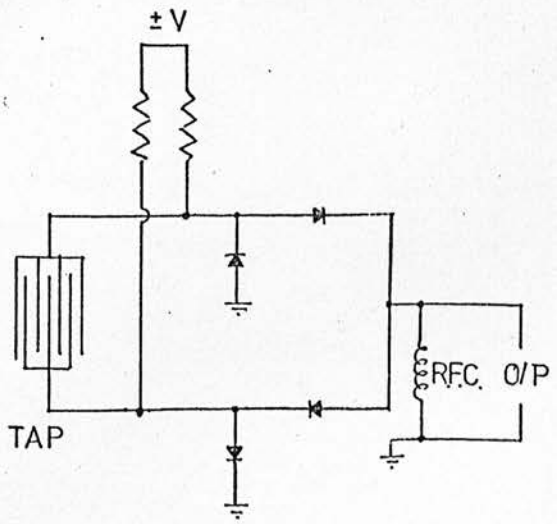


(d)

FIGURE 5.4 DOUBLE POLE DOUBLE THROW TAP SWITCHING CIRCUITS FOR SAW PAMF'S

(a) FOUR RING CIRCUIT

(b) HUNSINGER-FRANCK CIRCUIT

(c) SIMPLIFICATION OF (b) FOR INTEGRATED SWITCH CONSTRUCTION

(d) FURTHER MODIFICATION FOR SINGLE CONTROL INPUT

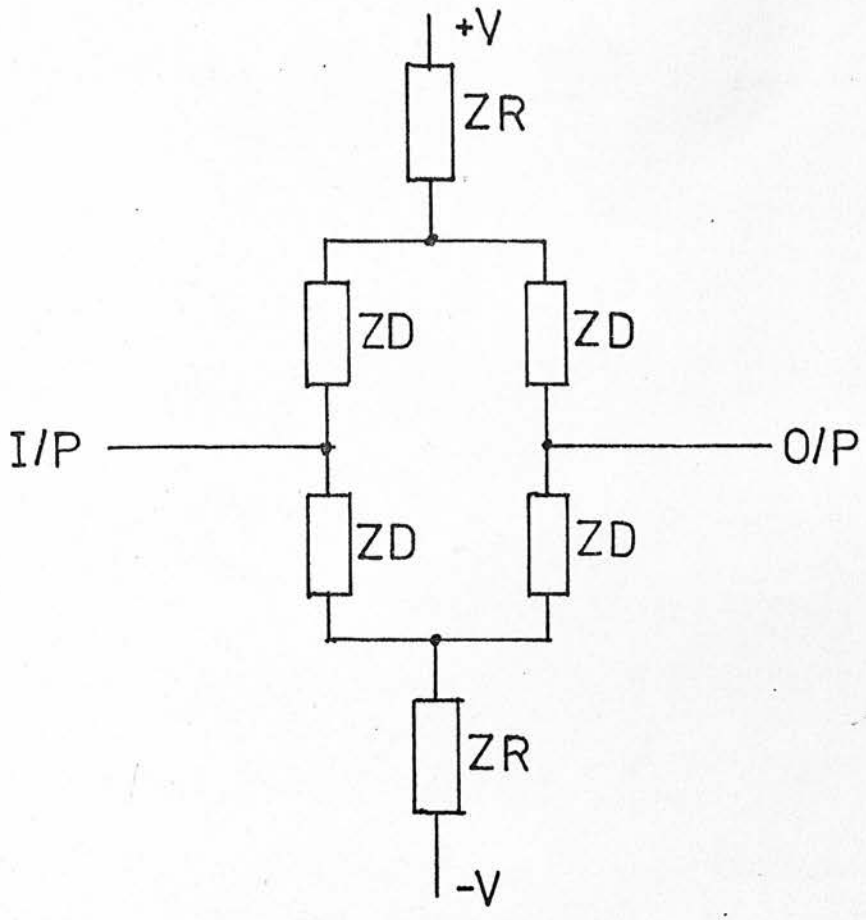


FIGURE 5.5 SINGLE RING CIRCUIT

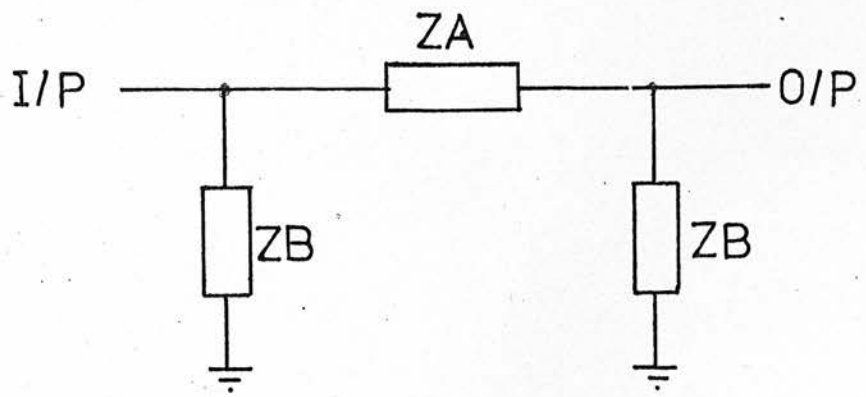


FIGURE 5.6 EQUIVALENT CIRCUIT OF A SINGLE RING

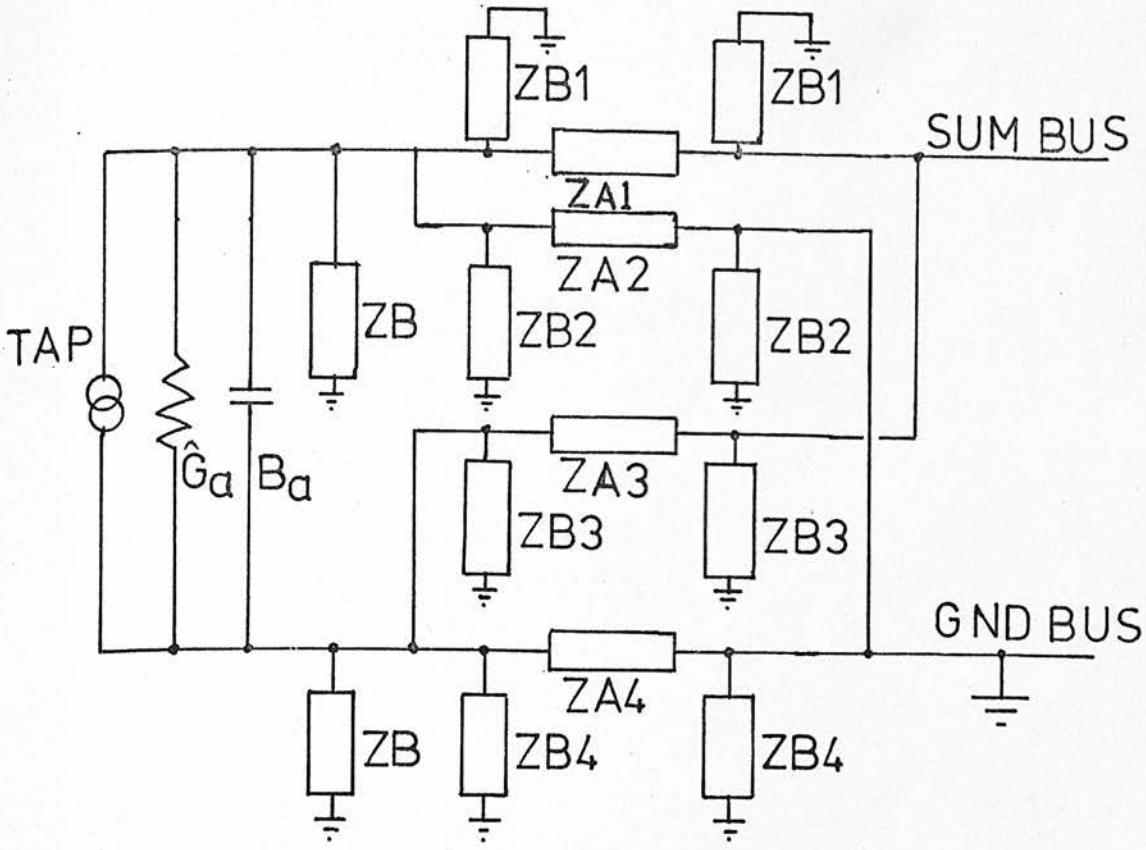


FIGURE 5.7 TAP AND ASSOCIATED SWITCHING CIRCUIT

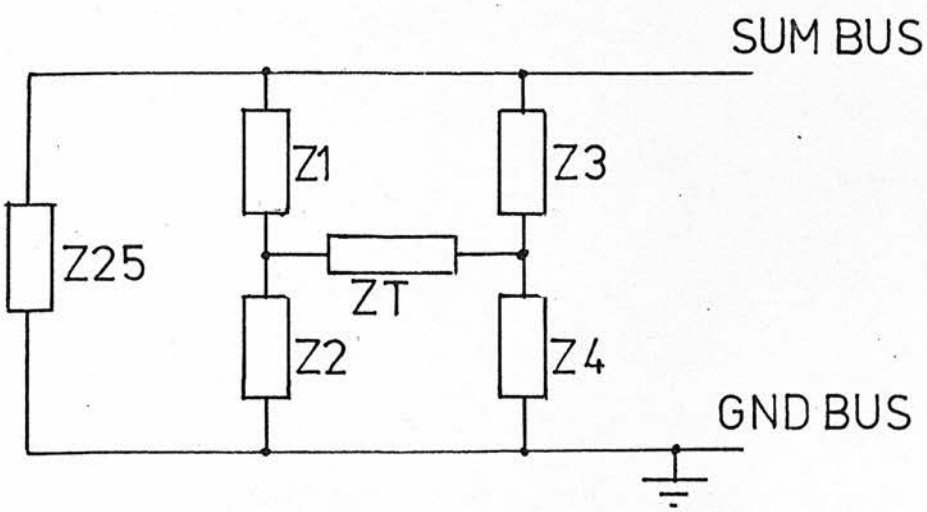


FIGURE 5.8 SIMPLIFIED EQUIVALENT CIRCUIT OF A TAP AND ITS ASSOCIATED SWITCH

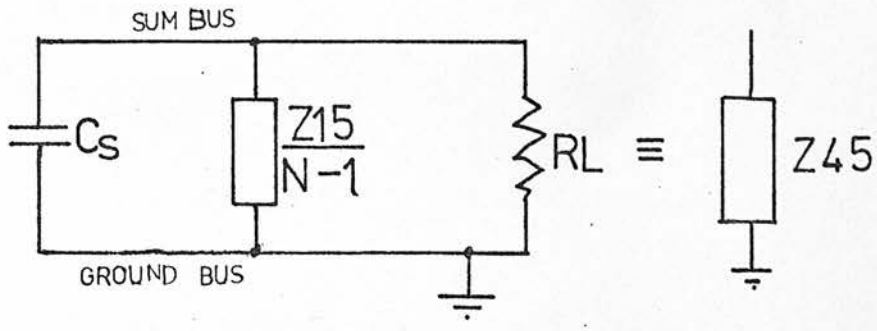


FIGURE 5.9 TOTAL LOAD ON SUM BUS

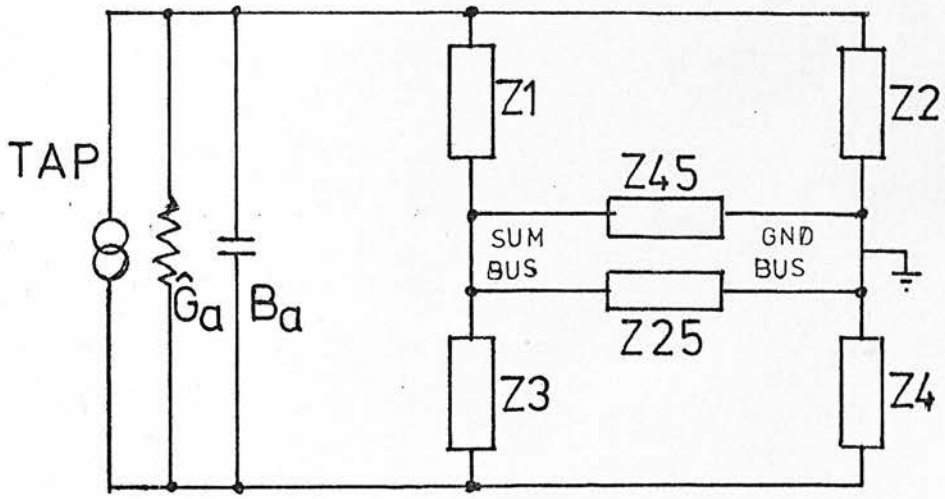


FIGURE 5.10 TOTAL LOAD ON A SINGLE TAP

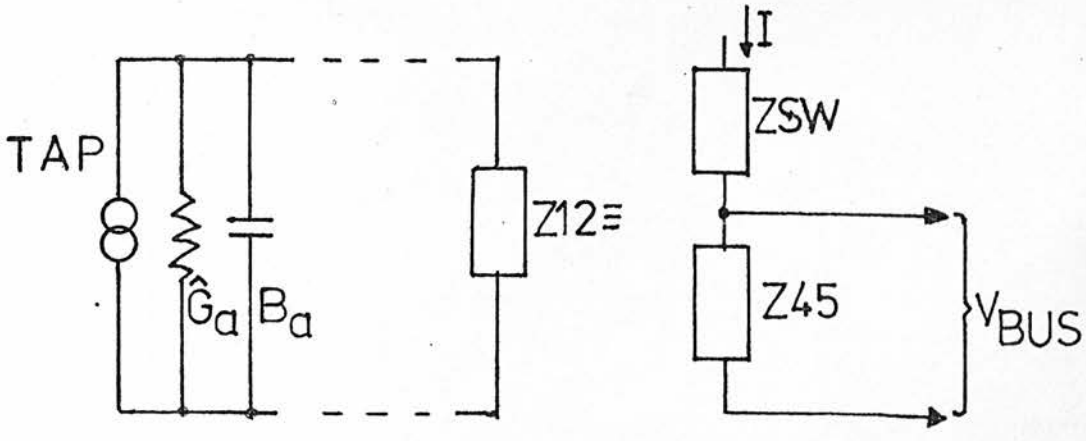


FIGURE 5.11 SERIES SWITCH EQUIVALENCE

# 6. CONSTRUCTION AND PERFORMANCE OF SAW PROGRAMMABLE ANALOGUE MATCHED FILTERS

## 6.1 TAP POLARITY SWITCHING

In parallel with the theoretical analysis presented in Chapter 5, simple practical experiments were performed to investigate the operation of a discrete component switching circuit.

Preliminary investigations were made by bonding out one tap from a 100 MHz SAW AMF for interfacing with a double pole throw (DPDT) switch. This was constructed on a printed circuit board using the circuit of Figure 5.4(b). *Hewlett Packard 5082-3039 PIN diodes, whose performance was detailed in Figure 5.2, were employed. Experimental evaluation indicated that there was no measurable increase in insertion loss over the signal obtained directly from the tap and, in addition, detection of the output showed that $180^{o}$ phase reversals were obtained on interchanging the programming input. Measurements performed on the alternative circuit of Figure 5.4(a), with the cheaper IN914 diodes , gave similar performance with $\sim \frac{1}{2}$ dB additional insertion loss.

These results indicated that serious consideration should be given to the construction of simple seven or eight tap programmable AMF's with discrete component switching. Before detailing the construction and evaluation of these devices it is necessary to review the basic measurement procedures which have been adopted to evaluate the signal processing performance of SAW AMF's.

## 6.2 AMF MEASUREMENT PROCEDURES

A full frequency and time domain measurement and characterisation

procedure for SAW AMF's has been previously reported[30] and it is not necessary to repeat the procedures in detail. However, it is relevant to introduce the test equipment and terminology, and provide a brief resumé of the measurement methods which have been adopted.

Frequency Domain Measurement

The SAW AMF's were designed with input and output interfaces of 50 Ω impedance for compatability with RF Laboratory test equipment. Input IDT matching was monitored with a swept frequency measurement using the Hewlett Packard 8414 Polar display of the HP 8410 network analyser with Smith Chart overlay, as described in Chapter 5. Measurement of the VSWR indicates how closely the IDT is matched and in addition, the transducer radiation resistance, $R_a$, can be obtained directly from the measurements. The 3 dB bandwidth of the input IDT could also be measured easily with the HP 8412 Phase Magnitude Display to ensure that the AMF possessed the desired frequency response.

Time Domain Measurement - Impulse and Pulse Response

The time domain impulse response of the AMF was obtained by exciting the device with a baseband pulse, of width less than or equal to one half cycle at the AMF centre frequency. This generated two acoustic waves. Each comprised an $E_I$ cycle acoustic pulse at the AMF centre frequency, $f_o$, where $E_I$ is the number of periods (finger pairs) in the input IDT. One of these waves propagated along the crystal surface below the tap array. Figure 6.1(b) represents diagramatically the test equipment employed to measure the impulse response of a SAW AMF. The fast rise time HP 8004 pulse generator provided the 5 nsec 5 volt pulses which were required to impulse a $f_o$ = 100 MHz AMF. However, it is often necessary with slower response generator (eg, HP 8003) to use a seperate circuit,

employing avalanche transistor breakdown, to provide the short, 5 nsec, impulse. Avalanche impulse generators are also advantageous as they give 15 volts amplitude improving the SNR of the displayed response. A HP 8447A wideband amplifier with flat gain and phase characteristic was used to amplify the signal prior to displaying the impulse response on a Tektronix 7904-7A19 VHF oscilloscope.

Measurement of the AMF insertion loss to one tap is more conveniently performed using the pulse testing equipment outlined in Figure 6.1(a). Here the pulse generator was used to gate out a pulse of RF carrier from a seperate HP 3200B VHF signal generator which was set at the AMF centre frequency. Pulses containing $E_I$ cycles or less of RF energy may be used without distorting the output waveform. The RF pulse, typically +7 dBm, was split into two equal power signals to provide a controllable reference signal for comparison of individual tap amplitudes. Device insertion loss was measured by substituting a 50 Ω variable attenuator, HP 355D, in place of the AMF and adjusting for equal amplitude in test and reference channels. Electromagnetic breakthrough and spurious reflection levels can also be measured with this technique.

During pulse and impulse tests the generator pulse repetition period must exceed the propagation delay under the tapping electrode otherwise a multiple response will be displayed on the oscilloscope. In an AMF which is coded with a PN sequence the code imbalance between 0 and $\pi$ phase taps is always 1, hence the insertion loss can be measured with a cw test. This averages out any tap-to-tap amplitude variations, but it introduces breakthrough and spurious signal components into the insertion loss measurement.

Time Domain Measurement - Response to the Matched Waveform

The SAW AMF correlation performance can also be measured using several different test signals. Figure 6.2(a) represents the *active* generation of a burst of encoded waveform. This was accomplished by gating out the required time delay of cw signal, at the AMF centre frequency, $f_o$, prior to phase modulation , in a Mini Circuits Laboratory (MCL) ZADI double balanced mixer, with the required PN code. The code was conveniently obtained from a HP 1930 Pseudo Random Bit Sequence (PRBS) generator which can be programmed for any desired code length or sequence. By comparison Figure 6.2(b) shows the *passive* generation of the test signal by impulsing a conjugate SAW AMF to generate the burst of PN-PSK coded test waveform. Passive generation gives the loop performance of a pair of AMF's.

In addition to evaluating the *aperiodic* AMF performance with a burst of coded signal, *periodic* testing with a repetitive coded waveform can easily be achieved by removing the gating unit and RF switch, shown dotted in the active generator system of Figure 6.2(a). When the AMF is coded with a PN m-sequence of length N, the periodic autocorrelation function has a single peak of amplitude N with unity time sidelobes (equation 3.3). These low sidelobe levels make this the most demanding test of AMF time domain performance.

Assessment of the correlation performance was made by measuring the insertion loss and peak to sidelobe ratio as described previously. Detailed study of the correlation peak indicated whether bandlimiting was present as the basewidth should be exactly two chips wide. Doppler performance of the matched filter[76] can also be evaluated with the active test signal by off-setting the carrier in the VHF signal generator.

All these time domain measurements apply to both fixed coded and programmable SAW AMF's. The additional parameters measured in PAMF's are the power consumption and reprogramming time. The power consumption of manually programmable AMF's is easily measured. Electronically programmable AMF's, where the programming voltages are obtained from logic signals, require separate hardwired tests to ascertain the switch power consumption.

Reprogramming delay measurements are only relevant in the fully electronically programmable AMF shown in Figure 5.1. Measurements were obtained by changing the tap coding from an all '0' to all '1' as the AMF is correlating a cw signal. The time delay incurred while the output changes phase gives a direct measurement of the reprogramming delay.

## 6.3 MANUALLY PROGRAMMABLE AMF's

### 6.3.1 DESIGN OF PAMF's WITH DISCRETE COMPONENT SWITCHES

With PAMF's it is advantageous to utilise an available SAW AMF mask design to permit a realistic performance comparison between the existing fixed coded AMF's and the new programmable devices. The EA 4 mask, which is designed for operation at 100 MHz on ST-X quartz substrates, was chosen as its structure incorporates tap bonding pads, Figure 4.2, which are convenient for interfacing with external switch circuitry. This structure used a 20 finger pair input IDT of 50 $\lambda$ (acoustic wavelength) aperture. Taps were designed as 3 finger pair IDT's of 80 $\lambda$ aperture.

Printed circuit board construction of the 4 ring switching circuit, Figure 5.4(a) was simulated with IN914 diodes and 10 K$\Omega$

resistors for analysis with the Programme included in Printout 1, Appendix B. It was intended to use the components with ± 12 V programming inputs to give a typical diode forward biased impedance of 80 Ω and reverse biased capacity of 0.8 pF (2 KΩ impedance at 100 MHz). The requirement for a large interconnection fan out between SAW device and PCB switches in the high component count switch was simulated by adding a 7 pF stray capacity on each bond lead and 5 pF on the sum bus output node of each switch. These values were derived from measurements madewith the network analyser and RX meter on the switch layout used in the single tap switching experiment, reported in Section 6.1.

Figure 6.3 shows a comparison of the predicted performance of EA 4 fixed coded and programmable AMF's derived from the computer analysis. The information was obtained from the second and third table of data in Printout 2, Appendix B. The solid curves give the electrical insertion loss in impulse and correlation response for fixed coded AMF's with 1 to 250 taps as shown previously in Figure 4.3. The dotted curves provide similar results for discrete component SAW PAMF's. The additional shunt loading of switch diodes and resistors causes a large increase in the device insertion loss. Typical features are 10 dB for a 7 tap PAMF rising to 30 dB for 100 taps. These shunt losses are also evident in the correlation response where a minimum insertion loss of 40 dB is predicted. In comparison < 10 dB loss was projected for fixed coded devices with > 63 taps.

In addition to indicating electrical performance parameters, the computer programme also analysed the electroacoustic reflections within these devices. The chain dotted curve of Figure 6.3 shows,

with respect to the *input acoustic wave*, the primary electro-acoustic signal reflected at each tap during an impulse test. It will be noted when comparing the fixed coded and programmable AMF's that the electro-acoustic reflection levels are enhanced by the presence of the switching circuits. In the fixed coded AMF, Figure 4.3, the reflection signal decreased with increasing numbers of taps. In contrast, the PAMF primary reflection at each tap has a constant amplitude of -75 dB. The discrepancy arises from the difference in tap loading in the two devices. In the PAMF each tap is loaded predominantly by the series switch. This isolates the tap from the sum bus and output circuit resulting in an almost constant acoustic to electric conversion loss, $\rho_{31}$, and hence primary reflected signal. However, the electrical losses in the switch are dependant on the number of taps and hence the PAMF impulse response insertion loss still increases with the greater numbers of taps as shown in Figure 6.3.

It is important to note the level of these electro-acoustic regenerated signals and compare them with acoustic wave impedance mismatch which is now known to degrade seriously SAW AMF performance. This latter mechanism, which was discussed in Chapter 4, gave a primary acoustic reflection coefficient of -35 dB in the simple EA 4 mask design. In contrast,the electro-acoustic regeneration in a one to thirty one tap programmable AMF was only -75 dB. At the time of these preliminary investigations the acoustic wave impedance mismatch effect had not been identified, and hence it was assumed that electro-acoustic regeneration was the dominant effect which was likely to degrade the PAMF signals processing performance. The computer programmes and data printouts of appendix B were therefore designed

to calculate the level of AMF spurious signals by summing primary and secondary electro-acoustic reflections across the encoded tap array. The worst case arises when the PAMF coding possesses the same relative phase on alternate taps, a condition which is unlikely to be met in the practical spread spectrum systems reported in Table 3.1. The programmes sum seperately the primary and secondary reflections at every second tap in the array to obtain values for the anticipated level of electrical spurious signals. This resulted in predictions of PAMF impulse response spurious levels <-40 dB for devices with < 100 taps.

The practical measurements, Section 6.3.2, showed considerable disagreement with these predictions. This was only explained later in the device development when acoustic wave impedance effects were better known and understood. It was then that it became apparent that reflection compensated tap geometries were essential to both fixed coded and programmable AMF's if acceptable signal processing performance was to be achieved. With the continual reporting of new developments[71,72] reducing the level of wave impedance mismatch reflections, it was not considered relevant to include their effect in the PAMF theory. This would duplicate identical studies which were being carried out on fixed coded AMF's. Instead, the improvements were noted and care was taken to ensure that electro-acoustic reflection levels could be kept to a value which was an order of magnitude smaller than any wave impedance mismatch reflections.

These points apart, conclusions can still be drawn from the computer derived curves of Figure 6.3. It was obvious that a severe degradation arose from the large additional shunt capacity, and it

is this dominant factor which limits the number of taps in the discrete component PAMF designs.

### 6.3.2 DEVICE PERFORMANCE

These practical results are based on measurements performed on three manually programmable AMF's constructed to operate at 100 MHz on ST-X quartz substrate material.

Figure 6.4(a) shows an 8 tap PAMF constructed using the circuit of Figure 5.4(a) with IN914 diodes. In pulse response, the device exhibited an insertion loss to the best tap of 60 $\pm$ 0.5 dB with $\pm$12 volt drive signals[60]. The increase of 10 dB over a hardwired AMF agreed with the theoretical prediction of Figure 6.3. A $\pm$3 dB tap amplitude variation was measured which was considerably in excess of the $\pm\frac{1}{2}$ dB when hardwired. This was caused by individual switch component tolerances and stray circuit loading. Electrical weighting was applied at the switches to obtain the impulse response shown in Figure 6.4(b) - trace (1). The response differed from the previous AMF responses shown in Figure 4.4 as the waveform envelope clearly shows the output each individual tap. This arose from the selection of alternate taps in the AMF structure, which was necessary to give an acceptable spacing (1.2 mm) to satisfactorily interface between the taps and switches. This also resulted in a consequent reduction in the AMF chip rate to $2\frac{1}{2}$ MHz.

Aperiodic autocorrelation of an actively generated seven chip Barker coded PSK sequence is shown in Figure 6.4(b) - trace (3) with a peak-to-sidelobe ratio of 15.5 $\pm$ 0.2 dB (theoretical 16.8 dB). Similar results were obtained with fixed coded devices from this mask

indicating that the switches were contributing no differential phase shift between taps. The PAMF required 50 mW DC power per tap with ±12 volt switch drive signals. Further assessment of the performance showed that reducing the supply potentials to ± 5 volt incurred less than a 1 dB addition to the insertion loss and degraded the autocorrelation peak-to-sidelobe ratio by a further 1 dB to 14.5 ± 0.2 dB. However, the total device power consumption was reduced from 400 mW to < 50 mW.

For comparison, the circuit of Figure 5.4(b) was evaluated with another 7 tap AMF structure, also on ST-X quartz substrate[87]. Similar components were used with the addition of 270 pF monobloc coupling capacitors. This device also exhibited large, ±3½ dB, tap-to-tap amplitude variation but gave only 5 dB additional insertion loss over the fixed coded version. A simplified computer analysis, Programme 2 , Appendix B, was developed for this switching circuit. The second table of data in printout 4 predicted 7 dB additional loss, giving a 3 dB improvement over the previous device, with this lower component count circuit. Autocorrelation performance of both devices were comparable. However, the simpler circuit operated satisfactorily with 5 volt drive signals requiring only 10 mW total DC power. Substitution of the HP 5082-3039 PIN diodes in place of the IN 914's, gave a further reduction of 1 dB in insertion loss. This improvement is of little consequence when the higher unit (£3 each) cost of these diodes is taken into account.

In the devices low output noise levels were only obtained when the switch layout was designed on double sided PCB with a screening groundplane as shown in Figure 6.4(a). Tap-to-tap isolation was

typically 30 dB, but on-to-off switch ratios of > 20 dB were difficult to obtain. This was caused by direct electromagnetic radiation between the tap interconnection wires and switches.

Measurements were also made on a 16 tap programmable AMF, utilising a professionally designed PCB with 4 ring switches, shown in Figure 6.4(c). In this device the SAW TDL was mounted within a screened box on a separate interconnection PCB. Taps were bonded to gold plated tracks which exited the sides of the box for discrete wiring to the switches. This construction, which unfortunately placed additional stray capacity on the taps, had inferior component screening and electromagnetic isolation when compared to previous designs. Experimental evaluation of the device showed electromagnetic leakage of signals between taps. In impulse response individual tap amplitudes were dependant on device coding. For example, when coded with all '1's the impulse response had approximately a 3 dB amplitude droop with, in addition, -10 dB spurious signals following the generated sequence. At the time of these experiments extensive computer analysis was performed with a variety of stray tap loadings in an attempt to simulate the high level of electrical spurious signals. The results all predicted that impulse response spurious levels of approximately -75 dB were typical for electro-acoustic regenerated signals. However, it is *now* known from subsequent researches conducted on fixed coded AMF designs, that the high spurious levels exhibited in the 16 tap PAMF were caused by summation of reflections from acoustic wave impedance mismatch.

These devices have practically demonstrated the feasibility of designing simple programmable AMF's with conventional IDT taps, each

individually interconnected through a diode polarity switch onto a common sum bus. However, the use of discrete components for switch realisation results in several limitations :

* Large insertion loss due to component and stray shunt load.

* Large physical size of switches limits signal-to-noise ratio.

* Interface between taps and switches limits chip rate.

* Acceptable performance is in doubt for devices with > 8 taps.

Attention was therefore focussed on obtaining an alternative technology for switching circuit fabrication which permits a reduction in switch size to improve insertion loss and output SNR,and fully exploit the available SAW AMF bandwidth. It is imperative to achieve fabrication of a switching matrix with a pitch of 620 μm to permit *direct* interfacing with the taps of a 5 MHz chip rate AMF.

## 6.4 INVESTIGATION OF SUITABLE TECHNOLOGIES FOR THE CONSTRUCTION OF ELECTRONICALLY PROGRAMMABLE AMF's

Dialogue was first established with semiconductor designers to investigate the integrated circuit (IC) technologies which were available for the fabrication of high fidelity PAMF switches. At the time, the discussions favoured implementation of the four ring circuit, Figure 5.4(a), which possessed no capacitors and hence was easily integrated, although subsequent research has shown that identical performance can be obtained with lower component count

circuits. Initial contact was established with the Plessey Company Limited, Allen Clark Research Centre, to investigate their Silicon on Sapphire (SOS) process and high speed bipolar process 3.

SOS is a recently developed technology[89] which, due to specialised component geometries and etching techniques, provides low capacity components which are ideal for PAMF switch construction. For example, vertical junction diodes of 20 μm junction area possessing only 0.02 pF zero bias capacity have been fabricated with this technology at the Autonetics division of North American Rockwell[86]. In addition, these diodes had only 10 Ω forward biased series resistance when 0.04 Ω cm resistivity material was used. The excellent isolating property of the sapphire substrate resulted in low parasitic capacitances on both diodes and resistors minimising PAMF shunt losses. Figure 6.5 compares the projected performance of programmable AMF's with several different switching circuit realisations. Fixed coded AMF characteristics are obtained from the second table of data and the SOS switch characteristics for the 4 ring circuit, from the 4th table of data in Printout 2, Appendix B. The excellent properties of the SOS diode switch gives a vast reduction in insertion loss and the low forward biased impedance reduces electro-acoustic reflections by 7 dB compared with the earlier PCB device. In addition,these reflections decrease with increasing numbers of taps in a manner similar to the fixed coded AMF, further illustrating the high fidelity of the SOS switch.

Another possible alternative IC technology for switch fabrication is the Plessey, high speed bipolar Process 3. This is a second generation process[90] with fine lateral geometries, shallow

0.4 μm, diffusions and thin 4 μm, epitaxy which produces isolated bipolar transistors within a 62 μm x 42 μm total device area. Transition frequency ($f_T$) of 2.5 GHz at 5 mA and current gain ($\beta$) of 40 to 100 are typical transistor performance figures. The process is currently used to fabricate a range of circuits including ECL digital counters capable of operating above 1 GHz and IF amplifiers with 200 MHz bandwidth, and 20 to 60 dB gain.

Process 3 base collector junction diodes possess only ½ pF reverse bias capacity with 18 V breakdown voltage. However, integrated circuit resistors must also be fabricated within the base diffusion and the large areas required to realise 10 kΩ values results in 1-2 pF of distributed capacitance. Figure 6.6 shows the layout of the diffusions for a PAMF switching circuit using this process. The layout is designed to include three tap switches within a semiconductor chip of 1444 μm x 676 μm active area, for packaging in a 16 lead DIL. This encapsulation necessitates either a tap interconnection fan out or reduction of PAMF chip rate to 1MHz to match tap-to-tap spacing to the DIL package dimensions. However, direct mounting of unencapsulated semiconductor chips alongside the SAW device, permits stitch bond interconnections to a 5 MHz chip rate AMF without any bandwidth restriction. Computer analysis of the Process 3 switching circuit, 5th table of data in Printout 2, Appendix B, shows that devices with 31 taps will have an insertion loss to the correlation peak of -29 dB. Although this result offers considerable improvement over the PCB design, the larger component and shunt capacity gives a performance which is considerably inferior to the SOS switching circuit. The computer results are presented graphically in Figure 6.5.

Hybrid construction, interfacing the SAW TDL to a thin film[91] switching circuit, offers another possible approach to the realisation of a prototype PAMF with the lower component count circuits of Figure 5.4(d). The fabrication of a high performance device with good dynamic range,> 40 dB, dictates that assembly techniques similar to those proposed for the IC device be employed, with the switching circuit included inside the screening box containing the AMF. This reduces the noise and spurious signal effects evident in the PCB device, but requires a switch design which is compatible with the SAW AMF tap-to-tap spacing. Beam lead diodes in 0.17 mm x 0.9 mm packages combined with 60 μm wide thin film resistors offers the potential to realise a switching circuit with a 620 μm pitch for direct interconnection to a 5 MHz chip rate AMF. Thick film construction was considered as a possible alternative but the minimum reproducable linewidth of 600 μm excluded its application. PIN diodes, which possess the low capacity required for PAMF switch fabrication, are unfortunately only readily available in beam lead packages from a single manufacturer, Alpha Industries of Woburn, Massachusetts. Figure 5.2 showed the VHF small signal characteristics of the D5840 diode which is the cheapest component in their range.

The projected performance of a hybrid PAMF fabricated using these diodes and 5 KΩ thin film bias resistors is also shown in Figure 6.5 for comparison against the other technologies. The analysis is based on Programme 2 - Printout 3, Appendix B - which was developed for the simpler switching circuit. The results used to derive the hybrid curves of Figure 6.5 were obtained from the 4th table of data in Printout 4 - Appendix B.

It is intended in this device to utilise a TTL MSI code storage and selection facility, to provide the capability ultimately for the fabrication of a fully electronically programmable AMF. In the final device it is intended to mount the code store on a PCB which uses 12½ thou wide tracks for simple interfacing between the wide pitch of the TTL circuitry and narrow pitch of the thin film switches. However, TTL switch drive gives output logic levels of 0.1 volt (low) and 3.6 volt (high) which is insufficient to drive the diode into the low impedance conduction region. Only 200 μA of current flows in the forward biased diode resulting in 400Ω impedance, see Figure 5.2. This high impedance increases the acoustic reflection levels at each tap to -62 dB as shown in Printout 4 - Appendix B. The increase in electric-acoustic reflection levels also results in a consequent increase in the relative amplitude of primary and secondary electrical spurious signals. However, performance degradation is not severe as these effects are still considerably smaller than the wave impedance mismatch,which is the dominant degrading effect limiting the performance of all simple first order AMF designs.

Prior to commencing the fabrication of a high technology device it is necessary to evaluate accurately the available technologies. Table 6.1 shows a cost and time scale analysis for the fabrication of two pairs of 32 tap programmable AMF's using the three technologies discussed here. The table specifically refers to the cost of *fabricating* four switching matrices, based on the circuits of Figure 5.4(a) for an integrated or SOS device and 5.4(d) for the hybrid AMF. It does not include the cost of AMF materials and processing or any code storage and selection hardware.

Integrated circuit technology is a natural choice for PAMF switches, especially when it is appreciated that serial registers and transfer store can also be fabricated on the same semiconductor chip. With SOS, the logic circuits can be realised with MOSFET's on a common sapphire substrate. This relatively new SOS technology is *not* currently available in the UK as a production process. A development process does exist, at the Plessey Company Limited, but it is designed for the specific requirements of MOS fabrication. Although these SOS diodes would possess an acceptable low capacity, typically 0.05 pF, further development is unlikely to reduce their forward biased impedance below 100 Ω at 1 mA. Appendix B also includes in the sixth table of data in Printout 1 a simulation of the expected performance of a PAMF using the Plessey SOS diodes. The device shows an increase in acoustic reflections signals, due to the high diode impedance, similar to that predicted for the hybrid device. In addition to giving inferior device performance compared to the Autonetics SOS processes, table 6.1, showed that the costs likely to be incurred in tailoring the Plessey process to meet our requirements were unacceptably high for prototype device construction.

The high speed silicon IC Process 3 is also attractive for switching circuit fabrication. It can readily achieve the narrow pitch between switching circuits with the complex 4 ring switch, as shown in Figure 6.6. When fabricating high chip rate PAMF's with >16 taps, it is impossible to use separately encapsulated switching circuits due to the layout problem. Semiconductor chips can be designed to accommodate any desired number of tap switches, but usually it is unrealistic to include more than 16 switches on a single semiconductor chip when a high yield is required.

It is obvious, therefore, that the construction of a 128 tap AMF will involve many wire bonds between the AMF and the semiconductor switches decreasing the overall reliability and reducing many of the advantages of integrated construction. Table 6.1 showed that integrated construction is both time consuming and outwith direct control, two factors of considerable importance in the PAMF development programme.

Although the initial design studies were based on an IC approach, it was finally decided to use thin film hybrid fabrication, with all the assembly performed in-house. As our requirements would be met by a small quantity of prototype devices, the high component cost of beam lead PIN diodes (£3 each) was offset by the relatively large mask making costs incurred in an IC approach. Thus, the hybrid approach offered reasonable cost, direct control and fast fabrication - 10 weeks for a 32 tap device. In addition, this approach possessed the flexibility to individually modify the AMF structure, switching circuit, or code store to obtain several iterations on the device design.

It must be noted that IC technology possesses the capability of easily incorporating the code storage and selection hardware within the device, which is attractive ultimately for the fabrication of production devices.

## 6.5 SAW HYBRID PAMF's

### 6.5.1 CONSTRUCTIONAL DETAILS

The programmable AMF, shown in Figure 6.8(a), consists of three separately constructed sub-assemblies. The hybrid microelectronic

circuitry was made on a 63 x 25 mm Corning 7059 glass substrate, allowing space for the SAW delay line. The latter was made on a 63 x 8 x 2.5 mm polished bar of ST-X quartz, subsequently cemented onto the glass substrate. This assembly was then cemented on a printed circuit board carrying fan-out leads and the TTL packages which form the shift register for code selection. The RF parts of the device, delay line and hybrid switching matrix were enclosed in an aluminium box which also screened the input transducer from the taps.

Tap switching circuits are detailed in another hybrid AMF, later in Figure 6.9(b). Here the AMF structure had 128 taps, though only 32 were connected to switching circuits on the device illustrated. The thin film resistors were fabricated using a nichrome-gold process. 200Ω/sq sheet resistance nichrome was evaporated onto the glass substrate, then overlayed with gold. Both evaporations were performed with an electron-beam heated source. The resistive and conducting patterns were defined using a Shipley positive photo-resist system combined with selective etches. The 5 KΩ resistors had a pitch of 620 μm per pair, with 60 x 1500 μm active areas and 200 μm wide bonding pads to accommodate the diodes. The resistor values varied by ± 5% which was considered adequate but improved photomasking combined with RF sputtering of the film can be employed to improve film quality and composition if required. The Alpha D5840 beam lead PIN diodes were bonded onto the gold overlay, bridging the gap between the resistor array and output summing bus. The bonding was performed with a pulse tip thermocompression ball bonder.

The quartz substrate with SAW structure was positioned between the resistor diode networks and secured with an adhesive varnish. Connection between the resistors and taps was made with gold wire, bonded between the gold and aluminium pads. A pulsed, thermo-compression ball bonding technique was used as this does not require any steady state heating of the device, but only an instantaneously pulsed heating of the bonding capillary when the preset bonding pressure is reached. This avoids any thermal degradation of the components and also provides wide freedom of choice for adhesives.

Interfacing the closely spaced thin film switches to standard encapsulated 8-stage TTL shift registers was accomplished by using a printed circuit board with 310 μm (12½ thou) wide metal tracks having the same period as the resistors pairs (620 μm). The tracks subsequently fan-out to shift register stages accommodated along the sides of the 5" x 9" board. The pulsed thermocompression ball bonding system was again selected to complete the connections between the thin film and printed circuit board. The copper tracks were gold plated in the bonding region to ensure good bond reliability. The remainder of the board was flow soldered both for protection and to facilitate connection of the TTL packages. A ground plane on the printed circuit board formed the rear face of the screening box, and a web in the box screened the input transducer from the taps.

### 6.5.2 SELECTION, GENERATION AND STORAGE OF PROGRAMMING CODES

Evaluation of an electronically programmable AMF required an infinite code store to investigate the device performance with many different codes. The electronically programmable SAW AMF's

described in the following two sections are designed with only a simple serial register incorporated on the PAMF printed circuit board. This was achieved with SN 74164, 8 chip (bit) TTL shift registers.

Programming is accomplished from the remote code selector, shown in Figure 6.7, which was developed to reduce the PAMF logic complexity. The code selector was designed with the capability of generating on banks of switches two independent 64 chip words for programming of AMF's with up to 128 taps. On depressing the read button, the codes are read off the switches and loaded into two separate 64 chip registers each comprising 8 SN 74198 elements. Releasing the read switch shifts the two codes out in serial format with a 64 pulse burst of internally generated clock pulses. These are synchronised to, but $180^{o}$ out of phase with, the two 64 chip words. A 1 MHz MC 4024 astable clock generator is gated with the shift command into two SN 74193 TTL programmable divider circuits to count and gate the necessary 64 clock pulses. This system permits any required code to be read and correctly located in the PAMF serial code store.

### 6.5.3 HYBRID PAMF EMPLOYING A DOUBLE POLE DOUBLE THROW SWITCH DESIGN

The performance of the 31 tap hybrid programmable AMF, shown in Figure 6.8(a), which used the DPDT switch of Figure 5.4(d), was assessed practically by direct comparison with fixed coded AMF's fabricated from the same EA 4 mask design. In addition its performance was compared against the theoretical predictions of Figure 6.5. The electrical performance is summarised in Table 6.2.

The upper trace of Figure 6.8(b) shows the impulse response of a typical EA 4 AMF, precoded with a 31 chip PN sequence. For comparison the lower trace shows the impulse response of the hybrid PAMF coded with the time reverse of the same 31 chip PN sequence. It is noted that a total of five taps are inoperative in this device. Taps 9, 15, 16, 17 and 18 give no output. As neither '1' or '0' phase signal was present,the fault is presumably caused by an open circuit resistor or faulty bond. Subsequent additional failures, which occurred at taps adjacent to those already affected, indicated that there was probably a scratch or other fault on the resistor tracks. It must also be noted that in impulse response, both the precoded and programmable device had the same level of spurious signals. It is known that the spurious signals in the fixed coded AMF were caused by acoustic wave impedance mismatch. Hence spurious in the PAMF, at the same amplitude level, confirmed the computer predictions that the low electro-acoustic regenerated spurious levels do not cause any further performance degradations.

Insertion loss of the PAMF in pulse response was measured as 57 $\pm$0.5 dB. Direct comparison against fixed coded devices leads to inaccuracies as a 2 to 3 dB input IDT matching tolerance is usually present in the individual AMF's. Comparison against a hardwired tap on the same PAMF gave a measured 3 $\pm$0.5 dB loss in the switch. This is in reasonable agreement with the 4½ dB predicted by the theoretical curves of Figure 6.5.

The centre trace of Figure 6.8(b) shows the PAMF correlation response for a loop test. Passive generation of the test signal was achieved in a fixed coded AMF (upper trace) prior to detection in the hybrid PAMF. The insertion loss to the correlation peak is

degraded to 29 ±0.5 dB as the 26 active taps gave a compression gain of only 28 dB. The peak to sidelobe ratio was measured as 12 ±0.2 dB, which differs from the 14 dB of the fixed coded AMF, Figure 4.4(b) due to faulty taps. The PAMF exhibited a peak to sidelobe ratio of only 16 ±0.2 dB when correlating a repetitive 31 chip PN sequence. In comparison, fixed coded AMF with 31 functional taps, achieved 21 ±0.2 dB,still possessing considerable degradation from the theoretical 30 dB.

The lower two photographs in Figures 6.8 serve to illustrate the inherent flexibility of coding possessed by *programmable* AMF's. In Figure 6.8(c) the processed signals are typical of burst mode Spread Spectrum systems. It shows the device performance when receiving two different 31 chip PSK sequences, Code A and Code B, which have been computer selected from a 127 chip m-sequence for low autocorrelation and cross correlation time sidelobe levels. In the upper trace the PAMF exhibits autocorrelation when the device is coded to recognise Code A. The centre trace shows the cross-correlation of the same device when the test signal is changed to the other signature, Code B. The third trace shows again the autocorrelation response when the PAMF is reprogrammed with Code B from the code selector. Simple envelope and threshold detectors[68] permit a receiver to distinguish between the two signatures and recognise only those signals coded with its own unique address. This code recognition forms the basis of several of the Spread Spectrum communication systems reported in Table 3.1.

Figure 6.8(d) shows the PAMF recognising several distinct subsequences of a longer continuous PN-PSK IF sequence. In all the

four traces the 31 tap hybrid PAMF is receiving the same 127 chip sequence. The device is reprogrammed between traces with a new 31 chip subsequence moving the autocorrelation peak to a different point in the long sequence. When the PAMF possesses the fast reprogramming capability outlined in Figure 5.1, then continuous reprogramming can be employed to serially process short segments of a long code to obtain the train of regularly spaced correlation peaks shown later in Figure 7.5. This latter concept forms the basis of the prototype serial parallel receiver, described in Chapter 7, which demonstrates the capability of combined SAW devices to effect a considerable increase in the time bandwidth product of Programmable PSK Matched Filters.

In addition to investigating the PAMF time domain performance, theoretical and practical studies were performed to study the variation of insertion loss with changes in load impedance and matching at the tapping electrode. Theoretical analysis indicated that hybrid devices with >50 taps, which have a large shunt capacity, favour a lower load resistance than 50 Ω for reduced loss. This can be seen by comparing the 4th and 6th Table of data in Printout 4, Appendix B. Practical verification was difficult as only 31 tap hybrid PAMF's were constructed. Measurements made on these devices by introducing wideband transformer coupling between the taps and the external load were inconclusive as they showed no appreciable variation in insertion loss with changes in load impedance.

Measurements on inductor matching of the taps to the external load gave lowest loss with a 0.065 μH Piconix variable inductor,

but the measured loss was identical to the unmatched condition. This value did confirm that the total shunt capacity of taps, diodes and strays was~50 pF which was the value selected in the computer analysis. It was concluded that direct interconnection to a 50 Ω load was likely to give the best PAMF performance.

The SN 74164 TTL MSI serial code store used in the PAMF did not possess open collector outputs hence only a 3.5 volt switch drive signal was available. This gave low bias currents, reducing the PAMF power consumption to ¾ mW, per tap at the expense of high diode impedance and relatively large electro acoustic spurious signals when compared to integrated PAMF's. This is seen by comparing the reflected signals of SOS PAMF's in the 4th table of data in Printout 2 with the hybrid PAMF, 4th table of data in Printout 4.

With the development of tap geometries with improved suppression of acoustic wave impedance mismatch reflections, it is likely that hybrid PAMF's could be limited to ≤31 taps if the impulse response electro-acoustic regenerated spurious is not to exceed a -40 dB level. (The 4th table of data in Printout 4 predicts, for a 31 tap PAMF with worst case tap coding, an impulse response insertion loss of 53.2 dB and primary electrical spurious levels of 91 dB.) However the electro-acoustic reflections can be suppressed by lowering the diode impedance with an increase in bias current. High level logic[92] with 0 and 20 volt logic levels is not recommended as the slow switching speeds, ~1 μsec, will seriously degrade the fast reprogramming capability. A better approach is to retain the original TTL code store and increase the depth of the thin film nichrome deposit to reduce the sheet resistivity

and hence the bias resistors values. The computer analysis presented in the 5th table of data in Printout 4 predicts a 20 dB reduction in the electrical reflection levels at each tap for a hybrid PAMF with 500 Ω bias resistors. However, the additional resistive shunt losses degrade the electrical insertion loss by a further 6 dB.

This modification has been incorporated in an improved layout of the DPDT switch which also reduces the number of wire bonds by removing the stitch bonded cross overs. This new switch layout has not been evaluated in a SAW hybrid PAMF. However, it offers the potential of improved switch performance for the fabrication of longer 64 or 128 tap hybrid PAMF's.

### 6.5.4 EVALUATION OF A HYBRID PAMF WITH A SIMPLIFIED SWITCH DESIGN

The hybrid PAMF reported in Section 6.5.3 employed a DPDT switch, designed to interface with three finger pair AMF taps to obtain high performance with low electrical insertion loss. However, the switch requires a significant number of expensive components, which introduces both fabrication difficulties and reliability problems in these PAMF's. The review of switching circuits in Chapter 5 indicated that PAMF's cannot easily be constructed with a circuit employing fewer than four active devices. Research was therefore initiated to obtain a novel design of PAMF which provided a significant reduction in the number of switch components.

The approach adopted[93] used a Single Pole Double Throw (SPDT) programming switch. Figure 6.9(c) illustrates the simplification

in switch design which has been achieved at the expense of increasedsophistication in the SAW AMF tap structure. The AMF tap was modified to a dual phase design outputing both 0 and $\pi$ phase samples of the propogating acoustic wave. This permited a SPDT switch to select the required output phase and isolate the other one. Since both tap phases must sample the acoustic wave simultaneously , they require to occupy the same physical position on the delay line. This was accomplished by segmenting the propagating wave into a dual acoustic beam.

In the new PAMF the tap-to-tap spacing has been decreased to 310 μm to give a 10 MHz chip rate capability. The desirability of using a ST-X quartz substrate, for temperature stable operation, would normally necessitate operation at 200 MHz to obtain 10 MHz chip rate with this low $k^2$ material, Table 1.1. However, fabrication of 200 MHz EA 3 fixed coded AMF's highlighted the practical difficulties in selectively etching a large fault-free array of taps with ~ 4 μm line width and spacing. In addition there are also difficulties in obtaining high value variable inductors, > ½ μH, for IDT matching, which possess a self resonant frequency in excess of 200 MHz. These problems were avoided by designing the new PAMF mask, the EA 6, for operation at 120 MHz. A wide aperture (115 λ) low resistance ($r_a$ = 20 Ω) input IDT was selected. It was designed with only 12 finger pairs to achieve a 8.5% fractional bandwidth of 10 MHz with wideband matching techniques[30]. Unfortunately there was a fault in the artwork resulting in the input IDT incorporating only 6 finger pairs hence excess bandwidth was available at the expense of additional loss.

As considerable time delay, typically 8 - 12 months, is inevitable between the design of an artwork and delivery of chrome masks, the EA 6 AMF design was settled while the fixed coded AMF's were still under evaluation. As a consequence the mask used a three finger pair tap design without any reflection compensation. 128 taps were included, each one comprising two separate transducers of 38 λ aperture with a common ground connection as shown in Figure 6.9(c).

For simplicity and ease of fabrication this PAMF used a modified version of the previous hybrid layout where the diodes were mounted side by side with a 620 μm pitch between switching circuits, shown schematically in Figure 6.9(c). For 10 MHz chip rate operation, alternate taps had to be interconnected to hybrid switches and code store on opposite sides of the device, see Figure 6.9(a). Figure 6.9(b) details the layout of the AMF taps and hybrid circuitry.

The upper trace of Figure 6.9(d) shows the impulse response of a prototype EA 6 AMF with 31 taps hardwired in a PN sequence. The device insertion loss was approximately 66 dB which is considerably higher than previous AMF's (~ 50 dB) due to the fault in the input IDT construction and the loss in the dual phase tap design. In addition the output envelope was not of constant amplitude, as the length of the input IDT did not equal the tap spacing . Tap amplitude variations of ± 2 dB were evident and spurious responses were only 15 dB below the desired output. The lower trace shows the loop performance of an EA 6 fixed coded and programmable AMF. The PAMF possessed a further 8 dB loss in

the switches compared with the 3 dB measured loss of the previous DPDT switch design. Although all the taps and switches were functional in this device the autocorrelation peak to sidelobe ratio was only 10 ±0.2 dB. These poor results indicated that there were severe degradations in the performance of this AMF.

The tap-to-tap amplitude variation in the fixed coded AMF impulse response is caused by acoustic wave impedance mismatch effects. Although only 31 taps were bonded out in the AMF the mask incorporated 128 taps which each generate an acoustic reflection. Measurement of the through transit and reflected acoustic signals after an impulse had propagated under the tapping electrode indicated that a higher level primary reflections, -30 dB, were present in this design. This was caused by the new tap geometry, which incorporated an additional connection in front of the tapping electrodes. In addition to enhanced primary reflections, the secondary reflections are also increased to -60 dB and they sum at each of the 128 taps to give the train of spurious acoustic pulses, shown in Figure 4.5. However, in the EA 6 AMF the amplitude of the first pulse N.SR1 is 128 times the secondary reflection coefficient which is only 20 dB below the incident acoustic impulse. In the previous EA 4 AMF there were only 35 taps hence the secondary acoustic reflections did not sum appreciably across the tap array. In any EA 6 AMF the *dominant* secondary acoustic reflections sum electrically across the encoded tap array giving rise to the large variations in individual tap amplitudes and the high level of spurious signals.

Although these effects cause a serious limitation in the performance of the fixed coded AMF, further degradations arise in

the PAMF where the unused half of the dual phase tap is no longer unconnected but is loaded by a reverse biased diode. Electrical resonance of this diode with the interconnection bonding wire gives rise to an electro-acoustic reflections which enhances the acoustic wave impedance reflection signal increasing both primary and secondary reflections. In the PAMF secondary reflections have been observed with an amplitude only 4 dB lower than the impulse after it has propagated below the tap structure. Similar measurements on the 35 tap EA 4 fixed coded and programmable AMF's indicated that the switching circuits caused *no* additional degradation to the through transit acoustic response of these devices.

The EA 6 mask design has illustrated,first, the serious problems of acoustic spurious signals in long (>32 tap) AMF's. Secondly,it was noted that the electrical load of the hybrid switching circuit on the dual phase tap caused a further significant degradation in device performance. It is anticipated that the electro-acoustic reflections could be reduced by replacing the SPDT switch with the DPDT design of Figure 5.4(d) which connects the other half of the tap to an antiphase sum bus. However, this solution makes the more complex dual phase tap design redundant.

Staples[7] has obviously also observed degrading reflections in SPDT PAMF's as he suggests an alternative approach where the unused half of the tap is grounded. This is less attractive than a simple DPDT switch design as 3 dB signal loss is automatically introduced. Both Staples' approach and the DPDT switch require four diodes removing the advantage of component reduction which was possessed by the original SPDT switch. It is concluded therefore that the SPDT switch is unsuitable for SAW PAMF fabrication.

A new mask, EA 9, Table 4.1, was designed with dual phase taps incorporating split finger electrodes[71] to suppress the acoustic wave impedance mismatch reflections. However the inferior performance of the SPDT switch resulted latterly in the rejection of this PAMF design in favour of the DPDT switch design reported in the previous section.

### 6.5.5 DEMONSTRATION AND MEASUREMENT OF FAST REPROGRAMMING CAPABILITY

The EA 4 hybrid PAMF with the DPDT switch design was selected for measurement of the reprogramming time delay. To obtain a fully electronically programmable AMF possessing a fast reprogramme capability,the original device shown in Figure 6.8(a) was redesigned with a printed circuit board which incorporated a TTL transfer store, Figure 5.1, between the original serial store and programming switches. The PAMF is shown in Figure 6.10(a).

Demonstration of the fast reprogramme capability was accomplished with a loop test where a PSK coded sequence was generated in a 31 tap precoded EA 4 AMF and detected in the new hybrid PAMF as shown in the bold outline of Figure 6.10(b). The code selector, described in Section 6.5.2, was used to generate simultaneously both the required AMF programming codes which were subsequently externally gated to code the PAMF sequentially with the forward and reverse codes. Reprogramming, with the transfer command, was performed through a pulse generator to give an infinite variation in the instant of reprogramming.

Figures 6.11(a) and (b) show the PAMF output responses. In the upper trace of Figure 6.11(a) the PAMF is coded for autocorrelation and in the lowest trace the coding is time reversed giving the familiar cross correlation response. The second trace

demonstrates the fast reprogramme capability by initially coding the PAMF for cross correlation and reprogramming with the auto-correlation code, while the coded sequence is propagating through the PAMF. Reprogramming occurs on the negative going edge of trace 3. This results in the second trace possessing leading sidelobes identical to the cross correlation response (lowest trace) prior to reprogramming to recognise the correlation peak and obtain trailing sidelobes identical to the autocorrelation response (upper trace).

Attempts to measure accurately the PAMF response time in this system were inconclusive. The use of a coded waveform makes it impossible to tell exactly when reprogramming is complete as the PAMF output envelope displays the varying amplitude of the correlation functions. Accurate measurements were therefore made with a cw test. This was accomplished by replacing the code selector and PAMF serial code store by a hardwired bus to permit the PAMF to be externally coded with an all'0' or all '1' code. Figure 6.11(b) illustrates the device operation. The transfer command is shown in the upper trace. The middle trace shows the tap code changing from '0' to '1' after a 30 nsec propagation delay in the TTL transfer register. The PAMF output drops to zero before returning with the opposite phase as seen in the lower trace. Reprogramming takes approximately 300 nsec. Additional measurements, made by hardwiring the switch drive, gave an increase in reprogramming time when the voltage was increased or decreased from the 3.5 volts drive provided from the TTL transfer store. Delays in excess of 1 μsec were obtained with a 20 volt High Level Logic[92] drive signal.

It was concluded that it is impossible to reprogramme this device within the chip time (200 nsec) but that the TTL MSI transfer store provides an interface voltage which gives acceptable reprogramming speed.

### 6.5.6 ACOUSTIC REFLECTION EFFECTS

The inherent flexibility of coding achieved within the PAMF permits any desired code word to be easily set on the taps to examine the effect of acoustic spurious signals on AMF performance. The EA 4 hybrid PAMF was chosen for this demonstration as the switch in this device has been shown in Section 6.5.3 to contribute no additional degradation to the AMF signal processing performance. The following experiments investigate only the effect of acoustic wave impedance mismatch reflections caused by the mass loading and electrical shorting at the tapping electrodes which were reported in Chapter 4. It was stated there that the interaction of an acoustic pulse with a 100 MHz 3 finger pair transducer results in a primary acoustic reflection of relative amplitude ~ -35 dB. Primary reflections have been represented diagramatically in Figure 4.5 as a series of pulses with identical phase, which propagate in the opposite direction to the input pulse with a pulse-to-pulse spacing of twice the tap-to-tap propagation delay. These reflections are the predominant degrading effect in TDL's with simple tap geometries employing< 50 taps.

The traces of Figure 6.11(c) demonstrate the electrical summation of these primary acoustic reflections across the encoded tap array of the EA 4 31 tap hybrid PAMF. The tap coding was

purposely set to reduce and emphasise the spurious output signal. The centretrace shows the impulse response of the device when coded with the simple sequence, 11001100 etc. Neglecting the faulty PAMF taps the device shows a good response with spurious signals of relative amplitude, < -25 dB. As alternate taps possess opposite phase coding, the acoustic reflection signals, which all have similar phase, cancel at the output electrical bus. However, there is a code imbalance in a device with an odd number of taps (31). Hence the output will give an electrical spurious signal equal to the voltage from 1 tap only. Thus theoretically electrical spurious signals should be -35 dB.

In the lower trace the AMF is reprogrammed with an all '1' code. Here the acoustic reflection signals, which all have the same phase, are present below a tap array which also possesses the same relative phase coding. This results in a coherent summation at alternate taps to give a voltage gain, G, of

$$G = 20 \log_{10} \frac{N}{2} \text{ dB} \qquad 6.1$$

when N is the number of taps in the AMF.

Thus in a perfect AMF summation at 16 taps gives 24 dB gain, generating the -11 dB output electrical spurious shown in the lower trace. In the upper trace the AMF is programmed with alternate '1' and '0' ie 101010 etc which also results in coherent summation at alternate taps with a -11 dB output electrical spurious. However, with this coding, after one tap propagation delay the reflected signals will sum under the '0' instead of the '1' taps causing the output spurious signal to regularly change phase.

It must be noted that these experiments have simulated the effect of both the best and the worst coding in the AMF. In practical systems the AMF's are normally coded with short PN sequences or subsequences of longer PN sequences where there is usually only a slight imbalance of '1' and '0's. Figure 6.8(b) traces (1) and (3) shows the impulse response of the EA 4 fixed coded and programmable AMF's when coded with a forward and time reversed 31 chip maximal length PN sequence. The responses had spurious levels of relative amplitude -20 dB. This high level occurs even although there is only a single imbalance of '1' and '0' in the PN code because an examination of *alternate* tap coding in the particular sequence used showed that there was an imbalance of 5 chips. This gives a 15 dB summation of the primary acoustic reflections causing the performance degradation in Figure 6.8(b) when compared with the centre trace of Figure 6.11(c).

These experiments have illustrated the mechanism which permits acoustic reflections to sum across an encoded tap array degrading the AMF impulse and correlation responses. It is obvious from the discussion that primary reflections must be decreased to improve the performance of existing 31 tap AMF's even when maximal length PN sequence coding is employed. In addition Section 6.5.4 showed that the summation of secondary reflections across the tap array further degrades the performance if the design of these simple devices is extended beyond 50 taps. It is for these reasons that the reflection compensated AMF structures of Bristol[71] and Darby[72] have been widely adopted.

## 6.6 TIME BANDWIDTH PRODUCT PREDICTIONS FOR SAW PROGRAMMABLE AMF's

The 31 tap 5 MHz chip rate hybrid PAMF constructed with the beam lead diode and thin film resistor DPDT switch has been shown to be an efficient device with low power consumption and switch insertion loss. In addition its signal processing performance was almost identical to comparable fixed coded AMF's. Device cost was not excessively high for prototype AMF's but there was evidence that the large number of interconnection bonds was limiting the yield and reliability of these devices. Although the electrical performance was inferior, considerable improvements in reliability were obtained with the simpler SPDT switch.

Other hybrid designs, such as that adopted by Fifer[85] for a 128 tap 10 MHz chip rate PAMF,employed a more sophisticated hybrid package which included the serial code store as unencapsulated semiconductor chips. He also experienced fabrication problems which required 4 sub-assemblies to be constructed and tested prior to assembly of the complete device. Although constructionally a more sophisticated device,this PAMF was less efficient (electrical insertion loss was ~100 dB) and it did not possess the fast reprogramme capability of the hybrid PAMF described in Section 6.5.5.

The 128 tap 10 MHz chip rate PAMF of Hagon[8], which employed a quartz TDL wire bonded to an integrated SOS switching circuit and MOS code store, clearly illustrated the *excellent* properties of the SOS diode switches. High performance was achieved with low spurious levels in a device which possessed only 3 dB switch insertion loss. The natural extension of this PAMF into a monolithic

device with Aluminium Nitride film for SAW propagation and a silicon layer for switches and code store mounted side by side on a common sapphire substrate represents a formidable task. High yield is of vital importance in semiconductor processing to minimise component cost. In addition,it is difficult to deposit a uniform Aluminium Nitride film possessing the necessary properties for SAW propagation. For these reasons it is probable that the large physical size of the monolithic PAMF will prohibit it from ever becoming a production item.

Forecasting the potential of SAW PAMF's it seems likely that the all hybrid PAMF with beam lead or flip chip active components will provide moderate cost prototype AMF's. They should possess the capability of processing signals with 20 MHz bandwidth but it is unlikely that they will incorporate more than 64 taps. A hybrid device which employs a series of SOS integrated switches will offer increased reliability and lower production costs and it is probably that they can be produced in small quantitites with up to 256 taps. Interconnection bonding will still limit the device bandwidth to approximately 20 MHz. The monolithic PAMF is projected to provide the ultimate in performance with device bandwidth of ~50 MHz but the fabrication yield is likely to limit the physical length of production devices to typically 128 taps.

| | SILICON-ON-SAPPHIRE | SILICON I.C. | HYBRID |
|---|---|---|---|
| DIODES | 0.02 pF, 10 Ω 1 mA | 0.25 pF, 100 Ω at 1 mA | 0.05 pF (PIN), 100 Ω at ½ mA |
| RESISTORS | diffused | diffused | thin film |
| FABRICATION | Few companies have technology available | Industrial production process | Simplest, and in-house |
| COST ANALYSIS | £<br>Masks 750<br>Process set-up 2500<br>Process 1 batch 900<br>£4150 | £<br>Masks 1000<br>Process 1 batch 560<br>£1560 | £<br>Masks in-house 50<br>Process in-house 50<br>Diode purchase 1560<br>£1660 |
| TIME SCALE (WEEKS) | Mask design 16<br>Mask fabrication 12<br>Process set-up and production 1st batch 20<br>Evaluation 4<br>Device construction 3<br>55 | Mask design 16<br>Mask fabrication 12<br>Process 1st batch 12<br>Device construction 3<br>47 | Mask design and fabrication 3<br>Thin film processing 6<br>Device construction 4<br>13 |

TABLE 6.1 TRADE-OFFS COMPARING SWITCHING-MATRIX TECHNOLOGIES FOR FOUR 32 - TAP PROGRAMMABLE AMF'S

| | TYPICAL FIXED CODED AMF | INFINITELY PROGRAMMABLE AMF |
|---|---|---|
| Centre Frequency (MHz) | 100 | |
| Code Chip (Bit) Rate (MHz) | 5 | |
| No of Taps | 31 | |
| Insertion Loss to a Single Tap (expansion) (dB) | 54 ± 0.5 | 57 ± 0.5 |
| Expansion Spurious Signals (coded 31 chip PN) (dB) | -20 | -20 |
| Insertion Loss to the Correlation Peak (pulse compression) (dB) | 24 ± 0.5 | 29 ± 0.5 |
| Compression Gain (dB) | 30 | 28 |
| Periodic Correlation Peak to Sidelobe Ratio (dB) (theoretical 30 dB) | 21 ± 0.2 | 16 ± 0.2 |
| Aperiodic Correlation Peak to Sidelobe Ratio (dB) (theoretical 15.8 dB) | 14 ± 0.2 | 12 ± 0.2 |

TABLE 6.2 EA 4 SAW AMF PERFORMANCE COMPARISON

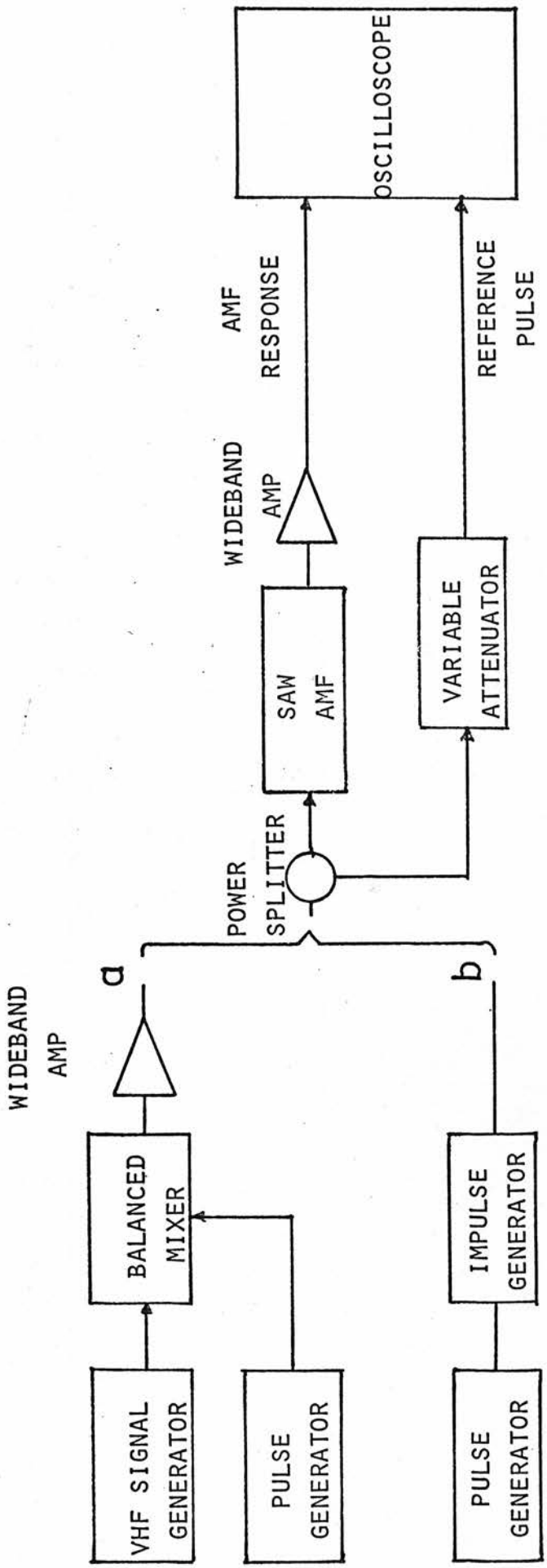


FIGURE 6.1 IMPULSE AND PULSE RESPONSE TEST ARRANGEMENT

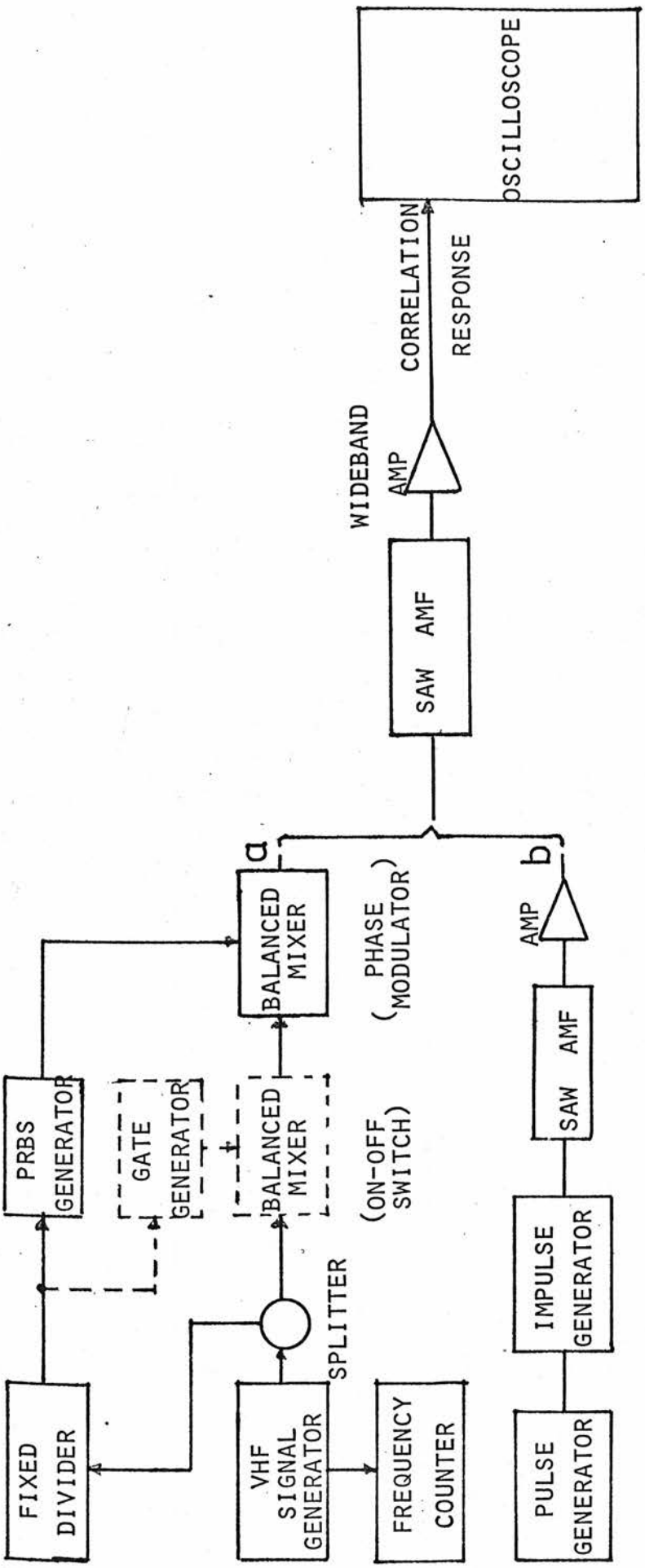


FIGURE 6.2 APERIODIC AUTOCORRELATION MEASUREMENT USING EITHER AN ACTIVE OR PASSIVE TEST SIGNAL

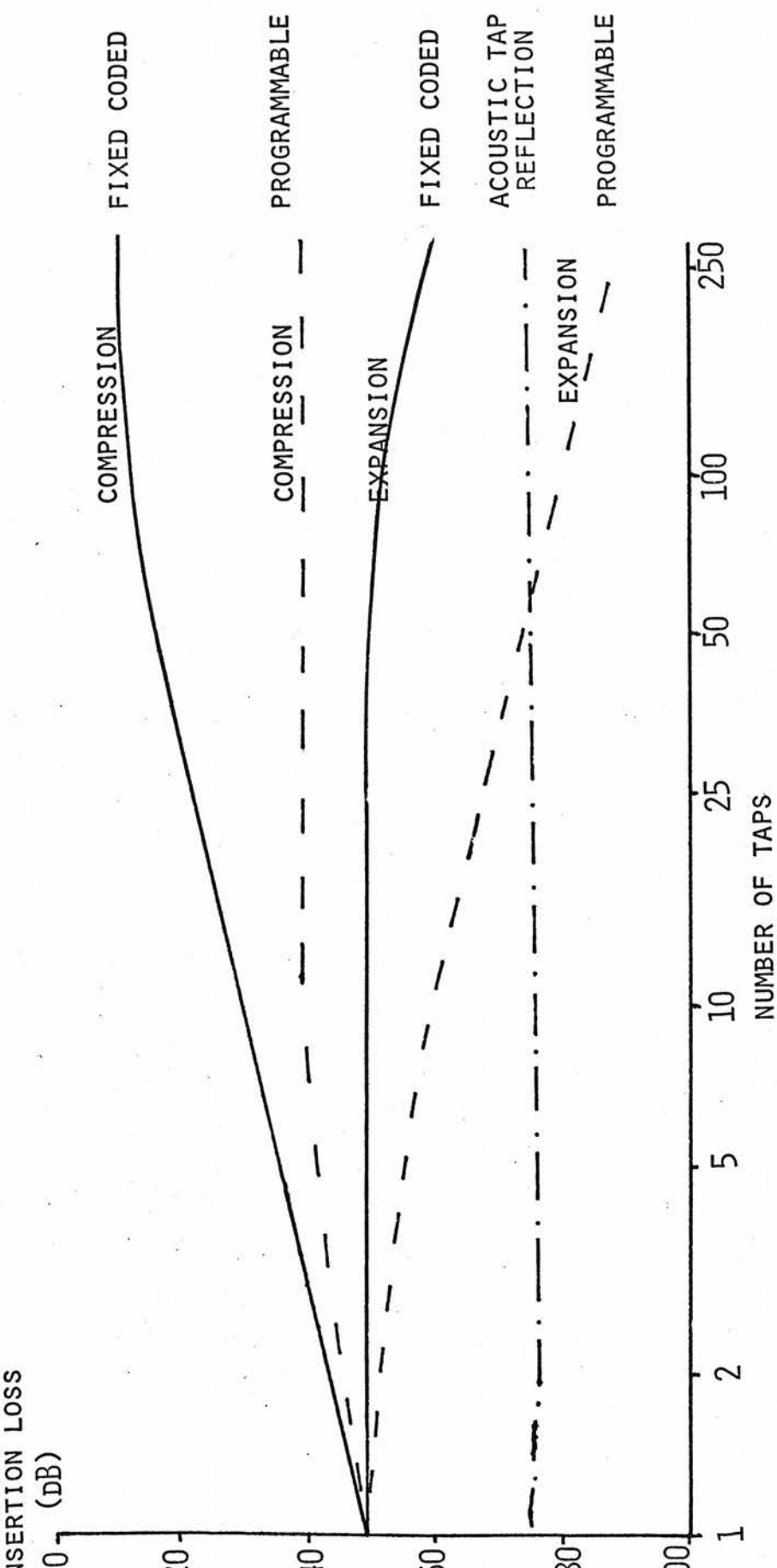


FIGURE 6.3 INSERTION LOSS COMPARISON FOR FIXED CODED AND PROGRAMMABLE AMF'S

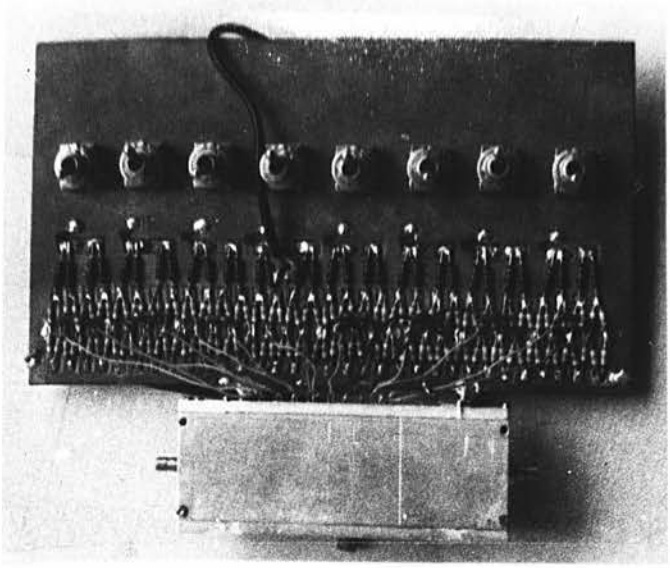

(a)

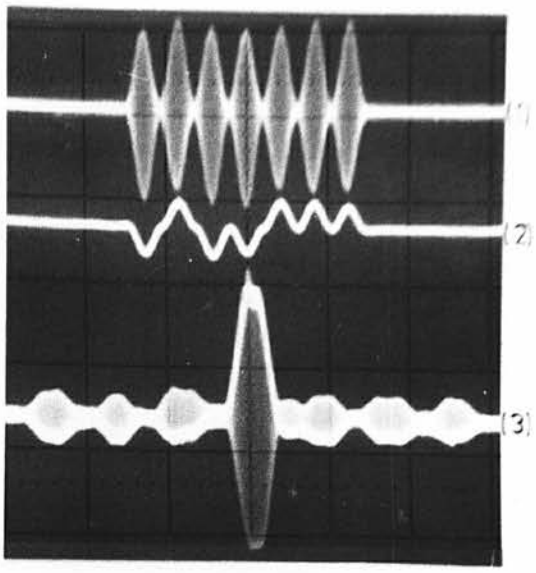


(b)

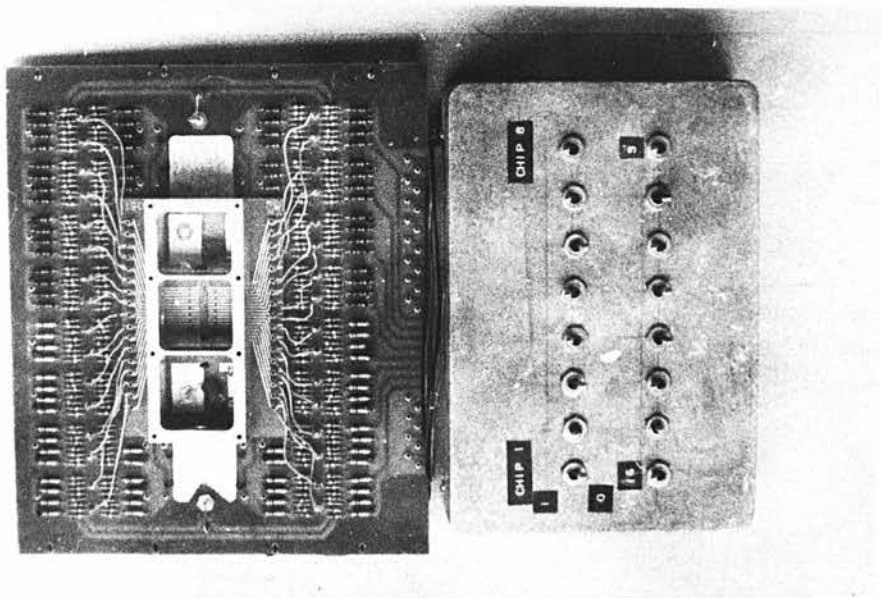


(c)

FIGURE 6.4 PROGRAMMABLE AMF'S EMPLOYING DISCRETE COMPONENT SWITCHES

(a) 8 TAP PAMF SHOWING SWITCH LAYOUT

(b) DETECTED PAMF PULSE AND CORRELATION RESPONSES (Horizontal scale 1 μsec per large division)

(c) 16 TAP SAW PAMF

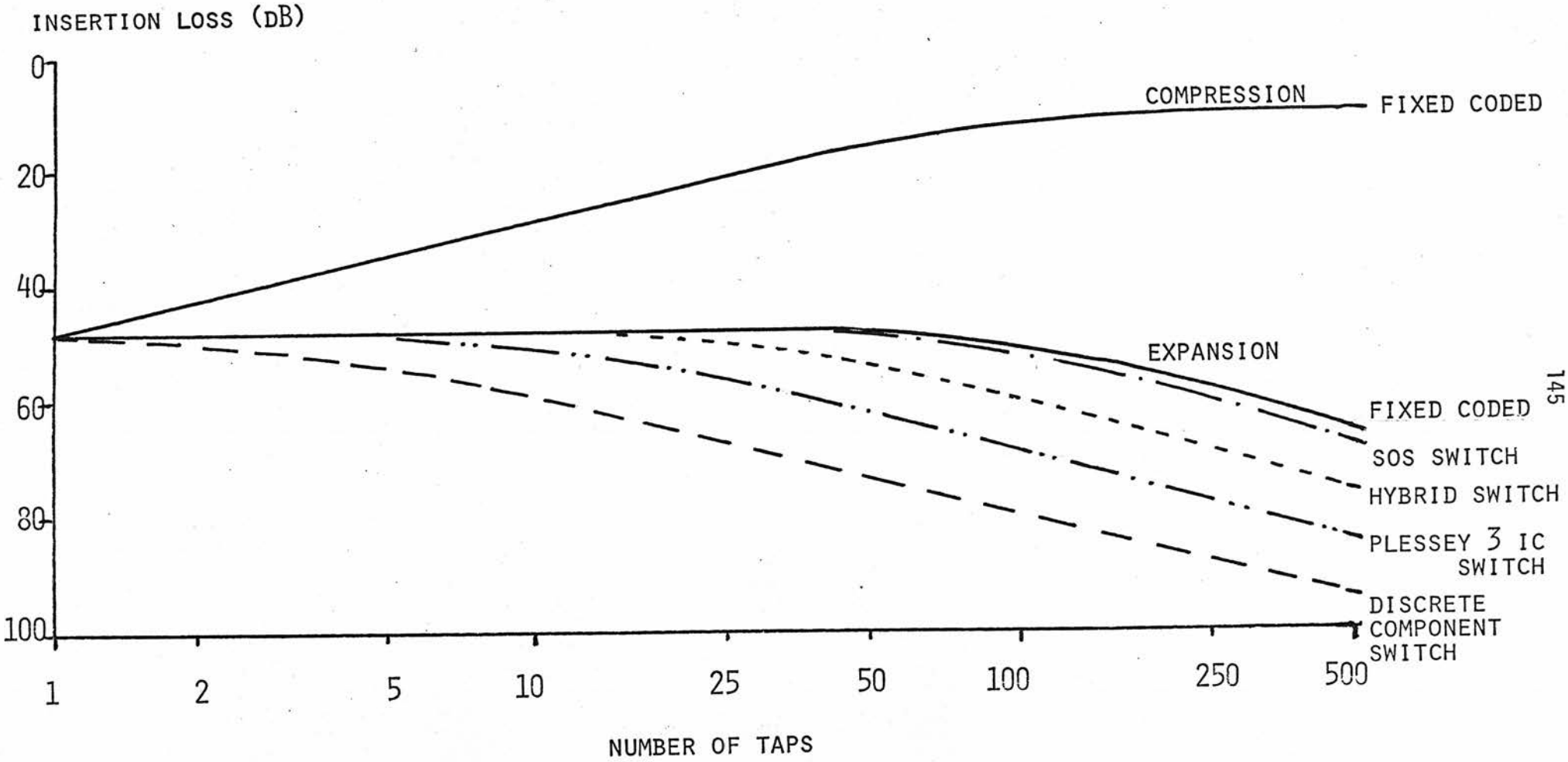


FIGURE 6.5 COMPUTER PREDICTIONS OF AMF INSERTION LOSS

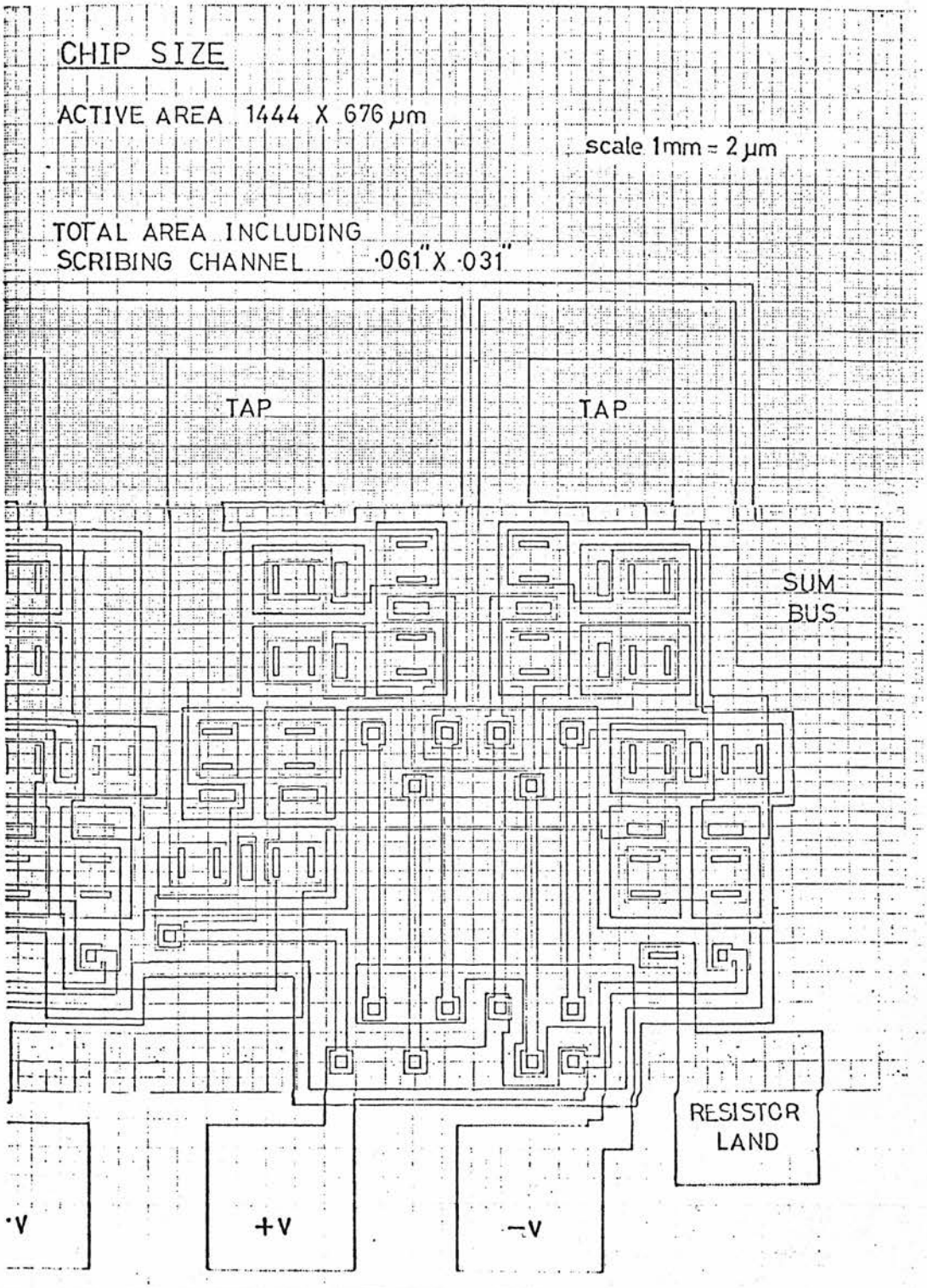


FIGURE 6.6 LAYOUT FOR ONE CELL OF AN INTEGRATED PAMF SWITCH COMPATIBLE WITH PLESSEY PROCESS 3 DESIGN RULES

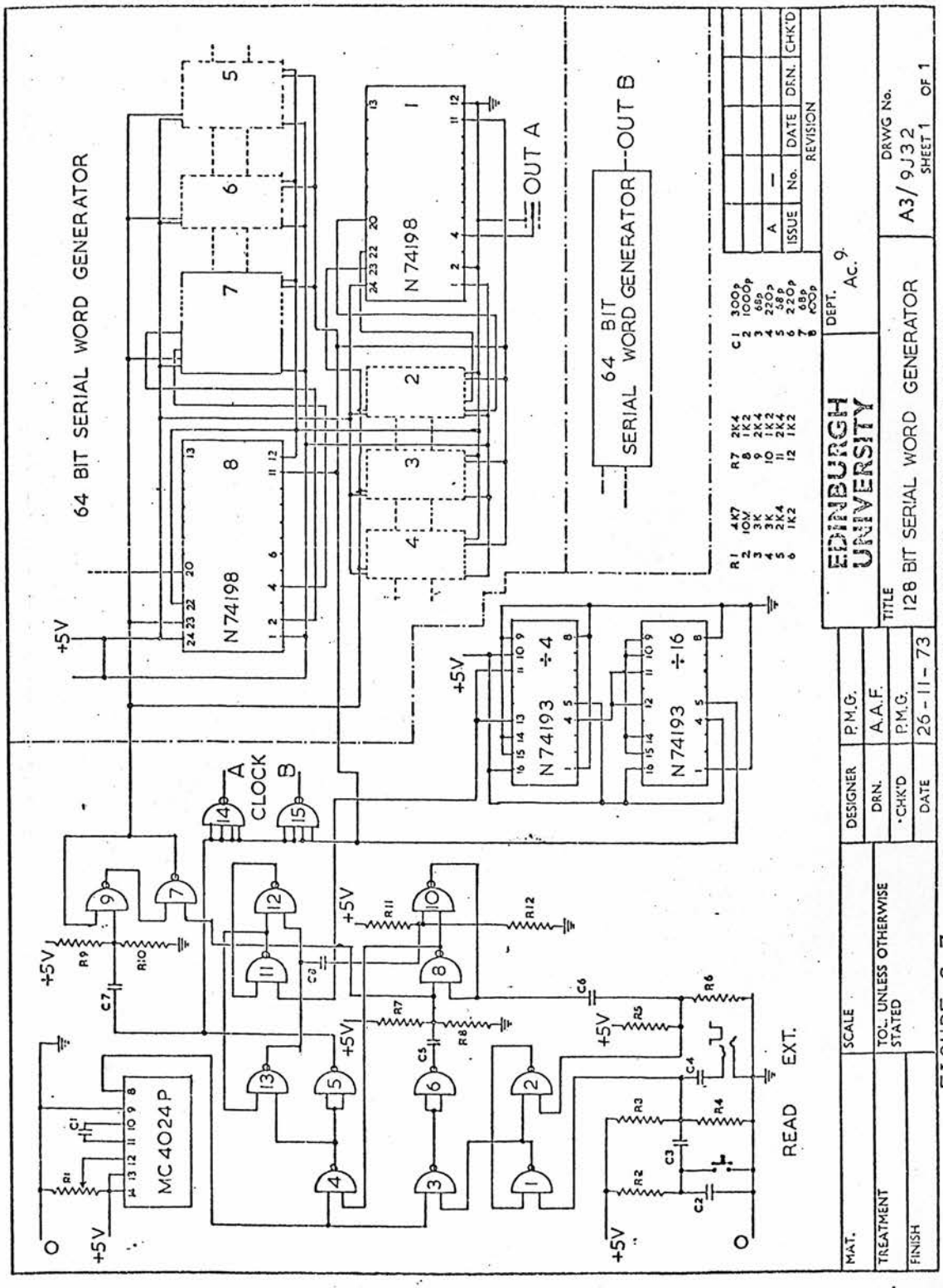


FIGURE 6.7 PROGRAMMABLE AMF REMOTE CODE SELECTOR

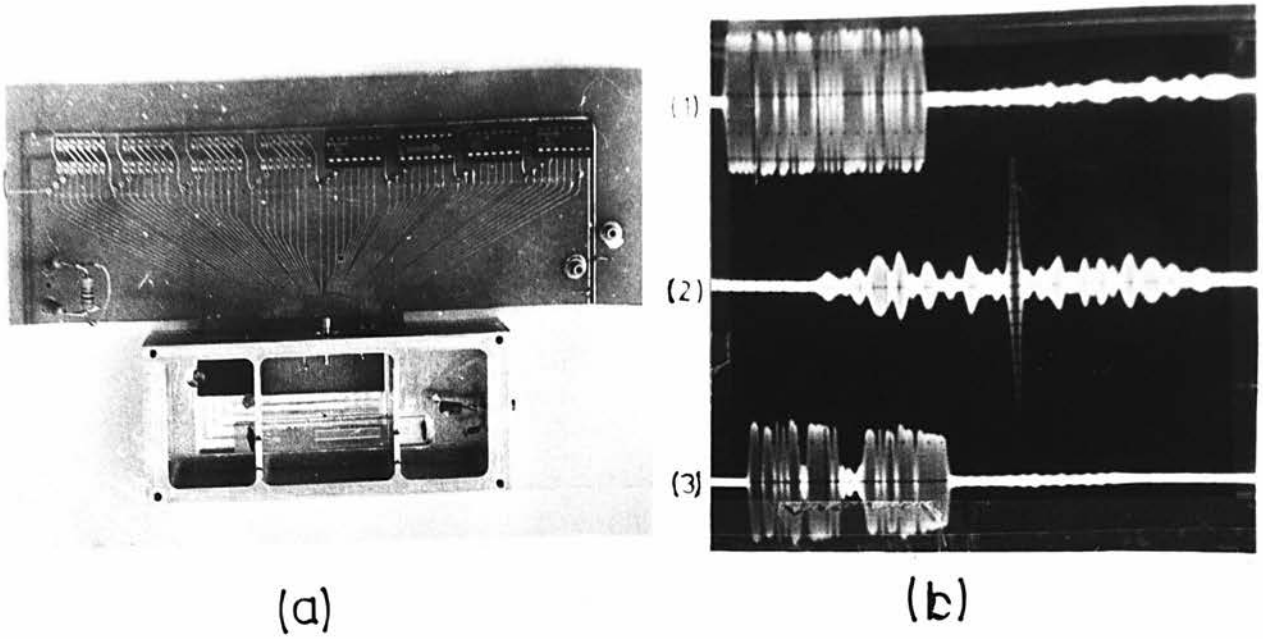


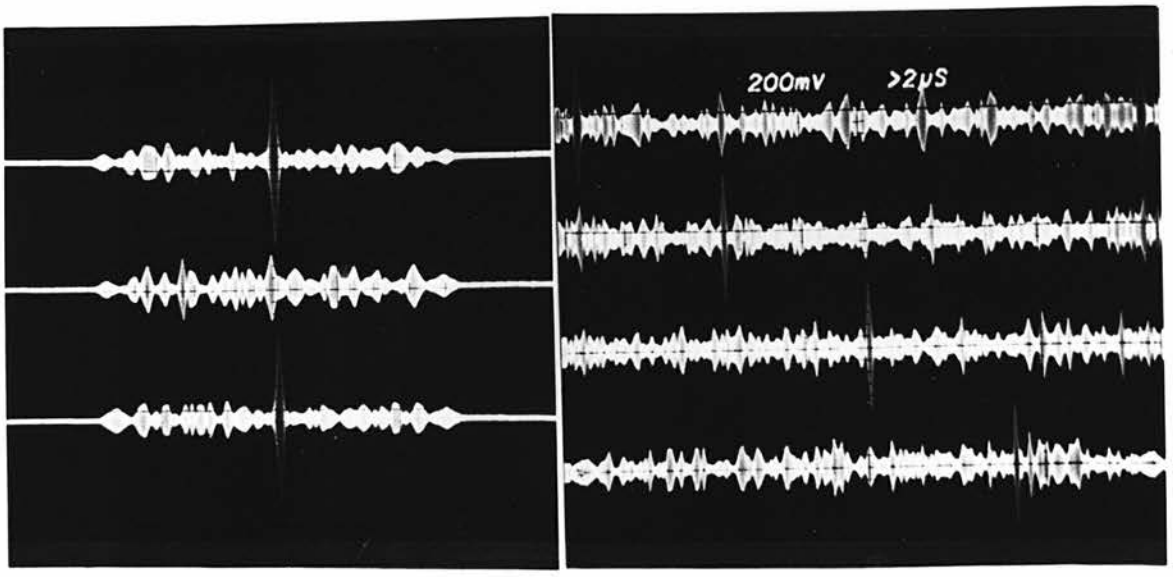


FIGURE 6.8 EA 4 SAW AMF WITH DOUBLE POLE DOUBLE THROW HYBRID SWITCH

(a) PHOTOGRAPH OF 31 TAP PAMF

(b) PRECODED AMF IMPULSE RESPONSE AND PAMF AUTOCORRELATION AND PULSE RESPONSES †

(c) PAMF CORRELATION PERFORMANCE WITH TWO DISTINCTLY CODED 31 CHIP SUBSEQUENCES †

(d) DETECTION OF A 127 CHIP SEQUENCE IN THE 31 TAP PAMF

(† horizontal scale 2 μsec per large division)

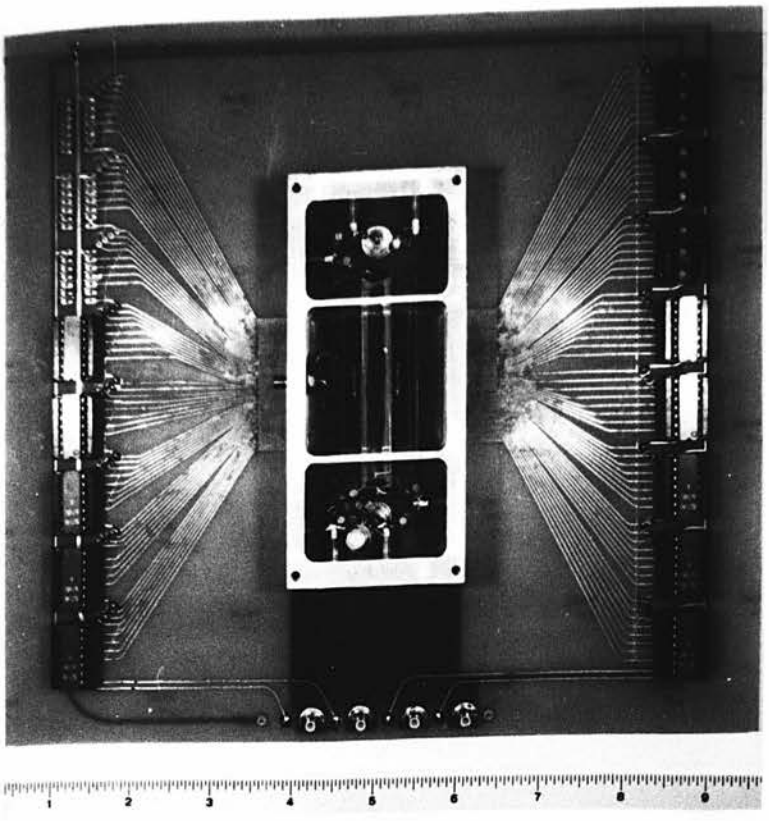

(a)

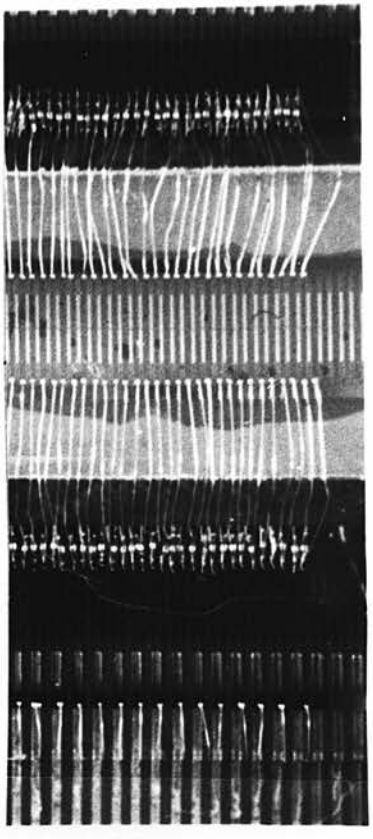

(b)

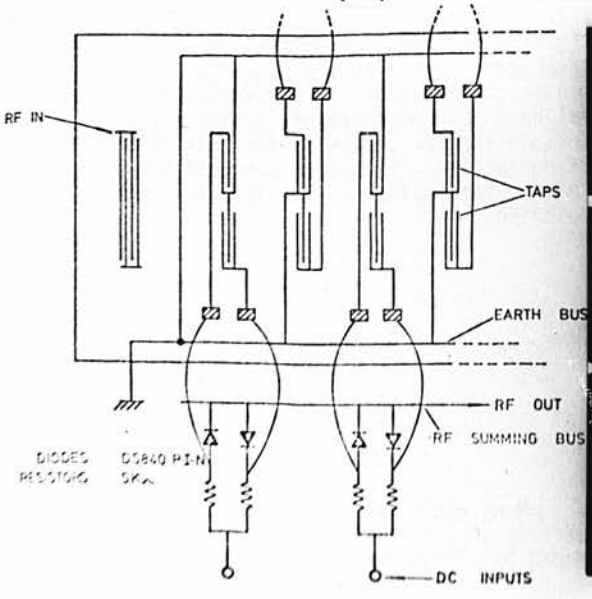


(c)

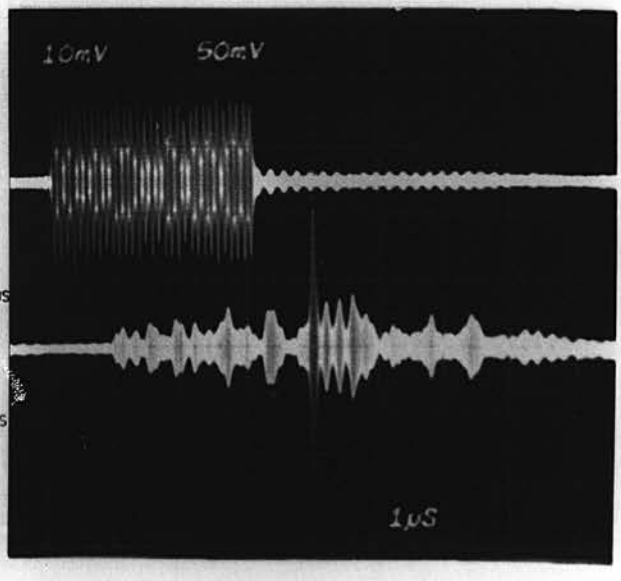


(d)

FIGURE 6.9 CONSTRUCTION AND PERFORMANCE OF THE EA 6 SAW PAMF EMPLOYING THE DUAL PHASE TAP DESIGN

(a) PHOTOGRAPH OF COMPLETE DEVICE
(b) DEVICE DETAIL HIGHLIGHTING HYBRID CONSTRUCTION
(c) SCHEMATIC OF SINGLE POLE SWITCH
(d) FIXED CODED AMF PULSE RESPONSE AND PAMF AUTOCORRELATION RESPONSE

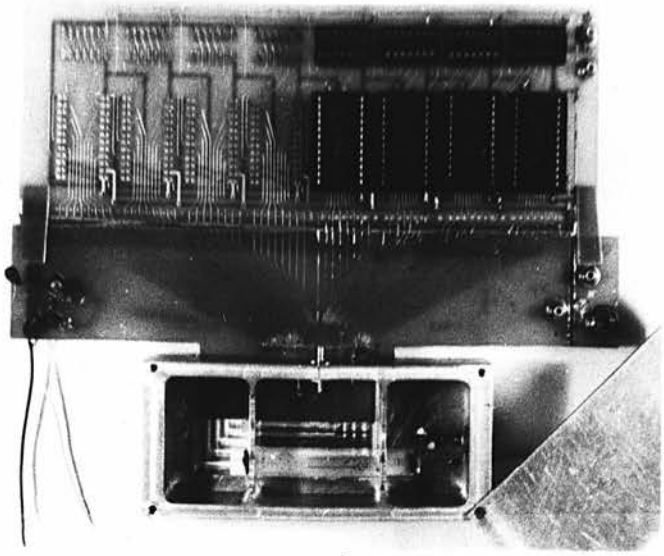

(a)

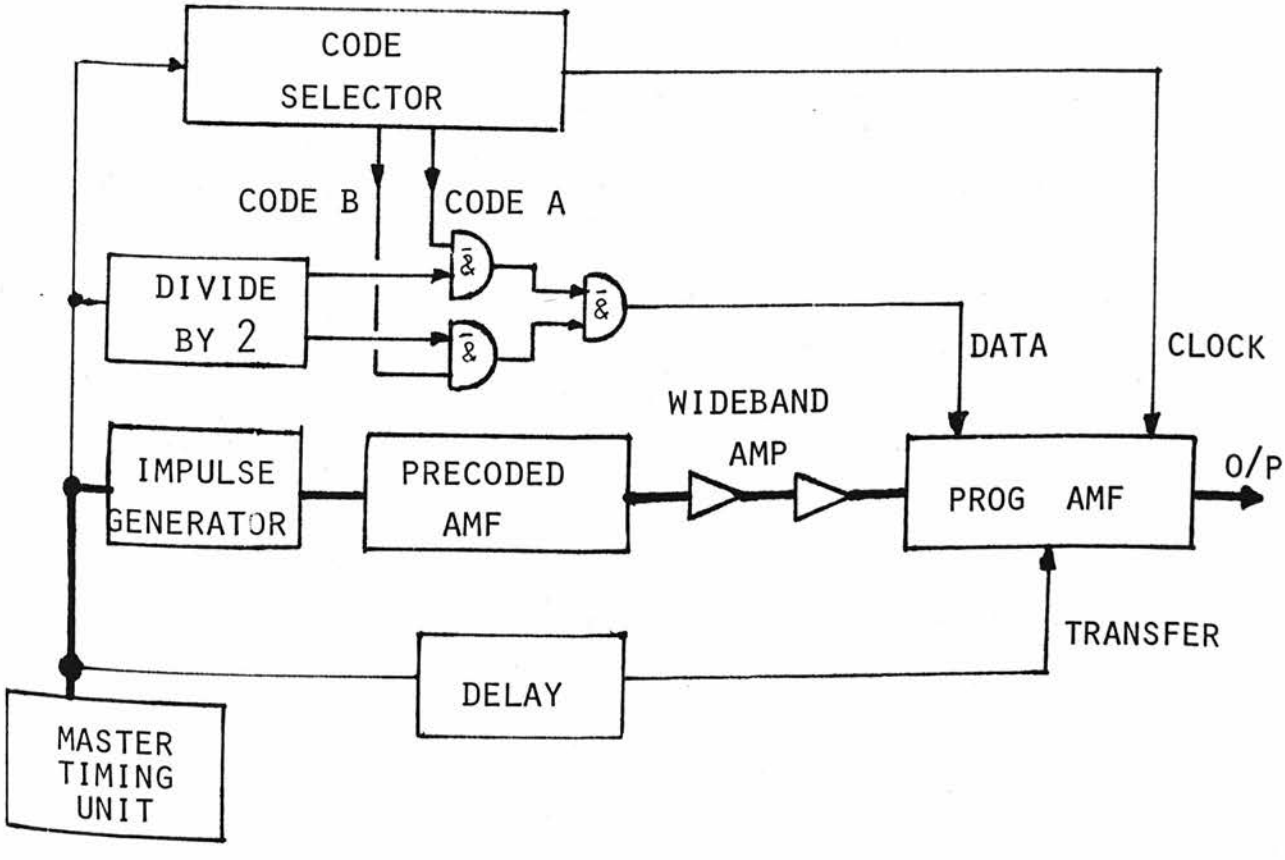


(b)

FIGURE 6.10 (A) FULLY ELECTRONICALLY PROGRAMMABLE 31 TAP EA 4 SAW AMF

(B) REPROGRAMMING TEST EQUIPMENT

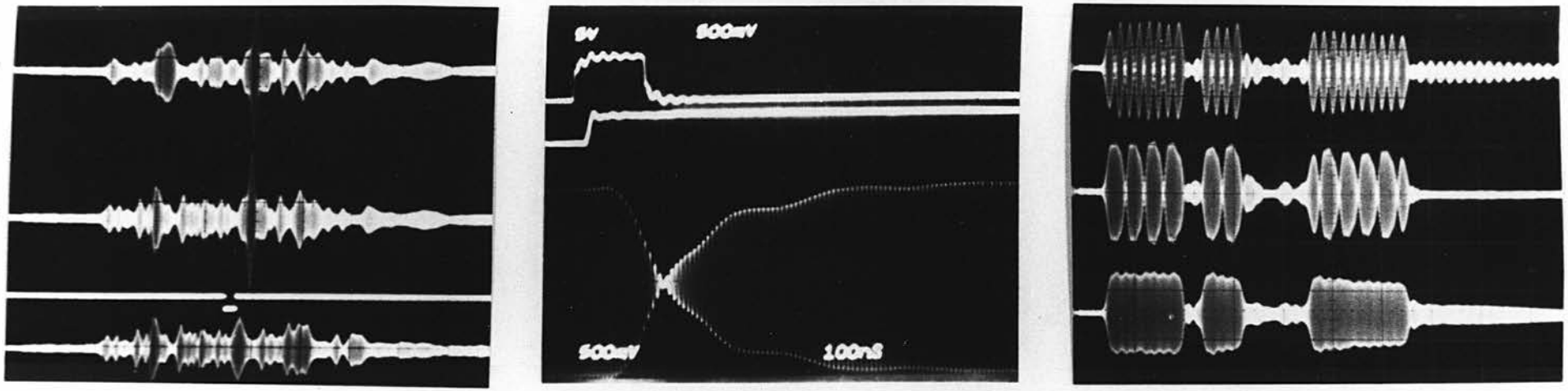


(a) (b) (c)

FIGURE 6.11 SAW ELECTRONICALLY PROGRAMMABLE AMF PERFORMANCE

(a) DEMONSTRATION OF THE FAST REPROGRAMME CAPABILITY

(b) DETAIL OF THE REPROGRAMMING DELAY

(c) IMPULSE RESPONSE SPURIOUS LEVELS WITH DIFFERENT AMF CODES

# 7. LARGE TIME BANDWIDTH PRODUCT PROGRAMMABLE MATCHED FILTER MODEM

## 7.1 THE SERIAL PARALLEL SIGNAL PROCESSING CONCEPT

Chapter 3 summarised many Spread Spectrum communication systems, highlighting the multitude of different signal coding formats currently used in these systems. All the reported systems used receivers which employ matched filtering techniques to permit the desired signal to be detected even when corrupted by noise and multisubscriber interference. The later chapters of the thesis have reviewed the high performance that was achieved when SAW techniques were used to fabricate fixed coded and programmable Analogue Matched Filters.

To date, the incorporation of these SAW components into simple communication modulator-demodulator (modem) configurations has favoured the use of fixed coded AMF's, primarily because designs of 127 tap AMF's are readily available. However, most practical systems require coded sequences of much longer time bandwidth (TB) product. This has necessitated the concatenation of several short coded sequences [94] from one or more AMF's if SAW techniques are to be applicable. Premature detection of the received signal in a short AMF, which cannot accommodate the complete code, is unsatisfactory as it does not achieve the full processing gain and hence is susceptable to interference and jamming. Other modems have evolved where several individual AMF's are combined with a single long wideband tapped delay line [55] to coherently process the complete coded sequence. These modems are still limited to sequence lengths of less than 50 μsec by the physical size of the substrate material. TB products of >1,000 are therefore difficult to obtain. In addition,

it is noted that all these modems are restricted, by the inflexibility of SAW precoded AMF's to the processing of fixed coded sequences. It is attractive therefore to investigate whether Electronically Programmable AMF's can be used to overcome this limitation.

The previous chapter concluded that the TB of SAW PAMF's was unlikely to exceed 256, which is considerably inferior to the 1,000 achieved with fixed coded AMF's[77] and modems[55]. This Chapter reports the extension of SAW *Programmable* Matched Filter capabilities beyond this limit using a Serial Parallel Signal Processing System. This technique was first reported by Burke[95] for the novel design of a large TB FH/PN receiver. In his coherent frequency synthesiser, the received signal was serially processed in a bank of frequency contiguous SAW precoded AMF's whose outputs were converted to a common IF for coherent summation in a SAW Recirculating Delay Line Integrator (RDLI)[96]. No practical results were reported,but Hunsinger[8] has demonstrated the performance of a SAW Serial Parallel Receiver (SPR) employing a single 127 tap fixed coded AMF and RDLI which achieved a TB of $10^3$.

This thesis reports the first demonstration of the detection of a continuous PN-PSK sequence in a SAW SPR which is capable of accommodating sequence lengths in excess of 1,000 chips. This fully *programmable* PN-PSK matched filter processes a signal which has a lower detectability than previous reported systems [55,94], making the receiver less sensitive to interference and jamming.

In the SPR, which is outlined in Figure 7.1, the input PN-PSK signal is initially processed in a *single* N tap SAW PAMF. This is reprogrammed M times, with updated N chip segments of a local reference code, to give a train of correlation peaks at the PAMF output. The

large time bandwidth is achieved by parallel summation of this train of correlation peaks in a SAW RDLI. Each individual peak is delayed making it time coincident with the following peak to achieve coherent summation of the entire sequence. In this manner, M seperate correlation peaks are integrated before the receiver is cleared with a dump pulse.

Although the receiver no longer possesses the fully asynchronous property of the SAW AMF, it requires only frame synchronisation to the local reference code, tolerating a received signal timing ambiguity equal to the propagation delay within the PAMF. With this slight penalty it is possible to design programmable PSK matched filters with TB's of $10^3$ to $10^4$ using a relatively simple PAMF with 100 taps and switching circuits. This immediately provides a vast cost reduction when compared to the $10^4$ switches required by a single PAMF.

The SAW modem described here can be used either to generate or to detect PSK IF signals. Since active code generation of PSK codes is relatively easy, this Chapter highlights receiver operation. It is here that the reduced hardware complexity of SAW techniques is especially attractive when compared with other microelectronic matched filtering realisations[29,30].

The SAW programmable PSK matched filter has immediate potential application in the Direct Sequence Spread Spectrum System[47]. It is here that the enhanced timing tolerance of the SAW SPR, compared to the existing active correlator, will provide more than an order of magnitude improvement in the system synchronisation (lock up) time.

## 7.2 THE SAW RECIRCULATING DELAY LINE

### 7.2.1 PRINCIPLE OF OPERATION

The block diagram of the RDL is included in Figure 7.1. The integrator sums a train of pulsed cw inputs, which are usually AMF correlation peaks, by delaying each pulse to make it time coincident with the following pulses in the train. It must provide exactly the correct delay to achieve coherence of the rf energy within the pulses. In addition, the loop gain must be maintained exactly at unity (K = 1) to obtain correct operation of the integrator. For an RDLI which is performing M recirculations, coherent summation gives a final signal voltage M times, and hence signal power $M^2$ times, the input level. Random noise adds incoherently to give an output noise power M times the input level.

$$\text{Hence, Processing Gain} = \frac{SNR_{OUT}}{SNR_{IN}} \qquad 7.1$$

$$= 10 \text{ Log}_{10} \left(\frac{M^2}{M}\right) \text{ dB} \qquad 7.2$$

$$= 10 \text{ Log}_{10} (M) \text{ dB} \qquad 7.3$$

Thus the serial parallel receiver shown in Figure 7.1 which incorporates an N tap PAMF has a total processing gain, with envelope detection :

$$\text{Receiver Processing Gain} = 10 \text{ Log}_{10} (N \times M) \text{ dB} \qquad 7.4$$

When operated with unity loop gain it is necessary to introduce a dump pulse which open circuits the loop after the Mth pulse has been added. This clears the integrator in readiness for the next train of

pulses. It also stabilises the loop against small variations in amplifier gain. Dump pulse duration must exceed $\tau$, the propagation delay in the RDL. Dumping is conveniently achieved by biasing a MCL ZAD 1 double balanced mixer to operate as an rf switch.

### 7.2.2 DESIGN CONSIDERATIONS

It is advisable to use an ST-X quartz substrate material for the RDL design to achieve temperature stable operation. Although the high coupling, hence low loss and large fractional bandwidth, of lithium niobate substrates is attractive, its high temperature coefficient, Table 1.1, and large triple transit responses makes it undesirable for RDL design.

Theory and experiment have shown that the SAW delay line is the critical component which affects the loop response. Both bandlimiting and spurious responses in the delay line are known to limit seriously the operation of the RDL.

#### Spurious Responses

Theoretical investigation of integrator performance[96,97] has analysed the effect of spurious signals and shown that both the *pulse* and *integration* responses of the RDL exhibit a decreasing signal to spurious ratio with increasing number of recirculations. In an RDL of infinite bandwidth with loop gain K, after successive recirculation of an input signal A, the output amplitude is given by the series

$$A\,[1 + K + K^2 + K^3 \ldots] = A\left[\frac{1}{(1-K)}\right] \qquad 7.5$$

If additionally the delay line has a time seperated spurious response S, it has been shown[97] that this signal builds up as the series

$$S\,[1 + 2K + 3K^2 + 4K^3 \ldots] \quad = \quad S\left[\frac{1}{(1-K)^2}\right] \qquad 7.6$$

Hence it is seen that the secondary response always grows faster than the required response by the factor $\frac{1}{(1-K)}$ .

Spurious responses in SAW delay lines are predominantly caused by bulk wave generation and reflection from the terminations and IDT's. Figure 7.2(a) shows the pulse response of an RDL incorporating a 100 MHz SAW delay line with a 20 period IDT's. The upper trace shows the response to a single 2 μsec wide input pulse which is continuously recirculated in a unity gain loop. Note that the delay line spurious signals, which are not evident in the first transit, appear after 3 recirculations and gradually increase in amplitude. The poor response shown here was caused by a reflection of amplitude -35 dB relative to the output pulse from a wax termination. The fault was later corrected with an angled tape absorber to give a spurious free RDL pulse response.

Triple transit pulses are not easily identified as they are time coincident with the pulses recirculated in the loop. However, they may be analysed theoretically using equations 7.5 and 7.6. It is interesting to calculate the expected degradation in a unity gain (K = 1) integrator, which is summing a train of 16 input pulses, to indicate the level of triple transit rejection required in the delay line. If the input pulse amplitude is A then equation 7.5 gives the final integrator signal output as 16A. From equation 7.6 it is

seen that the triple transit spurious response will sum over 14 recirculations to give an output

$$A \cdot S \cdot [1 + 2 + 3 + 4 \ldots 14] \qquad 7.7$$

where S is the relative amplitude of the triple transit compared to main delayed pulse.

$$\text{Hence, Total output} = A(16 + 105\,S) \qquad 7.8$$

If the triple transit pulse is to degrade the output by $<\frac{1}{2}$ dB then its magnitude must be <-41 dB.

This condition dictates that the delay lines must employ low Q electrical matching to reduce $\rho_{11}$. Measurements on the 12 period IDT delay line used in the SPR, whose performance is reported in Section 7.3.2, indicated that triple transit levels were ~ - 45 dB. This is equal, to within 1 dB, of calculated level for acoustic wave impedance mismatch reflections, indicating that the low Q matching was introducing negligible electro-acoustic reflection.

Bandlimiting

Any SAW delay line is a frequency filter whose response is governed by the design of the IDT's and matching networks. Recirculating integrators require a wide bandwidth to avoid degradation of the signal which undergoes multiple transits through the delay line IDT's. If sufficiently low Q inductor matching is used then acoustic bandlimiting is the predominant degrading mechanism. Bandlimiting increases the basewidth of the recirculated pulse and degrades the signal amplitude

as shown in Figure 7.2(a). The lower two traces show the response of the same delay line when the input signal bandwidth is increased by using pulsewidths of 1 μsec (middle trace) and ½ μsec (lower trace). Figure 7.3(a) compares the frequency response of two loosely coupled SAW delay lines. The trace with the narrow peak shows the response of a delay line employing 20 period IDT's in which the acoustic Q limits the 3 dB bandwidth to 4.5%. Reducing the Q by decreasing the number of IDT periods to 12 gives a higher insertion loss and the flatter frequency response shown in the other trace (3 dB bandwidth of 7%).

Figure 7.3 (b) illustrates acoustic bandlimiting diagramatically. The figure shows the time domain distortion when a pulsed cw electrical signal is converted, at an IDT, into an acoustic wave by summing the contributions from each electrode finger. The diagram shows particularly severe distortion which could have been reduced considerably by employing a narrower bandwidth electrical signal.

Acoustic bandlimiting has been studied with a computer analysis which applies the distortion shown in Figure 7.3(b) to the input and output IDT of a SAW delay line. The programme[96] evaluates both the pulse and integration response of an RDL for any bandwidth of input signal with either triangular or rectangular pulse envelopes. It is always assumed that the input cw frequency is matched to the delay line centre frequency, $f_o$. For an RDL with 20 period IDT's the computer programme predicts the 16th pulse amplitude as 99%, 88% and 57% with the input pulsewidths of 2 μsec, 1 μsec and ½ μsec. These results agree closely with the traces illustrated in Figure 7.2(a).

Degradation of these pulse amplitudes is reflected in degradation

of compression gain when the RDL is used in the integrating mode, RDLI. Figure 7.4 shows computer predictions of the RDLI performance when *integrating* a series of 16 triangular envelope signals which represent the PAMF correlation peaks generated in an SPR. Curves are presented for fixed degradation as a function of the delay line IDT periods and fractional bandwidth of the coded signal. The curves illustrate that the RDLI suffers a 2 dB degradation when recirculating a 5% bandwidth signal in a three period IDT delay line. These results demonstrate that single period IDT's are the optimum choice for the design of RDLI's. However the high insertion loss incurred is a severe disadvantage. 12 period IDT's are preferred for ease of stabilising the feedback loop, and thus they are subsequently used in the prototype SPR described in Section 7.3.2.

With dumping at the end of the integration period, it is possible to increase the loop gain above unity by ~ ½ dB to compensate for acoustic bandlimiting and achieve a linear signal growth. However a simple analysis, which neglects bandlimiting, shows that either an increase or decrease of 1 dB from unity in the loop gain, reduces the processing gain obtainable by~1 dB[98] within a sixteen transit integrator. Both programmes [96,98] take into account only the IDT amplitude response and further theoretical analysis is required therefore to establish the precise relationship between delay line frequency response and loop gain on the integrator signal processing performance.

This section has reported many problems that have been encountered in RDLI construction. However, it is important to note that SAW techniques compare favourably with other realisations such as those based on Charge Coupled Device Technology[62].

## 7.2.3 RECIRCULATING DELAY LINE PERFORMANCE EVALUATION

The SAW RDL was implemented with the components shown in Figure 7.1. Dumping and signal summation were conveniently achieved with a double balanced mixer and wideband transformer coupled summer, respectively. The loop gain was verified by introducing a narrow-band pulse into the RDL. Adjusting the gain, to make the 1st and 20th pulse have the same relative amplitude, $\pm \frac{1}{2}$ dB, was found to be the optimum method of setting the single transit loop gain to an accuracy of better than $\frac{1}{10}$ dB. Fine gain adjustment was obtained by varying the supply voltages of the Avantek UTA 417 B feedback amplifier.

RDL *pulse* response is shown in Figure 7.2 (a) and (b). Illustration (a) compared the response of the same 20 finger pair delay line to 3 different pulse widths while (b) shows the response of three different 100 MHz delay lines to the same 0.5 μsec pulse used in the lower trace of illustration (a). The upper trace of (b) was obtained with the original 20 period IDT delay line and the middle and lower traces with delay lines which incorporated 12 and 3 period IDT's respectively. The theory[96] again predicts that the 16th pulse will have a relative amplitude of 82% in the 12 period delay line and 100% in the 3 period line, which agrees closely with the observed results. These traces demonstrate the importance of ensuring that the delay line possesses sufficient acoustic bandwidth to minimise signal degradation.

Figure 7.2(c) shows the *integration* response of the 6.4 μsec 12 period IDT RDLI. The input signal is a continuous train of 100 MHz pulsed cw, generated at a 156.25 kHz repetition rate, matching

exactly delay in the integrator. The upper trace shows the integrator response, summing 120 pulses prior to dumping the loop. Integration occurs at a comb of input frequencies corresponding to the precise delay at which coherence is obtained between the cw in the input and recirculated pulse. Varying the 100 MHz carrier by $\pm$ 156.25 kHz adds or subtracts one cycle of the rf signal in the RDLI giving an integrator output of slightly reduced amplitude. The middle trace shows the integration of three of the 300 nsec wide input pulses after two recirculations. The lower trace shows the final pulse after 120 recirculations to illustrate the effect of band-limiting.

Although the RDLI can be used to coherently process any pulsed rf signals the main interest here is to use it to increase the time bandwidth product of SAW AMF's. Figure 7.2(d) shows the correlation response of the 6.4μsec integrator when summing a series of correlation peaks from a 31 tap EA 4 fixed coded AMF. A high fidelity of response is evident but no improvement in peak to sidelobe ratio is obtained from the concatenation of 20 identical short coded sequences. For Spread Spectrum applications this form of code synthesis does not achieve a large code alphabet, and in addition the receiver will be sensitive to cross correlation with the other subscriber codes. These disadvantages can be overcome only with the programmable matched filter modem which marries a SAW Programmable AMF with the RDLI's described here.

## 7.3 THE SURFACE ACOUSTIC WAVE SERIAL PARALLEL RECEIVER

### 7.3.1 TEST SYSTEM

The SAW Serial Parallel Receiver, shown in Figure 7.1, was constructed[99] with the 12 period IDT delay lines discussed earlier

and the 31 tap fully electronically programmable AMF reported in Section 6.5.5. The SPR was designed to process 100 MHz carrier signals PSK modulated at a 5 MHz chip rate.

The test system constructed to generate the SPR local reference code and the continuous PN-PSK IF input test signal is shown in Figure 7.5. These peripherals were necessary to permit an accurate evaluation of the receiver performance. HP 1930 Pseudo Random Bit Sequence (PRBS) code generators were used as they conveniently generate the long PN codes required to programme and test the SPR. The receiver local reference code was generated in the *Master* PRBS with a local 5 MHz clock. The PRBS output and clock pulses were directly interfaced with the PAMF serial code store. Coding of the PAMF was accomplished by the transfer command which reprogrammed the device in 32 chip code blocks. The command was obtained from a seperate 32 chip transfer counter. To achieve stable operation, for display on an oscilloscope, this counter was reset by the Master PRBS trigger pulse at the start of each sequence. This trigger pulse was also used to dump the contents of the RDLI loop.

With a code generator designed to provide the local reference PRBS and load it into the SPR it is necessary to obtain a test signal to evaluate the receiver performance. This was accomplished with an identical 1930 *Slave* PRBS which is reset from the Master PRBS with a delayed trigger pulse. Varying the delay controls the phasing between the two generators permitting measurement of the tolerance in receiver timing. Owing to the slow response of the 1930 reset input (< 1 μsec) it was convenient to reset the Slave PRBS for a complete code sequence. This was performed by the

external sixteen bit reset counter. The PRBS test signal is phase modulated,with a MCL ZAD 1 double balanced mixer, onto the output of a HP 8640 B VHF signal generator. A synthesised generator was chosen to stop carrier drift from degrading the evaluation of the large TB (> 1000) receiver . This system generates a test signal comprising a long burst of cw followed by fifteen repetitions of the desired coded sequence. The identical Master and Slave PRBS codes are selected either on front panel switches or by external programming inputs.

### 7.3.2 RECEIVER PERFORMANCE

The inset traces of Figure 7.5 show the SPR performance when correlating a continuous 127 chip PN-PSK sequence. The first trace shows the input 100 MHz test signal continuously modulated by a 127 chip code at a 5 MHz rate. The second trace shows the output of the 31 tap PAMF which is reprogrammed in 32 chip code blocks to give a correlation peak every 6.4 μsec. The continual reprogramming gives 4 accurately spaced correlation peaks in place of the single correlation peak which would be obtained from a fixed coded AMF. The 4 correlation peaks are coherently summed in the integrator as shown in the third trace.

Performance is further shown in Figure 7.6. Illustration (a), upper trace,shows the integration of a 2047 chip code in the SPR. This was obtained by reprogramming the PAMF 64 times during each code sequence. The test signal generates continuous 100 MHz cw signal prior to modulation with the repetative 2047 chip code. Hence,the start of the trace shows the SPR suppression of narrowband interference. The non-linear growth of signal is caused by the

delay line bandlimiting described in Section 7.2. Increasing the loop gain above unity by $\frac{1}{2}$ dB ($K \cong 1.05$) compensates for the non-linearity but degrades the theoretical processing gain achieved in the receiver[98]. The second trace shows a correlation peak at the PAMF output for comparison against an attenuated version of the final integrator output, lower trace, illustrating the severity of the bandlimiting.

Figure 7.6 compares, in (c), the noise free receiver performance against, in (d), that obtained under strong cochannel interference, typical of the conditions experienced at the receiver input in a DSSS system. The upper trace shows the input PN-PSK signal, the centre trace the PAMF output and the lower trace the integrator output. In (d) the input SNR is ~ -12 dB and after serial processing in the PAMF the SNR is improved to ~ 0 dB. Further signal integration in the RDLI gives a final SNR of ~ +12 dB. Degradations in processing gain are evident between observed 24 dB and theoretical 33 dB due mainly to faulty taps in the PAMF, signal breakthrough and bandlimiting in the RDLI. When operated with a more modest number of recirculations, eg 8, the modem was found to give a processing gain within 2 dB of theoretical.

Measurements on the modem have shown that the SPR tolerates a timing variation of $\pm$ 3.0 μsec in received signal without any loss in output signal amplitude. This is very close to the $\pm$ 3.2 μsec theoretically achievable. The sensitivity to Doppler in the SPR was measured as 1.1 $\pm$ 0.2 kHz for a 3 dB drop in final pulse amplitude and 2.5 $\pm$ 0.2 kHz offset for a null in the integrator output. These results agree closely with theory[30,76] which predicts

an offset to the first null of :

$$\Delta f = \pm \frac{f_o}{EL} \qquad 7.9$$

where $f_o$ = carrier frequency (100 MHz)

E = Number of cycles per chip, ie, PAMF input IDT Periods (20)

L = N x M = Number of chips in the integrator (2047)

giving a $\Delta f$ = 2.44 kHz.

Although the SPR is sensitive to changes in input frequency the structually imposed AMF tap coding sets the receiver code rate making it relatively insensitive to a small variation in the local clock frequency. These changes introduce only a slight alteration in the precise instants at which the PAMF is reprogrammed by the transfer command. A $\pm$ ½% variation in clock rate was found to reduce by 1 µsec and 3 µsec tolerance of the receiver to input signal timing. This property is potentially attractive for achieving improved synchronisation in a DSSS system using an SPR operating in a simple serial search mode. Other proposed search routines correlate the received signal against the local reference code for a fixed integration period. If an output is not obtained from the integrator, then a section of code must be skipped before attempting the next integration. This requires considerable sophistication in local code generator design when compared with a serial search routine.

Figure 7.6(b) compares the performance of the SPR with TB of 511 firstly at unity loop gain, upper trace, and secondly in the middle trace with a ½ dB reduction in loop gain (K = 0.95). With

reduced gain it is possible to dispense with the dump pulse as shown in the lower trace. This mode of operation makes the SAW SPR similar to the video integrators employed for radar signal processing[100]. Coherent input signals still integrate but the output decays when the pulse train stops or loses coherence. This is not clearly seen in the lower trace as the bandlimiting causes adjacent 511 chip coded sequences to merge, even though there is a one chip shift between sequences. This stable mode of RDLI operation might possibly be attractive for a DSSS search routine in which the receiver searches continuously for synchronisation until the SPR output exceeds some predetermined threshold.

## 7.4 SUMMARY

The programmable PSK matched filter has demonstrated the capabilities of SAW devices to achieve time bandwidth products which have been previously unobtainable in a single programmable SAW PAMF. When operated as a receiver, SPR mode, the modem achieved close to theoretical processing gain. The ability to tolerate enhanced timing ambiguity, compared to the active correlator, ideally suits it for the urgent requirement of reducing the lock up time in existing DSSS systems. Extension of the receiver concepts described here promises the capability to accommodate signals with delays > 1 msec. This development will permit SAW Spread Spectrum signal processors to be incorporated into many existing 2.4 K baud data rate systems.

The receiver did possess a degradation from the theoretical processing gain when the time bandwidth product exceeded 255. This arose predominantly from direct electromagnetic breakthrough of both

the input and programming signals in the PAMF and RDLI. Other practical deficiencies , such as small variations in loop gain with signal level, which limit the dynamic range of the RDLI to typically 25 dB,are also known to contribute to the degradation in processing gain. Further investigation of these deficiencies , combined with studies of SAW wrap around delay lines[101] which might also include a gain controlled InSb feedback amplifier[102], seem destined to offer substantial future performance improvements for large TB ($>10^3$) programmable matched filters receivers.

The application of the easily fabricated SAW acoustic convolver[5,64] in place of relatively complex PAMF, is also attractive for increasing receiver bandwidth and hence improving the matched filter TB product *particularly* in the context of wide band spread spectrum applications. Here the low convolver efficiency and consequent high drive levels required are likely to introduce further practical problems in the design of the high dynamic range SAW integrator. The convolver also requires additional microelectronic circuitry to generate a segmented and time reversed reference signal. However, the actively modulated reference is potentially attractive as it permits tracking of any Doppler shift which is present on the received signal, a function which cannot be performed with the SAW PAMF and RDLI.

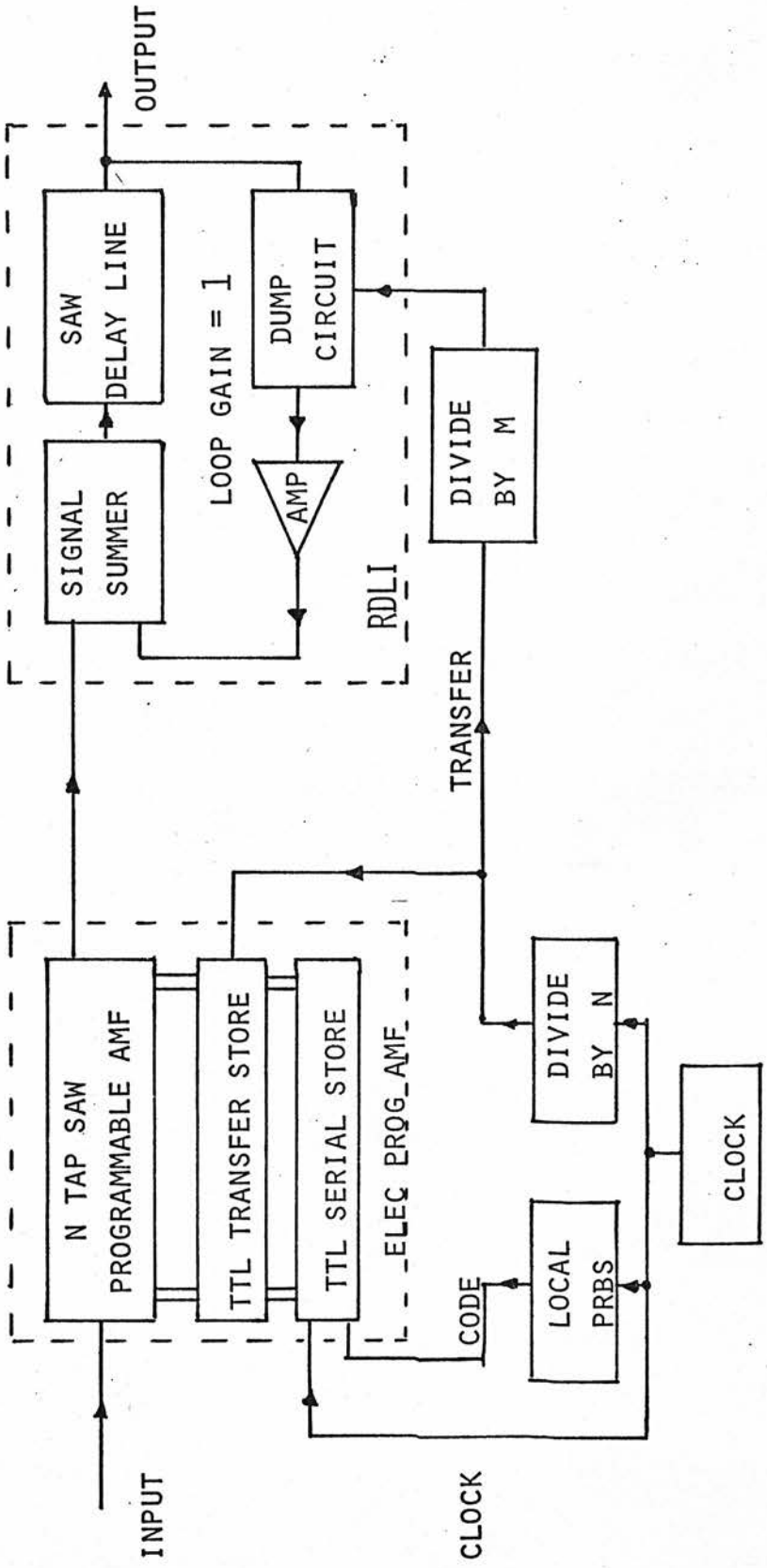


FIGURE 7.1 SAW PROGRAMMABLE SERIAL PARALLEL RECEIVER

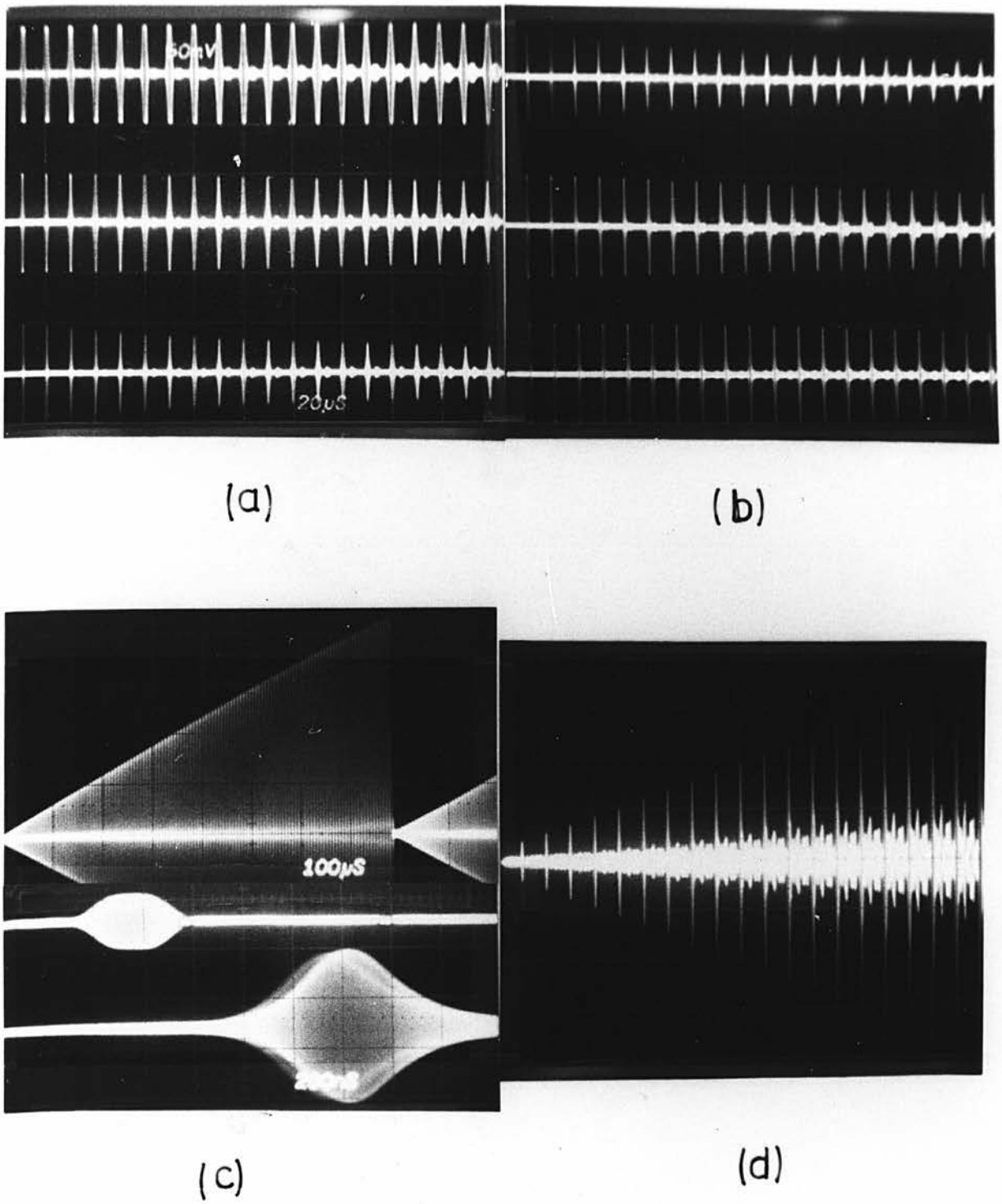


FIGURE 7.2 SAW RECIRCULATING DELAY LINE PERFORMANCE

(a) PULSE RESPONSES OF A 100 MHz SAW RDL INCORPORATING 20 PERIOD IDT's

(b) COMPARATIVE PULSE RESPONSES OF THREE 100 MHz SAW RDL's WITH 20, 12 and 3 PERIOD IDT's

(c) INTEGRATION RESPONSE OF AN RDLI WITH PULSED cw INPUTS

(d) RDLI RESPONSE WITH INPUT CORRELATION PEAKS FROM AN EA 4 FIXED CODED AMF

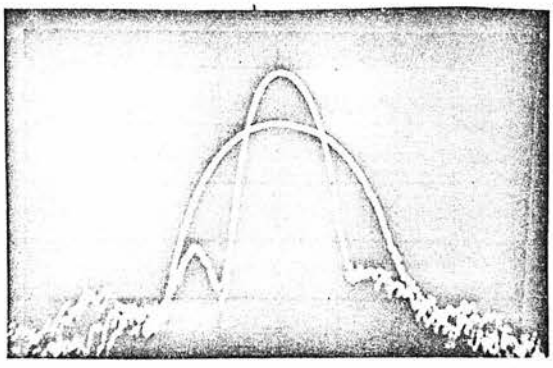

FIGURE 7.3

(a) FREQUENCY RESPONSES OF TWO SAW DELAY LINES WITH 12 and 20 PERIOD IDT's (vertical scale 10 dB per large division, horizontal scale 3 MHz per large division).

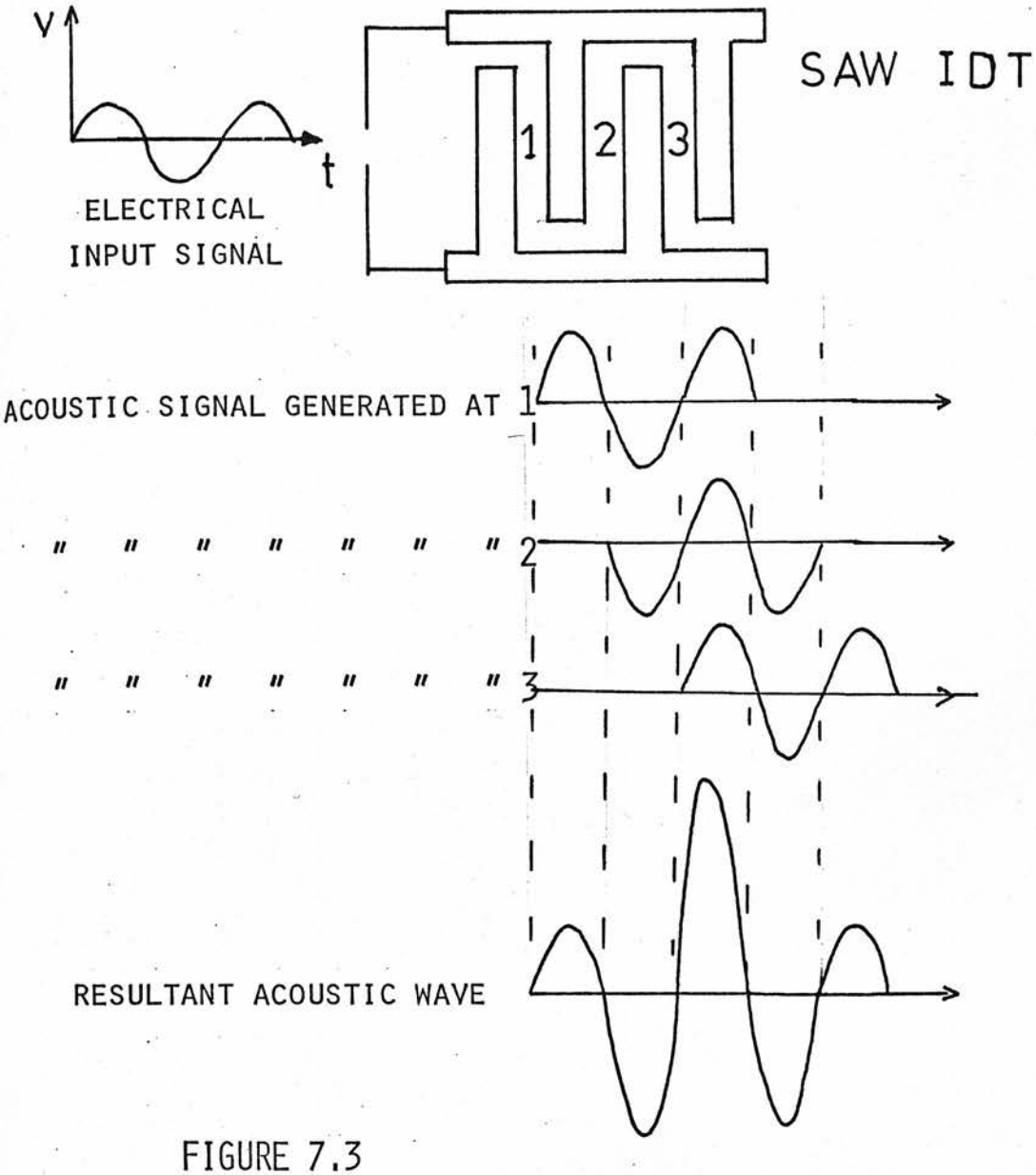


FIGURE 7.3

(b) HIGHLIGHTS THE DISTORTION WHEN AN INPUT ELECTRICAL SIGNAL IS CONVERTED TO AN ACOUSTIC WAVE AT A SAW IDT

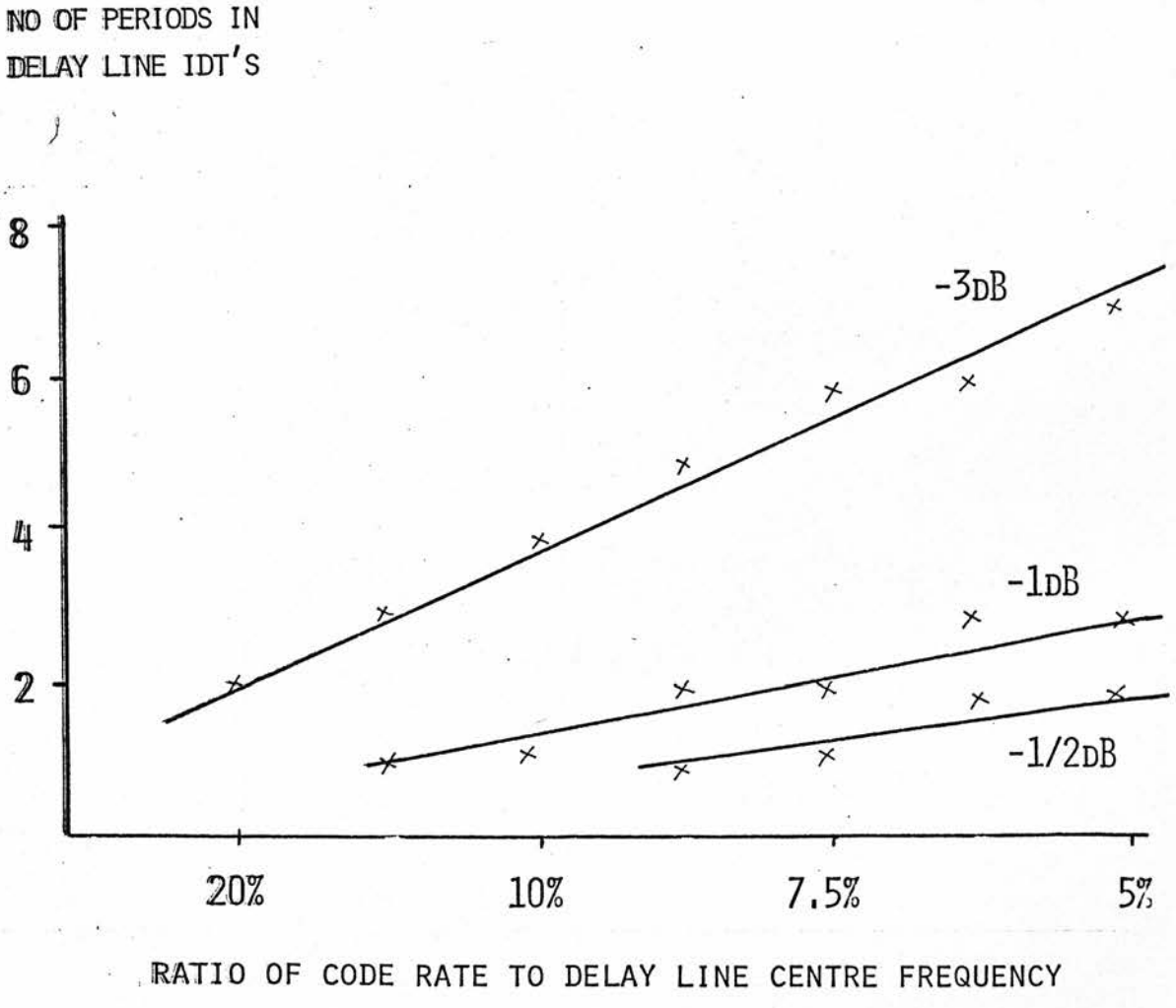


FIGURE 7.4 LOSS IN COMPRESSION GAIN DUE TO ACOUSTIC BANDLIMITING WHEN PERFORMING 16 TRANSITS THROUGH RDLI

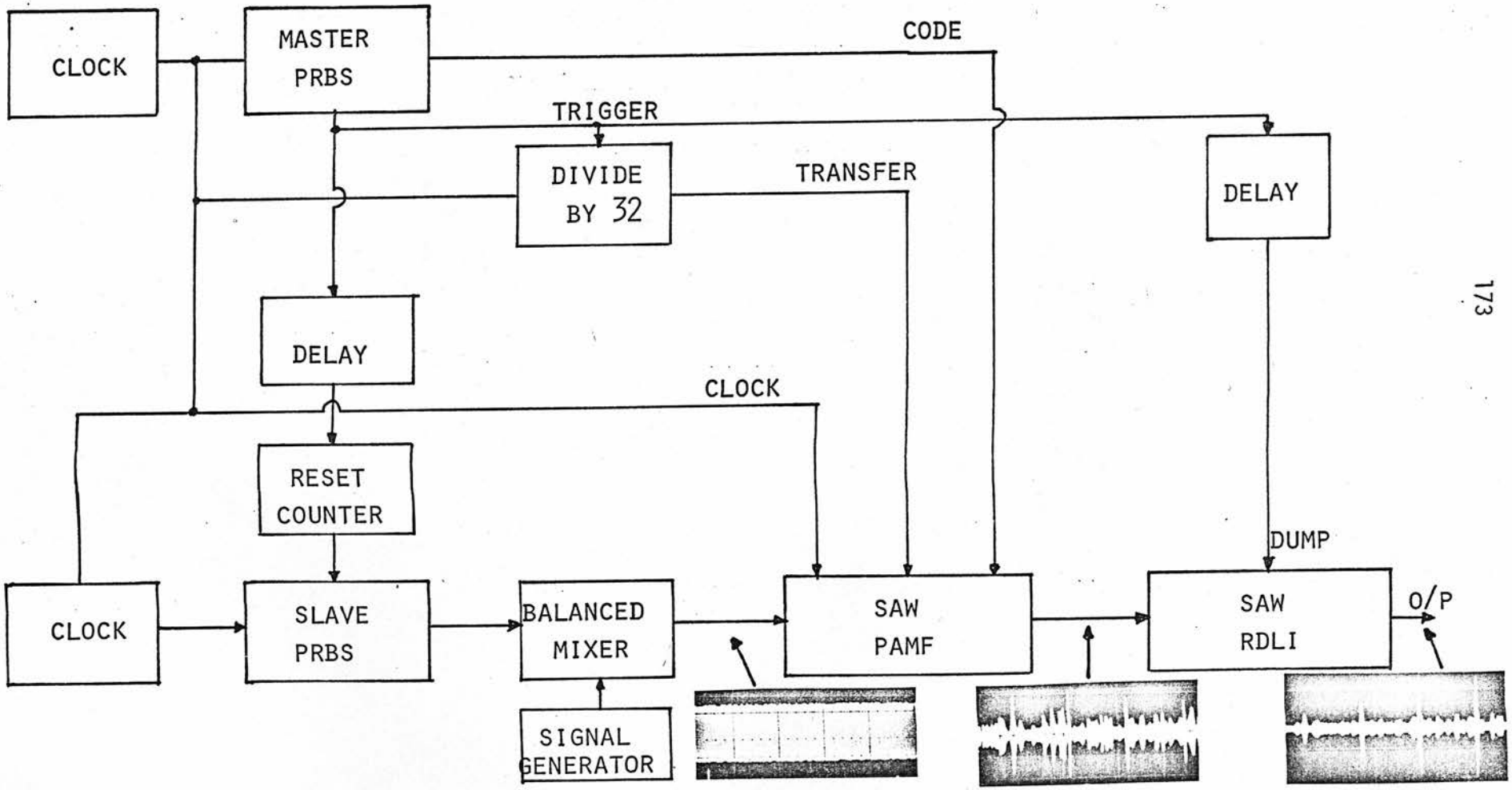


FIGURE 7.5 TEST ARRANGEMENT FOR EVALUATION OF SAW SERIAL PARALLEL RECEIVER

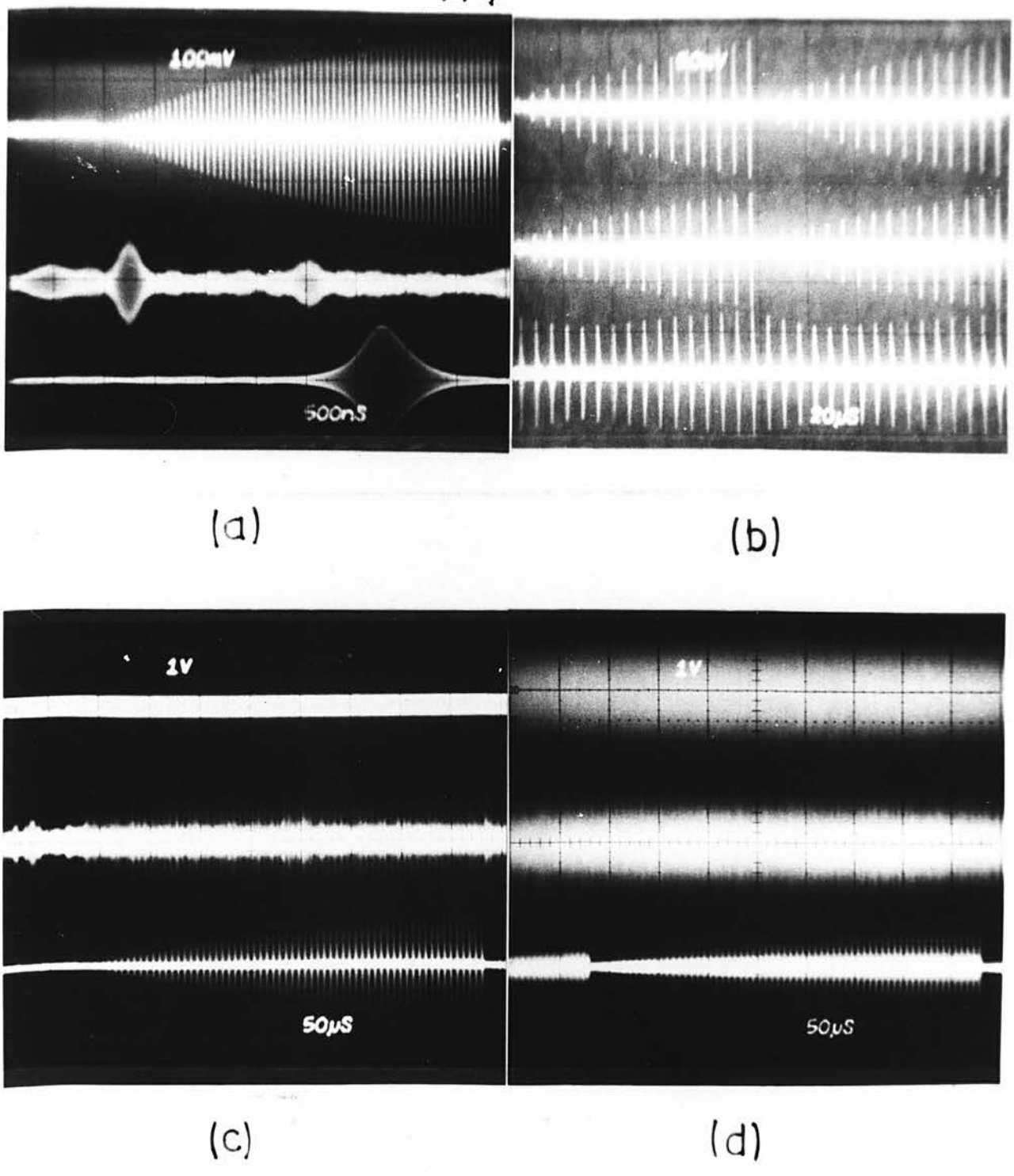


FIGURE 7.6 SAW SERIAL PARALLEL RECEIVER PERFORMANCE

(a) CORRELATION OF A 100 MHz SIGNAL BIPHASE MODULATED BY A 2047 CHIP CODE AT A 5 MHz RATE

(b) INTEGRATOR RESPONSE AT K = 1 and K = 0.95 WITH AND WITHOUT DUMP PULSES

(c) and (d) COMPARE THE SPR OPERATION UNDER NOISE FREE CONDITIONS WITH STRONG CO-CHANNEL INTERFERENCE

# 8. SAW COMPONENT APPLICATIONS IN AIR TRAFFIC CONTROL

## 8.1 INTRODUCTION

Chapters 2 and 3 of this thesis have thoroughly investigated the application of a broad range of SAW devices to conventional and Spread Spectrum communications. This Chapter studies some of the unique signal processing requirements of Air Traffic Control (ATC) systems[103,104], which encompass both communication and radar principles.

Several reviews have been presented on the procedures and equipments currently employed in ATC[28,104] which highlighted the similarities existing between ATC and conventional communications equipments. This Chapter does not duplicate the studies of the latter equipments in Chapter 2, but rather it attempts to review the new ATC system proposals and investigate the application of the novel signal processing capability of SAW devices. Therefore,it concentrates on the application of Spread Spectrum signal processing techniques to proposals such as the Civil AEROSAT North Atlantic ATC System[106,107], the Collision Avoidance Surveillance (CAS)[52] programme and the Integration of Communication Navigation and Identification (ICNI)[51] signals for military ATC.

## 8.2 CURRENT AIR TRAFFIC CONTROL SYSTEMS

### 8.2.1 PROCEDURES

The prime objectives of the ATC system are to provide safe, expeditious and economic operation of aircraft movements. The control of air traffic involves the use of a multitude of equipment hardware encompassing ground based surveillance and identification

equipments to enable the ground based controller to know the position and identity of aircraft; accurate on-board navigation equipment for pilot position determination; and voice communication equipment to handle message transfers between pilot and traffic control. Current ATC can be subdivided into terminal, continental and oceanic areas.[105] Terminal procedures involve the scheduling of take-offs and landings of aircraft to meet the available capacity. En route control over-land is accomplished by constraining the aircraft to fly along agreed airways. Transoceanic control involves a two-way structure of tracks or air corridors which are exclusively allocated across the North Atlantic by the oceanic planners. In all these flight phases exclusive ATC authority is maintained by the ground based controllers.

In contrast military ATC, McColl[104], involves a more comprehensive surveillance facility requiring tracking of both friendly and enemy aircraft. With large areas of airspace reserved for military use there are fewer constraints on the pilot who exercises exclusive control requiring the incorporation of navigation, surveillance and communication equipments of increased accuracy to meet the demanding requirements of intercept and strike manoeuvers.

### 8.2.2 EXISTING EQUIPMENTS

Table 8.1 highlights current and proposed ATC equipments[28] in the three main areas of communications, navigation and surveillance illustrating the duplication and integration of equipment functions. Existing communications are handled by voice procedures on either a VHF or HF net depending on the range to the ground-based antenna. LORAN and OMEGA are both examples of external reference hyperbolic

navigation systems[108] utilising one-way ground-derived signal transmissions. Conversely, the civil DME and military TACAN[109] overland equipments operate by two-way interrogation of a ground-sited transponding beacon. Inertial[108] is one example of a self-contained navigation equipment which is now fitted as standard in the jumbo jets. Primary and secondary radar[110] (SSR for civil and IFF for military applications) are the fundamental surveillance equipments. In summary the ATC system of the world's airways is a complex integration of airborne and ground based equipments, procedures and facilities embracing many different technologies.

### 8.2.3 DEFICIENCIES IN CURRENT SYSTEMS

Continental en route and terminal surveillance is all performed with ground based radar. However primary radar coverage cannot extend to oceanic crossings, and it is particularly subject to rain and ground clutter. This can be minimised with circular antenna polarisation or moving target indication. However, the use of a wider bandwidth chirp waveform with pulse compression[110] is attractive for reducing of the range cell to approximately the same size as the target aircraft. Typical parameters are a 25:1 pulse compression ratio with a 5 μsec transmitted pulse length, linearly frequency modulated over 5 MHz. SAW pulse compression networks have not found application in primary radar installations but they are in use in airborne radar[111] where the technological advantages of size and weight are more applicable.

To reduce the problems of ground and rain clutter on the primary radar display, and to aid target identification, ATC controllers make extensive use of the cooperative SSR data link. The SSR system

requires each aircraft to carry a transponder which replies to an interrogating signal from the ground, with a coded reply on a separate frequency. This eliminates the interference experienced in primary radar from other reflecting objects. The SSR signal may either be displayed independently on a Plan Position Indicator (PPI) or correlated with the primary radar returns for authentification of targets. Further processing of the reply signal data content in a code extractor permits the aircraft's identity or height to be displayed alongside the target. This system provides the basic data for computer processing in a terminal control system such as ARTS/MEDIATOR[112] which is used in heavily congested areas.

The SSR airborne transponder replies to an interrogation with an on-off keyed (OOK) sequence of up to 15 pulses, each 0.45 μsec long,[105] transmitted within a 20.3 μsec frame period. The system is susceptable to impulsive interference or 'fruit' which is caused by the ground based receiver detecting a transponder replying to interrogations from another SSR site. As these replies are not synchronised to the interrogation rate, they can be removed with plot extraction prior to the PPI display. Another interfering mechanism, 'garbling', is caused by two aircraft in close proximity both replying to an interrogation. The overlapping of replies often makes it impossible to decide which codes were transmitted. A new selective address system (ADSEL/DABS), described by Amlie[104], is under development to overcome the problem of 'fruit' and reduce the number of 'garbled' replies. However, in common with all ATC systems it is impossible to replace existing hardware overnight with an improved system.

A SAW tapped delay line can be used to resolve 'garbled' replies from aircraft with differential spacings of less than 3 km[113].

The input signal is fed into a SAW TDL which has been set to 'look for' a particular return, ie a specified OOK signal ('1's and'0's) which makes up the 20.3 μsec code. The signal from each of the taps is individually detected and the outputs from the '1' taps are summed to form the signal in Channel A, while the complementary Channel B, gives the sum of detected outputs from the '0' taps. When the correct code is received, the output from Channel A is the auto-correlation function of the code while Channel B gives the cross-correlation between the input code and its polarity complement ('1's and '0's interchanged). When the output voltage, Channel A-Channel B, is selected the time sidelobes for a 'correct' return are reduced giving a consequent reduction in false detection rate. Figure 8.1 shows the performance of a 15 tap SAW linear correlation receiver separating two identical returns with several different levels of overlap. It has demonstrated a significant improvement over the existing system at a cost which does not preclude incorporation into existing ground stations where 'garbling' is a problem.

A second SAW device, the Inverse Filter, has also been designed[13] to further improve this system. The matched filter[67] is known to give the optimum signal for threshold detection against white noise. By contrast, the inverse filter provides improved resolution of inter-symbol interference in communication systems and the clutter dominated returns experienced by many radar systems. These filters, which can be applied to any signal waveform, are potentially useful where system constraints do not permit the transmitted waveform to be chosen for optimum resolution and where signal to noise ratio is not a problem. The inverse filter has been reported[13] to provide an improvement in pulse compression ratio of nearly an order of magnitude over the matched

filter. It is anticipated that the application of the SAW inverse filter to the delay line tap design of the previous system will produce a shorter output pulse permitting resolution of overlapping returns with <70 metres spacing.

In addition to these problems, other deficiencies,arising predominantly from poor HF oceanic communications and the growth in air traffic movements,are pressurising ATC authorities to install automatic equipment. To this end, several major ATC system developments are under active consideration for deployment within the next two decades. The following section addresses the potential application of SAW signal processing techniques to some of these systems.

## 8.3 FUTURE AIR TRAFFIC CONTROL SYSTEMS

### 8.3.1 SYSTEMS CONCEPTS

This section reviews the basic concepts of several of the new ATC system proposals which were briefly mentioned in Section 8.1. The recently developed microwave satellite repeaters[38,106], Section 2.2.4, already have a proven record of reliable operation in civil communications. The large area coverage of a synchronous satellite, compared to several tens of SSR ground stations, suggests that satellites can offer considerable improvements in ATC surveillance and data handling systems[114].

One prototype satellite ATC system, AEROSAT, is now under development. However there are still many technical problems to be solved. The optimum choice of signalling technique for the satellite to mobile link is uncertain as the power budgets are very marginal[106,114]. Digital Spread Spectrum (SS) signalling techniques look attractive

especially when it is noted that there is a trend to partially replace voice by data. The low activity factor of ATC messages also favours SS accessing in place of conventional FDMA and TDMA techniques.

In addition to developments in signal processing,there is a desire in military ATC to Integrate the Communicaton Navigaton and Identification signalling functions into a common *comprehensive* equipment. Section 8.3.5 reports this development, which offers a reduction in power consumption, number of antennae and maintenance while improving spectral occupancy. *Conversely* the Collision Avoidance Surveillance (CAS) proposals, Section 8.3.4, aim to achieve comprehensive ground based surveillance with a *cheap* airborne transponder ranging system which will be carried by all aircraft.

It must be noted that this survey is in no way comprehensive. Other collision avoidance proposals, such as the RCA SECANT[115] system, are not reported here. This is important, as SECANT invokes a complete change in ATC philosophy, placing the onus for air safety back with the pilot.

### 8.3.2 AEROSAT

The North Atlantic Aeronautical Satellite System, AEROSAT[107], is intended to provide an extension of positive ATC surveillance and voice communication over the busiest oceanic air traffic route in the world. The system proposes initially to utilise two satellites accessed through two Oceanic Control Centres, with each satellite placed in synchronous orbit over the ends of the present oceanic track system[105].

Surveillance is to be performed with an active ranging system of 1 nmi accuracy based on chirp, multiple tone or digital techniques. This is accomplished by selectively interrogating the aircraft through one satellite[107] prior to detection and timing of the reply, containing onboard altitude information, which has been routed through the two satellites. To meet the traffic forecasts it is proposed to design six communications channels, three in each satellite. System planning allows the use of one Satellite voice channel as a 1.2 kilobaud DPSK data link to cover the entire control area. The specification of L Band transmissions is likely following the reservation of a substantial band from 1558.5 to 1660 MHz[105] for Aeronautical Radio Navigation and Communication.

It is intended to evaluate a pre-operational system using the ATS-6 satellite in 1975 to ascertain both the optimum voice modem and ranging techniques, and also to investigate fully the problem of multipath returns from sea reflections. As envisaged, the AEROSAT system which is likely to be the first operational Satellite ATC system, is to use narrowband signals which cannot be processed easily in currently existing SAW devices. However, following evaluation of the pre-operational system it may be necessary to use Spread Spectrum coding techniques with matched filter detectors to achieve satisfactory satellite to aircraft power budgets.

8.3.3 HIGH INTEGRITY L BAND DATA LINK

This data link confines reporting of position information to a single communications channel by utilising one-way signal transmissions combined with a selective address system. The arrangement of subscriber accessing on an unsynchronised poled basis is attractive for the accommodation of individual aircraft interrogation rates

suitable for both subsonic and supersonic transports. Accurate navigation information, which is now available on the flight deck from the new Inertial Navigation equipments, can be accommodated within a *fixed length* message format (eg, 120 bits) along with an address preamble. High integrity, the measure of the number of *correctly* received messages for a given number of messages outputed (or displayed), is vital in ATC data links. It can be achieved for fixed length messages by the application of the baseband encoding techniques of Parker[50].

The system incorporates a high level of message redundancy to avoid a '1' being interpreted as a '0', and vice versa in the receiver. With four-signature data encoding[50] one encodes both for data level '1' or '0', and for position, odd or even, in the message sequence. In the receiver, the detected baseband pulses are present on four wires feeding the decoding tri-state register. After clearing the register to the non-determinate state, in readiness for the next message, the first data bit,which appears as an odd '1' in Figure 8.2(a),clocks only the first stage to a '1' and removes the inhibit from the second stage. The received data therefore provides the decoder shift pulses necessary for asynchronous operation. With fixed length messages a single check bistable is required on the final stages to ascertain that no errors have been received before outputing the message onto the display.

The four signatures can be readily obtained by using four audio tones within the allocated frequency channel,which for L Band operation could be easily generated with the SAW oscillator discussed in Chapter 1. Detection is also possible with SAW MFSK filters as described by Lever[8]. Spread Spectrum techniques using asynchronous SAW AMF's

are attractive for this system. Two signatures can be realised with two chirp pulses : one positive slope and the other negative slope. A further pair of chirp waveforms with a different centre frequency make up the four signatures. PN-PSK coding could also be employed but large TB's are necessary to reduce the cross-correlation products to acceptable levels[59].

The overall system operation, which is represented in Figure 8.2(b), encompasses the feeding of the incoming data stream in the transmitter into a four signature encoder which routes the data on to four busses to impulse the associated filter and generate the required coded signature. The filter outputs, at IF, are then summed, amplified and upconverted to L Band. In the receiver the down-converted IF signal is fed into the four conjugate matched filters, each of which gives an output on one of four lines which lead to the tri-state decoder.

In conclusion,this system is ideally suited to the selective addressing of aircraft on long oceanic crossings for obtaining automatic *error free* direct readout of onboard inertial navigation equipment without any aircrew participation. It is anticipated that the system would easily accommodate the requirements for ground based surveillance in the AEROSAT system.

### 8.3.4 RANGE DIFFERENCING NAVIGATION AND SURVEILLANCE SYSTEMS

Figure 8.3 shows the concept of active and passive navigation systems[78] employing either round trip or one-way signal transmissions for ranging by propagation time measurement. The use of PN-PSK Spread Spectrum coding techniques is advantageous both to distinguish the required signal and to measure accurately the time of arrival.

These techniques, which have been demonstrated with chirp signals[53], will require an accurate trade-off against cw tone ranging to establish which system is best suited to any specific application.

In addition to navigation systems there are proposals for surveillance systems[52], for use primarily in the Continental United States, which have as an essential requirement the inclusion of all aircraft. The proposed method of operation involves a one-way ranging system for bandwidth conservancy. Each aircraft is equipped with a beacon transponder radiating a unique coded ranging signal[78], which is routed to a ground based control centre through several widely spaced satellites. As no synchronisation exists between the aircraft and the ground station, the use of four or more satellites permits the calculation of absolute user position. For accurate receiver timing and separation of the returns from the many aircraft in the system, it is proposed to PN-PSK modulate the transmissions with a coded sequence. This permits the use of a matched filter in the receiver to detect the required signal and to provide a timing accuracy equal to one chip of modulating code.

With this system, it is impossible to obtain the necessary 100,000 codes, for unique identification of each aircraft. It is proposed to generate these identities using unique combinations of codes, pulse repetition rates, pulse placements and transmission frequencies. For example, one proposal[52] utilises a single transmission frequency of 1.6 GHz with a modulation rate of 10 MHz. With 25 different 511 chip PN-PSK codes it is possible to obtain a quarter of a million unique addresses. The received signals could be recognised and timed, as shown in Figure 8.4 prior to inputing

the PRP analysing and tracking computer which predicts any likely conflicts. SAW devices have been evaluated seriously for both generation and detection of the coded sequences used in this system.

### 8.3.5 INTEGRATION OF COMMUNICATIONS NAVIGATION AND IDENTIFICATION EQUIPMENTS

ICNI is a *military* concept requiring a signal format of high security and information fidelity when subjected to multipath returns, interference, jamming and spoofing signals. The design of any system requires careful balance to provide the improved operating capability at reasonable cost. The Mitre prototype system[8, 51] utilises a single communications channel, common to all users, and organises subscriber allocation with a TDMA system. One way transmission provides bandwidth conservation removing the self interference experienced in the SSR two way transmission systems. The system parameters have been developed principally for the United States Air Force tactical theatre of operations requiring a capacity of 100 accesses per second with a 600 bit maximum message length and coverage range of 600 miles diameter.

A typical subscriber might utilise one 10 msec slot per 10 second time frame to transmit position, identity, mission, fuel and ordinance status etc with ample provision for error detection and correction, utilising an onboard clock to time the start of transmission. The 10 msec time slot is split into three parts[51], a 200 μsec synchronisation preamble, a 600 bit message block and finally a 2 msec guard period to avoid interference with transmissions in adjacent slots. Single time slot allocation may be

used in several modes, accommodating simple time ordered signalling as previously described or discrete address interrogation and reply including data exchange with another subscriber. In addition, voice traffic from a 2.4 K baud vocoder can be accommodated by allocating 4 time slots per second to one subscriber. To combat the problems of jamming and interference, it is intended to utilise a bandwidth of 10-100 MHz with both PN-PSK and frequency hopped Spread Spectrum techniques. SS coding with matched filter detection also enables minimisation of the transmitter profile reducing the visibility of the transmitted signal and hence the effectiveness of any hostile monitoring.

The choice of operational frequency represents a compromise between a low frequency which offers the greatest range at low power against a high frequency which permits a larger instantaneous bandwidth to provide improved interference and multipath protection. With SS coding techniques the transmitted signal exhibits a flat spectral power density and it is hoped that the organised TDMA transmission will permit utilisation of the already allocated TACAN band (960-1210 MHz)[109] for co-existence of both signals without any severe mutual interference. This is attractive for obtaining the necessary ~100 MHz allocation required for the new system without disrupting existing equipments and frequency allocations.

It is known that the performance of SAW devices is receiving critical examination for this system. In addition simple SAW Serial Parallel Receivers, employing precoded AMF's, have been constructed as prototype synchronisers for the ICNI system. However, accurate *performance and cost evaluations* are necessary to ascertain whether SAW or the competing CMOS DMF techniques will be finally selected.

## 8.4 CONCLUSIONS

Following early discussions of simple retrofit applications for SAW devices in the SSR system, this Chapter has attempted to review several of the new ATC system proposals where SAW AMF's might possibly be incorporated into these equipments. The recent work of Setrin[55] designing a block encoding-decoding modem for a new IFF transponder interrogation system, and Bushs' [56] Spread Spectrum TV data link for Remotely Piloted Vehicles[116], illustrates the seriousness with which SAW components are being evaluated for military ATC. It is considered a natural extension that civil systems planners will shortly adopt a more critical appraisal of SAW signal processing techniques.

In addition to the ATC systems discussed here, other applications could easily be found for SAW devices in, for example, the new Microwave Landing Systems[117]. These systems, which are currently based on C Band signal transmissions employing either a Doppler or Scanning Beam System,are under development for improved, more flexible, curved runway approach paths. Clark[8] discusses another important operational requirement, *Clear Air Turbulence*, which technology has as yet been unable to solve. Investigations using optical infra-red radiometry techniques have to date suffered from a high rate of false alarm. The unique integration and correlation and other signal processing techniques available with SAW devices could possibly be translated to optical components to solve this problem.

In conclusion, it can be stated convincinly that, the sophisticated signal processing techniques of new ATC systems seem destined, in the near future, to open up a new market-place for SAW components.

| OPERATIONAL AREA | EXISTING EQUIPMENTS | | | NEW EQUIPMENT TRENDS | | |
|---|---|---|---|---|---|---|
| | COMMUNICATIONS | NAVIGATION | SURVEILLANCE | COMMUNICATIONS | NAVIGATION | SURVEILLANCE |
| TERMINAL<br>CONTINENTAL (OVERLAND) | VHF RADIO | ILS<br>VOR/DME<br>TACAN | PRIMARY RADAR<br>SSR/IFF | SATCOMS | MLS<br>AIR DERIVED COLLISION AVOIDANCE AND SATELLITE RANGING | GROUND PROCESSED SATELLITE CAS AND NEW IFF |
| OCEANIC | HF RADIO | LORAN/OMEGA | NONE | AEROSAT | INERTIAL | AEROSAT |
| | | | | ICNI FOR COMPREHENSIVE SYSTEM | | |

TABLE 8.1 CLASSIFICATION OF MAJOR AIR TRAFFIC CONTROL EQUIPMENTS

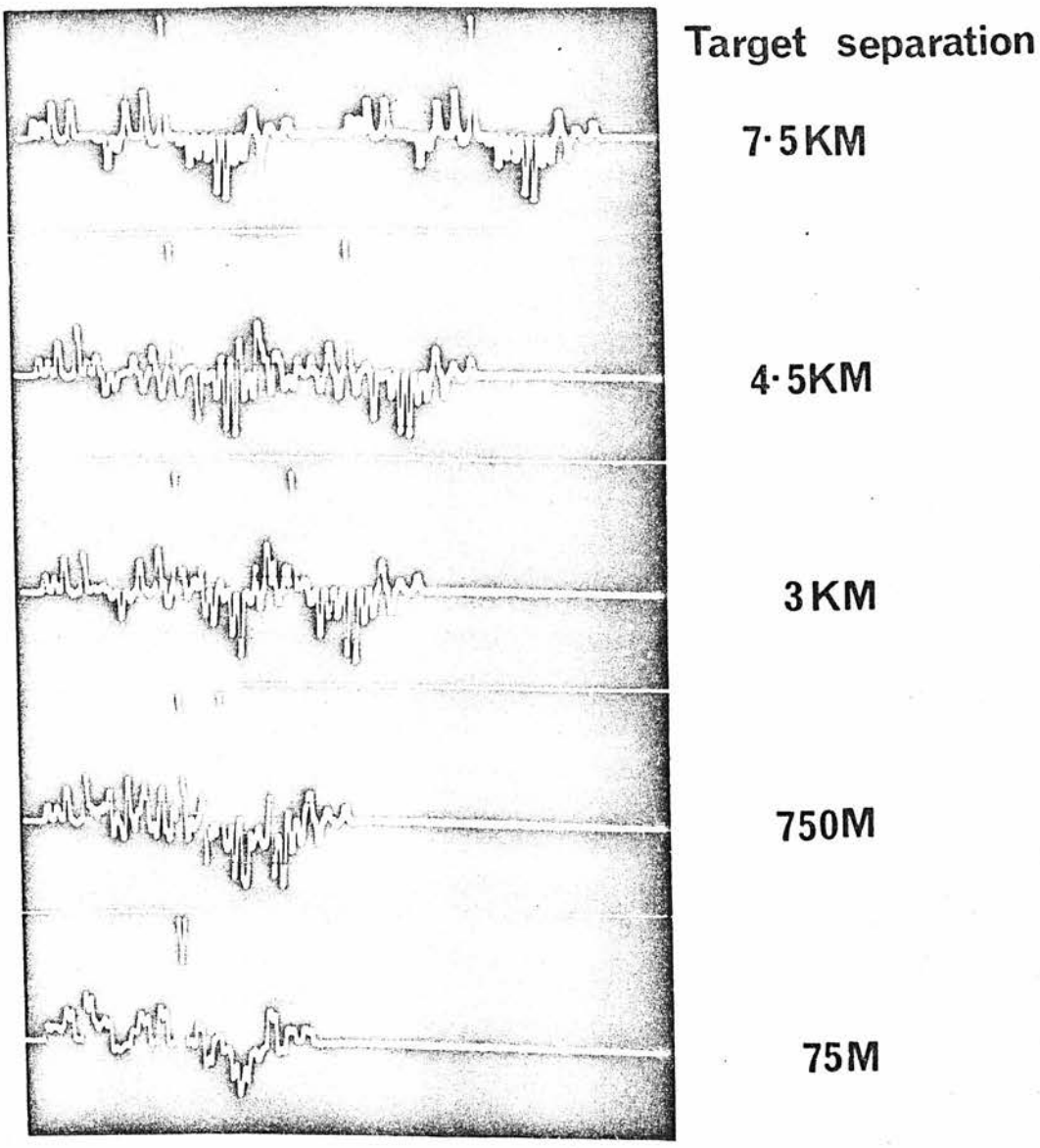


FIGURE 8.1 SEPARATION OF TWO IDENTICAL OVERLAPPING SECONDARY SURVEILLANCE RADAR SIGNALS IN A SAW TAPPED DELAY LINE DECODER -

(courtesy G Moule, RRE)

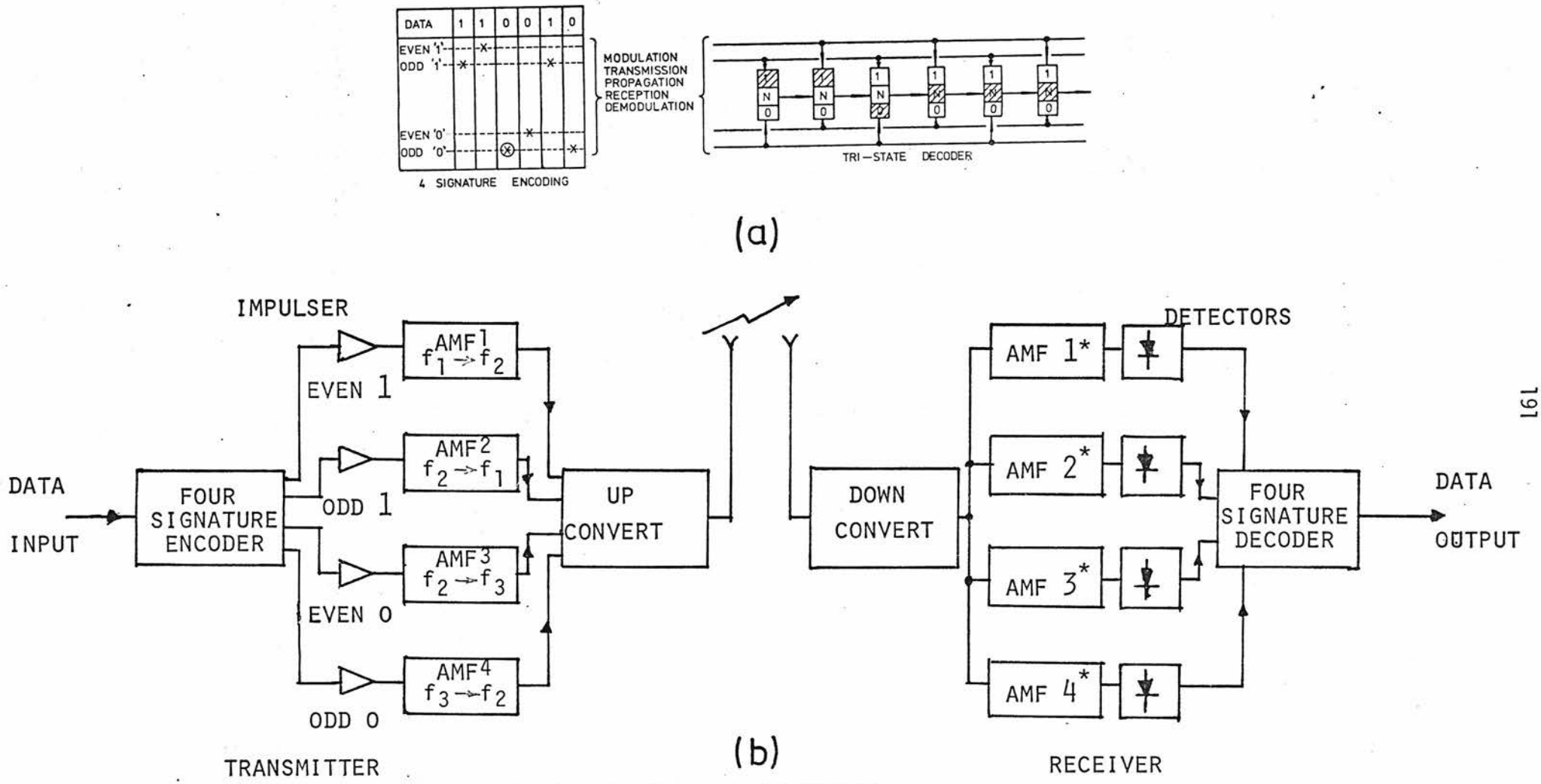


FIGURE 8.2 FOUR SIGNATURE DATA ENCODING AND DECODING

(a) CODE FORMAT HIGHLIGHTING OPERATION OF THE TRISTATE RECEIVER LOGIC

(b) SCHEMATIC OF THE SAW TRANSCEIVER

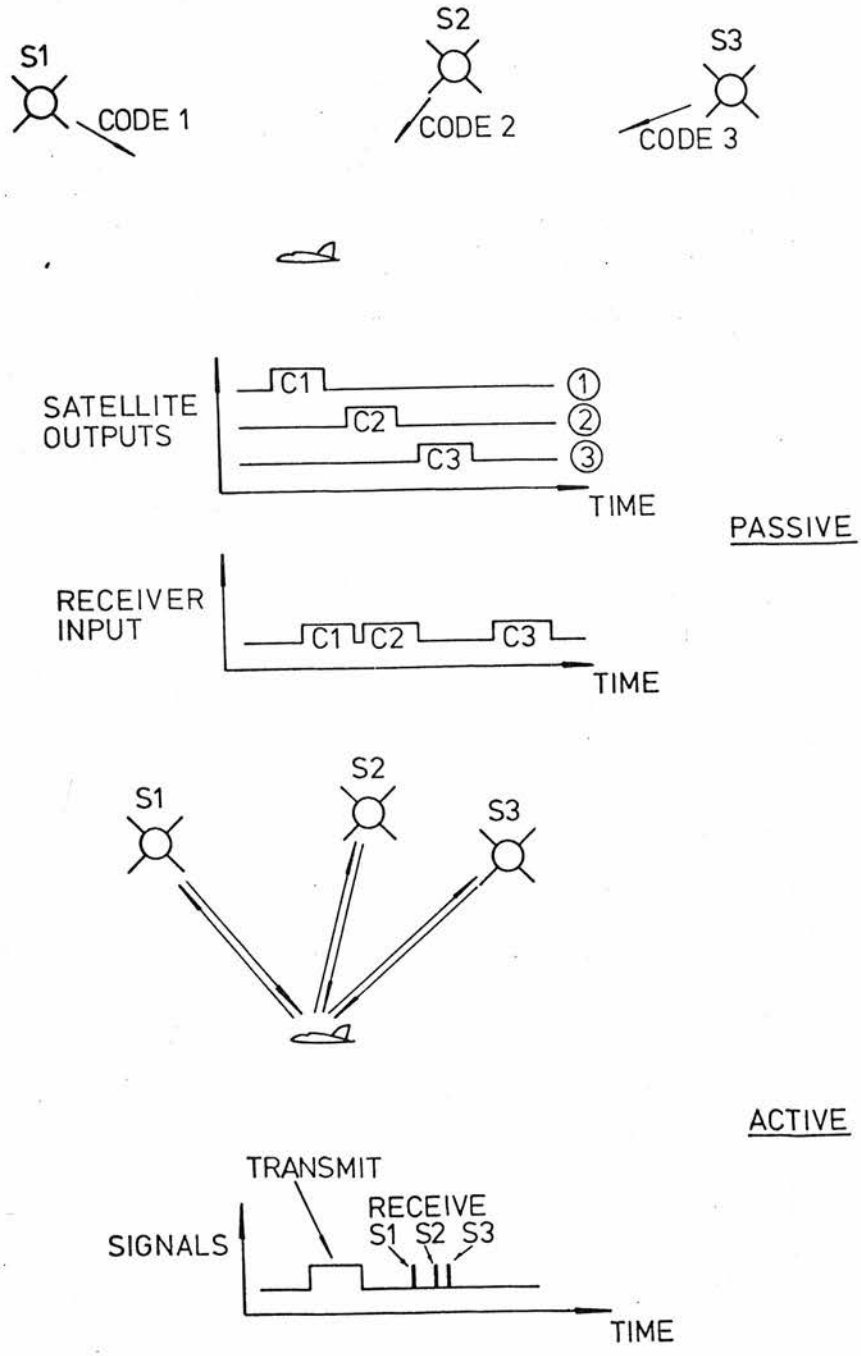


FIGURE 8.3 SATELLITE RANGING TECHNIQUES FOR AERONAUTICAL NAVIGATION

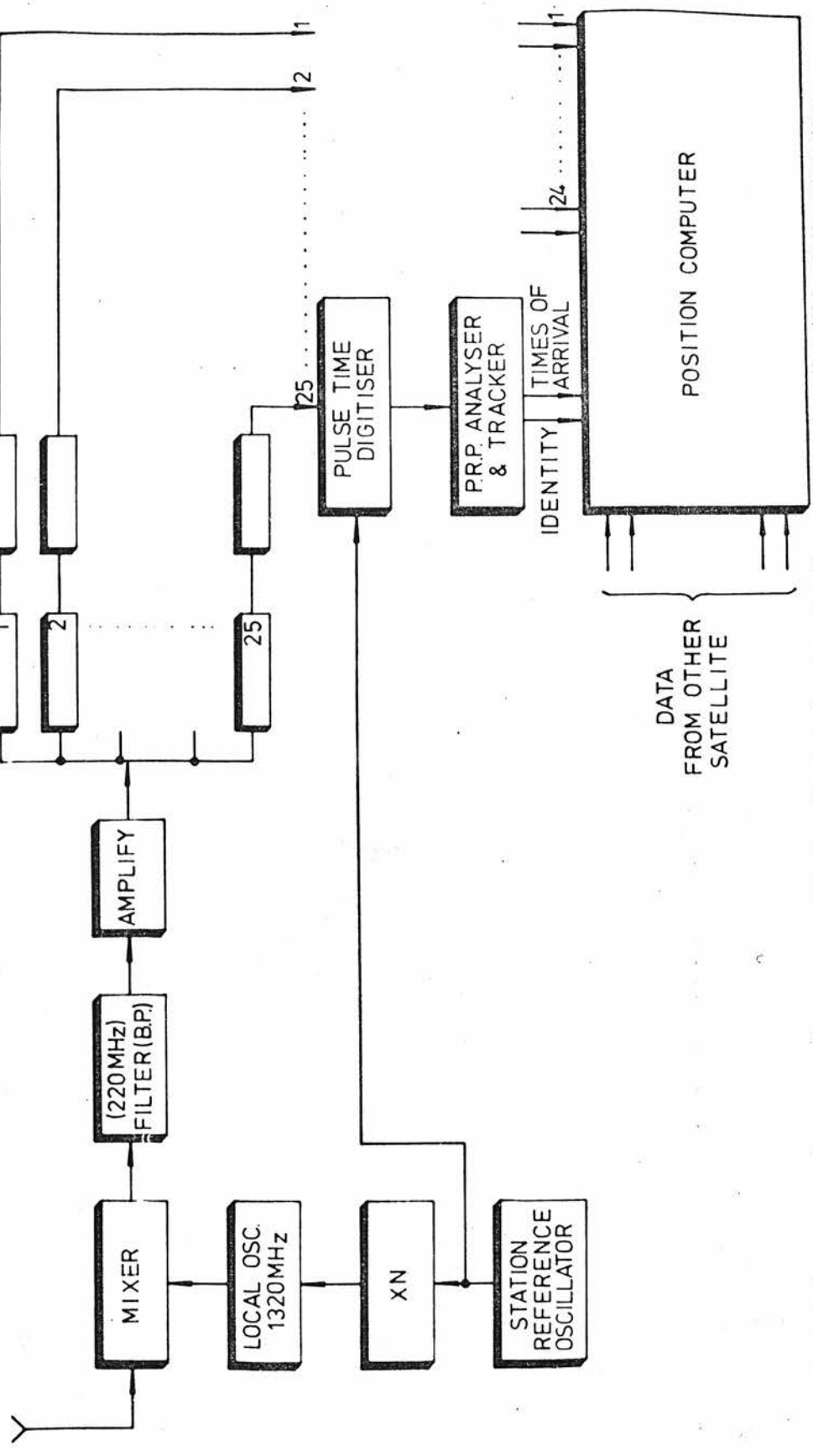


FIGURE 8.4 GROUND PROCESSING EQUIPMENT FOR COLLISION AVOIDANCE SURVEILLANCE SYSTEM EMPLOYING SAW AMF SIGNAL DETECTORS

# 9. FINAL REMARKS

## 9.1 SUMMARY

This thesis has reviewed the broad range of devices which can be fabricated using Surface Acoustic Wave (SAW) technology. To date, the major breakthrough in SAW device applications has occurred in military airborne radar. Here, SAW pulse compression filters have demonstrated impressive, close to theoretical, performance with high dynamic range and good temperature stability. The successful incorporation of SAW components can be traced directly to the competitive performance, reliability, reproducability and cost effectiveness of these fixed coded devices. This development has resulted in systems' designers seriously considering other SAW components such as bandpass filters and oscillators for the next generation of radar equipments.

Recent developments have introduced the requirement [8,118] to combine SAW with integrated circuit (IC) technology. It was noted in Chapter 1 that the simple planar construction of SAW devices is compatible with, but simpler than, existing IC fabrication techniques. The oscillator is the first SAW device to exploit this marriage which allows each technology to provide its own distinctive contribution. The relative simplicity of the oscillator structure,combined with its high tolerance of fabrication faults, permits these stable SAW sources to be designed for fundamental operation at VHF and above. This represents a considerable advance over the capabilities of existing bulk acoustic wave resonators.

The thesis has noted these developments and attempted to examine the application of SAW devices to analogue and digital communication

and Air Traffic Control (ATC) systems. The introductory survey on Civil Communications systems, Chapter 2, showed that the component requirements of current equipments and the SAW device parameters are closely aligned. It has been reported that high dynamic range SAW linear transversal filters, are capable of operating between HF and low microwave frequencies. Most devices have been designed at VHF where the centre frequency and percentage bandwidths are compatible with the IF stages of existing equipments. The capability of SAW technology to extend signal processing to UHF is predicted to offer potential applications for SAW devices in new uprated high capacity, communications equipments.

Economics is currently the major stumbling block hindering their immediate incorporation into existing equipments. This is typified by the development, over the last six years, of the SAW colour TV IF filter. In the intervening period,existing technology has also advanced to match the competition from SAW. However, Zenith Radio[26] is now fabricating these filters in pilot production, for incorporation into a selected number of domestic receivers.

The description in Chapter 3, of the alternative Spread Spectrum accessing techniques for communication and ATC highlighted the importance of matched filters for the generation and detection of the coded signals used in these systems. The passive, fixed coded, SAW Analogue Matched Filters (AMF), reported in Chapter 4, are especially attractive as they have demonstrated high fidelity signal processing performance. However,it was identified that programmability is a necessary requirement before SAW AMF's can

retrofit the Direct Sequence Spread Spectrum (DSSS) system to give the urgently required reduction in the receiver lock up time.

The analysis of SAW Programmable Analogue Matched Filter (PAMF) design in Chapter 5 permitted a realistic theoretical evaluation of the many technologies which are available for device fabrication. Following a competitive trade-off, Chapter 6, hybrid construction was finally selected for PAMF fabrication as it was best suited to this Department's microelectronic processing facilities. Fully asynchronous thirty-one tap Electronically Programmable AMF's, designed to operate at 100 MHz with a 5 MHz chip rate, were constructed with low power consuming beam lead PIN diode and thin film nichrome resistor programming switches. Code generation and storage was accomplished within TTL peripherals permitting the PAMF to be reprogrammed in only 300 nsec. The demonstrated signal processing performance of these devices was almost indistinguishable from identical fixed coded AMF's. However, these relatively short PAMF's were expensive (~ £500 material cost) and they exhibited low reliability due to the large numbers of interconnection bonds.

Comparison with devices constructed concurrently in the USA highlights the author's prediction of ultimately superior performance for PAMF's incorporating Silicon on Sapphire (SOS) integrated switches. These latter devices are capable of extension to greater numbers of taps, ie, 128. However, yield in production will still be a major consideration. It is *forecast* that hybrid PAMF's with integrated SOS switches will be limited to 256 taps, while fully integrated devices will be limited to 128 taps.

Thus, further development is required to realise the high time bandwidth product ($10^3$ - $10^4$) matched filters necessary to improve the lock up time of DSSS systems. A Serial Parallel Receiver (SPR) in which a SAW Electronically Programmable AMF was combined with a SAW Recirculating Delay Line Integrator (RDLI) was evaluated in Chapter 7. The SPR was constructed and demonstrated correlating a 100 MHz carrier PN-PSK modulated at a 5 MHz rate by a 2047 chip coded sequence. Although not fully asynchronous,the receiver was shown to possess a timing ambiguity of $\pm$3.0 μsec, which gave a considerable improvement over the active correlators used in existing equipments.

The receiver was found to be limited to time bandwidth products of ~255 by delay line bandlimiting, triple transit responses and direct electromagnetic breakthrough when less than a 2 dB degradation in processing gain was required. These effects all require further investigation before the maximum time bandwidth product can be predicted for these SAW Programmable PSK Matched Filters. However, it is anticipated that time bandwidth products of 5,000 will soon be obtainable in high performance SAW SPR's.

## 9.2 FUTURE RESEARCH REQUIREMENTS

It is seen from this thesis that SAW devices possess a *predictable, high fidelity* performance which puts the technology in a strong position for applications in Radar, Communications and ATC equipments. However, it has also been reported that, with the exception of Radar systems, few applications exist today.

It is therefore important that a strong link is formed between the device and systems designers. The SAW device designer must be

prepared to develop sub-system modules which fully exploit the unique signal processing capabilities of his devices. Areas requiring further investigation include the design of adaptive frequency filters, self adaptive transversal equalisers and fast Fourier Transform processors, which are all based on the transversal filter design expertise existing today. The construction of these modules is predicted to offer signal processing functions whose capabilities considerably exceed that obtainable with existing circuit techniques.

To keep ahead of the competition from digital microelectronic signal processors, it is also important to exploit the marriage of SAW with the complementary Charge Coupled Device (CCD) and epitaxial Yttrium Iron Garnet (YIG) technologies. The combination of SAW with CCD appears to offer another solution to overcome the restricted time delay achievable within the SAW device. This is attractive for the fabrication of two dimensional Discrete Fourier Transform processors with very large time bandwidth, ($10^6$), products. The combination of the SAW oscillator with a tunable YIG bandpass filter should permit the construction of new wideband digitally controlled microwave frequency synthesisers.

It is concluded that there is a definite requirement for a meaningful dialogue between SAW and system designers before the full exploitation of these components can be achieved. This development is vital if Surface Acoustic Wave technology is to maintain, into the next decade, the competitive position it holds today.

# REFERENCES


1. Lord Rayleigh "On waves propagating along the plane surface of an elastic solid", Proc London Math Soc, Vol 17, pp 4-11, Nov 1885.

2. R M White and F W Voltmer, "Direct piezoelectric coupling to surface elastic waves", App Phys Lett, Vol 7, pp 314-316, Dec 1965.

3. J J Campbell and W R Jones "A method of estimating optimal cuts and propagation directions for excitation of piezoelectric surface waves", IEEE Trans SU-15, pp 209-217, Oct 1968.

4. A J Slobodmik and E D Conway, Microwave Acoustics Handbook Air Force Res Lab, AFCRL-70-00164, March 1970.

5. J D Maines and E G S Paige "Surface acoustic wave components devices and applications", Proc IEE Reviews, pp 1078-1110, Oct 1973.

6. M G Holland and L T Claiborne "Practical surface acoustic wave devices", Proc IEEE Vol 62, No 5, pp 582-611, May 1974.

7. Microwave Acoustic Signal Processing, Special Issue - IEEE Transactions Microwave Theory and Techniques, MTT-21, No 4, April 1973.

8. Component performance and systems applications of surface acoustic wave devices, IEE Conference Publication No 109, Sept 1973.

9. W R Smith et al "Analysis of interdigital surface wave transducers by use of an equivalent circuit model", IEEE Trans MTT-17, No 11, pp 856-872, Nov 1969.

10. A J Bahr "Fabrication techniques for surface acoustic wave devices", IEE Conf Publication No 109, pp 22-31, Sept 1973.

11. H E Kallman "Transveral Filters", Proc IRE Vol 28, pp 302-310, July 1940.

12. R F Mitchell, "Surface acoustic wave transveral filters, their use and limitations", IEE Conf Publ No 109, pp 130-140, Sept 1973.

13. J D Maines et al "Inverse filters: design and performance using surface acoustic waves", Proc IEEE Ultrasonics Symp, 73, CHO 807-8 SU, pp 437-440, 1973.

14. K M Lakin and H J Shaw "Surface wave delay line amplifiers", IEEE Trans MTT-17, No 11, pp 912-920, Nov 1969.

15. Introsonics, "The touch sensitive digitiser", 1972 Information available from Introsinics Ltd, Stillsville, Ontario, Canada.

16. J Burnswig et al "Electronically controllable time delay", IEEE G-MTT Int Microwave Symp 73-CHO-736-9 MTT, pp 134-136, 1973.

17. J F Havlice et al "A new acoustic imaging device", Proc IEEE Ultrasonics Symposium 73-CHO-807-8 SU, pp 13-17, 1973.

18. I Kaufman and J W Foltz, "Self scanned optical sensors using elastic surface waves", Proc IEEE 57, pp 2081-2082, 1969.

19. H Seidel and D L White "Ultrasonic surface-wave guides", US Patent 3406358, 1968.

20. A Rønnekleiv and O Kjoestad "Mellomfreskvenstrinn for PSK-PCM demodulator basert pa akustiske over flatebolger", Trondheim Technical College, Report No K225, Sept 1971.

21. S L Quilsci and H J Shaw "Helical surface-acoustic-wave delay line", Elect Lett 8, pp 625-626, 1972.

22. H van de Vaart and L R Schissler, "Acoustic surface wave recirculating memory", IEEE Trans MTT-21, No 4, pp 236-243, April 1973.

23. S C-C Tseng and G C Powell, "SAW device implementation of complementary sequences for image processing", IEE Conf Publ No 109, pp 255-269, Sept 1973.

24. R H Tancrell "Analytic design of surface wave bandpass filters" IEEE Trans SU-21 No 1, pp 12-22, Jan 1974.

25. L T Claiborne et al "VHF/UHF bandpass filters using SAW device technology", Microwave Journal 17 No 5, pp 35-40, May 1974.

26. 1974 IEE Ultrasonics Symposium Proceedings 74-CHO-816-1 SU, Milwaukee, Nov 1974.

27. M Lewis "Surface Acoustic Wave Oscillators", Proc Microwave 73, pp 437-441, Brighton, England, June 1973.

28. J H Collins, P M Grant and J D Maines, "An assessment of SAW device performance in relation to potential systems applications" presented at 21st Microwave Research Institute Symposium, Brooklyn Polytechnic, April 1974.

29. "Electronic system based on acousto-electronic integrated circuits employing heteroepitaxial materials", Final Contract Report, B/SR/8696, University of Edinburgh, October 1974.

30. B J Darby "Surface acoustic wave analogue matched filter realisation and applications in digital spread spectrum systems", PhD Thesis, University of Edinburgh, May 1974.

31. P M Grant and J H Collins "Surface Acoustic wave devices application in microwave radio relay systems", IEE Conf Publ No 109, pp 299-308, Sept 1973.

32. P M Grant, J D Adam and J H Collins "Surface wave device applications in microwave communication systems", IEEE Trans COM-22 No 9, pp 1410-1419, Sept 1974.

33. W J Bray "Possible roles for guided wave systems in the future telecommunications network", IEE Conference on Trunk; Telecommunications, October 1970.

34. D Dorsi "A survey of microwave terrestrial communications", Proc Microwave 73, Brighton, England, pp 77-89, June 1973.

35. T R Rowbotham "Short hop radio-relay system work at 20 GHz", Proc Microwave 73, Brighton, England, pp 112-116, June 1973.

36. Communications in Japan, Special Issue IEEE Transactions on Communications, COM-20, No 4, August 1972.

37. C L Cuccia "Phase shift keying: the optimum modulation technique for digicom", Microwave Systems News, Vol 3, No 14, p 3, Jan 1973.

38. COMSAT Technical Review Vol 2, No 2, 1972.

39. Mobile Radio Communication, Special Issue, IEEE Transaction on Communications COM-21, No 11, Nov 1973.

40. S V Bearse "The year of giant growth arrives for land mobile communications", Microwaves 13, No 1, pp 38-47, Jan 1974.

41. J R Brinkley "The future of Mobile Radio Paging services in Europe", Paper 3.4, Proc Communications 1974, Brighton, England, June 1974.

42. T Watanabe and T Kurskawa "140 MHz IF main amplifiers for 2700 channel microwave repeaters", IEEE Trans COM-18, No 5, pp 651-662, 1970.

43. R Coakley "A survey of measurement techniques for microwave communication systems", Proc Microwave 73, pp 189-196, Brighton, 1973.

44. K G Plass "Acoustic surface wave bandstop filter for UHF frequencies", Proc 1973 European Microwave Conference, Paper C 8.3.

45. C M Kudsia et al "Lightweight GFEC waveguide multiplexer for satellite application", Proc Microwave 74, Montreux, pp 585-589.

46. J Noordanus "Frequency Synthesis - a survey of techniques", IEEE Trans COM-17, No 2, pp 257-271, April 1969.

47. Spread Spectrum Communications, Agard lecture series LS-58, Bolkesjo, Norway, May 1973.

48. M G Unkauf "An acoustic surface wave modem for time variant dispersive channels", Paper 8-3, 21st Microwave Research Institute Symposium, Brooklyn Polytechnic, April 1974.

49. H K Robin et al "Multitone signaling system employing quenched resonators for use on noisy teleprinter circuits", Proc IEE Vol 110, No 9, pp 1554-1568, 1963.

50. B D Parker "Design of an air to ground asynchronous digital communication system for ATC", IEE Conf Publ No 28.

51. C E Ellingson "A practical design of an ICNI system", Agard Conf Proc, No 105, Edinburgh, 1972.

52. D D Otten et al "Satellites for domestic air traffic control", 3rd AIAA Comm Sat Conf, Los Angeles, April 1970.

53. J Burnsweig and J Wooldridge "Ranging and data transmission using digitally encoded FM chirp surface acoustic wave filters", IEEE Trans MTT-21, No 4, pp 272-279, April 1973.

54. B J Hunsinger "Spread spectrum processors", Ultrasonics 11, pp 254-262, 1973.

55. M Setrin et al "An IFF system using block programmable surface wave signal expander and compressor", Proc IEEE Ultrasonics Symposium 73-CHO-807- 8 SU, pp 316-323, 1973.

56. H Bush et al "Application of chirp SWD for spread spectrum communications", Proc IEEE Ultrasonics Symposium, 73-CHO-807-8 SU, pp 494-497, 1973.

57. I S Reed and H Blasbalg, "Multipath tolerant ranging and data transfer techniques for air-ground and ground-air links", Proc IEEE Vol 58, pp 422-429, March 1970.

58. Golomb, S W (ed) Digital Communications with Space Applications, Prentice-Hall, 1964.

59. R Gold "Study of correlation properties of binary sequences" Air Force Avionics Laboratory Report, AFAL-TR-67-311, Wright Patterson Air Force Base, Ohio, November 1967.

60. P M Grant and J H Collins "Synchronisation acquisition and data transfer utilising a programmable SAW AMF", Elect Lett, 8, No 12, June 1972.

61. M G Unkauf "Spread spectrum communications and modems", Paper M.1, IEEE Ultrasonics Symposium, Miami, December 1971.

62. The Technology and Applications of Charge Coupled Devices, CCD 74 Conf Proc, University of Edinburgh, Sept 1974.

63. S T Constanza, P J Hagon and L A MacNiven "Analog matched filter using tapped acoustic surface wave delay lines", IEEE Trans MTT-17, No 11, pp 1042-1043, Nov 1969.

64. D P Morgan et al "Asynchronous operation of a SAW convolver", IEEE Ultrasonics Symposium, 72, CHO-708-8 SU, pp 296-299, 1972.

65. A M McCalmont "Multiple-access discrete address communication systems", IEEE Spectrum 4, 8, pp 87-94, August 1967.

66. J H Bagley "Specification of the communications system", IEE Skynet Conf Publ, No 63, pp 12-18, 1970.

67. G L Turin "An introduction to matched filters", Trans IRE IT-6, No 3, pp 311-329, 1960.

68. B J Darby, P M Grant and J H Collins "Performance of SAW matched filter modems in noise and interference limited environments" Paper D1, Proc Ultrasonics International Conf, London 1973.

69. R H Tancrell and M G Holland "Acoustic surface wave filters", Proc IEEE 59, No 3, pp 393-409, March 1971.

70. P H Carr "Reduction of reflections in surface wave delay lines with Quarter Wave Taps", Proc IEEE 60, No 9, pp 1103-1104, Sept 1972.

71. T W Bristol et al "Application of double electrodes in acoustic surface wave device design", also G W Judd "An improved tapping transducer geometry for surface wave phase coded delay lines", IEEE Ultrasonics Symposium 72-CHO-708-8 SU, pp 343-345 and 373-376, 1972.

72. B J Darby "Suppression of spurious acoustic signals in phase coded surface acoustic wave AMF's using a dual tap geometry", IEEE Trans SU-20 No 4, pp 382-384, Oct 1973.

73. T S Fisher et al "Surface Wave correlator with inclined transducer", Elect Lett, 9, No 3, pp 55, February 1973.

74. K V Lever "An analysis of the effect of random fabrication errors on the performance of SAW pseudo random sequence correlators", Hirst Research Centre, CVD Memo No 71, 1971.

75. D T Bell "Phase errors in long surface wave devices", IEEE Ultrasonics Symposium 72-CHO-708-8 SU, pp 420-423, 1972.

76. P H Carr et al "The effect of temperature and Doppler shift on the performance of elastic surface wave encoders and decoders", IEEE Trans SU-19, No 3, pp 357-367, July 1972.

77. C F Vasile and R La Rosa "1000 bit surface wave matched filter", Elect Lett, 8, No 19, pp 479-480, Sept 1972.

78. J H Collins and P M Grant "The role of surface acoustic wave technology in future communication systems", Ultrasonics 10, pp 59-72, March 1972.

79. L T Claiborne et al "MOSFET Ultrasonic surface wave detectors for programmable matched filters", App Phys Lett, 19, No 3, pp 58-60, August 1971.

80. P Defranould "MOSFET surface detectors for high frequency signal processing", Paper 7.4, European Microwave Conference, 1973.

81. G D O'Clock et al "Switchable acoustic surface wave sequence generator", Proc IEEE, pp 1536-1537, Oct 1971.

82. F S Hickernell "Design and performance of a ZnO/Si-MOSFET monolithic quadraphase programmable correlator", IEEE Ultrasonics Symposium 73-CHO-807-8 SU, pp 324-328, 1973.

83. M Bruun "Electronic properties of gallium arsenide field effect transistor structure used as a detector for surface acoustic waves", Elect Lett, 8, pp 215-216, April 1972.

84. E W Greeneich and R S Muller "Acoustic wave detection via a piezoelectric field effect transducer", App Phys Lett, 20, pp 156-158, February 1971.

85. W C Fifer et al "Switchable acoustic matched filter", Rome Air Development Centre Report, RADC-TR-72-72, April 1972.

86. P J Hagon et al "Integrated programmable analogue matched filters for spread spectrum applications", Proc IEEE Ultrasonics Symposium 73-CHO-807-8 SU, pp 333-335, 1973.

87. D Stewart "Design, construction and testing of a programmable analogue matched filter", Student Project Report, Edinburgh University, HSP 144, May 1972.

88. B J Hunsinger and A R Franck "Programmable surface wave tapped delay line", IEEE Trans SU-18, No 3, pp 152-155, July 1971.

89. R S Ronen and P H Robinson "Recent advances in thin film silicon devices on sapphire substrates", Proc IEEE 59, pp 1506-1510, October 1971.

90. D E Hooper "The advanced bipolar IC process", New Electronics, pp 28-35, April 1974.

91. R W Berry et al, Thin Film Technology, Van Norstrand Press, 1968.

92. C Cavazzuti and G Fusaroti "High level logic handbook", SGS ATES, August 1972.

93. R D Lambert, P M Grant, D P Morgan and J H Collins "Programmable surface acoustic wave devices utilising hybrid microelectronic techniques", Radio and Electronic Engineer, 44, No 7, pp 343-357, July 1974.

94. C H Moor and C F Stolwyk "Concatenated surface wave processors", Proc IEEE Ultrasonics Symposium, 73-CHO-807-8 SU, pp 336-339, 1973.

95. A G Burke "A frequency hopped pseudo noise modem using surface wave techniques", G MTT Symposium Proc, Boulder, Colorado, Paper 42/2, 1973.

96. J Brown "An investigation of recirculating delay line integrators using surface acoustic wave delay lines", Student Project Report, Edinburgh University, HSP 161, May 1974.

97. H Urkowitz "Delay line secondary responses in AM and FM sweep integrators", J Fran Inst, 269, No 1, pp 1-23, Jan 1960.

98. DCVD Annual Report RU5-2, University of Edinburgh, December 1974.

99. P M Grant, J Brown and J H Collins "Large time bandwidth project programmable SAW PSK matched filter", pp 382-385, IEEE Ultrasonics Symposium 74-CHO-896-1 SU , 1974.

100. M S Zimmerman et al "A long memory delay line analog recirculator", IRE Nat Conv Rec, 7, 2, pp 70-78, 1959.

101. F Y Cho et al "Surface waves circulating on piezoelectric substrates", App Phys Lett, 18, No 7, pp 298-301, April 1971.

102. J Henaff et al "Wrap around ASW delay line with lens guidance and monolithic amplification", App Phys Lett 25, No 5, pp 256-258, Sept 1974.

103. Air Traffic Control Systems, AGARD Conf Publ No 105, Edinburgh, June 1972.

104. Special Issue of IEEE Transactions on Communications, Aeronautical Communications, COM 21, No 5, May 1973.

105. P M Grant et al "Potential applications of acoustic matched filters to Air Traffic Control systems", IEEE Trans MTT-21, No 4, pp 288-300, April 1973.

106. "Satellite systems for mobile communications and surveillance", IEE Conf Publ No 95, March 1973.

107. R W Meier "North Atlantic aeronautical satellite system development", Proc IEEE, Vol 59, pp 448-455, March 1970.

108. G E Beck, Navigation Systems, Van Nostrand Reinhold, London, 1971.

109. S H Dodington "Recent developments of the TACAN navigation system", Electrical Communication, 44, pp 316-321, 1969.

110. M I Skolnik Introduction to Radar Systems, McGraw-Hill, 1962.

111. J N Johnston "Dispersive sub-system for pulse compression in radar using SAW devices", Proc Microwave 73, pp 460-464, June 1973.

112. "Mediator ATC system comes into operation", Radio and Electronic Engineer, Vol 41, p 181, April 1971.

113. G L Moule "The reduction of garbling in secondary surveillance radar", IEE Conf Publ No 109, pp 337-343, Sept 1973.

114. D E Findley "Satellite considerations in future ATC systems", AGARD Conf Proc 105, ATC System, Paper 30 1972 .

115. J L Parsons "SECANT - A solution to the problems of mid-air collisions", AGARD Conf Proc 105, ATC Systems, Paper 23, 1972.

116. R T Davis "Mini RPV's for cheap and no risk air power", Microwaves 13, No 10, pp 40-48, October 1974.

117. Microwave Landing Systems, Special Issue Microwave Systems News, Vol 4, No 5, Oct/Nov 1974.

118. Surface Acoustic Wave Devices in ECM , Microwaves, December 1974/ January 1975

# APPENDIX A

## SAW INTER DIGITAL TRANSDUCER SCATTERING PARAMETERS

The simple bidirectional SAW IDT can be represented as a network with a single electrical port 3 and two acoustic ports 1 and 2 as shown in Figure A.1. The power scattering parameters, which define the levels of acoustic and electric transmitted and reflected signals, are conveniently derived from the crossfield model of the IDT,[69] which gives an accurate fit for both Quartz and Lithium Niobate substrate materials[9]. Consider the IDT shown in Figure A.2 with an electrical admittance $\hat{G}_a$ and susceptance $B_a$ (predominantly $2\pi f_o C_T$) which is connected to an electrical generator of admittance $G_G$ and susceptance $B_G$.

The voltage across the IDT terminals is given by

$$V_T = \frac{I}{\sqrt{(\hat{G}_a + G_G)^2 + (\omega_o C_T + B_G)^2}} \qquad A.1$$

Acoustic power delivered into the IDT, $P_A$, is

$$P_A = V_T{}^2 \hat{G}_a = \frac{I^2 \hat{G}_a}{(\hat{G}_a + G_G)^2 + (\omega_o C_T + B_G)^2} \qquad A.2$$

For the matched condition $\hat{G}_a = G_G$ and the generator susceptance is chosen to resonate the IDT interelectrode capacitance.

$$\therefore \omega_o C_T = -B_G$$

and

$$P_{INPUT} = \frac{I^2 G_G}{(\hat{G}_a + G_G)^2} = \frac{I^2}{4G_G} \qquad A.3$$

Due to the symmetry of the IDT design, power is radiated equally from both ports 1 and 2. The conversion loss, $\rho_{31}$, is defined as[9]

$$\therefore \rho_{31} = \frac{\text{Acoustic power transmitted from port 1}}{\text{Electrical power available from the matched generator at port 3}} \quad \text{A.4}$$

$$= \frac{\frac{1}{2} \cdot \text{Acoustic power generated in IDT}}{\text{Matched input power at port 3}} \quad \text{A.5}$$

$$= \frac{\frac{1}{2} \cdot I^2 \cdot \hat{G}_a \cdot 4 \cdot G_G}{[(\hat{G}_a + G_G)^2 + (\omega_o C_T + B_G)^2] \cdot I^2} \quad \text{A.6}$$

$$= \frac{2 \cdot \hat{G}_a \cdot G_G}{(\hat{G}_a + G_G)^2 + (\omega_o C_T + B_G)^2} \quad \text{A.7}$$

$$= \frac{2 \cdot b}{(1 + b)^2 + a^2} \quad \text{A.8}$$

where $$b = \frac{G_G}{\hat{G}_a} \quad \text{A.9}$$

and $$a = \frac{(B_G + \omega_o C_T)}{\hat{G}_a} \quad \text{A.10}$$

by reciprocity and symmetry it is seen that $\rho_{31} = \rho_{13}$ hence equation A.8 is valid both for generation and detection of surface acoustic waves. It can also be shown[9] that for an acoustic wave incident at port 1 with an electrical load at port 3

reflection coefficient $\rho_{11} = \dfrac{1}{(1+b)^2 + a^2}$ A.11

transmission coefficient $\rho_{21} = \dfrac{b^2 + a^2}{(1+b)^2 + a^2}$ A.12

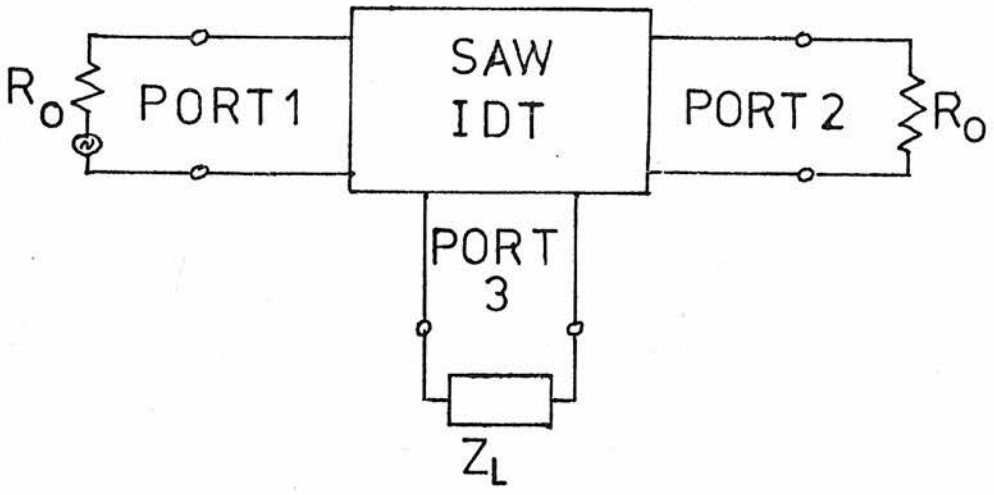


FIGURE A1

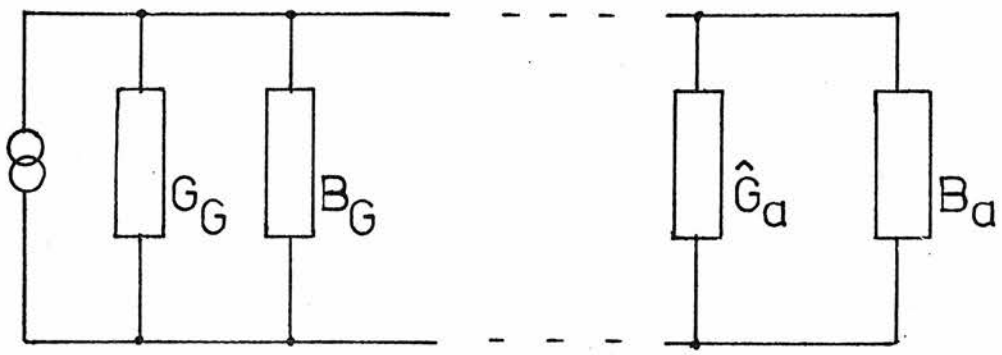


FIGURE A2

# APPENDIX B

## SAW PAMF ANALYSIS PROGRAMMES

This appendix contains the computer programmes and data printouts used to theoretically analyse the operation of the SAW PAMF switching circuits. The accompanying flow chart illustrates how the programmes were built up from the analysis reported in Section 5.4 of the Thesis. The programme developed to analyse the four ring DPDT switch of Figure 5.4(a) is contained in the first page of Printout. Printout 2 shows the data obtained from this programme for precoded, fixed coded, discrete component and integrated SAW Programmable AMF's.

Printout 3 gives the modified programme which was developed for the simpler switch shown in Figure 5.4(d) and the fourth page of Printout shows the predicted performance data for discrete component and hybrid PAMF's incorporating this switching circuit.

Other simplified PAMF analysis programmes have also been developed in which the forward biased diode resistance, RD, is always considered to be smaller than the reverse biased diode capacitive reactance, $\frac{1}{2.\pi.f.CD}$. This assumption, which has subsequently been verified by Staples[7], permits the tap, diode and interconnection capacities to be added directly at the sum bus, removing the necessity for complex algebraic computations. The approximation gave results which agree closely, $\pm$ 2 dB, with the comprehensive analysis presented in this Appendix for short, <127 tap, SAW PAMF's.

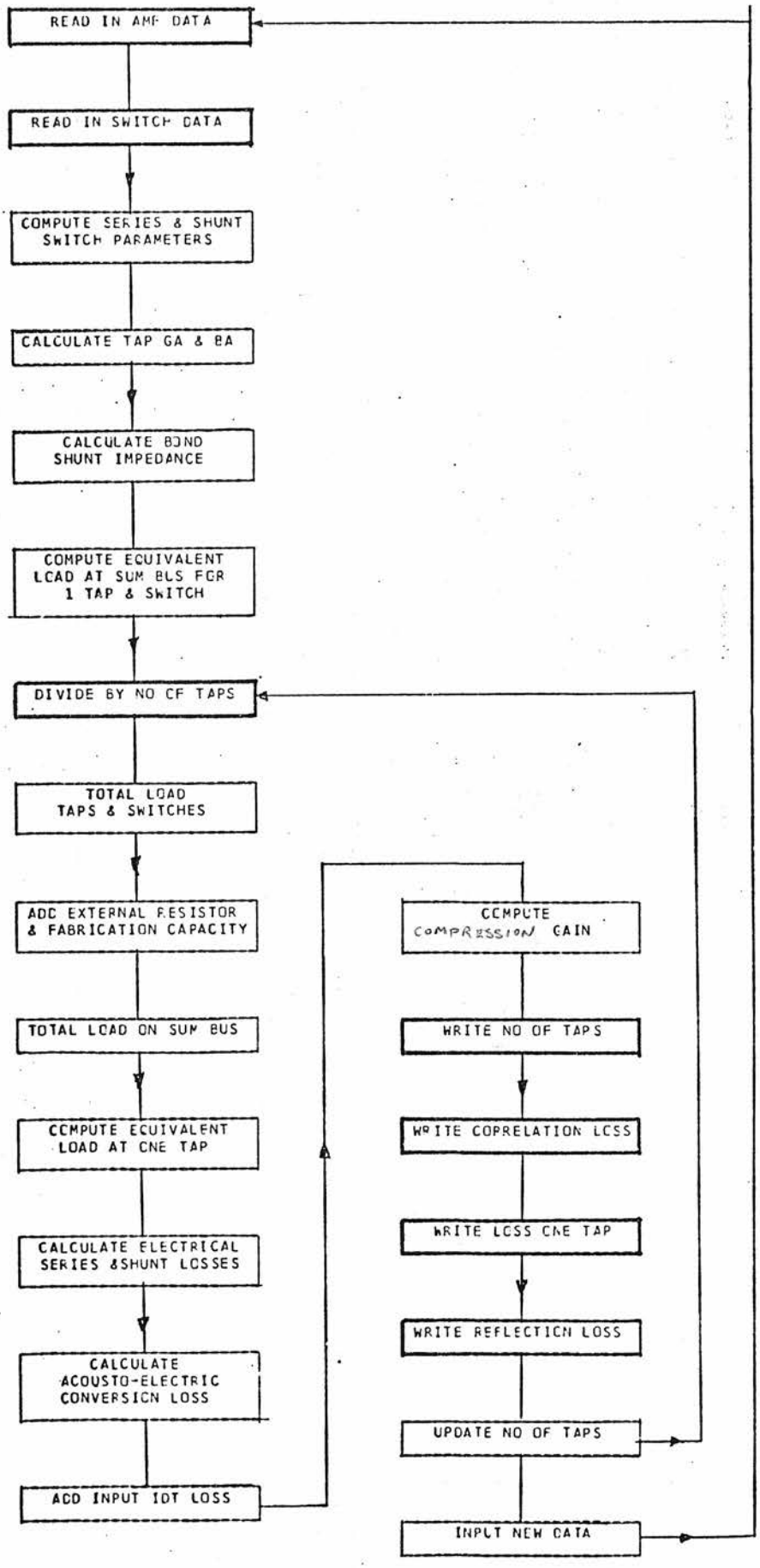


PROGRAMME FLOW CHART

## PROGRAMME 1

```
C     TO CALCULATE 4 RING  PROGRAMMABLE AMF INSERTION LOSS
      IMPLICIT COMPLEX*8 (Z,Y)
      REAL INLOA,INLOB,INLOC,INLOD,INLOE,INLOF,INLOG,KSQ
   40 READ(5,1) FREQ,KSQ,FINGPR,TAPAPT,CSQ,BEMWID
   45 READ(5,14)
   41 READ(5,8) RLO,RXT,CXT,CBOND
   29 IF(RLO.EQ.0)STOP
   42 READ(5,53) ZBIAS,ZONSW,ZOFSW
      Z10=ZONSW
      Z11=ZBIAS
      Z12=2*Z10*Z11+Z10**2
      Z13=Z12/Z10
      Z14=Z12/Z11
      Z20=Z14/2
      Z21=Z13/2
      Z10=ZOFSW
      Z11=ZBIAS
      Z12=2*Z10*Z11+Z10**2
      Z13=Z12/Z10
      Z14=Z12/Z11
      Z22=Z14/2
      Z23=Z13/2
      REG=1
      LABEL=0
      CTAPTO=TAPAPT*CSQ*FINGPR
      CTAPAC=BEMWID*CSQ*FINGPR
      GA=4*2*FREQ*CTAPAC*KSQ*FINGPR
      BA=2*3.142*FREQ*CTAPAC
      WRITE(6,30)
      WRITE(6,14)
      WRITE(6,20) FREQ,KSQ,FINGPR,CTAPTO,GA,BA
      WRITE(6,21) RLO,RXT,CXT,CBOND,CTAPAC
      WRITE(6,25) ZBIAS
      WRITE(6,26) ZONSW
      WRITE(6,27) ZOFSW
      WRITE(6,23)
      Y40=GA*(1.,0.)+(0.,1.)*BA
      Z40=1/Y40
      XB=-1/(2*3.142*FREQ*(CTAPTO-CTAPAC))
      XT=AIMAG(Z40)
      R5=REAL(Z40)
      R5=R5*XB/XT
      Z41=R5*(1.,0.)+(0.,1.)*XB
      Z42=Z40*Z41/(Z40+Z41)
      Z30=Z42
      XC=-1/(2*3.142*FREQ*CBOND)
      Z43=(0.,1.)*XC
      Z25=Z21*Z23/(Z21+Z23)
      Z1=Z20
      Z2=Z22*Z25/(Z22+Z25)
      Z3=Z22
      Z4=Z20*Z25/(Z20+Z25)
      Z5=Z30
      Z2=Z2*Z43/(Z2+Z43)
      Z4=Z4*Z43/(Z4+Z43)
      Z6=Z1*Z3/(Z1+Z3+Z5)
      Z7=Z1*Z5/(Z1+Z3+Z5)
      Z8=Z3*Z5/(Z1+Z3+Z5)
      Z9=Z7+Z2
      Z10=Z8+Z4
      Z11=Z9*Z10/(Z9+Z10)
      Z12=Z11+Z6
      Z12=Z12*Z25/(Z12+Z25)
      Z15=Z12
   50 LABEL=1+LABEL
      TAP=2**REG-1
      BP=2*3.142*FREQ*CXT*TAP
      RP=RLO
      GP=1/RP
      Y1=GP*(1.,0.)+(0.,1.)*BP
      IF(TAP.EQ.1.0) GO TO 35
      Z13=Z15/(TAP-1.0)
      Y13=1/Z13
      G13=REAL(Y13)
      RTASH=1/G13
      Y45=Y1+Y13
   36 Z45=1/Y45
      Z30=Z45
      Z5=Z30*Z25/(Z30+Z25)
      Z6=Z1*Z2/(Z1+Z2+Z5)
      Z7=Z1*Z5/(Z1+Z2+Z5)
      Z8=Z2*Z5/(Z1+Z2+Z5)
      Z9=Z7+Z3
      Z10=Z8+Z4
      Z11=Z9*Z10/(Z9+Z10)
      Z12=Z11+Z6
      RTALO=REAL(Z12)
      Y12=1/Z12
      G12=REAL(Y12)
      BP=AIMAG(Y12)
      RL=REAL(Z45)
      R1=RL/RTALO
      R2=RTASH/(RTASH+RP)
      INLOA=10*ALOG10(RL/RTALO*RTASH/(RTASH+RP))
      RP=1/G12
      XP=-1/BP
      XC=-1/BA
      XTOTAL=XP*XC/(XP+XC)
      GL=G12
      B=GL/GA
      BT=-1/XTOTAL
      BT=ABS(BT)
      A=BT/GA
      INLOB=10*ALOG10((2*B)/((1+B)*(1+B)+A*A))
      INLOC=INLOA+INLOB-8
      PROGAN=20*ALOG10(TAP)
      INLOD=INLOC+PROGAN
      INLOA=10*ALOG10(1/((1+B)*(1+B)+A*A))
      INLOE=INLOA
      INLOF=INLOA+PROGAN-6+INLOC
      INLOG=2*INLOA+2*PROGAN-6-3+INLOC
      WRITE(6,24) TAP,INLOD,INLOC,INLOE,INLOF,INLOG
      GO TO (101,102,103,104,105,106,107,108,109), LABEL
  101 REG=3
      GO TO 50
  102 REG=4
      GO TO 50
  103 REG=5
      GO TO 50
  104 REG=6
      GO TO 50
  105 REG=7
      GO TO 50
  106 REG=8
      GO TO 50
  107 REG=9
      GO TO 50
  108 REG=10
      GO TO 50
  109 GO TO 45
   35 Y45=Y1
      RTASH=1000000.
      GO TO 36
    1 FORMAT(6E10.3)
    8 FORMAT(4E10.3)
   14 FORMAT(55H                                                    )
   20 FORMAT(/,'  ','FREQ',3PE12.0,5X,'KSQ',0PE12.4,5X,'FINGPR',1PE12.4
     C,5X,'TOTL TAPC',0PE12.3,5X,'GA',E12.4,5X,'BA',E12.4)
   21 FORMAT(/,'  ','RLOAD ',2PE12.0,5X,'RXT',2PE12.0,5X,'CXT',0PE12.2,
     C5X,'CBOND',E12.3,5X,'ACTIVE TAPC',E12.3)
   23 FORMAT(/,10X,'TAPS',14X,'COP LOSS',10X,'INS LOSS',10X,'REFL SIG',8X
     C,'PRIM  REFL',8X,'SECY  REFL')
   24 FORMAT(2X,E15.3,3X,2PE15.1,3X,2PE15.1,3X,2PE15.1,3X,2PE15.1,3X,
     C2PE15.1)
   25 FORMAT(/,'  BIAS IMPEDANCE',1PE10.0,5X,'J',1PE10.0)
   26 FORMAT(1X,' ONSW IMPEDANCE',1PE10.0,5X,'J',1PE10.0)
   27 FORMAT(1X,' OFSW IMPEDANCE',1PE10.0,5X,'J',1PE10.0)
   30 FORMAT(////,'                          ')
   53 FORMAT(6E10.3)
      END
```

## PRINTOUT 1

EA4 PRECODED AMF

FREQ 10C.E 06 KSC 0.1960E-02 FINCPR 3.0000E 00 TOTL TAPC 0.386E-12 GA 0.1126E-05 BA 0.1505E-03
RLOAD 50.E 00 RXT 10.E 05 CXT 0.50E-13 CBOND C.100E-15 ACTIVE TAPC 0.239E-12
BIAS IMPEDANCE 1.E 10 J 0.
ONSW IMPEDANCE 1.E-07 J 0.
OFSW IMPEDANCE 0. J -1.E 15

| TAP | COR LOSS | INS LOSS | REFL SIG | PRIM REFL | SECY REFL |
|---|---|---|---|---|---|
| 0.100E 01 | -47.5E CC | -47.5E 00 | -85.0E 00 | -13.8E C1 | -22.6E 01 |
| 0.70CE 01 | -30.6E CC | -47.5E CC | -85.CE CC | -12.2E 01 | -19.3E 01 |
| C.15CE 02 | -24.1E CC | -47.7E 00 | -85.2E 00 | -11.5E C1 | -18.0E 01 |
| 0.31CE 02 | -18.4E 00 | -48.2E CC | -85.7E C0 | -11.CE C1 | -16.9E 01 |
| C.63CE 02 | -13.9E CC | -49.5E CC | -87.4E 00 | -10.7E 01 | -16.2E C1 |
| 0.127E 03 | -11.5E C0 | -53.5E 00 | -91.CE C0 | -10.9E 01 | -16.CE C1 |
| 0.255E 03 | -1C.6E CC | -58.7E 00 | -96.2E 0C | -11.3E C1 | -16.4E C1 |
| 0.511E 03 | -10.3E 00 | -64.5E 00 | -10.2E 01 | -11.8E 01 | -16.9E C1 |
| 0.102E 04 | -10.2E 0C | -70.4E 00 | -10.8E 01 | -12.4E 01 | -17.5E 01 |

EA4 FIXED CODED AMF

FREQ 1CC.E C6 KSQ C.1960E-C2 FINGPR 3.0CC0E C0 TOTL TAPC 0.386E-12 GA 0.1126E-05 BA C.1505E-03
RLOAD 50.E 00 RXT 10.E 05 CXT 0.25E-12 CBCND 0.100E-13 ACTIVE TAPC 0.239E-12
BIAS IMPEDANCE 1.E 1C J 0.
CNSW IMPEDANCE 1.E-07 J 0.
OFSW IMPEDANCE 0. J -1.E 15

| TAP | COR LOSS | INS LOSS | REFL SIG | PRIM REFL | SECY REFL |
|---|---|---|---|---|---|
| C.1CCE 01 | -47.5E 0C | -47.5E 0C | -85.CE 00 | -13.8E C1 | -22.6E 01 |
| 0.7CCE C1 | -30.7E 0C | -47.6E C0 | -85.1E C0 | -12.2E C1 | -19.3E 01 |
| 0.15CE C2 | -24.3E 00 | -47.9E 0C | -85.4E C0 | -11.6E 01 | -18.1E C1 |
| 0.31CE 02 | -19.1E CC | -48.5E 00 | -86.4E CC | -11.2E 01 | -17.1E 01 |
| 0.630E 02 | -15.7E 00 | -51.7E 00 | -89.2E C0 | -11.1E 01 | -16.7E 01 |
| 0.127E C3 | -14.2E CC | -56.3E 00 | -93.8E CC | -11.4E C1 | -16.9E 01 |
| 0.255E 03 | -13.8E CC | -61.9E C0 | -99.4E CC | -11.9E 01 | -17.4E 01 |
| 0.511E 03 | -13.7E CC | -67.8E 00 | -10.5E 01 | -12.5E C1 | -17.9E 01 |
| 0.102E 04 | -13.6E CC | -73.8E CC | -11.1E C1 | -13.1E 01 | -18.5E 01 |

EA4 4 RING PCB PROG AMF (1N914)

FREQ 10C.E 06 KSQ 0.1960E-02 FINGPR 3.0CCCE 00 TOTL TAPC C.386E-12 GA C.1126E-05 BA C.1505E-03
RLOAD 50.E 00 RXT 10.E 05 CXT 0.50E-11 CBOND 0.700E-11 ACTIVE TAPC 0.239E-12
BIAS IMPEDANCE 1.E 04 J 0.
ONSW IMPEDANCE 8.E C1 J C.
OFSW IMPEDANCE 0. J -2.E 03

| TAP | COR LOSS | INS LOSS | REFL SIG | PRIM REFL | SECY REFL |
|---|---|---|---|---|---|
| 0.10CE 01 | -47.7E CC | -47.7E 0C | -74.2E CC | -12.8E 01 | -20.5E 01 |
| C.7CCE C1 | -40.3E CC | -57.2E 00 | -75.5E 00 | -12.2E 01 | -18.3E 01 |
| 0.15CE 02 | -39.9E 00 | -63.4E 00 | -75.7E C0 | -12.2E 01 | -17.7E 01 |
| 0.31CE 02 | -39.8E CC | -69.7E C0 | -75.7E 00 | -12.2E 01 | -17.CE C1 |
| 0.630E 02 | -39.8E 00 | -75.8E 00 | -75.7E C0 | -12.1E 01 | -16.4E 01 |
| 0.127E 03 | -39.8E CC | -81.9E 00 | -75.6E C0 | -12.1E 01 | -15.8E C1 |
| 0.255E 03 | -39.8E 00 | -87.9E 00 | -75.6E C0 | -12.1E 01 | -15.2E C1 |
| 0.511E 03 | -39.8E 0C | -94.0E 00 | -75.6E 0C | -12.1E 01 | -14.6E C1 |
| 0.102E 04 | -39.8E 00 | -10.0E 01 | -75.6E 00 | -12.1E 01 | -14.CE C1 |

EA4 4 RING SCS IC PROG AMF (AUTONETICS)

FREQ 10C.E 06 KSQ 0.1960E-02 FINGPR 3.0CC0E 00 TOTL TAPC 0.386E-12 GA 0.1126E-05 BA 0.1505E-03
RLOAD 50.E 00 RXT 1C.E 05 CXT 0.10E-12 CBCND 0.200E-13 ACTIVE TAPC 0.239E-12
BIAS IMPEDANCE 1.E 04 J 0.
ONSW IMPEDANCE 1.E C1 J 0.
OFSW IMPEDANCE 0. J -8.E 04

| TAP | COR LOSS | INS LOSS | REFL SIG | PRIM REFL | SECY REFL |
|---|---|---|---|---|---|
| 0.10CE 01 | -47.5E 00 | -47.5E 00 | -82.1E 00 | -13.6E 01 | -22.1E 01 |
| 0.70CE 01 | -31.2E CC | -48.1E 00 | -82.6E C0 | -12.0E 01 | -18.8E C1 |
| 0.15CE 02 | -25.4E 00 | -48.9E 00 | -83.2E C0 | -11.5E 01 | -17.7E C1 |
| 0.31CE 02 | -20.7E C0 | -50.6E 00 | -84.4E 00 | -11.1E 01 | -16.9E C1 |
| C.63CE 02 | -17.5E 0C | -53.5E 00 | -86.4E C0 | -11.0E 01 | -16.3E 01 |
| 0.127E 03 | -15.7E 0C | -57.8E 00 | -88.7E C0 | -11.CE C1 | -16.CE C1 |
| 0.255E 03 | -14.8E 00 | -62.9E C0 | -90.7E CC | -11.1E 01 | -15.7E 01 |
| 0.511E 03 | -14.4E 00 | -68.5E 00 | -91.8E C0 | -11.2E 01 | -15.3E C1 |
| 0.102E 04 | -14.2E 0C | -74.4E C0 | -92.4E CC | -11.3E 01 | -14.8E 01 |

EA4 4 RING IC PROG AMF (PLESSEY 3)

FREQ 10C.E 06 KSQ C.1960E-02 FINGPR 3.0000E 00 TOTL TAPC 0.386E-12 GA 0.1126E-05 EA 0.1505E-03
RLOAD 50.E 00 RXT 10.E C5 CXT 0.50E-12 CBOND 0.250E-12 ACTIVE TAPC 0.239E-12
BIAS IMPEDANCE 1.E 03 J -3.E 03
CNSW IMPEDANCE 5.E 01 J 0.
OFSW IMPEDANCE 0. J -4.E 03

| TAP | COR LOSS | INS LOSS | REFL SIG | PRIM REFL | SECY REFL |
|---|---|---|---|---|---|
| 0.1CCE C1 | -47.5E CC | -47.5E 00 | -75.6E CC | -12.9E C1 | -20.8E 01 |
| 0.70CE C1 | -32.9E CC | -49.8E 00 | -76.7E CC | -11.6E 01 | -17.8E 01 |
| 0.150E 02 | -3C.0E CC | -53.5E 00 | -77.8E 00 | -11.4E C1 | -17.1E 01 |
| 0.31CE 02 | -28.9E CC | -5E.7E CC | -78.6E CC | -11.3E 01 | -16.5E 01 |
| C.63CE 02 | -28.6E CC | -64.5E 00 | -78.9E 00 | -11.3E 01 | -15.9E 01 |
| 0.127E 03 | -28.4E 0C | -7C.5E CC | -79.CE C0 | -11.3E C1 | -15.3E 01 |
| 0.255E 03 | -28.4E CC | -76.5E CC | -79.0E 00 | -11.3E 01 | -14.7E C1 |
| 0.511E 03 | -28.4E 00 | -82.5E 00 | -79.0E 00 | -11.3E 01 | -14.1E C1 |
| 0.102E 04 | -28.4E CC | -88.6E 00 | -79.CE C0 | -11.3E 01 | -13.5E C1 |

EA4 4 RING SOS IC PROG AMF (PLESSEY)

FREQ 10C.E 06 KSQ C.1960E-02 FINGPR 3.0CC0E 00 TOTL TAPC C.386E-12 GA C.1126E-05 BA 0.1505E-03
RLOAD 50.E 00 RXT 10.E C5 CXT 0.10E-12 CBCND C.200E-13 ACTIVE TAPC 0.239E-12
BIAS IMPEDANCE 1.E C4 J 0.
CNSW IMPEDANCE 1.E C2 J 0.
OFSW IMPEDANCE 0. J -3.E C4

| TAP | COR LOSS | INS LOSS | REFL SIG | PRIM REFL | SECY REFL |
|---|---|---|---|---|---|
| 0.100E 01 | -47.5E CC | -47.5E 00 | -71.1E C0 | -12.5E 01 | -19.9E C1 |
| C.70CE C1 | -31.3E 00 | -48.2E 00 | -71.3E C0 | -10.9E 01 | -16.6E C1 |
| 0.150E 02 | -25.6E 0C | -49.2E 00 | -71.5E C0 | -10.3E 01 | -15.4E C1 |
| C.31CE C2 | -21.3E 00 | -51.1E 00 | -71.8E 00 | -99.1E 0C | -14.4E 01 |
| C.63CE 02 | -18.4E CC | -54.4E 00 | -72.3E 00 | -96.6E C0 | -13.6E C1 |
| 0.127E 03 | -16.8E 0C | -58.8E CC | -72.6E 00 | -95.4E C0 | -12.9E 01 |
| 0.255E C3 | -16.0E 00 | -64.1E 00 | -72.8E CC | -94.8E 00 | -12.3E C1 |
| 0.511E 03 | -15.6E CC | -69.8E 00 | -72.9E CC | -94.5E 00 | -11.CE 01 |
| 0.102E 04 | -15.4E 00 | -75.6E 00 | -73.CE C0 | -94.4E 00 | -11.0E 01 |

PRINTOUT 2

## PROGRAMME 2

```
C     TO CALCULATE 4 DIODE PROGRAMMABLE AMP INSERTION LOSS
      IMPLICIT COMPLEX*8 (Z,Y)
      REAL INLOA,INLOB,INLOC,INLOD,INLOE,INLOF,INLOG,KSQ
   40 READ(5,1) FREQ,KSQ,FINGPR,TAPAPT,CSO,BEMWID
   45 READ(5,14)
   41 READ(5,8) RLO,RXT,CXT,CBOND
   29 IF(RLO.EQ.0)STOP
   42 READ(5,1)  ZBIAS,ZONSW,ZOFSW
      Z20=ZONSW
      Z21=ZBIAS
      Z22=ZOFSW
      Z23=ZBIAS
      REG=1
      LABEL=0
      CTAPTO=TAPAPT*CSO*FINGPR
      CTAPAC=BEMWID*CSO*FINGPR
      GA=4*2*FREQ*CTAPAC*KSQ*FINGPR
      BA=2*3.142*FREQ*CTAPAC
      WRITE(6,30)
      WRITE(6,14)
      WRITE(6,20) FREQ,KSQ,FINGPR,CTAPTO,GA,BA
      WRITE(6,21) RLO,RXT,CXT,CBOND,CTAPAC
      WRITE(6,25) ZBIAS
      WRITE(6,26) ZONSW
      WRITE(6,27) ZOFSW
      WRITE(6,23)
      Y40=GA*(1.,0.)+(0.,1.)*BA
      Z40=1/Y40
      XB=-1/(2*3.142*FREQ*(CTAPTO-CTAPAC))
      XT=AIMAG(Z40)
      R5=REAL(Z40)
      R5=R5*XB/XT
      Z41=R5*(1.,0.)+(0.,1.)*XB
      Z42=Z40*Z41/(Z40+Z41)
      Z30=Z42
      XC=-1/(2*3.142*FREQ*CBOND)
      Z43=(0.,1.)*XC
      Z1=Z20
      Z2=Z22*Z23/(Z22+Z23)
      Z3=Z22
      Z4=Z20*Z23/(Z20+Z23)
      Z5=Z30
      Z2=Z2*Z43/(Z2+Z43)
      Z4=Z4*Z43/(Z4+Z43)
      Z6=Z1*Z3/(Z1+Z3+Z5)
      Z7=Z1*Z5/(Z1+Z3+Z5)
      Z8=Z3*Z5/(Z1+Z3+Z5)
      Z9=Z7+Z2
      Z10=Z8+Z4
      Z11=Z9*Z10/(Z9+Z10)
      Z12=Z11+Z6
      Z15=Z12
   50 LABEL=1+LABEL
      TAP=2**REG-1
      BP=2*3.142*FREQ*CXT*TAP
      RP=RLO
      GP=1/RP
      Y1=GP*(1.,0.)+(0.,1.)*BP
      IF(TAP.EQ.1.0) GO TO 35
      Z13=Z15/(TAP-1.0)
      Y13=1/Z13
      G13=REAL(Y13)
      RTASH=1/G13
      Y45=Y1+Y13
   36 Z45=1/Y45
      Z30=Z45
      Z5=Z30
      Z6=Z1*Z2/(Z1+Z2+Z5)
      Z7=Z1*Z5/(Z1+Z2+Z5)
      Z8=Z2*Z5/(Z1+Z2+Z5)
      Z9=Z7+Z3
      Z10=Z8+Z4
      Z11=Z9*Z10/(Z9+Z10)
      Z12=Z11+Z6
      RTALO=REAL(Z12)
      Y12=1/Z12
      G12=REAL(Y12)
      BP=AIMAG(Y12)
      RL=REAL(Z45)
      R1=RL/RTALO
      R2=RTASH/(RTASH+RP)
      INLOA=10*ALOG10(RL/RTALO*RTASH/
     C                                (RTASH+RP))
      RP=1/G12
      XP=-1/BP
      XC=-1/BA
      XTOTAL=XP*XC/(XP+XC)
      GL=G12
      B=GL/GA
      BT=-1/XTOTAL
      BT=ABS(BT)
      A=BT/GA
      INLOB=10*ALOG10((2*B)/((1+B)*(1+B)+A*A))
      INLOC=INLOA+INLOB-8
      PROGAN=20*ALOG10(TAP)
      INLOD=INLOC+PROGAN
      INLOA=10*ALOG10(1/((1+B)*(1+B)+A*A))
      INLOE=INLOA
      INLOF=INLOA+PROGAN-6+INLOC
      INLOG=2*INLOA+2*PROGAN-6-3+INLOC
      WRITE(6,24) TAP,INLOD,INLOC,INLOE,INLOF,INLOG
      GO TO (101,102,103,104,105,106,107,108,109), LABEL
  101 REG=3
      GO TO 50
  102 REG=4
      GO TO 50
  103 REG=5
      GO TO 50
  104 REG=6
      GO TO 50
  105 REG=7
      GO TO 50
  106 REG=8
      GO TO 50
  107 REG=9
      GO TO 50
  108 REG=10
      GO TO 50
  109 GO TO 45
   35 Y45=Y1
      RTASH=1000000.
      GO TO 36
    1 FORMAT(6E10.3)
    8 FORMAT(4E10.3)
   14 FORMAT(48H                                                )
   20 FORMAT(/,'  ','FREQ',3PE12.0,5X,'KSQ',0PE12.4,5X,'FINGPR',1PE12.4
     C,5X,'TOTL TAPC',0PE12.3,5X,'GA',E12.4,5X,'BA',E12.4)
   21 FORMAT(/,'  ','RLOAD ',2PE12.0,5X,'RXT',2PE12.0,5X,'CXT',0PE12.2,
     C5X,'CBOND',E12.3,5X,'ACTIVE TAPC',E12.3)
   23 FORMAT(/,10X,'TAP',14X,'COR LOSS',10X,'INS LOSS',10X,'REFL SIG',8X
     C,'PPIM  REFL',8X,'SECY  REFL')
   24 FORMAT(2X,E15.3,3X,2PE15.1,3X,2PE15.1,3X,2PE15.1,3X,2PE15.1,3X,
     C2PE15.1)
   25 FORMAT(/,'  BIAS IMPEDANCE',1PE10.0,5X,'J',1PE10.0)
   26 FORMAT(1X,' CNSW IMPEDANCE',1PE10.0,5X,'J',1PE10.0)
   27 FORMAT(1X,' OFSW IMPEDANCE',1PE10.0,5X,'J',1PE10.0)
   30 FORMAT(////,'                          ')
      END
```

## PRINTOUT 3

EA4 PRECODED AMF

FREQ 100.E 06 KSQ 0.1960E-02 FINGPR 3.0000E 00 TOTL TAPC 0.386E-12 GA 0.1126E-05 BA 0.1505E-03
RLOAD 50.E 00 RXT 10.E 05 CXT 0.50E-13 CBCND 0.10CE-15 ACTIVE TAPC 0.239E-12
BIAS IMPEDANCE 1.E 10 J 0.
CNSW IMPEDANCE 1.E-07 J 0.
OFSW IMPEDANCE 0. J -1.E 15

| TAP | COR LOSS | INS LOSS | REFL SIG | PRIM REFL | SECY REFL |
|---|---|---|---|---|---|
| 0.100E 01 | -47.5E CC | -47.5E 00 | -85.0E 00 | -13.8E C1 | -22.6E 01 |
| 0.70CE 01 | -30.6E CC | -47.5E C0 | -85.CE CC | -12.2E C1 | -19.3E 01 |
| C.15CE 02 | -24.1E CC | -47.7E 00 | -85.2E 00 | -11.5E C1 | -18.0E 01 |
| 0.31CE 02 | -18.4E C0 | -48.2E 00 | -85.7E 00 | -11.CE C1 | -16.9E 01 |
| 0.63CE 02 | -13.9E CC | -49.9E CC | -87.4E 0C | -10.7E 01 | -16.2E C1 |
| 0.127E 03 | -11.5E C0 | -53.5E 00 | -91.CE C0 | -10.9E 01 | -16.0E 01 |
| 0.255E 03 | -1C.6E CC | -58.7E 00 | -96.2E CC | -11.3E C1 | -16.4E C1 |
| 0.511E 03 | -10.3E 0C | -64.5E 00 | -10.2E 01 | -11.6E 01 | -16.9E 01 |
| 0.102E 04 | -10.2E 0C | -70.4E 00 | -10.8E 01 | -12.4E 01 | -17.5E 01 |

EA4 4 DICDE PCB PROG AMF (1NS14)

FREQ 10C.E 06 KSQ C.196CE-02 FINGPR 3.0C00E 00 TOTL TAPC 0.386E-12 GA C.1126E-05 BA 0.1505E-03
RLCAC 50.E 00 RXT 1C.E C5 CXT 0.30E-11 CBCND C.500E-11 ACTIVE TAPC 0.239E-12
BIAS IMPEDANCE 4.E 03 J C.
CNSW IMPEDANCE 8.E 01 J 0.
OFSW IMPEDANCE 0. J -2.E C3

| TAP | COR LCSS | INS LCSS | REFL SIG | PRIM REFL | SECY REFL |
|---|---|---|---|---|---|
| 0.100E 01 | -47.6E CC | -47.6F 00 | -73.7E 00 | -12.7E 01 | -20.4E 01 |
| C.7CCE 01 | -37.9E C0 | -54.8E 00 | -75.2E CC | -11.9E C1 | -18.CE C1 |
| 0.15CE 02 | -37.2E CC | -6C.7E 00 | -75.4E 00 | -11.9E C1 | -17.4E C1 |
| 0.31CE 02 | -37.1E 0C | -66.9E 00 | -75.5E C0 | -11.9F 01 | -16.7E 01 |
| 0.62CE 02 | -37.0E 0C | -73.CE 00 | -75.5E 00 | -11.8E C1 | -16.1E C1 |
| 0.127E 03 | -37.0E 00 | -79.1E 00 | -75.5E 0C | -11.8E 01 | -15.5E 01 |
| C.255E 03 | -37.0E 00 | -85.1E 00 | -75.5E C0 | -11.8E 01 | -14.9E C1 |
| 0.511E 03 | -37.0E CC | -91.2E C0 | -75.5E CC | -11.8E C1 | -14.3E 01 |
| 0.102E 04 | -37.0E 0C | -97.2E 00 | -75.5E 00 | -11.8E 01 | -13.7E 01 |

EA4 4 DICDE PCB PROG AMF (HP PIN)

FREQ 100.E 06 KSQ 0.1960E-02 FINGPR 3.0000E 00 TCTL TAPC 0.386E-12 GA 0.1126E-05 BA C.15C5E-03
RLCAD 50.E 00 RXT 10.E 05 CXT 0.30E-11 CBCND 0.500E-11 ACTIVE TAPC 0.239E-12
BIAS IMPEDANCE 4.E 03 J 0.
CNSW IMPEDANCE 5.E 01 J 0.
OFSW IMPEDANCE 0. J -6.E 03

| TAP | COR LCSS | INS LOSS | REFL SIG | PRIM REFL | SECY REFL |
|---|---|---|---|---|---|
| 0.10CE 01 | -47.6E CC | -47.6E C0 | -76.2E 0C | -13.CE 01 | -20.9E 01 |
| C.7CCE 01 | -37.2E CC | -54.1E 00 | -78.4E 00 | -12.2E C1 | -18.6E 01 |
| 0.15CE 02 | -36.5E 00 | -60.0E 00 | -79.CE C0 | -12.1E 01 | -16.0E 01 |
| 0.31CE 02 | -36.3E CC | -66.1E 0C | -79.2E 00 | -12.1E C1 | -17.4E 01 |
| 0.62CE 02 | -36.3E 00 | -72.2E 00 | -79.2E 0C | -12.1E 01 | -16.8E C1 |
| 0.127E 03 | -36.3E CC | -78.3E 00 | -79.2E 00 | -12.1E C1 | -16.2E C1 |
| 0.255E 03 | -36.3E 00 | -84.4E 00 | -79.2E C0 | -12.1E 01 | -15.6E C1 |
| 0.511E 03 | -36.3E 00 | -90.4E 00 | -79.2E 00 | -12.1E 01 | -15.CE C1 |
| C.1C2E C4 | -36.3E 00 | -96.4E 00 | -79.2E 00 | -12.1E 01 | -14.3E 01 |

EA4 4 DIODE HYBRID PROG AMF (ALFHA)

FREQ 10C.E 06 KSQ 0.1960E-02 FINGPR 3.0C00E 00 TCTL TAPC C.386E-12 GA C.1126E-05 EA 0.1505E-03
RLOAD 50.E 00 RXT 10.E 05 CXT 0.30E-12 CBCND 0.200E-12 ACTIVE TAPC 0.239E-12
BIAS IMPEDANCE 5.E 03 J 0.
ONSW IMPEDANCE 4.E C2 J 0.
CFSW IMPEDANCE 0. J -6.E 03

| TAP | COR LCSS | INS LCSS | REFL SIG | PRIM REFL | SECY REFL |
|---|---|---|---|---|---|
| 0.10CE 01 | -47.7E C0 | -47.7E 00 | -61.3E 00 | -11.5E 01 | -17.9E 01 |
| 0.70CE 01 | -31.8E CC | -48.7E 00 | -61.4E 00 | -99.2E 00 | -14.7E 01 |
| C.15CE 02 | -26.7E 00 | -50.2E 00 | -61.5E C0 | -94.3E C0 | -13.5E C1 |
| 0.310E 02 | -23.4E 0C | -53.2E 00 | -61.6E C0 | -91.0E 00 | -12.6E 01 |
| 0.63CE 02 | -21.6E 00 | -57.6E 00 | -61.7E 00 | -89.3E 00 | -11.8E 01 |
| 0.127E 03 | -20.8E 0C | -62.8E 00 | -61.8E C0 | -88.5E C0 | -11.1E C1 |
| 0.255E 03 | -20.4E 0C | -68.5E 00 | -61.8E 00 | -88.2E C0 | -10.5E 01 |
| 0.511E 03 | -20.2E 00 | -74.4E 00 | -61.8E C0 | -88.0E 00 | -9E.6E C0 |
| 0.102E 04 | -20.2E CC | -80.4E 00 | -61.8E CC | -88.0E C0 | -92.5E 00 |

EA4 4 DIODE HYBRID PROG AMF (ALFHA)

FREQ 1CC.E C6 KSQ 0.1960E-02 FINGPR 3.0000E 00 TOTL TAPC 0.386E-12 GA 0.1126E-05 EA 0.1505E-03
RLOAD 50.E 00 RXT 1C.E 05 CXT 0.30E-12 CBCND C.20CE-12 ACTIVE TAPC C.239E-12
BIAS IMPEDANCE 5.E 02 J 0.
CNSW IMPEDANCE 4.E 01 J 0.
CFSW IMPEDANCE 0. J -6.E C3

| TAP | COR LCSS | INS LCSS | REFL SIG | PRIM REFL | SECY REFL |
|---|---|---|---|---|---|
| 0.10CE 01 | -47.5E CC | -47.5E 00 | -77.9E 00 | -13.1E C1 | -21.2E 01 |
| 0.70CE 01 | -34.6E CC | -51.5E CC | -79.CE CC | -12.CE 01 | -18.5E 01 |
| 0.15CE 02 | -31.5E CC | -55.CE 00 | -79.8E 00 | -11.7E 01 | -17.7E 01 |
| 0.31CE 02 | -29.7E 00 | -59.5E 0C | -80.5E CC | -11.6E C1 | -17.0E 01 |
| 0.63CE 02 | -28.7E CC | -64.7E CC | -81.0E C0 | -11.6E C1 | -16.4E C1 |
| 0.127E 03 | -28.2E C0 | -70.3E 00 | -81.2E 0C | -11.5E 01 | -15.8E 01 |
| 0.255E 03 | -27.9E CC | -76.0E 00 | -81.4E 00 | -11.5F C1 | -15.2E C1 |
| 0.511E 03 | -27.8E 00 | -82.0E 00 | -81.5E 00 | -11.5E C1 | -14.6E C1 |
| 0.102E 04 | -27.7E 0C | -87.9E 00 | -81.5E 00 | -11.5E 01 | -14.CE C1 |

EA4 4 CICDE HYBRIC PROG AMF 1C CHM LCAD

FREQ 10C.E 06 KSQ C.196CE-02 FINGPR 3.0000E 00 TOTL TAPC 0.386E-12 GA C.1126E-05 BA 0.1505E-03
RLCAC 10.E 00 PXT 1C.E 05 CXT 0.30E-12 CBCND C.200E-12 ACTIVE TAPC 0.239E-12
BIAS IMPEDANCE 5.E 03 J 0.
CNSW IMPEDANCE 4.E 02 J 0.
OFSW IMPEDANCE 0. J -6.E C3

| TAP | COR LCSS | INS LCSS | REFL SIG | PRIM REFL | SECY REFL |
|---|---|---|---|---|---|
| 0.100E 01 | -54.6E CC | -54.6E 00 | -61.7E 0C | -12.2E 01 | -18.7E 01 |
| C.70CE 01 | -37.9E 00 | -54.8E 00 | -61.7E 00 | -10.6E C1 | -15.3E C1 |
| 0.15CE 02 | -31.5E 0C | -55.1E 00 | -61.7E 0C | -99.2E 00 | -14.0E 01 |
| C.31CE C2 | -25.8E 0C | -55.6E 00 | -61.7E C0 | -93.5F CC | -12.8E 01 |
| 0.62CE 02 | -20.9E CC | -56.9E 00 | -61.7E 00 | -88.6E C0 | -11.7E 01 |
| 0.127E 03 | -17.2E 00 | -59.3E 0C | -61.8E C0 | -85.0E C0 | -10.8E 01 |
| C.255E 03 | -15.1E 0C | -63.2E 00 | -61.8E CC | -82.8E CC | -9S.9E CC |
| 0.511E C3 | -14.0E CC | -68.2E 00 | -61.8E CC | -81.8E 00 | -92.4E 00 |
| 0.102E 04 | -13.5E 00 | -73.7E 0C | -61.8E C0 | -81.3E 00 | -85.9E 0C |

PRINTOUT 4

# APPENDIX C

## LIST OF AUTHOR'S PUBLICATIONS

† denotes the publications which are bound in with this thesis.


1. J H Collins and P M Grant "The role of surface acoustic wave technology in future communication systems", Ultrasonics, 10, pp 59-72, March 1972.

2. P M Grant and J H Collins "Synchronisation acquisition and data transfer utilising a programmable surface acoustic wave analogue matched filter", Electronics Letters, 8, No 12, pp 299-301, 15th June 1972.

3. B J Darby, P M Grant and J H Collins, "Performance of surface acoustic wave matched filter modems in noise and interference limited environments", Ultrasonics International Conference Proceedings, Paper D1, pp 314-321, London, March 1973.

4. † P M Grant, J H Collins, B J Darby and D P Morgan "Potential applications of acoustic matched filters to air traffic control systems", IEEE Trans MTT, Special Issue on Microwave Acoustics, MTT-21, pp 288-300, April 1973, also IEEE Trans Sonics and Ultrasonics, SU-20, pp 206-218, April 1973.

5. † R D Lambert, P M Grant, D P Morgan and J H Collins, "Programmable surface acoustic wave devices utilising hybrid microelectronic techniques", IERE Conference Proceedings, No 27, on "Hybrid Microelectronics", pp 161-171, September 1973, also Radio and Electronic Engineer, 44 No 7, pp 343-357, July 1974.

6. P M Grant and J H Collins "Surface acoustic wave device applications in microwave radio-relay systems", IEE Conference Publication, No 109, pp 299-308, 1973.

7. B J Darby, P M Grant, J H Collins and I M Crosby, "Performance of aperiodic spread spectrum modems incorporating surface acoustic wave analogue matched filters", IEE Conference Publication, No 109, pp 319-328, 1973.

8. B J Darby, P M Grant and J H Collins "High performance communication modems incorporating surface acoustic wave analogue matched filters", IEEE Ultrasonic Symposium Proceedings, pp 329-332, 73 -CHO-807-8SU, 1973.

9. P M Grant, R D Lambert, D P Morgan and B J Darby, "Hybrid microelectronic programmable surface acoustic wave matched filters", Paper 12.3, Proc IEEE International Electron Devices Meeting, pp 236-239, Washington, 1973.

10. B J Darby and P M Grant "Key applications of SAW devices in communication links", Microwave Systems News, 3, No 6, pp 73-77, December/January 1974.

11. † B J Darby and P M Grant "Spread spectrum communication modem designs employing surface acoustic wave analogue matched filters", Proceedings 5th Microwave Communications Conference, pp 110-120, Budapest, June 1974.

12. † P M Grant, J D Adam and J H Collins "Surface wave device applications in microwave communication systems", IEEE Trans COM, Special Issue on Communications Research in Europe, COM 22, No 9, pp 1410-1419, September 1974.

13. J H Collins, P M Grant and J D Maines "An assessment of SAW device performance in relation to potential systems applications", Proceedings 21st MRI Symposium on Optical and Acoustical Microelectronics, Paper 2.3, Brooklyn Polytechnic, April 1974.

14. P M Grant, J Brown and J H Collins "Large time bandwidth product programmable SAW PSK matched filter module", pp 382-385, IEEE Ultrasonics Symposium Proceedings, 74-CHO-896-1SU, 1974.

15. P M Grant, D P Morgan, J M Hannah and J H Collins, "Fast synchronisation for spread spectrum communications by correlation in surface acoustic wave devices", to be presented at Ultrasonics International Conference, London, March 1975.

# POTENTIAL APPLICATIONS OF ACOUSTIC MATCHED FILTERS TO AIR-TRAFFIC CONTROL SYSTEMS (*INVITED PAPER*)

BY

P. M. GRANT, J. H. COLLINS, B. J. DARBY, AND D. P. MORGAN

*Reprinted from* IEEE TRANSACTIONS
ON *MICROWAVE THEORY AND TECHNIQUES*
Volume MTT-21, Number 4, April, 1973
pp. 288-300

# Potential Applications of Acoustic Matched Filters to Air-Traffic Control Systems

PETER M. GRANT, JEFFREY H. COLLINS, BARRY J. DARBY, AND DAVID P. MORGAN

*Invited Paper*

*Abstract*—**The potential role of acoustic matched filters in the demanding field of civil and military air-traffic control (ATC) systems is examined. Highlighted are the problems of current ATC systems and the significant aspects of acoustic matched filters and their expeditious usage in modems employing band spreading for a multisubscriber environment and certain envisaged ATC systems deemed necessary for future traffic growth that could benefit materially from acoustic technology.**

## I. Introduction

THE long-term applications of acoustic matched filters to the demanding field of civil and military air-traffic control (ATC) systems are examined. Highlighted is the fact that at current levels of air traffic, existing systems possess a capability just in excess of that required to handle the peak load of today, and further that although projected growth is to be handled in the short term by upgrading and supplementing present systems, particularly with computer complexes, such an approach does not represent a viable long-term solution. In logical sequence this paper contains three parts: current ATC systems in the United States, Great Britain, and Europe, and their basic deficiencies and lessons for future designs (Sections II through V); the significant and unique features of acoustic matched filters and their performance status as devices and in modem usage (Section VI); and envisaged ATC systems which are necessary to meet forecast traffic requirements emphasizing these systems that acoustic technology impacts (Sections VII and VIII). Liberal deployment of references for existing ATC systems serves to minimize the length of the paper, and the Appendix contains a glossary of commonly used ATC abbreviations.

## II. Current ATC Procedures

Following the first powered flight of the Wright brothers on December 17, 1903, air traffic soon reached a congested state necessitating the imposition of procedural rules [1]. The control of air traffic requires the use of a multitude of equipment hardware encompassing ground-based surveillance and identification equipment to enable the controller to know the position and identity of aircraft, accurate onboard navigation equipment for pilot position determination, and voice communication equipment to handle message transfers between pilot and traffic control. The procedures adopted for civil ATC have evolved over many years through international cooperation [2] of government control bodies (e.g., the FAA and CAA) aided by the intrinsic global nature of air traffic. For example, European air-traffic handling systems have evolved by consultation between the major European organizations resulting in the Eurocontrol authority with exclusive responsibility for the upper airspace.

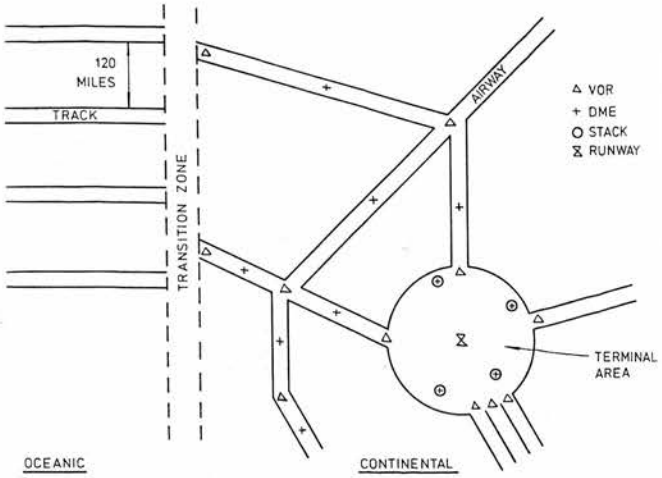


Fig. 1. Typical example of present airways system.

Current civil ATC can be subdivided into terminal, continental (overland), and oceanic areas (Fig. 1), all of which have a ground-based controller. Before entering an ATC system the airline must file a flight plan to enable the routing of each aircraft through the control network. Accepted flight plans are then entered as flight progress strips to enable controller monitoring of progress against schedule. Terminal area procedures [3] involve the scheduling of takeoffs and landings of aircraft to meet the available capacity. En route control [4] overland is accomplished by constraining the aircraft to fly along agreed airways. Transoceanic control involves a two-way structure of tracks or air corridors that are exclusively allocated across the North Atlantic by the oceanic planners [5]. Separation standards for all three areas are maintained by the ground-based controllers who possess exclusive ATC authority.

Military ATC [6] involves a more comprehensive surveillance facility requiring tracking of both friendly and enemy aircraft. With large areas of airspace reserved for military use there are fewer constraints on the pilot who exercises exclusive control requiring the incorporation of navigation, surveillance, and communication equipment of increased accuracy to meet the demanding requirements of intercept and strike maneuvers.

## III. Classification, Functional Capability, and Operating Limitations of Existing ATC Systems

### A. Classification and Functional Capability

Tables I and II detail current ATC equipments and frequency allocations in the three main areas of communications, navigation, and surveillance.

Manuscript received October 27, 1972; revised November 27, 1972. This work was supported by the British Science Research Council and the DCVD (United Kingdom Ministry of Defence PE).

The authors are with the Department of Electrical Engineering, University of Edinburgh, Edinburgh, Scotland.

TABLE I
CLASSIFICATION OF EXISTING ATC EQUIPMENT

| | Communications | Navigation | | Surveillance |
|---|---|---|---|---|
| | | Radio | Other Techniques | |
| Line of Sight | | TACAN ILS<br>DME VOR | compass<br>sextant | radar<br>IFF/SSR |
| Short range (continental) | VHF radio | DECCA ADF<br>console | altimeter<br>area navigation<br>inertial | ARTS/MEDIATOR<br>MADAP |
| Long range (oceanic) | HF radio | LORAN<br>OMEGA<br>Doppler | inertial | onboard radio position reporting |

TABLE II
FREQUENCY ALLOCATIONS FOR ATC EQUIPMENTS

| Equipment | Frequency Allocation | Reference |
|---|---|---|
| OMEGA | 10–14 kHz | [8], [9] |
| LORAN C/DECCA | 90–110 kHz | [7]–[9] |
| ADF/CONSOL | 200–1800 kHz | [9] |
| LORAN A | 1.7–2.0 MHz | [7], [8] |
| HF communications | 3–30 MHz | [7] |
| VHF FM communications | 30–70 MHz | [7] |
| ILS (localizer) | 108–112 MHz | [7] |
| VOR | 108–118 MHz | [9] |
| VHF (civil) | 118–136 MHz | [7] |
| UHF (military) | 225–400 MHz | [7] |
| ILS (glide) | 330–335 MHz | [7] |
| TACAN/DME | 960–1210 MHz | [10] |
| IFF/SSR | 1030–1090 MHz | [16] |
| SATCOM/radio navigation | 1535–1660 MHz | [28] |
| Collision avoidance | 1592–1622 MHz | [32] |
| Radar | 2.75–3.60 GHz | [15] |
| Radio altimeter | 4.2–4.4 GHz | [9] |
| MLS | 5.0–5.25 GHz | [14] |
| Radar | 9.07–9.50 GHz | [15] |
| Doppler navigation | 8.75–9.50 GHz | [12] |
| MLS | 15.4–15.7 GHz | [14] |

Communications are handled by voice procedures on either a VHF or HF net [7] depending on the range to the ground-based antenna. DECCA, LORAN, and OMEGA are all examples of external reference hyperbolic navigation systems [7], [8] that utilize one-way ground-derived signal transmissions. The civil DME [9] and military TACAN [10] overland equipments operate by two-way interrogation of a ground-sited transponding beacon. Inertial [11] and Doppler [12] are examples of self-contained navigation equipments, although more expensive, inertial navigation systems are currently fitted as standard in the 747 [13] and are superseding Doppler equipment in 707 and DC8 aircraft. Primary [15] and secondary radar [16] (SSR for civil and IFF for military applications) are the fundamental equipments used for continental, en route, and terminal surveillance (Fig. 2).

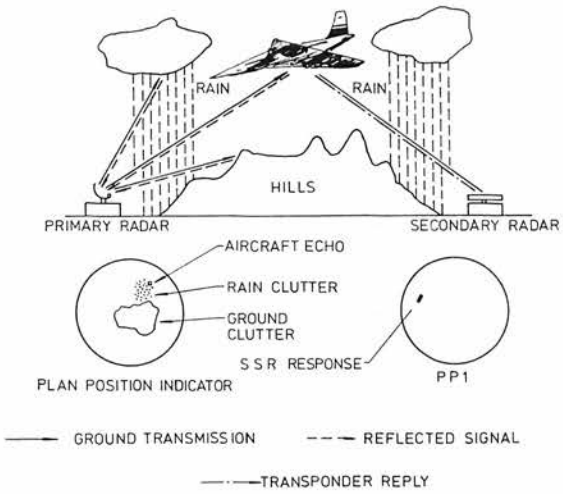


Fig. 2. Principles of primary and secondary radar.

Both civil computer-aided congested area (terminal control) systems, i.e., ARTS and MEDIATOR [17], and military systems, SAGE (United States) and LINESMAN (Great Britain) make extensive use of secondary radar to obtain accurate identification and authentication of primary radar returns.

*B. Operational Limitations*

Primary radar, whose coverage cannot extend to oceanic crossings like the Atlantic, is particularly subject to rain and ground clutter. Rain clutter can be reduced either by using an MTI system or with a wider bandwidth chirp waveform and pulse compression [18], thus reducing the range cell. Modest compression ratios, e.g., 25, are adequate, and surface acoustic wave (SAW) technology is readily applicable, particularly in airborne radar where size and weight are more significant.

Secondary radar [16] is not affected by clutter. Here an airborne transponder replies to the transmitted signal at a different frequency (Fig. 3). Confusion due to "fruit" and "garble," i.e., unwanted replies, is presently reduced by plot extraction on a PPI, although an alternative method using selective address (ADSEL or DABS) is also under development [19].

HF radio communication links over the North Atlantic are presently marginally reliable, provided a suitable "family" of channels is available to overcome propagation effects. The requirement for improved voice and data link facilities is apparent [20] due to the increase in subsonic air traffic and the introduction of supersonic aircraft. This necessitates consideration of new systems employing satellite repeaters [21].

Due to the requirement for high reliability in airborne equipment there is a built-in redundancy both of equipments

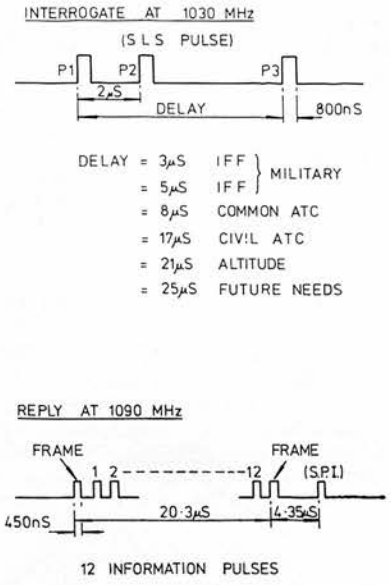


Fig. 3. Present SSR signal format.

and systems hardware, placing heavy pressure on both controllers and aircrew who must perform constant display monitoring. Several alternative schemes are under consideration to perform a level of integration of these equipments and displays in both military and civil environments.

## IV. Projected Growth of Civil Air Traffic Indicating Further Deficiencies in Existing Systems

In the United States the projected aircraft fleet for the year 2000 is approximately 1 million, with the peak airborne count exceeding 50 000 [22]. Here there is a preponderance of private fliers which results in a mix of VFR and IFR, as the private aircraft are not all equipped with SSR. Problems of congestion can be overcome either by installing onboard collision avoidance equipment or by imposing a discipline to restrict private aircraft from using congested areas.

The main problem in Europe, where air traffic is double the estimates of 5 years ago, covers the preponderance of protected areas resulting in congestion of the upper airspace, where route crossings now exceed 20 per hour. The MADAP system [23] situated near Brussels is a data processing system to handle the flight plans and SSR returns from aircraft in the upper airspace over Belgium, Luxemburg, The Netherlands, and West Germany. Although just commissioned, it is already inadequate to handle existing traffic.

The North Atlantic ATC system with its large peak summer load (524 crossings in one day in 1971) is becoming severely congested. A quarter million annual flights are forecast by 1980 [24] with 160 aircraft simultaneously outside line-of-sight communications. The high accuracy of inertial navigation equipment, which is currently fitted on most aircraft (Section III-A) that use the North Atlantic track system, can permit the use of composite tracks with reduced separations.

## V. Design Considerations Relevant to Future ATC Systems

### A. Procedures

It is helpful to comment on possible modifications to ATC procedures and to review design considerations for ATC systems before discussing the relevance of acoustic matched filters. Existing control procedures rely on a ground-based controller with total responsibility for the aircraft in his sector. Systems, such as the McDonnel Douglas EROS, Bendix IMAGE, and RCA SECANT [25], [26] provide the pilot directly with air-derived collision avoidance information placing the onus on him to make an avoiding maneuver without consulting any ground controller. The advent of area navigation on overland routes involves consideration of systems such as intermittent positive control (IPC) [19] that sends positive commands from the ground to selected low priority aircraft to avoid potential collisions.

### B. Satellite Hardware Considerations

Microwave satellite repeaters with their demonstrated capability and reliability for communications [27] are under active consideration for the functions of communication, navigation, and surveillance [28] in ATC systems. A synchronous satellite provides an area of coverage well in excess of that obtained from a single ground station. This enables a single repeater to operate, for example, over the majority of the United States without the mutual interference currently experienced from the many ground stations deploying SSR systems [16]. In RF link design the usual prime consideration is bandwidth conservation for optimum utilization of the available spectrum. Fixed ground-to-ground and satellite-to-ground microwave communications are essentially directional links employing high-gain narrow-beamwidth antennas. Here, bandwidth conservancy is not of prime importance as spuriously radiated spectral products are acceptably small. Links between aircraft and satellites are generally omnidirectional, which often results in critical power budgeting requirements because of the low antenna gains. One solution for optimizing the signal-to-noise ratio is to allocate many distinct exclusively assigned frequency channels in the satellite repeater. This complication of expensive satellite hardware is unnecessary when a single wide-band channel is utilized into which all subscribers are accessed on a code selection basis [28]. This is a natural application for matched filter reception techniques based on acoustic technology.

Consideration must be given also to interrelating the oscillator stability requirements with the Doppler shift expected on signals transmitted between a supersonic aircraft and ground terminal or synchronous satellite. The Doppler shift encountered on a 1.6-GHz $L$-band link with an aircraft flying at Mach 3.5 is typically 5 kHz [29], demanding an oscillator frequency stability better than $3\times10^{-6}$. This is a formidable requirement for microwave solid-state sources. These observations predicate the use of wide channel allocations ($>100$ kHz) with simultaneous access of several subscribers for optimal channel utilization.

### C. Propagation Effects

Propagation effects such as atmospheric distortion, attenuation, and ducting are broad-band phenomena. Further, a severe problem in communicating with an aircraft over sea on a satellite link is the sea-reflected multipath return [29]. The separation of the direct and multipath return can be accomplished with antenna directivity, suitable antenna polarization, or spread spectrum coding of the transmitted signal [29], which again predicates acoustic matched filter techniques. However, practical measurements to establish the magnitude of the multipath return [30] are inconclusive.

### D. Examples of Integration of ATC Equipments or Signals

An important consideration in the implementation of new systems involves the proposed level of equipment integration, particularly in military environments. Table II shows that aircraft currently contain a multitude of equipments. Equipment simplification starts with a progressive integration of the outputs of the existing equipments onto a common data processing system with a single sophisticated display, and progresses through integration of equipment operating in the same frequency band to the combination of the functions of communication, navigation, and identification into a single signal format. The totally integrated ICNI system [31], detailed in Section VII-C, is envisaged primarily for military applications where high security is mandatory. Its inherently high accuracy (typical positional errors less than 10 ft) solves the problem of providing a single navigation equipment for both terminal and en route control, a factor also of considerable interest to civil operators. Such equipment redesign will enable a vast reduction in the onboard power consumption, number of antennas required, spectral occupation, operation and maintenance costs, and will give increased accuracy, reliability, security, and interference protection. These latter features again point towards acoustic matched filter techniques. The collision avoidance surveillance (CAS) [25], [26] systems that involve the processing of air-derived signals to compute position of all aircraft within the system are intended primarily for the private pilot and thus price of usage is his key consideration. These systems position the expensive hardware in satellite-sited repeaters and ground processors to avoid avionics equipment costs.

### E. Voice and Data Link Considerations

ATC reporting based on short messages (<600 bit) does not justify the use of the voice link, which is already becoming overloaded. Instead all these could be accommodated on a single data channel [20] with a message format containing aircraft identity (30 bit), flight level (12 bit), and present position (44 bit). ATC messages necessitate a very high integrity data link as a single bit error can potentially result in a collision, particularly in a congested terminal area. The allocation of exclusive time slots (TDMA) for each aircraft represents a complicated and expensive solution to this problem, due to the necessity for accurate onboard clocks. The design of a novel completely asynchronous system which includes a message addressing capability [33] is described in Section VIII.

New techniques to provide a multiple access capability for voice traffic over, for example, the North Atlantic are also under consideration [21], [34]. Short messages with low channel occupancy preclude the use of uneconomic FDMA and TDMA systems which use a large bandwidth when the system accommodates a large number of aircraft. A random access discrete address (RADA) system [35] might represent a better technique where multiple access of a large number of subscribers is required. To realize a RADA system the baseband (vocoded) transmissions from each aircraft are bandspread by encoding each digit with a distinctive IF signature. The IF signature is used for both address and modulation. The design of the system, discussed in Section VI, results in interference which is proportional to the number of active subscribers. A given optimum usage can be designed into the system.

### F. Summary

It is preferable to finalize ATC procedures prior to concluding the final design of new ATC systems such as those detailed in Sections VII and VIII. Future deployment of satellites is predicted to obtain the maximum possible area coverage with a single system further accentuating the movement of ATC functions from VHF into microwave communications [14]. Band spreading, in preference to conventional FDMA, techniques are becoming attractive with the advent of acoustic matched filters and the need to cope with multipath environments. The areas of partial replacement of voice by data links and the integration of both ATC signal formats and equipments are justifying increased emphasis in the light of predicted overloading for existing ATC systems.

The necessary complexity in both signal formats and equipment hardware can be partially offset by the application of novel flexible signal processing techniques, especially by those realizable in SAW devices. Thus, it is considered relevant to examine briefly the significant and unique features of SAW technology.

## VI. Performance and Modem Design with Acoustic Matched Filters

### A. Introduction

Communication with low error rate in the presence of noise and interference is achieved efficiently by signal processing [36] prior to transmission and the corresponding inverse process at the receiver. This encoding and decoding involves the assignment of a particular code word (signature) to each message. The code word is selected from an appropriate "alphabet" of signal waveforms chosen such that their transmission makes the *best* use of the given noisy channel. Coded waveforms have also proved attractive for radar systems [18] where the definitions of noise and interference must be extended to include clutter. The signal waveforms after transmission through the channel arrive at the receiver in a corrupted form where an estimate (decoding) must be made in optimum fashion as to which message was sent. This involves the taking of a decision on the presence or absence of the received RF signals. These results are governed by the setting of a decision threshold that must be designed for a minimum probability of error. For any required maximum error rate with a specified signature and signal-to-noise ratio there exists an upper and lower threshold bound. Lower thresholds result in a higher probability of *false alarms* (noise voltages exceeding the threshold), and higher thresholds result in a greater probability of *missing* a received signature. Therefore, an acceptable compromise must balance the *false-alarm* rate and the *miss* rate. Now, if the signal-to-noise ratio at the threshold stage input is increased, the threshold can be raised for a given *false-alarm* probability. On the basis of maximizing both output signal-to-noise ratio and probability of detection for a linear filter, when the additive part of the channel disturbance is stationary, white, and Gaussian, the matched filter is the optimum primary signal processor [37].

### B. Performance of Acoustic Matched Filters

Impulsing a matched filter generates the time-reversed replica of the matched signal. Hence, the encoding and decoding operations can be accomplished, within certain technology bounds, with conjugate matched filter pairs. Fig. 4(a) (upper trace) shows a phase-shift keyed (PSK) IF signature gen-

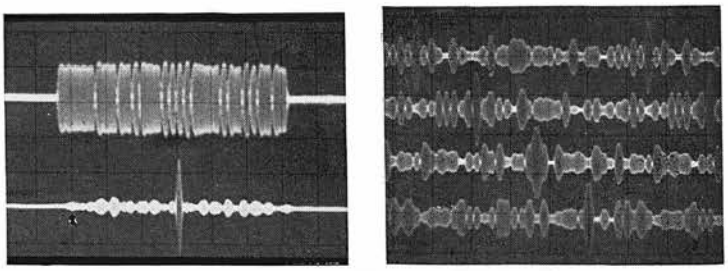

(a) (b)

Fig. 4. (a) Top trace: Impulse response of AMF binary phase coded with 31-chip $m$ sequence at 5-MHz chip rate on 90-MHz carrier (1 $\mu$s/large-scale div.). Lower trace: Aperiodic autocorrelation with same device (2 $\mu$s/large-scale div.). (b) Demonstration of synchronization acquisition for periodic autocorrelation functions of parent 31-chip $m$ sequence with 4 distinct 7-chip subsequences.

TABLE III

SUMMARY OF KEY ADVANTAGES OF ACOUSTIC MATCHED FILTERS

| Feature | Radar | Communications |
|---|---|---|
| Processing gain (provided prior to detection in devices) | reduced peak power for same range power: can be compatible with communications | increased signal to noise in band-spreading system |
| Band spreading | increased resolution<br>increased jamming immunity | multipath resolution<br>interference rejection<br>increased jamming immunity<br>less LO stability required |
| Waveform flexibility[a] | optimize for best clutter rejection | multiple addresses and signatures |
| Passive generation[a] | simple realizations of complex waveform | easy frequency hopping |
| Passive detection | permits truly asynchronous operation | permits truly asynchronous systems |
| Programmability[a] | electromagnetic compatibility, reduce crosstalk | random access by variable address (RADA)<br>improved security |

*Note:* Asynchronous tailor-made passive devices performing linear filtering.
[a] Features possessed particularly by surface acoustic wave devices.

TABLE IV

OPERATING RANGES AND PRACTICAL DATA FOR MATCHED FILTERS

| | | Operating Ranges | | | Practical Data | | | |
|---|---|---|---|---|---|---|---|---|
| | Device | $f_0$ (MHz) | $T$ ($\mu$s) | $B$ (MHz) | $TB$ | Sidelobe[b] Level (dB) | Insertion[c] Loss (dB) | Reference |
| Electromagnetic | lumped circuit | 0.2– 30 | 1000–10 | 0.02– 5 | 50 | −28 | | [39] |
| | tapped RF cable[a] | 100 – 500 | <1 | 50 – 300 | 100 | −30 | 50 | [40] |
| | folded tape waveguide | 500 –2500 | <1 | 200 –1000 | 720 | | 24 | [41] |
| Acoustic | magnetostrictive wire (tapped) | 0.5– 2 | 1000–10 | 0.1 – 2 | 500 | | 90 | [42] |
| | strip | 1 – 30 | 1000–30 | 0.1 – 5 | 64 | −23 | | [43] |
| | diffraction grating | 30 – 500 | 40– 1 | 10 – 250 | 160 | −40 | 29 | [44] |
| | love wave | 1 – 100 | 200–10 | 0.5 – 100 | 60 | −20 | 50 | [45] |
| | SAW IDT[a] | 20 – 300 | 50– 2 | 1 – 50 | 1000 | −25 | | [46]–[48] |
| | SAW grooved grating | 20 – 300 | 100– 2 | 1 – 100 | 1500 | | 37 | [49] |
| | convolver[a] | 20 –1000 | 40– 2 | 1 – 100 | 31 | theoretical | 90 | [50] |
| Microelectronic | digital[a] | baseband | 5000–10 | 0.1 – 20 | 127 | theoretical | N/A | [51] |
| | analog[a] | baseband | 1000 | 0.01– 15 | 13 | theoretical | N/A | [52] |

[a] Programmable devices.
[b] Sidelobe levels are quoted relative to the correlation peak.
[c] For CW at center frequency.

erated by impulsing surface acoustic wave analog matched filter (SAW AMF) and its detection in the conjugate AMF (lower trace). Coded time-domain signatures, such as PSK and chirp, with flat frequency spectra offer operational advantages when hard limiters are incorporated in receivers enabling subscribers at widely differing ranges to be accommodated.

Table III summarizes the key advantages that can be obtained with suitable waveform design and acoustic matched filter detection. A comparison of the operating ranges and known practical data of various acoustic devices with electromagnetic and microelectronic techniques is given in Table IV. New operating ranges ideal for many important radar and communications systems are reported in this issue of this

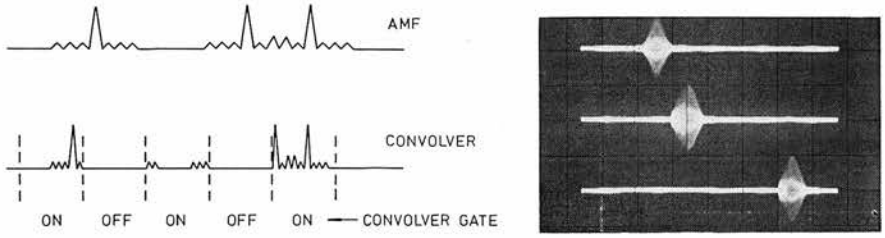


Fig. 5. (a) Schematic showing a received radar signal after processing in a matched filter, and the same signal after processing in convolver operating asynchronously (see Section VI-B). For simplicity, the transmitter pulse is taken as a 7-chip Barker coded waveform, and the three target returns are shown with the same amplitude. (b) Experimental result for an asynchronous convolver using rectangular RF pulses for the signal and reference. The three traces correspond to three values of signal delay, covering a range greater than the propagation delay in the device.

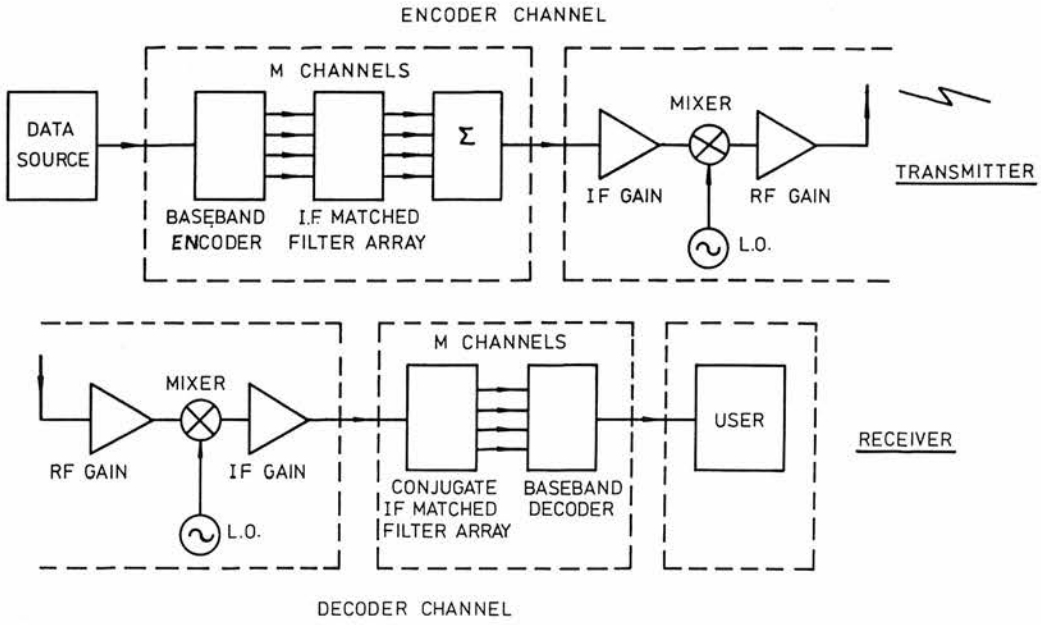


Fig. 6. *M*-ary modem using SAW matched filters for efficient encoding and decoding operations.

TRANSACTIONS. Further, development is necessary to realize devices for long delays (~1 ms) with processing gain ~100 for narrow-band (~100-kHz) systems; time–bandwidth products in excess of 1000 to reduce search times in synchronization; fast reprogramming (<100-ns) PSK filters processing 10-Mchip/s signals for ICNI; very high chip rate (>100-Mchip/s) devices for secure coded radio altimeter applications.

One crucial advantage of the acoustic filters (especially SAW) is their inherently asynchronous operation at RF, giving rise to fully asynchronous systems (see Sections VI-C and VIII-D) and powerful techniques for synchronization acquisition [53] in secure communications. For, secure spread spectrum applications, programmability is necessary and acoustic devices with the most promising features are the SAW programmable AMF and the nonlinear convolver. Fig. 4(b) illustrates the principle of synchronization acquisition [47] with a 7-tap SAW programmable AMF which is used to correlate four distinct 7-chip subsequences of a 31-chip waveform. Convolvers are not inherently asynchronous owing to the requirement for an accurately timed reference to ensure complete overlap of signal and reference in the region where their interaction is sensed. However, by using a repetitive reference signal and appropriate gating [54], asynchronous operation may be achieved. The output produced is shown schematically in Fig. 5(a). For visual display [Fig. 5(b)] the time segmentation effect is removed by arresting the time base when the output is gated off.

One further problem concerns the timing of the autocorrelation peak that is not directly related to the input signal timing due to the time segmentation effect. True timing is obtained in a *real-time recovery* unit using the reference timing information. Additional hardware is therefore required for applications that require asynchronous operation and true timing output. For comparison, a programmable PSK filter, although having limited programmability compared with the convolver, requires only tap switching circuitry and a read-only memory for code vector selection.

### *C. Definition and Characteristics of Band-Spread Communications Modems*

It is now possible to indicate how matched filters might fit into communication systems by investigation of a simple modem (Fig. 6). Consider the encoder and decoder processors split into baseband and IF sections. At the transmitter, digital data from a source (e.g., computer terminal or vocoder) is fed into a baseband encoder. Each message is assigned one or more of $M$ code words generated first at IF, by impulsing

TABLE V

EFFECT OF TIME–BANDWIDTH PRODUCT ON MINIMUM SIGNAL-TO-(NOISE PLUS INTERFERENCE) RATIO

| $B_ST$ | min $(S/I+N)_{i/p}$ dB | Relative Improvement (dB) |
|---|---|---|
| 1 | 11.5 | 0 |
| 13 | 0.4 | 11.1 |
| 31 | −3.4 | 14.9 |
| 127 | −9.5 | 21.0 |
| 511 | −15.5 | 27.0 |

*Note:* $P$ upper bound $= 10^{-5}$ for $\gamma = 1$.

the appropriate matched filter, and then translated to RF by mixing with a local oscillator. Each matched filter has a distinct *signature*, or code word, characterized by 1) waveform, e.g., phase-shift-modulated sequences such as the pseudonoise [55] and Barker [56] sequences, or frequency-modulated signals such as the linear chirp [18]; 2) center, or carrier frequency and modulation bandwidth; 3) relative delay (the delay is of importance in some frequency hopping schemes).

The choice of signature *alphabet* depends on the system requirements, e.g., number of users, mode of operation, i.e., coordinated or uncoordinated, propagation characteristics of the channel, desired level of message integrity, etc. At the receiver, the incoming signal is down-converted to IF and recognized in a conjugate matched filter array. Following demodulation of the matched filter output, a threshold detector stage makes the required decisions and sends pulses into the baseband decoder, whose output is a reconstruction of the source data stream.

The type of demodulator used can effect the error rate, which is dependent on the received signal-to-noise plus interference and the time–bandwidth product of the transmitted code waveform. In practice, the use of envelope demodulation instead of the preferred [36] phase or synchronous demodulation, which results in an effective 3-dB increase in error rate, is commonly necessary due to the difficulty of extracting phase information. Large time–bandwidth product codes are therefore required to ensure sufficient signal-to-noise ratios for a given false-alarm rate.

In [57], the equation relating false-alarm probability, $P$ to Gaussian disturbances and waveform time–bandwidth product for an envelope detector in the worst case situation, where the bandwidths of signal $B_S$ and interference $B_I$ are equal, is

$$P = \exp - \left[\gamma^2 B_S T \left(\frac{S}{I+N}\right)\right] \tag{1}$$

where $\gamma$ is a normalizing threshold constant and $S$, $N$, and $I$ are the signal, noise, and interference powers, respectively. Table V shows the minimum input signal-to-(noise plus interference) ratio which can be tolerated to obtain a false-alarm probability not exceeding $10^{-5}$ for various values of time–bandwidth product, taking $\gamma = 1$.

### *D. Experiments on a Simple M-ary SAW AMF Modem*

We have shown experimentally [58] that a matched filter expansion–compression loop offers a useful improvement in detection probability for a signal in noise and strong interference. However, in practice a simple loop does not make best use of the given channel. The $M$-ary system (Fig. 6) increases the efficiency of the communications channel. To illustrate the

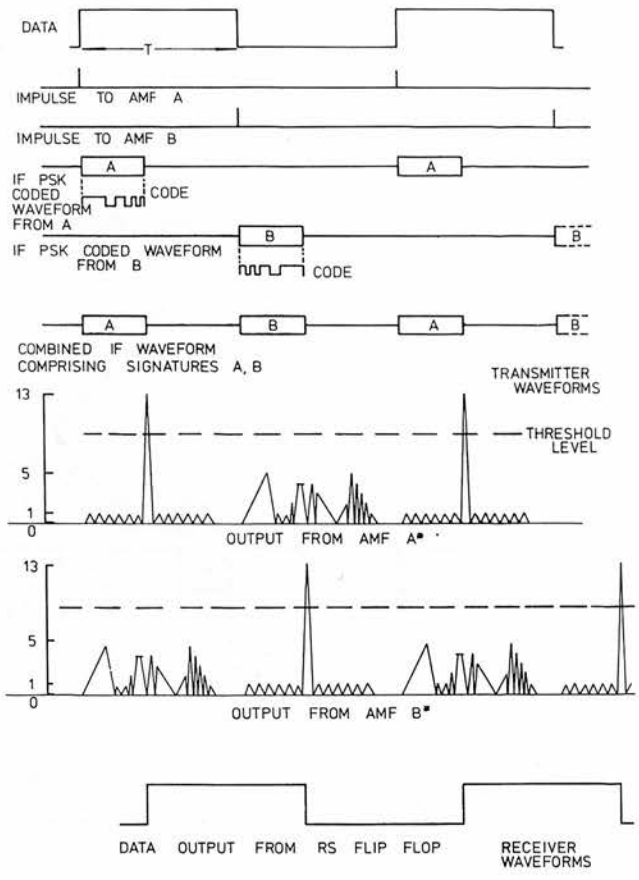


Fig. 7. Waveform diagram for simple two-signature $M$-ary SAW AMF modem.

$M$-ary principle, experiments were conducted for the simple case where $M = 2$. Thus, in each $T$ s one binary digit is transmitted and the corresponding data rate, $1/T$ bit/s, is subject to the maximum rate, $2B_S$, given by the sampling theorem.

The waveforms corresponding to the modem experiment are indicated in Fig. 7. For convenience four identical 13-chip Barker coded devices are used. Thus the two signatures generated ($A$ and $B$) were simply the Barker Code (1111100110101) and its time reverse (1010110011111). The cross correlation with the time-reverse sequence has peaks of relative height (5:13). These cross-correlation peaks arise from the imbalance of "1" and "0" states in the sequence and are not representative of the best autocorrelation and cross-correlation functions obtainable with selected binary PSK sequences [59]. In the receiver, the conjugate matched filters $A^*$ and $B^*$ have maximum response to codes $A$ and $B$, respectively. However, unlike the simple loop experiment, the threshold must be set halfway between the top of the auto-correlation peak and the top of the cross-correlation peak. This causes a degradation in performance because of the reduction in usable threshold range. The outputs of the threshold detectors are connected to set and reset a flip-flop which regenerates the data stream. Thus it is noted that a significant feature of SAW matched filters is their ability to retrieve data without synchronization preambles, enabling the construction of a truely asynchronous data detection system (as detailed in Section VIII).

The transfer of data (a 7-bit pseudonoise sequence) has been demonstrated at a clock rate of 25 kHz with low error rate ($< 10^{-7}$) in a noise and interference free coaxial wire link.

Error rates of less than $10^{-4}$ have been measured for simultaneous signal-to-noise and signal-to-"in-band" interference ratios of +8 dB. Selected signatures would enable the threshold to be lowered to the optimum [58] level and hence the error rate could be minimized.

The number of usable signatures and frequency slots is usually not sufficient in a simple $M$-ary system to provide random and simultaneous multiple access to a large number of subscribers. In Section VII the problems of selecting a sufficient number of codes with bounded cross correlations is highlighted in range differencing surveillance systems. The following two subsections indicate briefly certain possible implementations of SAW matched filters to previously published multiple access systems.

### *E. Time-Domain Multiple Access*

Reed and Blasbalg [60] described a time-domain multiple access (TDMA) $M$-ary system using the (7, 2) octal Reed–Solomon [61] code to generate a time–frequency pattern for each signal waveform. These codes exhibit orthogonality with an almost flat power spectrum, in addition, pseudorandom frequency hopping into eight channels is employed to combat multipath. The seven subpulses of each signature are *uncoded* 1.8-$\mu$s bursts of RF selected from eight possible frequency slots, the total message bandwidth being 5 MHz and the total RF bandwidth 40 MHz. A synchronized receiver first removes the pseudorandom frequency hop, then each subpulse is detected by its appropriate matched filter and maximum likelihood decoding extracts the data. This multiple frequency-shift keyed (FSK) system accommodates 4000 users at a data rate of 100 bit/s per user.

SAW matched filters can be used both to generate and detect the uncoded subpulses for the time–frequency pattern. Further, programmable AMF's duplicated in each of the eight pseudorandomly selected frequency slots would remove the synthesized local oscillator and only involve synchronous baseband gating of the matched filter outputs.

### *F. Random Access Discrete Address (RADA) Modem Implementation*

In address communication systems (Section V-E) a number of individual signatures constitute an address resulting in many different combinations providing a large address alphabet. Many subscribers can send arbitrary messages over a common wide-band channel at the same time and in the same geographical area by addressing each communication. The transmitted waveform has to carry both address and modulation. The most promising addressing technique is the exclusive allocation of a time–frequency pattern to each receiver, and possible modulation techniques are the digital delta modulation, quantized pulse position modulation (PPM), pulse code modulation, and analog PPM or pulse frequency modulation.

The number of addresses is determined inherently by the size of the time–frequency matrix. The selection of addresses depends on the system details. Certain solutions are outlined in the paper by Blasbalg *et al.* [62]. They propose a multiple FSK pseudonoise addressing modem, into which SAW matched filters could be fitted. A guide to the number of *unique* addresses $A$, obtained from a time–frequency matrix, is given by Magnuski [35]

$$A = \frac{F!}{(F-N)!N!} \times \frac{(T-1)!}{(T-N)!} \qquad (2)$$

where $F$ denotes the number of frequency slots, $T$ the number of time slots, and $N$ the number of coded sequences transmitted in the address. As a simple example, consider four frequency slots ($F=4$), five time slots ($T=5$), and three identical code sequences per address ($N=3$), yielding 48 unique addresses. These addresses are *quasi-orthogonal* in that two addresses may coincide in more than one time–frequency box. Their resolution becomes increasingly difficult as the mutual cochannel interference increases. A solution has been proposed by Chesler [63] combining $M$-ary and RADA techniques. A number of addresses $M$ are assigned to each receiver providing an optimum value of $M$ for which a minimum probability of error is obtained for each matrix size and channel utilization.

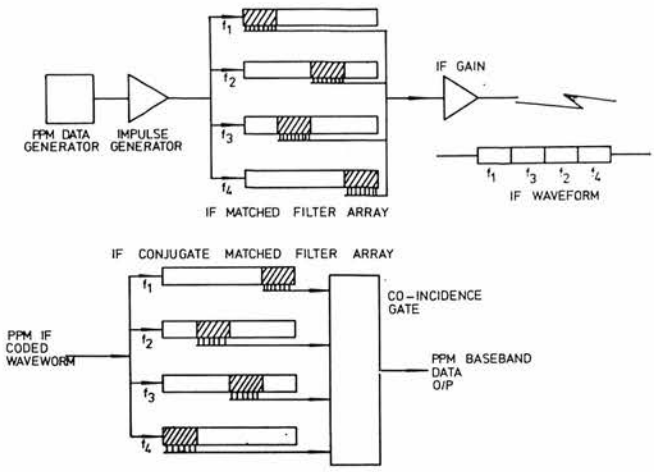


Fig. 8. Random access discrete address using SAW AMF's and SAW delay lines for encoding and decoding addressed PPM data.

TABLE VI
FUTURE ATC SYSTEMS

| | Simple ← | | → Comprehensive |
|---|---|---|---|
| Ground-based and onboard equipment | radar (primary and secondary) | air-derived collision avoidance (SECANT) | ICNI |
| Satellite transponder systems | inertial navigation reporting | AEROSAT | collision avoidance range differencing system |

A simple realization of a RADA modem for transferring PPM data is shown in Fig. 8. The recognition of both coded IF waveforms and the time–frequency pattern is necessary as this represents the receiver's address. For short coded waveforms, recognition of the time–frequency pattern may be accomplished through expeditious use of SAW delay lines to ensure that correct correlation in each frequency slot occurs in the same time slot. A coincidence gate performs the baseband decoding necessary to regenerate the PPM signal.

## VII. POSSIBLE FUTURE ATC SYSTEMS

### *A. Classification*

Following the review of properties, obtainable parameters, and advantages of utilizing acoustic matched filters in ATC, this section discusses certain representative new ATC systems under development for possible implementation in the late 1970's and beyond. These systems are classified in Table VI via a matrix scheme comprising simple though comprehensive

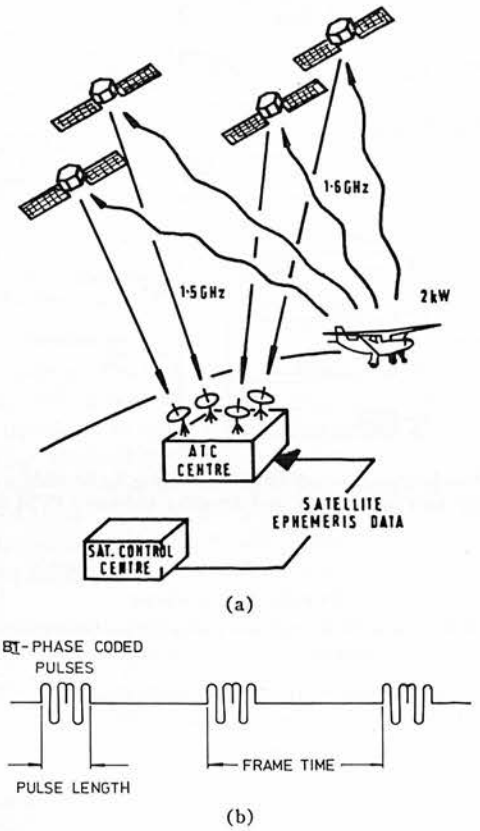


Fig. 9. Satellite range differencing systems. (a) Inclined eccentric orbiting satellites with ATC transponders. (b) Signal format.

systems. Space limitations preclude discussions of the important military IFF area where widespread interest in SAW matched filter techniques is currently being shown.

### *B. Range Differencing Surveillance Systems*

These systems [28] which are primarily intended for use in the continental United States (CONUS) have as an essential requirement the inclusion of all aircraft. The proposed method of operation involves a one-way ranging system, for bandwidth conservancy, where each aircraft is equipped with a beacon transponder which generates a unique coded ranging signal [32]. The use of an upper hemispherical coverage antenna enables routing of the transmitted signal through several widely spaced satellites back to a ground-based control center (Fig. 9). As no synchronization exists between the aircraft and the ground station, the use of four or more satellites enables calculation of absolute user position. For accurate receiver timing and separation of the returns from the many aircraft in the system, it is proposed to biphase modulate the transmissions with a coded sequence. This enables usage of a matched filter in the receiver to extract the required signal from among the multiple retransmitted satellite signals and to provide a timing accuracy equal to 1 chip of modulating code. The system ranging accuracy is therefore governed by the bandwidth of the transmitted signal. However, it is impossible to obtain the required 100 000 codes [59] for unique identification of each aircraft. Proposals have been submitted by TRW, Boeing, and Autonetics [28] to generate these identities using unique combinations of codes, pulse repetition rates, pulse placements, and transmission frequencies (Table VII).

The TRW LIT system [32] utilizes a single transmission

TABLE VII
RANGE DIFFERENCING CAS SYSTEMS

| Parameters of System | TRW | Boeing | Autonetics |
|---|---|---|---|
| Pulse length ($\mu$/s) | 51.1 | 255 | 20 (for 1 pulse) |
| Modulation rate (MHz) | 10 | 2 | 10 |
| Code length (chips) | 511 | 511 | 200 |
| Number of codes | 25 | 16 | 10 |
| Number of frequencies | 1 | 1 | 10 |
| Frame time (s) | 1.0–1.1 | 1.0–1.3 | N/A |
| Frame spacings ($\mu$s) | 10 | 50 | N/A |
| Number of frame addresses | 10 K | 6 K | 100×100 |
| Number of identifications | ¼ million | 100 K | 1 million |
| Accuracy of position (ft) | 250 | 300 | 260 |
| Transmitter peak power (kW) | 3.5 | 2 | 1 |

frequency of 1.6 GHz with a modulation rate of 10 MHz and a quarter of a million addresses as detailed in Table VII. The received signals, after recognition and timing, are fed into a PRP analyzing and tracking computer which predicts any likely conflicts. SAW AMF have been fabricated for generation and detection of the coded sequences used in this system. The Boeing proposals feature a similar LIT system of reduced accuracy due to the use of a signal of only 2-MHz bandwidth.

The Autonetics [28] proposal that covers not only simple surveillance but also en route navigation and communication, employs a pulse triplet containing the unique address. Air-to-ground communication messages can be sent 3 bit at a time by using the pulse triplet in a PPM format enabling the accomplishment of ranging and communications on the same signal format. This system represents a more comprehensive update version of the TRW and Boeing systems.

It should be noted that these surveillance systems transmit an identity pulse enabling the calculation of absolute position. However, the installation of accurate inertial navigation equipment offers an alternative surveillance system (discussed in Section VII) which transfers onboard navaid data to a ground controller over an asynchronous data link.

### *C. Integration of Communications, Navigation, and Identification Equipments*

ICNI [31], which was initially discussed in Section V-D, is a military concept requiring a signal format of high security and information fidelity when subjected to multipath returns, interference, jamming, and spoofing signals.

The proposed system utilizes a single communications channel that is common to all users with subscriber allocations organized on a TDMA system [31]. One-way transmission provides bandwidth conservation and removes the self-interference experiences in two-way transmission systems (SSR [16], SECANT [26], etc.). A typical subscriber would utilize one 10-ms slot per 10-s time frame to transmit position, identity, mission, fuel, and ordinance status, etc., with ample provision for error detection and correction, utilizing an onboard clock to time the start of transmission. The single time slot allocation may be used in several modes, accommodating simple time ordered signaling as previously described or discrete address interrogation and reply including data exchange with another subscriber [31].

To combat the problems of jamming and interference, it is intended to utilize a moderate bandwidth (10 MHz) with both pseudorandom band spreading and frequency agile techniques. Band-spread coding with matched filter detection also enables minimization of the transmitter profile reducing the visibility of the transmitted signal and the effectiveness of any

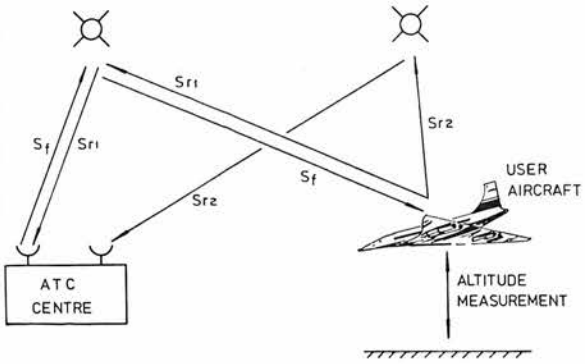


Fig. 10. Active tone ranging system.

hostile monitoring. These coding techniques which exhibit a reasonably flat spectral power density could permit utilization of the previously allocated TACAN band (960–1210 MHz) [10] for coexistence of both signals without any severe mutual interference. The bandwidths proposed for this system are between 10 and 25 MHz, which are easily accommodated by SAW AMF's. These AMF's, which perform rapid synchronization acquisition (Fig. 4), have been constructed to detect the 127-chip synchronization preambles [31]. It is anticipated that distinctly coded preambles will exceed the total currently achievable device delay, requiring a programmable AMF with the capability of changing code within a chip period. SAW matched filters are also expected to find many application in the detection of message data. This system highlights the advantages of a single signal format incorporating the functions of communication and ranging at the same transmitted power level without mutual interference.

### D. AEROSAT

The North Atlantic aeronautical satellite system AEROSAT comprises a joint verture by FAA and ESRO to provide an extension of positive ATC surveillance [21], voice, and high data rate functions [64] over the busiest oceanic air-traffic route in the world. In establishing a communications link over the North Atlantic a synchronous satellite represents the optimum choice of signal routing repeater. The specification of *L*-band transmission for ATC is expedient following the reservation of a substantial band from 1535 to 1660 MHz for aeronautical radio navigation and communication (Table II). The system is to be controlled and accessed through two oceanic control centers, one situated on each side of the Atlantic, with communication facilities to the existing ATC centers at Gander and Shanwick.

The AEROSAT system proposes initially to utilize two satellites, each one placed in synchronous orbit over the ends of the present track system. Surveillance is to be performed with a ranging system of 1-nmi ($1\sigma$) accuracy based on chirp [65], multiple tones, or digital ranging techniques [66]. Active ranging (Fig. 10) is accomplished by selectively interrogating the aircraft through one satellite (*Sf*) prior to detection and timing on the reply (*Sr*), containing onboard altitude information, that has been routed through the two satellites. To meet the traffic forecasts it is proposed to design six communications channels, three in each satellite, using simplex operation with narrow-band FM modulation. Systems planning includes one 1.2-kBd DPSK data link to cover the entire area which uses one of the satellite voice channels.

The requirements for each satellite therefore include the capability of simultaneously relaying two surveillance signals, providing three communication channels, accepting and acting on telemetry tracking and command signals, and performing necessary frequency conversions on all signals. Power budgets have been derived for both uplinks and downlinks that highlight the requirement to evaluate the tradeoffs in aircraft installation costs (e.g., antenna phased array designs), spacecraft weight, and transponder reliability.

It is intended to evaluate a preoperational system using the ATS-F satellite in 1974 to ascertain both the optimum voice modem and ranging techniques and also to evaluate fully the problem of multipath returns from sea reflections. The AEROSAT system, which is likely to be the first operational satellite ATC system, as envisaged uses signals with time–bandwidth products that exceed the capabilities of currently existing SAW devices. However, the use of acoustic strip delay lines could present significant technological advantages when performing the signal processing functions. Should the design and construction of onboard electronically steered phase arrays be impossible, then band-spreading techniques with SAW matched filter detectors could represent a significant technique for achieving the required aircraft to satellite power budgets.

## VIII. Novel High-Integrity *L*-Band Data Link for ATC

### A. Introduction

Pending the deployment of AEROSAT, no ground-based surveillance exists for the North Atlantic crossing. It was previously stated in Section III-A that all large aircraft will shortly be equipped with sophisticated and accurate inertial navigational equipments. This section describes a simple high-integrity *L*-band data link to output onboard navaid data which contains SAW matched filters, and the features of fully asynchronous operation with built-in error checking procedures for verification of message authenticity.

### B. Accessing Procedures

It is intended to confine reporting of position information to a single communications channel utilizing one-way signal transmissions combined with a selective address system. This differs from the ICNI concept by arranging subscriber accessing on an unsynchronized poled basis to accommodate individual aircraft interrogation rates suitable for both subsonic and SST. Navigation information which is always a message of known length (Section V-E) can therefore be accommodated within a fixed length message format (e.g., 120 bit), which includes address information. High integrity, the probability that a message will be received and outputed correctly, is vital in ATC data links. Throughput, which is a measure of the number of outputed messages for a given number of transmitted messages, is of lesser importance as it can be overcome by further interrogation. High integrity can be achieved for fixed length messages by the application of suitable baseband encoding techniques [33], [67].

### C. High-Integrity Encoding–Decoding Procedure

Matched filters giving improved detection probabilities by processing at IF do not provide high integrity without baseband error detection techniques. In a system using binary registers, this is achieved through a high level of message redundancy to avoid the absence of a "1" being interpreted as a "0" in the receiver. The application of tristate receiver logic, described by Parker [67], where reception of either a "1" or "0" data bit always constitutes a change of state, offers a

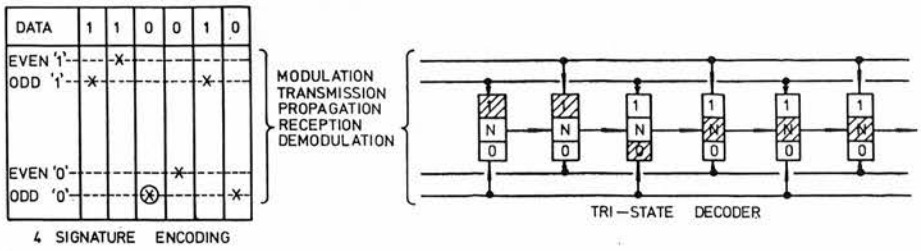


Fig. 11. Four-signature encoding and high-integrity decoding utilizing a tristate logic shift register.

significant improvement. A four-signature data encoding system allows encoding both for data level and for position in the message sequence. Fig. 11 shows the encoding in the transmitter of each data bit into one of four signatures. In the receiver, the detected baseband pulses are present on four wires feeding the decoding register. After clearing the register to the nondeterminate state, the first bit of message, which appears as an odd "0" clocks the first stage only to a "0" (because all other odd stages are inhibited) and removes the inhibit from the second stage. The receiving logic therefore ensures that even bits cannot be entered into odd states and vice versa. If one bit of the message is missing at the receiver the next bit, which possesses the incorrect positional information, is rejected. Then all the following bits are entered two stages in advance of their correct position resulting in a nondeterminate state in the last two stages. The occurrence of an odd and even bit overlap results in a register overflow. A single check bistable is employed to ascertain that no errors have been received before outputing the message onto the display. This illustrates a cheap and efficient method of realizing a self-checking high-integrity data detection system. It is fully asynchronous since the previous data bit provides the decoder shift pulses.

### *D. Modulation Format*

The choice of waveforms for the four distinctive signatures will be governed by ease of generation and detection and by other factors influencing the system performance. The four signatures can be readily obtained by using four audio tones within the allocated frequency channel. However, for an *L*-band channel this involves problems of oscillator stability (Section V-C). Band-spreading techniques using SAW AMF's, which are asynchronous devices, have potential advantages in that discrimination between signatures can be achieved, multipath returns can be resolved, and the system will be less sensitive to interference and jamming (Table IV). Two signatures can be realized with two chirp pulses, one positive slope and the other negative slope. A further pair of chirp waveforms with a different center frequency make up the four signatures. PSK waveforms could also be employed but large time–bandwidth products are necessary to reduce the cross-correlation products to acceptable levels [59].

The overall system operation, which is represented in Fig. 6 with $M=4$, encompasses the feeding of incoming data stream in the transmitter into a four-signature encoder which routes the data on to four busses to impulse the associated filter and generate the required signature [68]. The filter outputs, at IF, are then summed, amplified, and up-converted to *L* band. In the receiver the down-converted IF signal is fed into the four conjugate chirp filters, each of which gives an output on one of four lines which lead to the tristate decoder.

### *E. Conclusions*

The system as described is fully asynchronous and provides significant advantages, in privacy of transmitted signal and high message integrity, over existing and proposed data links. In addition, each of the individual facets of the system (Section VIII-A) uses proven techniques which if married should produce an easily engineered and operated system incorporating additional data link facilities to further reduce the communication channels load. It is concluded that the transmission of real-time navaid data represents a powerful technique for cost-effective surveillance system on oceanic crossings. However, the system as described has many wider areas of application to aircraft and battlefield IFF (high-integrity ADSEL/DABS concept), air-to-air computer dumping, and air-to-ground sonar buoy surveillance.

## IX. Conclusions

Implementation of new ATC systems involves cooperation between a large number of parties, implying a long time scale prior to implementation. It is therefore important that device designers and system planners should immediately coordinate their efforts to evaluate the performance of acoustic wave technology in a real-world situation. Highlighted are system philosophies for new microwave ATC systems incorporating matched filters which offer attractive band-spread coding in place of more conventional multiple access techniques. Acoustic matched filters, particularly surface-wave filters, have many advantages, e.g., economics and performance reliability, although strong competition can be expected from LSI semiconductor technology, despite the additional complexity necessary to achieve large dynamic range and asynchronous operation. In the interest of brevity we have excluded discussion of other acoustic devices, such as frequency filters, delay lines, and UHF oscillators for applications such as FDMA data transmission, radio altimeter, and selective address SSR. It can be concluded that ATC systems development has reached a critical phase due to the congestion of air traffic, and that signal processing in acoustic devices can offer significant advantages in the next generation of ATC systems.

## Appendix

### Glossary of ATC Terminology

| | |
|---|---|
| ADF | Automatic direction finding. |
| ADSEL | Address selective SSR. |
| AEROSAT | Aeronautical satellite system (North Atlantic). |
| AGARD | Advisory Group for Aerospace Research and Development. |
| ATC | Air-traffic control. |
| ARINC | Aeronautical Radio Incorporated. |
| ARTS | Automated radar terminal system. |

| | |
|---|---|
| ATS | Advanced technology satellite. |
| CAA | Civil aviation authority (United Kingdom). |
| CAS | Collision avoidance surveillance. |
| CONUS | Continental United States. |
| DABS | Discrete address beacon SSR. |
| DME | Distance measuring equipment. |
| EROS | Eliminate range zero system. |
| ESRO | European Space Research Organization. |
| FAA | Federal Aviation Administration (United States). |
| ICAO | International Civil Aviation Organization. |
| ICNI | Integrated communications navigation and identification. |
| IFF | Identification friend or foe. |
| IFR | Instrument flight rules. |
| ILS | Instrument landing systems. |
| IMAGE | Intruder monitoring ground equipment. |
| IPC | Intermittent positive control. |
| LIT | Location identification transponder. |
| MADAP | Maastrich automatic data processing equipment. |
| MLS | Microwave landing systems. |
| PPI | Plan position indicator. |
| SAGE | Semiautomatic ground environment. |
| SECANT | Separation and control of aircraft by nonsynchronous techniques. |
| SSR | Secondary surveillance radar. |
| SST | Supersonic transport. |
| TACAN | Tactical air navigation system. |
| VFR | Visible flight rules. |
| VOR | VHF omniranging. |

## Acknowledgment

The authors wish to thank Dollman Electronics and Microwave and Electronic Systems Ltd. for permission to describe their high-integrity *L*-band data link patent which originated in discussions between B. D. Parker, M. J. Moran, and J. N. Johnston; J. O. Clark, E. H. Boyenval, T. G. Thorne, C. Ullyatt, C. Ellingson, and D. Hitchings for positive contributions on ATC systems and philosophies; R. D. Lambert for SAW device fabrication; and J. G. Sutherland for experimental work.

## References

[1] *Instrument Flying Handbook*, Dep. Transportation FAA, Washington, D. C., AC 61-27A, 1968.
[2] *International Standards and Recommended Practices, Annex 11: Aeronautical Communications*, Int. Civil Aviation Organization (ICAO) publ.
[3] "Terminal air traffic control," DOT/FAA Air Traffic Services, Washington, D.C., no. 7110.8A, Apr. 1971.
[4] "En route ATC," FAA Air Traffic Services, Washington, D. C., no. 7110.9, Oct. 1967.
[5] C. C. Jackson, "The separation of air traffic over the North Atlantic," *Flight Int.*, vol. 89, pp. 967–970, June 1966.
[6] D. L. Stevenson, "UK Military and Civil ATC in harmony," *Interavia*, 1971.
[7] R. F. Hansford, *Radio Aids to Civil Aviation*. London, England: Heywood and Company, 1960.
[8] F. S. Stringer, "Hyperbolic radio navigation systems," *Wireless World*, vol. 75, pp. 355–365, 1969.
[9] G. E. Beck, *Navigation Systems*. London, England: Van Nostrand-Reinhold, 1971.
[10] S. H. Dodington, "Recent developments of the TACAN navigation system," *Elec. Commun.*, vol. 44, pp. 316–321, 1969.
[11] C. F. O'Donnell, *Inertial Navigation: Analysis and Design*. New York: McGraw-Hill.
[12] J. E. Clegg and T. G. Thorne, "Doppler navigation," *Proc. Inst. Elec. Eng.*, paper 2568R, Mar. 1958.
[13] A Carousel IV inertial navigation system manufactured by AC Electronics in conformity with ARINC specification 561.
[14] "Microwave landing systems," *Microwave J.*, vol. 15, Jan. 1972.
[15] M. I. Skolnik, *Introduction to Radar Systems*. New York: McGraw-Hill, 1962.
[16] K. N. Shaw and A. A. Simolunas, "System capability of ATC radar beacon system," *Proc. IEEE*, vol. 58, pp. 430–437, Mar. 1970.
[17] "Mediator ATC system comes into operation," *Radio Electron. Eng.*, vol. 41, p. 181, Apr. 1971.
[18] J. R. Klauder, A. C. Price, S. Darlington, and W. J. Albersheim, "Theory and design of chirp radars," *Bell Syst. Tech. J.*, vol. 39, pp. 745–808, July 1960.
[19] G. E. Lundquist, "Status and trends in civil ATC control systems," in *AGARD Conf. Proc.*, no. 105, *ATC Systems*, paper 7, 1972.
[20] N. A. Blake and J. C. Nelson, "A projection of future ATC data processing requirements," *Proc. IEEE*, vol. 58, pp. 391–396, Mar. 1970.
[21] R. W. Meier, "North Atlantic aeronautical satellite system development," *Proc. IEEE*, vol. 53, pp. 448–455, Mar. 1970.
[22] "Report of the DOT air traffic control advisory committee 1969," U. S. Government Publ.
[23] G. H. Trow, "ATC in the Eurocontrol area," in *AGARD Conf. Proc.*, no. 105, *ATC Systems*, paper 2, 1972.
[24] "North Atlantic air traffic forecasts," NATCS, paper CP-11, Mar. 1971.
[25] W. F. Arnold, "CAS causes conflict," *Electronics*, p. 69, Dec. 20, 1971.
[26] J. L. Parsons, "SECANT—A solution to the problems of mid-air collisions," in *AGARD Conf. Proc.*, no. 105, *ATC Systems*, paper 23, 1972.
[27] J. G. Peunte, W. G. Schmidt, and A. M. Werth, "Multiple-access techniques for commercial satellites," *Proc. IEEE*, vol. 59, pp. 218–229, Feb. 1971.
[28] D. E. Findley, "Satellite considerations in future ATC systems," in *AGARD Conf. Proc.*, no. 105, *ATC Systems*, paper 30, 1972.
[29] G. W. Barnes, D. Hirst, and D. J. James, "Chirp modulation system in aeronautical satellites," in *AGARD Conf. Proc.*, no. 87, *Avionics in Spacecraft*, 1971.
[30] "ESRO ATC balloon-aircraft satellite simulation experiment," European Space Research Organization, June 1971.
[31] C. E. Ellingson, "A practical design of an ICNI system," in *AGARD Conf. Proc.*, no. 105, *ATC Systems*, paper 32, 1972.
[32] D. D. Otten, J. H. Craigie, A. Garabedian, and D. D. Morrison, "Satellite for domestic air traffic control," presented at the AIAA 3rd Communication Satellite Systems Conf., Los Angeles, Calif., Apr. 1970.
[33] B. D. Parker, "Design of an air to ground asynchronous digital communication system for ATC," in *Air Traffic Control Engineering and Design*, Inst. Elec. Eng. Conf. Publ. no. 28.
[34] "System definition and design study of a pre-operational aeronautical satellite system," British Aircraft Corp., phase 1, Final Rep., July 1971.
[35] M. Magnuski, "Address communication systems," in *Communication Systems Engineering Handbook*, D. Hamsher, Ed. New York: McGraw-Hill, 1953, ch. 18.
[36] R. M. Fano, *Transmission of Information*. New York: Wiley, 1961.
[37] G. L. Turin, "An introduction to matched filters," *IRE Trans. Information Theory*, vol. IT-6, pp. 311–329, June 1960.
[38] *IEEE Trans. Microwave Theory Tech.* (*Special Issue on Microwave Acoustic Signal Processing*), this issue.
[39] K. W. F. Steward, "A practical dispersive network system," *Marconi Rev.*, vol. 28, pp. 254–272, 1965.
[40] B. Loesch, E. M. Hofstetter, and J. P. Perry, "A technique for synthesising signals and their matched filters," M.I.T. Lincoln Lab., Cambridge, Mass., Tech. Rep. 475, Dec. 1969.
[41] H. S. Hewitt, "A computer designed 720 to 1 microwave compression filter," *IEEE Trans. Microwave Theory Tech.*, vol. MTT-15, pp. 687–694, Dec. 1967.
[42] T. Martin, private communication.
[43] J. H. Eveleth, "A survey of ultrasonic delay lines operating below 100 Mc/s," *Proc. IEEE*, vol. 53, pp. 1406–1428, Oct. 1965.
[44] Anderson Laboratories, Inc., IMCON series.
[45] C. Lardat, C. Maerfeld, and P. Tournois, "Theory and performance of acoustical dispersive surface wave delay lines," *Proc. IEEE*, vol. 59, pp. 355–368, Mar. 1971.
[46] J. Burnsweig and E. H. Gregory, "High performance surface wave signal processing filters," presented at the Int. Filter Symp., Los Angeles, Calif., Apr. 15, 1972.
[47] P. M. Grant and J. H. Collins, "Synchronisation acquisition and data transfer utilising a programmable surface-acoustic-wave analogue matched filter," *Electron. Lett.*, vol. 8, pp. 299–301, 1972.
[48] C. F. Vasile and R. LaRosa, "1000 bit surface wave matched filter," *Electron. Lett.*, vol. 8, pp. 479–480, 1972.
[49] R. C. Williamson and H. I. Smith, "Large time bandwidth product surface wave pulse compressor employing reflective gratings," *Electron. Lett.*, vol. 8, pp. 401–402, 1972.
[50] D. P. Morgan, B. J. Darby, and J. H. Collins, "Programmable cor-

relator using parametric interactions in acoustic surface waves," *Electron. Lett.*, vol. 8, pp. 40–42, 1972.
[51] G. C. Bagley, "Radar pulse-compression by random phase-coding," *Radio Electron. Eng.*, vol. 36, pp. 5–15, July 1968.
[52] D. R. Collins, W. H. Bailey, W. M. Gosney, and D. D. Buss, "Charge coupled device analogue matched filters," *Electron. Lett.*, vol. 8, pp. 328–329, 1972.
[53] J. H. Collins and P. M. Grant, "The role of surface acoustic wave technology in communications systems," *Ultrasonics*, vol. 10, pp. 59–71, Mar. 1972.
[54] D. P. Morgan, J. H. Collins, and J. G. Sutherland, "Asynchronous operation of a surface acoustic wave convolver," in *Proc. 1972 IEEE Ultrasonics Symp.*, 72 CMO 708-8 SU, pp. 296–299.
[55] *Digital Communications with Space Applications*, S. W. Golamb, ed. Englewood Cliffs, N. J.: Prentice-Hall, 1964.
[56] R. H. Barker, "Group synchronisation of binary digital systems," in *Communications Theory*, W. Jackson, Ed. New York: Academic Press, pp. 273–287, 1953.
[57] R. J. Mayher and R. O. Meyers, "Utilization of matched filters in cochannel interference suppression," *IEEE Trans. Electromagn. Compat.*, vol. EMC-10, pp. 285–292, June 1968.
[58] B. J. Darby, P. M. Grant, and J. H. Collins, "Performance of surface acoustic wave matched filter modems in noise and interference limited environments," to be presented at the 1973 Int. Ultrasonics Conf., London, England, Mar. 27–29, 1973.
[59] R. Gold, "Study of correlation properties of binary sequences," U. S. Air Force Avionics Lab., Wright-Patterson AFB, Ohio, Tech. Rep. AFAL-TR-67-311, 1967.
[60] I. S. Reed and H. Blasbalg, "Multipath tolerant ranging and data transfer techniques for air-to-ground and ground-to-air links," *Proc. IEEE*, vol. 58, p. 422–429, Mar. 1970.
[61] I. S. Reed and G. Solomon, "Polynomial codes over certain finite fields," *J. Soc. Ind. Appl. Math.*, vol. 8, pp. 300–314, 1960.
[62] H. Blasbalg, D. Freeman, and R. Keeler, "Random-access communications using frequency shifted pseudo-noise signals," in *IEEE Int. Convention Rec.*, vol. 12, pt. 6, pp. 192–216, 1964.
[63] D. Chesler, "Performance of a multiple address RADA system," *IEEE Trans. Commun. Technol.*, vol. COM-14, pp. 369–372, Aug. 1966.
[64] D. Leverington, "An appraisal of an aeronautical satellite system," *J. British Interplanatory Soc.*, vol. 24, pp. 263–272, 1971.
[65] J. Burnsweig and J. Wooldridge, "Ranging and data transmission using digital encoded FM-chirp surface acoustic wave filters," this issue, pp. 272–279.
[66] H. Wunnenberg, "Tone ranging versus digital ranging," European Space Research Organization, Tech. Note ATCS/368/HW/EG.
[67] B. D. Parker, "Improvements in or relating to data transmission systems," U.K. Patent Spec. 1246218.
[68] J. N. Johnston and B. D. Parker, provisional patent application filed.

# Surface Wave Device Applications in Microwave Communication Systems

PETER M. GRANT, J. DOUGLAS ADAM, AND JEFFREY H. COLLINS

Reprinted by permission from
IEEE TRANSACTIONS ON COMMUNICATIONS
Vol. COM-22, No. 9, September 1974

# Surface Wave Device Applications in Microwave Communication Systems

PETER M. GRANT, J. DOUGLAS ADAM, AND JEFFREY H. COLLINS, SENIOR MEMBER, IEEE

*Abstract*—**The application of certain prototype devices, already realized in the complementary surface acoustic wave (SAW) and magnetostatic wave (MSW) technologies, is examined in the context of analogue and digital microwave communications equipments. The specifications of Gaussian response IF bandpass filters and satellite channel multiplexing filters are detailed in the context of SAW designs. Extensions of SAW filter technology to the construction of IF remodulating modems incorporating frequency modulated oscillators and discriminators are examined. Stable SAW oscillators are also reviewed in the context of lightweight, rugged, space-qualified local oscillator drives. The application of MSW technology to the design of a group delay equalizer for millimetric waveguide long-haul digital communications equipments is surveyed. Finally, the paper addresses the design of fixed and variable delay lines realized in both technologies, and SAW code generators, for application to path-length equalization and testing of high data rate microwave radio relay systems, respectively.**

## I. CURRENT TRENDS IN MICROWAVE COMMUNICATION SYSTEMS

MICROWAVE communication systems, both civil and military, are growing phenomenally throughout the world. For example, the consumption of telecommunications equipment is forecasted to double over the next seven years with Latin America, Asia, and Africa having the most basic needs. In the more highly developed countries, pressures for telephone and private-line equipment continue to mount with demands for color and conference TV, computer-to-computer data dumping for banks, and facsimile transmissions. This paper notes this explosive growth and addresses the following question. What impact could surface acoustic wave (SAW) and magnetostatic wave (MSW) solid-state technologies make on the long-term hardware implementation of these systems? Experimental results discussed here have been derived from a number of organizations, including our own. Therefore, it is the object of the paper to assess only these results in the context of IF processing in microwave communication systems.

It is not deemed necessary to review existing analogue and digital microwave radio relay equipments for terrestrial [1] and satellite [2] applications. All solid-state equipments are now available for terrestrial analogue equipments and considerable effort is being devoted to the design of digital transmission systems [3] which exhibit high compatibility with existing microelectronic interfacing equipment. Attention is focussed in this paper on microwave carriers between 2 and 20 GHz. However, specific problems of the millimeter waveguide system referenced elsewhere in this issue [4] and UHF mobile equipments are also discussed.

Section II of the paper reviews the status of surface acoustic wave (SAW) [5] and magnetostatic wave (MSW) [6] technologies and discusses how their respective parameter bounds affect their areas of application. Sections III and IV specify the requirements of frequency filters, local oscillators, and frequency discriminators primarily in the context of analogue microwave radio relay equipments. Their performance is delineated when realized in SAW technology. Sections V and VI discuss the problems of group delay equalization in millimeter overmoded waveguide systems and path-length equalization in a 20-GHz space-diversity pole line system [7]. MSW devices are explored as a potential solution to the problems of these future digital communications systems. Section VII discusses SAW code generators in the context of digital link testing and remarks briefly on the applications of SAW real-time Fourier transformers to the area. Finally, Section VIII highlights the advantages of SAW and MSW devices when compared with conventional circuit realizations and specifies trends.

## II. REVIEW OF SAW AND MSW TECHNOLOGIES

### A. Introduction to SAW

The well-reviewed surface acoustic wave (SAW) technology [5] can realize IF devices possessing broad bandwidth signal delays, custom-designed frequency responses, and coded signal generation and detection capability for matched filtering applications. All devices employ a single crystal piezoelectric substrate in which a sound wave propagates nondispersively along the surface, in a manner analogous to earthquake waves bounded to the earth's crust. The ability to arbitrarily sample or modify the propagating wave electrically and the extremely short wavelength, 30 $\mu$m at 100 MHz, which is 5 orders of magnitude smaller than that exhibited by electromagnetic devices, and their passive and reproducible nature, make the technology attractive for many real-time signal-processing functions.

Serious interest in SAW commenced in 1967 with the development of the interdigital electrode transducer

Manuscript received November 16, 1973. This work was supported in part by the British Science Research Council and in part by the British Post Office.

The authors are with the Department of Electrical Engineering, University of Edinburgh, Edinburgh, Scotland.

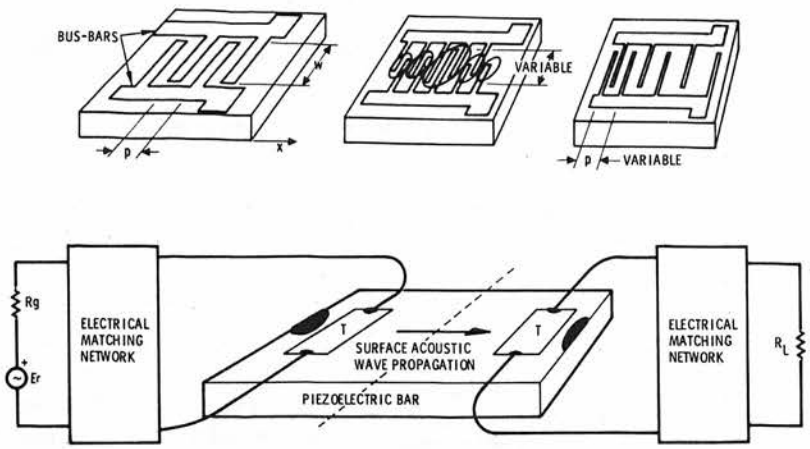


Fig. 1. Surface acoustic wave delay line schematic detailing metallized electrode interdigital transducer structure incorporating the following. (a) Constant periodicity, $p$, uniform weighting, $w$. (b) Apodization for amplitude weighting. (c) Frequency-weighted geometry.

(IDT) [8], [9] which permitted efficient transduction between electromagnetic and acoustic energy. The IDT consists of a set of interleaved metal electrodes and is fabricated by photoetching a deposited metal film. In the simplest form, the width and spacing of electrodes is equal and uniform throughout the pattern, as shown in Fig. 1(a). Electrical excitation of the transducer with a sinusoidal voltage produces a periodic electric field which penetrates into the piezoelectric substrate. The substrate responds by periodically expanding and contracting in unison with these fields. Suitable choice of substrate orientation produces two surface acoustic wave beams of aperture $W$ propagating normal to the IDT electrodes, without significant beam steering or diffraction. Peak output occurs at the synchronous frequency $f_0$ where

$$f_0 = v/p \tag{1}$$

and $v$ equals SAW velocity and $p$ equals transducer periodic length. Under this condition of acoustic synchronism, the stress contributions of all electrodes add in phase analogous to an end fire antenna array. Delay lines are simply fabricated with two transducers, as shown in the lower diagram of Fig. 1. IDT design can incorporate *any* desired amplitude and phase weighting by adjusting electrode overlap [Fig. 1(b)] and electrode spacings [Fig. 1(c)] to computer synthesize a wide range of frequency responses.

Device performance is constrained always by the parameters of the piezoelectric substrate material chosen. Quartz, lithium niobate, bismuth germanium oxide, aluminium nitride, and PZT ceramics are all favored media for SAW propagation [10], see Table I. The factors of strong piezoelectric coupling $k^2$, which permit high percentage bandwidth, low acoustic propagation loss for efficient operation, and low acoustic velocity for large signal time delay, all require to be evaluated in the context of specific device specifications. The commonly used ST-cut of quartz has a very low temperature coefficient of delay (~3 ppm/°C), but weak electromagnetic coupling which limits available bandwidths to 5–10 percent. Consequent delay line insertion loss is typically 10 dB, 6 dB of which arises from the bidirectional nature of the two IDT's. The high-$k^2$, closely coupled lithium niobate permits fabrication of delay lines with 8-dB insertion loss and 40 percent bandwidth. However, for large structures second-order effects, such as bulk mode generation, limit the fidelity of device operation. Both these materials can handle predominately VHF/UHF signals between 10 and 500 MHz.

The acoustic velocity of approximatelv 3 km/s permits up to 50-$\mu$s total delay to be accommodated within a 6 in substrate. The maximum frequency, 700 MHz, is currently limited by the resolution of photolithographically controlled etching to about 1 $\mu$m. This can be overcome by alternative masking techniques, such as electron beam fabrication, or by operating at harmonics of the IDT. However, for operation above $L$ band, the high propagation loss (several dB/$\mu$s) results in low delay line efficiencies and limits the available $Q$'s of filters. Low frequency operation is limited by the width of substrates available to achieve the necessary aperture $W$ for 50-$\Omega$ transducer design.

The simple construction procedure has led to the fabrication of delay lines which find applications in recirculating memories [11], fusing, and electronic countermeasures (ECM) systems. The ability to arbitrarily weight the transducer to obtain custom-designed frequency-selective delay lines has led to specialized IF frequency filters for TV receivers [12], and communications systems, which will be discussed later. SAW devices also find applications as matched filter processors of linear FM [13] and PSK [14] coded signatures for radar, communication, and air-traffic control (ATC) systems [15], providing a significant hardware reduction is achieved when compared to a microelectronic processor.

### *B. Introduction to MSW*

Magnetostatic waves (MSW) [6] are slow electromagnetic waves at microwave frequencies which propagate in narrow linewidth ferrimagnetic materials, notably yttrium iron garnet (YIG), subjected to a steady mag-

TABLE I
KEY PROPERTIES OF ATTRACTIVE SAW SUBSTRATE MATERIALS

| Material | Crystal Cut and Orientation | Piezoelectric Coupling Constant ($k^2$) percent | Optimum Device Bandwidth (percent) | Delay per Unit Length ($\mu$s/cm) | Temperature Coefficient (ppm/°C) |
|---|---|---|---|---|---|
| PZT | Basal plane | 4.3 | 23 | 4.5 | 120 |
| $Bi_{12}GeO_{20}$ | (111), (01$\bar{1}$) | 1.2 | 14 | 5.9 | 128 |
| $LiNbO_3$ | YZ | 4.3 | 22 | 2.9 | 91 |
| Quartz | ST, X | 0.17 | 5 | 3.2 | 0 |
| AlN/Sapphire | XZ | 0.63 | 10 | 1.6 | 42 |

etic bias field, $H$. Due to their low propagation velocity $C/10$ where $C$ is the velocity of light) and the small ample sizes ($<3$ cm on a side) used, the behavior of MSW an be accurately predicted by solving Maxwell's equations n the magnetostatic limit combined with the Polder ensor permeability [16] of the ferrite and the appropriate ample boundary conditions. MSW are inherently dispersive. The wave number is dependent on the magnetic ias field and signal frequency in the range $k = 10$ cm$^{-1}$ o $k = 10^4$ cm$^{-1}$. Time delays may be adjusted within the ange 1 ns/cm to 2 $\mu$s/cm, the upper limit being determined by the wave attenuation which for typical YIG is 0 dB/$\mu$s. Magnetostatic waves can propagate in the range 5 GHz to at least 20 GHz. MSW have been studied in etail for almost two decades, but their serious application to microwave signal-processing functions has awaited he production of low-loss single-crystal YIG deposited n the nonmagnetic garnet substrate gadolinium gallium arnet (GGG), by the process of liquid phase epitaxy 17]. YIG films can readily be grown with thickness beween 1 $\mu$m and 100 $\mu$m of area $\sim$4 cm$^2$ and exhibit ferriagnetic resonance linewidths [16] as low as 0.06 Oe 18]. The inherently uniform magnetic field inside a thin agnetic film allows wave propagation at a constant wavenumber in contrast to the position dependent demagetizing field and hence varying $k$ found in bulk crystal ods and plates [19].

Three orientations of a rectangular YIG film with respect to magnetic bias field are shown in Fig. 2 along with he appropriate dispersion diagram. All possess the comon features of a passband determined by the bias field. The volume modes (MSVW), Fig. 2(a) and (b), possess a sine or cosine variation of RF magnetization in the film ransverse to the direction of propagation, and an expoential decay in the RF magnetic field outside the film. The surface mode (MSSW), Fig. 2(c), fields decay away rom the film surface inside and outside the film. The ields are confined to one surface for a given propagation irection and bias field direction. A reversal of either bias ield direction or propagation direction will switch the ave to the opposite surface. This process is termed field isplacement.

Magnetostatic wave generation is achieved efficiently y placing a short-circuited transmission line across one nd of the YIG film so that the microwave magnetic ields of the transmission line are perpendicular to the ias field. In this configuration the RF magnetic field of he line couples to the MSW magnetization. Output coupling is simply the reverse of this procedure. With correct design, transduction losses can be as low as 3 dB per coupler. The bandwidth of this simple coupler is only limited in operation by the width of the strip, which must be less than $\lambda/2$ of the magnetostatic wave.

More complex coupling structures may be devised, for example, the meanderline transducer which is the magnetic analogue of the SAW interdigital transducer. This transducer, in principle, allows the frequency filtering inherent with IDT's in SAW to be carried out with MSW. MSW epitaxial film technology is directly compatible with planar microwave integrated circuit (MIC) technology. The YIG film on its GGG substrate may be placed on top of or buried in the MIC alumina substrate. Alternatively, the MIC conductor patterns may be deposited on the garnet substrate with the active YIG areas defined by selective etching techniques.

Signal-processing functions which have been realized to date [19] include dispersive delay lines, fixed delay lines, tapped delay lines, isolation, beamsteering, and convolution. Use of selective etching to fabricate MSW waveguiding structures where one transverse dimension is the order of a wavelength, promises that several functions can be integrated on one substrate.

### C. Comparison of SAW and MSW

SAW and MSW technologies perform many similar signal-processing functions which rely on spatial real-time tapping of the propagating wave and the ability to vary the phase and group delay characteristics to fit a desired specification. SAW and MSW are not, however, in direct competition, as each has areas in which it excels. The parameter bounds of the two technologies are highlighted in Fig. 3 in terms of the present limits of delay and operating frequency. From an engineering viewpoint, MSW is in its infancy compared with SAW. However, it should achieve ultimately the same degree of sophistication with emphasis upon the unique feature of MSW delay lines, namely *electronically* variable delay.

## III. FREQUENCY FILTERS FOR COMMUNICATIONS SYSTEMS

SAW IF filters [20] are applicable in both analogue and digital terrestrial communication systems and in multiplexers for the analogue hypergroups of FDM assemblages. Harmonic operation opens up the possibility of lightweight channel multiplexing filters for satellite applications. Specifically, five typical applications of SAW frequency filtering are addressed in this section.

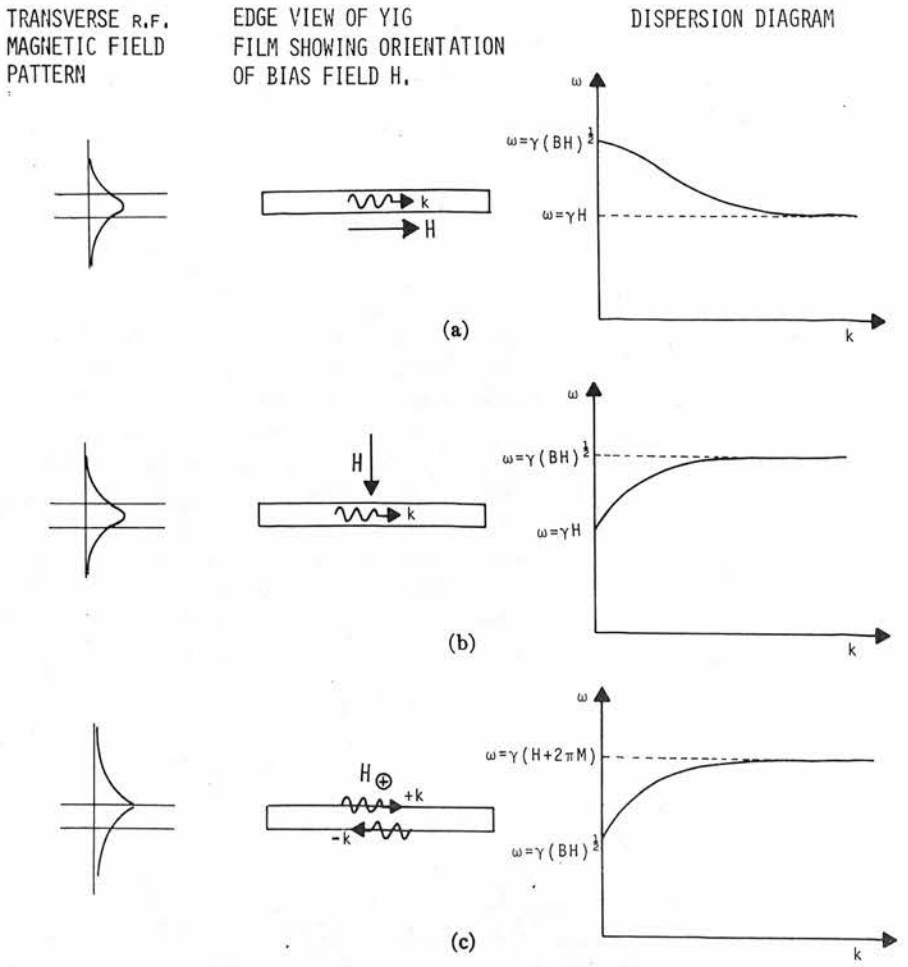


Fig. 2. Magnetostatic wave propagation modes in YIG films. In all cases, $\omega$ denotes angular frequency of excitation, $\gamma$ denotes the gyromagnetic ratio of 2.8 MHz/Oe, $B$ denotes the magnetic flux density, $M$ denotes the YIG saturation magnetization of 1780 Gauss, $k$ denotes the wave vector, and $H$ denotes the internal dc field which is related to the bias field through the YIG sample demagnetizing factors. (a) Bias field in plane of film, parallel to propagation direction. Volume mode—backward wave. (b) Bias field perpendicular to plane of film. Volume mode—forward wave. (c) Bias field in plane of film perpendicular to direction of propagation, surface mode.

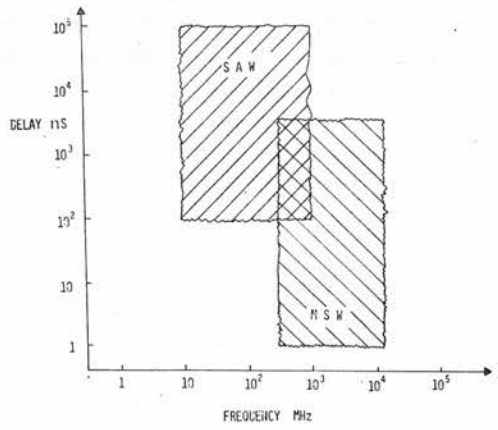


Fig. 3. Typical parameter bounds for surface acoustic wave and magnetostatic wave technologies.

SAW bandpass filters [21] have been designed with 0.25 to 40 percent passbands. As stated in Section II-A, independent control of amplitude and phase response is achieved by adjusting finger overlap and spacing, enabling a linear phase response to be obtained in the passband. Marginally cost-effective IF filters (<70p estimated quantity price) have already been produced for the passband and sound traps required in domestic color television receivers.

The essential requirements of 140-MHz IF filters [22] for 2700-channel analogue repeaters are delineated in Table II. SAW technology can readily achieve the ±15-MHz 1-dB bandwidth, with 0.1-dB ripple and 50-dB out-of-band rejection. These links are specified for low AM/PM conversion, permitting only 10-ns group delay variation over a 5-repeater hop, requiring each IF amplifier to possess <3 ns variation over a 50-dB automatic gain control (AGC) range. Conventional realization necessitates the design and cascading of a series of low-pass and high-pass filter stages with additional elements for group delay equalization. This results in a network with 10 to 20 adjustments, and a complicated and time-consuming alignment procedure.

SAW designs possess the flexibility to incorporate most group delay variations, thus designing out the necessity for external equalization networks. SAW frequency filters are also applicable to digital communication systems. For

TABLE II
SAW ESSENTIALS OF IF FILTER SPECIFICATION FOR 2700-CHANNEL REPEATER

| | |
|---|---|
| Center Frequency | 140 MHz |
| Insertion Loss | <8 dB |
| Passband Width | ±15 MHz (−1 dB) |
| | ±25 MHz (−3 dB) |
| Passband Ripple | <0.1 dB (±15 MHz) |
| Stopband Attenuation | >50 dB (@ ±40, ±80 MHz) |
| Group Delay Variation | 0.1 ns (±15 MHz) |

TABLE III
TYPICAL SATELLITE CHANNEL MULTIPLEXING FILTER SPECIFICATION

| | |
|---|---|
| Center Frequency ($f_c$) | 4 GHz |
| Insertion Loss | <15 dB |
| Passband Width | ±20 MHz |
| Passband Ripple | <0.22 dB |
| Stopband Attenuation (between 30 and 550 MHz from $f_c$) | >40 dB |
| Group Delay Variation | 6 ns (±16 MHz) |

xample, a Gaussian response IF filter for a 32-channel CM system operates at 70 MHz center frequency with ±2½-MHz 3-dB bandwidth and stopbands 35 dB down t ±7½ MHz. A group delay variation over the 3-MHz nter of band must be maintained within 3 ns. A SAW sign can meet this specification. Potential applications lso exist for frequency filters in the separation and transtion of multiplexed telephone traffic. The British Post ffice specification for a Band 3 hypergroup filter permits dB variation in insertion loss within the 8.620–12.336-IHz passband [23] and requires 50-dB rejection of the djacent Band 2 at 8.120 MHz. Studies are being conucted by the French Post Office to separate a large ypergroup FDM assemblage, with a bank of 10 SAW lters [24]. Individual filters are designed to select 4-MHz ide channels within the 20- to 70-MHz allocation, with 20-dB insertion loss.

The current INTELSAT IV repeaters [25] perform traight frequency translation from 6 GHz (receive) to GHz (transmit). Although a 500-MHz wide broad-band ront end is employed, the 12–36-MHz wide channels are eparated for power amplification in individual TWT's. he input and output multiplexers incorporate 6 to 10 ection Chebyshev waveguide filters each weighing apox 4 kg. Their large physical size and the likelihood of uture satellites having more transponders has focussed ttention on lightweight methods of realizing these filters. AW is an attractive possibility, providing the highequency IDT fabrication problems alluded to Section II-A can be overcome. Currently, 3-GHz SAW operation as been demonstrated with electron beam techniques. A ombination of this technique with harmonic operation f the IDT is predicted to overcome the 4-GHz barrier. he consequent 15-dB insertion loss penalty of a SAW evice would be overcome with transistor amplifiers. A asible specification is shown in Table III, containing he key features of low attenuation ripple (<0.2 dB) and lope (<0.12 dB/MHz), with a 10-ns group delay varition over 86 percent of the passband. The use of 10 ercent guard bands between channels requires a sharp irt selectivity with 35-dB attenuation at 0.75 percent ff-center frequency.

The explosive growth of UHF mobile communications sults in the necessity to allocate adjacent channels for ansmitters situated in close geographical proximity. Reivers must therefore incorporate stable bandstop filters o suppress the undesired channel. SAW technology can alize these filters [26] when the signal is divided to feed parallel combination of a SAW delay line and compensating attenuation and phase-shift network. Phase cancellation results from the summation yielding a comb-shaped frequency response with nulls whose spacing is controlled by the SAW delay line. Operation has been demonstrated [26] with a lithium niobate line at 430 MHz, exhibiting a nominal 10-dB insertion loss with 22-kHz wide 10-dB stopbands. The requirement of UHF mobile equipments demands 20-dB stopbands, each 5 kHz wide, necessitating the temperature-stable ST-cut quartz substrate. These examples of bandpass and bandstop filters, designed to meet comprehensive specifications, illustrate the seriousness which system designers are placing on the potential of SAW technology for communications equipment hardware realizations.

## IV. SAW DISCRIMINATORS AND LOCAL OSCILLATOR FOR ANALOGUE COMMUNICATION MODEMS

Analogue communication systems currently demodulate IF signals in a triple-tuned circuit FM discriminator, to convert back to the baseband assemblage of stacked telephone channels. IF discrimination can be achieved with both bulk and SAW devices, as described by Hartemann [27]. One approach used SAW filters operating at slightly different center frequencies with each output individually rectified, prior to voltage subtraction. This provides a linear relationship between input frequency and output voltage over a frequency band defined by the difference between the two transducer frequencies. Currently, better than 1 mV/kHz sensitivity is obtained with 2 percent linearity over 5 percent bandwidth. Devices use quartz substrates to obtain 0.03 ppm/°C temperature sensitivity, which is far better than the 100 ppm/°C of tuned-circuit discriminators.

SAW analogue FM discriminators for radio relay equipments require extension to accommodate 20 percent bandwidth with improvement to 1 percent linearity. Narrow-bandwidth high linearity 0.1-percent devices also have potential application in microwave link analysis equipments. SAW discriminators possess the capability of operating up to $L$-band frequencies, which is relevant to high-capacity analogue communication systems. Quartz-substrate phase discriminators with high stability zero crossover also find application in locking unstabilized high-power local oscillators to a bulk quartz plate or SAW reference oscillator.

Stable local oscillators are required extensively for frequency translation in microwave communication equipments [28]. Conventional crystal oscillators have funda-

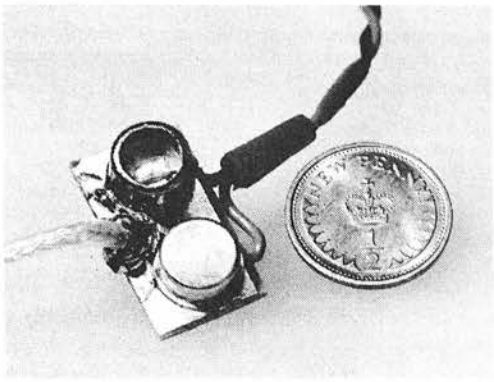

Fig. 4. Highlights microminiaturization of a 720-MHz SAW oscillator. (Courtesy M. Lewis, *Microwave Syst. News*, Nov. 1973.)

TABLE IV
SPACE-QUALIFIED LOCAL OSCILLATOR DRIVE SPECIFICATION

| | |
|---|---|
| Frequency | 500 MHz |
| Short-Term Stability (over $\frac{1}{4}$ second) | 1 in $10^{10}$ |
| Long-Term Stability (over 3 years) | 1 in $10^6$ |
| Temperature Stability (over $-10$°C to $+50$°C) | 1 in $10^6$ |
| Output Power | 5 mW |
| Overall Efficiency | >1 percent |

mental frequencies up to 30 MHz and become more fragile as the frequency increases. Harmonic operation permits extension to 150 MHz, necessitating further multiplication to achieve microwave frequencies. A simple frequency-selective SAW delay line, with the addition of a high-gain feedback loop, forms an oscillator with no mode ambiguity which achieves fundamental operation to 700 MHz [29]. Fig. 4 shows a SAW oscillator designed for 720-MHz operation. ST-cut quartz is attractive for stable oscillation and rugged devices. Experimental SAW oscillators exhibit overall efficiences comparable with a quartz bulk oscillator and transistor multiplier chain—500-mW dc input for 5-mW RF output at 700 MHz. Custom-designed amplifiers which are predicted to reduce power consumption by an order of magnitude make these devices especially attractive for a space-qualified local oscillator drive, whose typical requirements are highlighted in Table IV. Short-term stabilities (<1 second) of 1 part in $10^{10}$ are required while SAW oscillators are achieving 1 part in $10^9$. Long-term aging of several ppm per month has been achieved, but is still inferior to existing oscillator performance. Improvements in preparation of the quartz surfaces seem destined to alleviate this shortcoming.

These oscillators can be easily amplitude, phase, or frequency modulated for accurate trimming or data modulation. The FM capability permits consideration of an all SAW IF analogue communications modem incorporating an oscillator-discriminator pair. With voltage excitation of a varactor diode across the IDT, a SAW modem generates and detects modulation depths of 2.5 percent which represents a significant advance over the 0.1 percent achievable with bulk quartz oscillators.

## V. MAGNETOSTATIC WAVE GROUP DELAY EQUALIZER

Experimental millimeter wave trunk communication systems using the low loss $TE_{01}$ propagation in overmoded circular waveguide are currently reaching field-trial stages in Great Britain and other countries. The British Post Office system, which has been described by White *et al.* elsewhere in this issue [4], operates with 50-mm diameter helical copper guide. The available bandwidth above 32 GHz has been divided into two bands. Band I, from 32 to 50 GHz, will use channels 500-MHz wide and a repeater IF of 1.25-GHz center frequency. Band II, from 52 to 80 GHz, will use channels 1-GHz wide and a repeater IF center frequency of 2.5 GHz.

The group delay variation inherent in circular waveguide propagation must be equalized if optimum use is to be made of the available bandwidth. The linear group delay variation introduced by a 14.58-km waveguide length, in Band I over a 500-MHz channel width, varies monotonically from 42 ns at 32 GHz to 12 ns at 48 GHz, and, in Band II, over a 1-GHz channel width, from 18 ns at 52 GHz to 4 ns at 88 GHz. Equalization will be performed on the IF signals before regeneration. Thus an equalizer will be required for each channel at each repeater.

Presently available group delay equalizers include the folded-tape meanderline [30], the resonant ring equalizer [31] and bridge "T" lumped component networks [32]. All can be made to satisfy the system dispersion and linearity requirements. They have, however, characteristics which are *fixed* during manufacture and cannot be varied easily *in situ*. This is an undesirable situation, since the amount of equalization required will not be known precisely until the waveguide is laid. In general, due to geographical factors, each channel at each repeater in a trunk system will require a unique amount of equalization.

The unique feature of magnetostatic wave delay lines is that they are electronically variable via the magnetic bias field and this makes them attractive for this application [33]. Fig. 5 shows a theoretical plot of delay against frequency in Band I for a 20-$\mu$m thick YIG film operated in the surface wave mode [Fig. 2(c)] demonstrating the dependence of the delay upon the magnetic bias field. The delay is inversely proportional to the thickness of the film. The opposite sense of dispersion, delay decreasing with increasing frequency, is obtained by operating in the backward volume wave mode, [Fig. 2(a)].

Recent experiments in our laboratory have demonstrated that a simple magnetostatic delay line can be designed to approximate the linear group delay variation required. In a typical example, a 22-$\mu$m film excited by 100-$\mu$m wide microstrip couplers, spaced 1 cm apart, operating in the surface mode, showed an approximately linear delay variation with frequency of 15 ns over a 500-MHz band centered on 1.25 GHz, Fig. 6. The insertion loss midband was 12 dB with band edges a further 6 dB down. The bias field requirement was only 76 Oe, and is

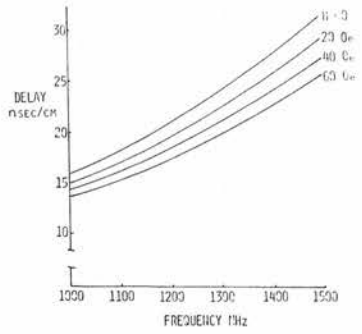


Fig. 5. Theoretical plot of delay versus frequency of magnetostatic wave. Surface mode propagation, with bias field as parameter, in a transversely magnetized YIG film of thickness 20 $\mu$m. Note that the characteristics show the key feature of electronically variable delay.

thus readily adjustable for trimming the equalizer characteristics.

Before the magnetostatic group delay equalizer can be used in a practical system, the slope linearity must be improved to within $\pm 0.5$ ns, and the phase ripple removed. The nonlinearity will be brought within acceptable limits through the use of magnetic, dielectric and conducting layers overlayed on the YIG surface. Phase ripple, which can be identified with Fresnel ripple, and spurious magnetostatic modes will be removed by operation away from the sharp low-frequency edge of the magnetostatic wave passband, by absorption of undesired magnetostatic modes, and by external electromagnetic matching techniques.

Magnetostatic wave devices using epitaxial materials are compatible with planar MIC technology. An entire subassembly may be deposited on a 2 × 2-cm garnet substrate. Thus an adjustable group delay equalizer with integral input and output matching and ferrite bias magnet may be produced in a one-cubic-inch volume.

## VI. IF DELAY LINES FOR DIGITAL COMMUNICATION MODEMS

Space-diversity communication systems, such as the British Post Office 20-GHz poleline system [7], employ two or more geographically separated transmission routes with wide repeater spacings. Path switching in the terminal receiver is used to overcome the narrow fade margins by selecting the route which offers the lowest error rate under high precipitation conditions. Data must not be lost during switching. One approach is to use a compensating IF delay line to synchronize the signal from both paths. This concept is similar to the differential absolute delay equalization (DADE), that is utilized on analogue systems carrying data under voice (DUV) traffic, avoiding loss of data when a standby link is switched into circuit.

A typical link of 100-km length employing 7 repeaters can be expected to exhibit a path-length difference of 3 to 4 km, owing to geographical repeater siting problems. Path-length equalization may be approximated with fixed delay lines, to accommodate 2-, 1-, $\frac{1}{2}$-, $\frac{1}{4}$-km differential spacings having 8-, 4-, 2-, and 1-$\mu$s delays realized on YZ

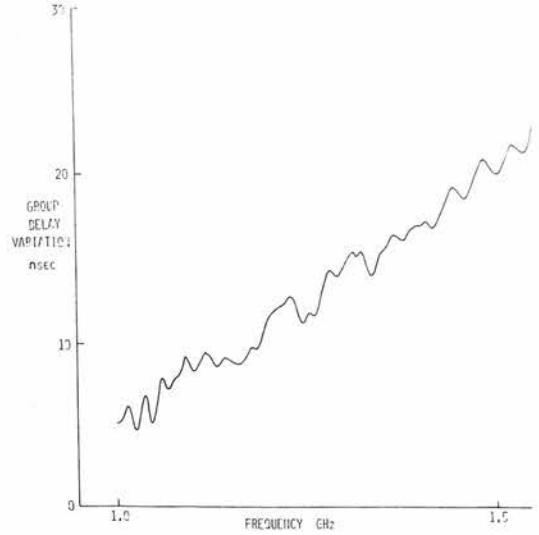


Fig. 6. Experimental results of variation in group delay versus frequency of a magnetostatic surface wave in a YIG film of thickness 21 $\mu$m with a bias field of 76 Oe. These results are relevant directly to the field trial of the British Post Office $TE_{01}$ millimetric waveguide system planned for 1975.

lithium niobate at 1.2-GHz center frequency and 132-MHz 3-dB bandwidth. Device insertion loss of <20 dB and group delay variations of approximately 2 ns would be required. However, route switching without loss of data requires synchronization to within half a bit, necessitating a variable delay line of 1-$\mu$s maximum delay and 4-ns setting accuracy. This can be achieved with a pair of dispersive SAW filters [34] or, more efficiently, with a magnetic bias field adjustable MSW device.

As stated in Section II-B, simple magnetostatic delay lines are inherently dispersive, but it has recently been demonstrated [35] that by spacing a metal plate a few thousandths of an inch from a YIG film surface, nondispersive operation can be obtained over a limited bandwidth with the bias field arrangement of Fig. 2(c). The basic device arrangement is shown in Fig. 7(a) with a 10-$\mu$m thick YIG film on a GGG substrate of dimensions 1.5 cm × 0.7 cm × 1.25 mm. Excitation was by microstrip couplers 75-$\mu$m wide with glass as the dielectric spacer. Fig. 7(b) shows Bongianni's results for the time delay of the magnetostatic wave propagating on the lower surface of the film $(+y)$ as a function of frequency between 2 and 3 GHz with the dielectric thickness as a parameter. Constant delay characteristics, within 5 ns, were obtained over a 200-MHz bandwidth at 2.3 GHz. The minimum insertion loss was 15 dB with triple transit suppression of 45 dB on the delayed signal pulse. Direct feedthrough was less than 50 dB. The location of the constant delay region in the delay/versus frequency characteristic of the device is determined by the ratio of the YIG/dielectric thickness $d/t$ and magnetic bias field. Suitable adjustment of $d/t$ will result in 10 percent bandwidth being available for time delays in the range 10 ns to 1 $\mu$s with insertion losses of less than 10 dB for short delays and 30 dB for 1 $\mu$s delay.

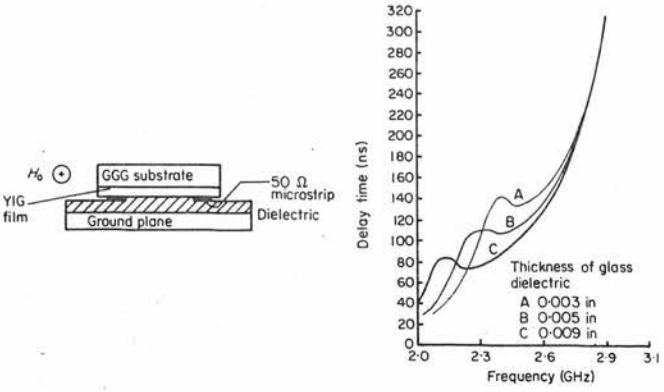


Fig. 7. Realization of nondispersive magnetostatic wave delay line. (a) Microstrip arrangement using a dielectric layered structure. (b) Delay versus frequency as a function of dielectric thickness.

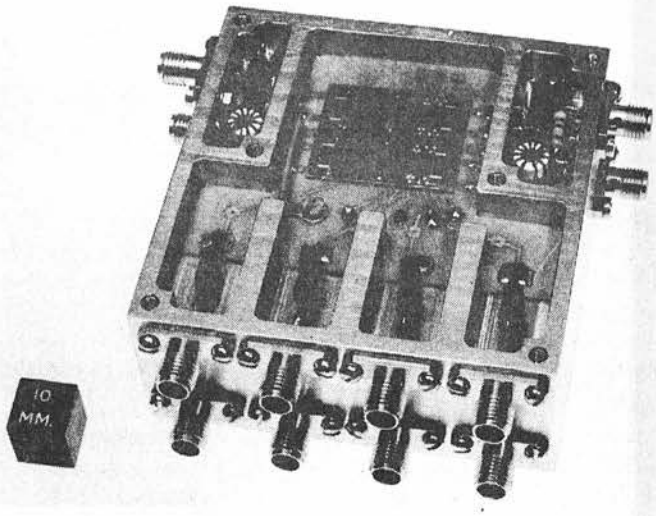


Fig. 8. SAW PSK code generator on a 100-MHz IF carrier at 20 MBd equivalent to 100-stage register. (Courtesy Standard Telecommunications Laboratories, England.)

## VII. IF MODULATORS AND DEMODULATORS FOR DIGITAL COMMUNICATIONS

Regenerative digital communications repeaters employ a demodulator to convert the received signal from PSK IF to baseband. Optimization of the signal-to-noise ratio can be performed with a bit-matched filter which permits the best decision to be made as to the relative phase of the received signal [36]. SAW technology can be used to decode PCM, PPM, MFSK, PSK, or DPSK signals. Experiments conducted with simple uncoded SAW bit matched filters for use in a MFSK system [37] showed receiver performance within 1 dB of theoretical, equivalent to that achieved with conventional quenched resonator devices. However, in most systems, the SAW devices can be implemented directly at VHF/UHF frequencies, precluding the necessity for IF processing. Studies on the error rate performance of a 192-MBd 4-phase DPSK Gray demodulator [38] highlighted the potential application of SAW technology to achieve both the stable delays and accurate filtering necessary for efficient operation.

Evaluation of any communication system during commissioning or service is most conveniently performed with a measurement which simulates the system traffic [39]. Digital systems are often tested by modulating the IF signal with a long binary pseudonoise sequence. When an identical code generator is employed in the receiver and synchronized to the received data, a simple comparator can perform an error rate count to assess the quality of transmission and performance of terminal and repeater equipments. This is a performance measurement, similar to the white noise test, and not a diagnostic procedure such as link analysis, which highlights the degrading factors of AM/PM conversion, gain, and phase linearity.

Conventional code generators employ microelectronic shift registers with logical feedback. However, when fabricating registers exceeding 20 stages at clock rates over 100 MHz, factors such as propagation delays, clock synchronization, and power dissipation problems become acute. SAW technology offers a solution by producing a modulated IF signal output without any mixer and oscillator. In the pseudonoise generator demonstrated by Morgan [40], the microelectronic shift register is replaced by a SAW delay line incorporating one input transducer and two feedback taps. The tap outputs are amplified and summed, prior to gating positive or negative impulses on to the input transducer.

Fig. 8 shows a prototype SAW PSK code generator of Crisp [41]. It is equivalent to a 100-stage shift register with a 100-MHz IF output, PSK modulated at 20 MBd. Current fabrication techniques permit these devices to be extended to 300-stage registers at 150 MBd, for minimal increase in power consumption. Such a device consumes typically 15 mW/bit, exhibiting an order of magnitude improvement over standard emitter-coupled logic circuit techniques.

The ability of SAW devices to compute fast Fourier transform algorithms in real time [42] with speeds in excess of 1 MHz, possessing an order of magnitude improvement over existing digital processors, offers exciting new potential for this technology in many applications areas. The design of a SAW convolver directly interfaced with the computer executive control should enable achievement of a broad-band microwave link diagnostic equipment with 60-dB dynamic range. When Fourier analysis is applied to selected codes, such a system promises the provision of a new generation of high-speed microwave-link analysis equipments. The development of SAW fast Fourier transform processors is predicted to open up a significant new application area for this technology.

## CONCLUSIONS

Table V summarizes the applications to microwave radio relay systems of a range of devices realized in the

TABLE V
SUMMARY OF RELEVANT SAW AND MSW DEVICE APPLICATIONS TO MICROWAVE COMMUNICATIONS

| Device | Applications Area | Advantages | Disadvantages |
|---|---|---|---|
| SAW Frequency Filter (Fundamental) | IF Filters | No Adjustments Light Weight | |
| SAW Frequency Filter (Harmonic) | Satellite Channel Multiplexing Filters | Design Out Group Delay Variations | High Insertion Loss |
| SAW Oscillator | Space Qualified Local Oscillator Drive and Analogue Communications Modulator | High Operating IF, Easy Harmonic Selection | Poor Long-Term Stability |
| SAW Discriminator | Analogue Communications Demodulator | High Operating IF | Moderate Operating Bandwidth, Moderate Linearity to Date |
| MSW Group Delay Equalizer | Equalize Waveguide Dispersion in Millimetric Trunk Systems | Adjustable Delay Slope | Phase Ripple and Delay Linearity Evident |
| SAW Fixed Delay Lines | Delay Equalization for Digital Links Employing Space Diversity | Stable and Accurate Delay | Marginal Bandwidth on Temperature Stable Substrates |
| MSW Variable Delay Line | Delay Equalization for Digital Links Employing Space Diversity | Electronically Adjustable. Operate at GHz IF | Moderate Insertion Loss for $\mu$s Delays |
| SAW Bit Matched Filter | Digital IF to Baseband Decoder | Optimizes SNR | Difficult to Achieve Highest Data Rates Required |
| SAW Pseudonoise Generator | Acceptance Testing of Digital Links | Direct IF Modulation | Fixed Data Rate |

complementary SAW and MSW technologies. Space limitations have precluded a comparison and accurate cost analysis with other technological implementations of equivalent functions. However the key features of miniaturization, accurate design, and cost effectiveness have been stressed. SAW technology should first impact IF frequency filters, with inbuilt group delay equalization, and analogue communication IF modems employing frequency-modulated signal formats. Growth in digital systems is presenting new application areas, such as group delay and path-length equalization, which offer challenging opportunities also to MSW designs. Finally, it is noted that communications growth is predicted to use higher IF and transmission frequencies which, in the future, will favor both SAW and MSW versus competing technologies.

## ACKNOWLEDGMENT

The authors would like to thank the staffs of Hewlett Packard Ltd., the British Post Office, Microwave & Electronic Systems Ltd., the University of Edinburgh, and the University of Trondheim for their contributions.

## REFERENCES

[1] D. Dorsi, "A survey of microwave terrestrial communication systems," in *Proc. Microwave 73*, pp. 77–89, 1973.
[2] C. L. Cuccia, "Progress towards million channel satellite communications systems," in *Proc. Microwave 73*, pp. 3–11, 1973.
[3] Sarguent, "The design of quarternary PSK systems for high capacity terrestrial and satellite communications."
[4] R. W. White, M. B. Read, and A. J. Moore, "Recent British work on millimetric waveguide systems," this issue, pp. 1378–1390.
[5] D. P. Morgan, "Surface acoustic wave devices and applications: Part 1—An introductory review," *Ultrasonics*, vol. 11, no. 3, p. 121–131, 1973.
G. S. Kino and H. Matthews, "Signal processing in acoustic surface wave devices," *IEEE Spectrum*, vol. 8, pp. 22–35, Aug. 1971.
*Microwave J.*, special issue, vol. 13, Mar. 1970.
[6] J. H. Collins and F. A. Pizzarello, "Propagating magnetic waves in thick films—A complementary technology to surface wave acoustics," *Int. J. Electron.*, vol. 34, no. 3, pp. 319–351, 1973.
[7] T. R. Rowbotham, "Short-hop radio-relay system work at 20 GHz," in *Proc. Microwave 73*, pp. 112–118, 1973.
[8] R. M. White and F. W. Voltmer, "Direct piezoelectric coupling to surface elastic waves," *Appl. Phys. Lett.*, vol. 7, p. 314, 1965.
[9] W. R. Smith, H. M. Gerard, J. H. Collins, T. M. Reeder, and H. J. Shaw, "Analysis of interdigital surface wave transducers by use of an equivalent circuit model," *IEEE Trans. Microwave Theory Tech.*, vol. MTT-17, pp. 856–864, Nov. 1969.
[10] J. H. Collins, P. J. Hagon, and G. R. Pulliam, "Evaluation of single crystal piezoelectric materials for surface acoustic wave applications," *Ultrasonics*, vol. 8, no. 10, pp. 218–226, 1970.
[11] H. van de Vaart and L. R. Schissler, "Acoustic surface-wave recirculating memory," *IEEE Trans. Microwave Theory Tech.*, vol. MTT-21, pp. 236–243, Apr. 1973.
[12] R. F. Mitchell, "Acoustic surface wave filters," *Philips Tech. Rev.*, vol. 32, p. 179, 1971.
[13] J. D. Maines and J. N. Johnston, "Surface acoustic wave devices and applications: Part 2—Pulse compression systems," *Ultrasonics*, vol. 11, no. 5, pp. 211–217, 1973.
[14] S. T. Costanza, P. J. Hagon, and L. A. MacNevin, "Analog matched filter using tapped acoustic surface wave delay line," *IEEE Trans. Microwave Theory Tech.* (Corresp.), vol. MTT-17, pp. 1042–1043, Nov. 1969.
[15] P. M. Grant, J. H. Collins, B. J. Darby, and D. P. Morgan, "Potential applications of acoustic matched filters to air-traffic control systems," *IEEE Trans. Microwave Theory Tech.*, vol. MTT-21, pp. 288–300, Apr. 1973.
[16] B. Lax and K. J. Button, *Microwave Ferrites and Ferrimagnetics*. New York: McGraw-Hill, 1972.
[17] H. J. Levinstein, S. Licht, R. W. Landorf, and S. L. Blank, "Growth of high-quality garnet thin films from supercooled melts," *Appl. Phys. Lett.*, vol. 19, no. 11, pp. 486–488, 1971.
[18] J. D. Adam, J. M. Owens, and J. H. Collins, "Studies of FMR linewidth in thick YIG films grown by liquid phase epitaxy," in *Proc. 19th Conf. Magnetism and Magnetic Materials*, Boston, Mass., Nov. 13–16, 1973.
[19] J. H. Collins, J. D. Adam, and J. M. Owens, "Microwave device applications of epitaxial ferrimagnetic films," in *Proc. European Solid State Devices Conf.*, 1972, pp. 83–126.

[20] C. S. Hartmann, D. T. Bell, Jr., and R. C. Rosenfeld, "Impulse model design of acoustic surface-wave filters," *IEEE Trans. Microwave Theory Tech.*, vol. MTT-21, pp. 162–175, Apr. 1973.
[21] R. F. Mitchell, "Surface acoustic wave transversal filters, their use and limitations," in *Inst. Elec. Eng. Aviemore Conf. Proc.*, no. 109, 1973, pp. 130–140.
[22] T. Watanabe and T. Kurokawa, "140-MHz IF main amplifiers for 2700-channel microwave repeaters," *IEEE Trans. Commun. Technol.*, vol. COM-18, pp. 651–662, Oct. 1970.
[23] British Post Office, Line Frequency Chart, A458.
[24] B. Serzec, private communication.
[25] *COMSAT Tech. Rev.*, vol. 2, Fall 1972.
[26] K. G. Plass, "Acoustic surface wave bandstop filters for UHF frequencies," in *Proc. European Microwave Conf.*, 1973, paper C 8.3.
[27] P. Hartemann, "Surface acoustic wave phase and frequency discriminators," in *Inst. Elec. Eng. Conf. Proc.*, no. 109, pp. 152–166, 1973.
[28] P. M. Grant and J. H. Collins, "Surface acoustic wave device applications in microwave radio-relay systems," in *Inst. Elec. Eng. Conf. Proc.*, no. 109, pp. 299–308, 1973.
[29] M. F. Lewis, "The design, performance and limitations of SAW oscillators," in *Inst. Elec. Eng. Conf. Proc.*, no. 109, pp. 63–72, 1973.
[30] P. J. Tu, "A computer-aided design of a microwave delay equalizer," *IEEE Trans. Microwave Theory Tech.*, vol. MTT-17, pp. 626–634, Aug. 1969.
[31] B. Wardrop, "Strip line microwave group delay equalisers," *Marconi Rev.*, pp. 150–177, 2nd Quarter 1970.
[32] P. S. Brandon, "The design of methods for lumped-constant dispersive networks suitable for pulse compression radar," *Marconi Rev.*, pp. 225–253, 4th Quarter 1965.
[33] J. D. Adam and J. H. Collins, British Patent Application, 42943/73.
[34] J. Burnsweig, W. T. Gosser, and S. H. Arneson, "Electronically controllable time delay," in *Proc., Int. Microwave Symp.*, Boulder, Colo., 1973, pp. 134–136.
[35] W. L. Bongianni, "Magnetostatic propagation in a dielectric layered structure," *J. Appl. Phys.*, vol. 43, no. 6, pp. 2541–2548, 1972.
[36] C. L. Cuccia, "Phase shift keying: The optimum modulation technique for digicom," *Microwave Syst. News*, vol. 3, p. 3, Jan. 1973.
[37] K. V. Lever, E. Patterson, D. G. Scotter, and B. G. Feasey, "Assessment and performance of matched filters for MFSK communications," in *Inst. Elec. Eng. Conf. Proc.*, no. 109, pp. 329–332, 1973.
[38] A. Rønnekleiv and O. Kjoestad, "Mellomfrekvenstrinn for PSK-PCM demodulator basert pa akustiske over flatebolger," Trondheim Tech. College, Rep. K225.
[39] R. Coackley, "A survey of measurement techniques for microwave communication systems," in *Proc. Microwave 73*, pp. 189–196, 1973.
[40] D. P. Morgan and J. G. Sutherland, "Generation of pseudo-noise sequences using surface acoustic waves," *IEEE Trans. Microwave Theory Tech.*, vol. MTT-21, p. 306, 1973.
[41] J. J. Crisp and J. S. Heeks, "The application of SAW devices to code generation," in *Inst. Elec. Eng. Conf. Proc.*, no. 109, pp. 270–277, 1973.
[42] J. M. Alsup, R. W. Means, and H. J. Whitehouse, "Real time discrete Fourier transforms using surface acoustic wave devices," in *Inst. Elec. Eng. Conf. Proc.*, no. 109, pp. 278–286, 1973.

★

**Peter M. Grant** was born in St. Andrews, Scotland, on June 20, 1944. He received the B.Sc. degree in electronic engineering from the Heriot-Watt University, Edinburgh, Scotland, in 1966.

From 1966 to 1970 he worked as a Development Engineer with the Plessey Company, Ltd., England, at both the Allen Clark Research Centre and Havant, designing frequency synthesizers and standards for mobile military communications. Following a year as Senior MOS Applications Engineer with Emihus Microcomponents, Glenrothes, Scotland, he was appointed to a Research Fellowship at the University of Edinburgh, Edinburgh, Scotland, to study the applications of surface acoustic wave devices to communication systems.

Mr. Grant is a member of the Institution of Electrical Engineers, London.

★

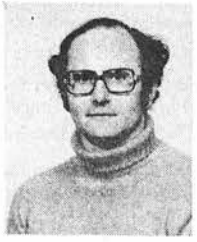

**J. Douglas Adam** was born in Stirling, Scotland, on March 21, 1943. He received the B.Sc. degree in electrical engineering from the University of Strathclyde, Glasgow, Scotland, in 1965, the M.Sc. degree in materials science and the Ph.D. degree from the University of Glasgow, Glasgow, Scotland, in 1967 and 1969, respectively. His doctoral thesis was on magnetoelastic wave propagation in yttrium iron garnet (YIG).

From 1969 to 1971 he was a Research Fellow at the University of Glasgow, working on the vapor phase growth of epitaxial YIG films. He is presently a Research Fellow at the University of Edinburgh, Edinburgh, Scotland, working on wave propagation in epitaxial YIG films and their applications to communication systems.

★

**Jeffrey H. Collins** (SM'73) was born in Luton, England, on April 22, 1930. He received the B.Sc. degree in physics and the M.Sc. degree in mathematics from the University of London, London, England, in 1951 and 1954, respectively.

From 1951 to 1956, his experience in microwave tubes and ferrite parametric amplifiers was obtained during employment at the GEC Hirst Research Centre, England, and at Ferranti, Ltd, Edinburgh, Scotland. From 1957 to 1967, he was with the Electrical Engineering Department, University of Glasgow, Glasgow, Scotland, where he taught in the fields of network theory and materials science, and researched microwave ferrites and microwave acoustics. During the scholastic years 1966–1968, he was a Research Engineer in the W. W. Hansen Laboratories of Physics, Stanford University, Stanford, Calif., engaged in research on surface acoustic waves, magnetic garnet delay lines, optoacoustic interactions, and pulse compression applications. From 1968 to 1970 he was Director of Physical Sciences at the Electronics Division of Rockwell International, Calif. In 1970 he returned to Scotland, where he is currently Professor of Industrial Electronics at the University of Edinburgh, Edinburgh, Scotland.

Prof. Collins is a Fellow of the Institution of Electrical Engineers (IEE), of the Institution of Electronics and Radio Engineers (IERE), London, and of the British Institute of Physics.

Reprinted by permission from
IEEE TRANSACTIONS ON COMMUNICATIONS
Vol. COM-22, No. 9, September 1974

UDC 534.21: 621.372.54: 621.3.049.776

# Programmable surface acoustic wave devices utilizing hybrid microelectronic techniques

**R. D. LAMBERT***

**P. M. GRANT,** B.Sc., C.Eng., M.I.E.E.†

**D. P. MORGAN,** M.A., M.Sc., Ph.D.†

and

**Professor J. H. COLLINS,**
M.Sc., F.Inst.P., C.Eng., F.I.E.E., F.I.E.R.E.†

*Based on a paper presented at the IERE Conference on Hybrid Microelectronics held in Canterbury on 25th to 27th September 1973.*

**SUMMARY**

Programmable matched filters can be realized using surface acoustic wave propagation in conjunction with external microelectronic circuitry. Here two devices, a programmable analogue matched filter and a diode convolver, are discussed, highlighting the similarities in constructional technique. Specific device requirements include an r.f. circuit which for 10 MHz signal bandwidth must possess a 310 $\mu$m pitch. Factors influencing the choice of the thin film hybrid microelectronic technique are outlined and the design, fabrication and performance details are described.

*Formerly at the University of Edinburgh; now with General Instrument Microelectronics Ltd., Glenrothes, Fife, Scotland.
† Department of Electrical Engineering, University of Edinburgh, King's Buildings, Mayfield Road, Edinburgh EH9 3JL.

## 1 Introduction

Many radar and communication systems[1,2] now utilize signal formats consisting of sequences of coded waveforms, or *signatures*, to overcome propagation effects, improve detection probabilities and permit multiple access capability. Signature generation (expansion) in the transmitter and detection (compression) at the receiver can be performed with a suitable filter designed to match to the transmitted signal. Such a matched filter[2] has an impulse response which is the time-reverse of the signature and thus performs correlation. The correlation process selectivity enhances the required signal as compared to noise and interference, giving a characteristic narrow correlation peak preceded and followed by a number of time sidelobes when the desired signal is received. The particular waveforms considered here are phase-shift keyed (p.s.k.) modulated r.f. carriers where each of the contiguous time segments of modulating code is known as a chip. For a binary coded signal the r.f. phase is therefore 0 or $\pi$ rad during each chip period depending on the particular code used.

This paper examines the design and construction of matched filters, fabricated by combining thin film hybrid and surface acoustic wave (SAW) technology. Specifically, programmable devices are considered where the response can be electronically controlled to correlate a large variety of coded waveforms. Programmability has wide ranging attractions including: high level security, adaptability to overcome variable interference, and multiple address capability—facets which cannot be conveniently achieved with a bank of fixed coded filters. The devices under consideration are the programmable analogue matched filter a.m.f. and diode convolver, which pose similar technological and fabrication problems and are conveniently fabricated with hybrid microelectronic technology.

Section 2 details the background to realizing matched filters with SAW techniques and describes the implementation and performance of the two devices with conventional discrete component hardware. Sections 3 and 4 describe technological considerations and detail the design and construction of a hybrid programmable a.m.f., then outline the performance achieved and compare SAW a.m.f.s against competing technologies. In conclusion, Section 5 outlines the future programme required to evaluate applications potential of these devices.

## 2 Surface Acoustic Wave Programmable Matched Filters

SAW devices are generally constructed using polished piezoelectric substrates, where the acoustic wave is launched by the application of a suitable electric field.[3] This is achieved efficiently by the interdigital transducer, shown schematically in Fig. 1, which consists of interleaved metal electrodes photoetched from a deposited metal film. The transducer, which can also detect these waves, applies a field whose spatial periodicity corresponds to the SAW wavelength, typically 30 µm for a frequency of 100 MHz.

Figure 1 shows the structure of an a.m.f., whose

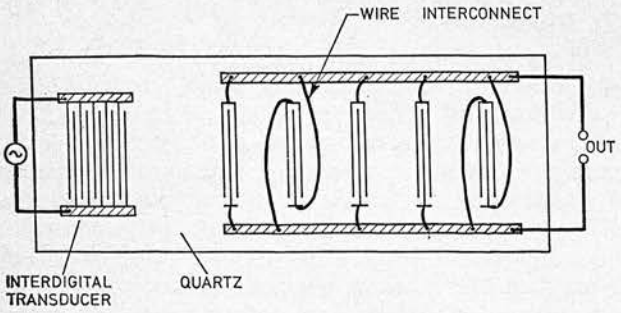


(a) Fixed-coded analogue matched filter.

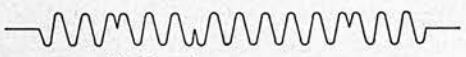

(b) Impulse response.

**Fig. 1**

impulse response is required to be the p.s.k. waveform shown. When an impulse is applied at the left transducer, a surface wave packet with a corresponding number of periods is produced. The packet is subsequently sampled in turn by a series of taps, which are simply transducers with a relatively small number of electrodes. When the taps are spaced by a distance corresponding to the duration of the wave packet, the device expands the impulse into a continuous p.s.k. waveform where the phase of the signal from an individual tap is determined simply by the polarity of the connexions as shown in Fig. 1.

The substrate material is usually chosen to be quartz, since the ST-cut of this material gives a very low temperature coefficient of delay (less than 3 parts/$10^6$/deg C). The weak electromechanical coupling in this material helps to reduce second-order effects, an important factor since the number of electrodes is large. On the other hand, it leads to relatively large insertion loss, typically 50 dB in expansion. The SAW velocity, 3158 m/s, implies attractively compact size (< 5 cm) for a device with 13 μs delay.

### 2.1 Programmable Analogue Matched Filters

The a.m.f. can be made programmable by using an electronic switching network between the taps and summing bus to control the phase contribution of individual taps, in accordance with a binary code stored in an associated shift register (Fig. 2). Reprogramming to a new code is accomplished simply by reading the desired code from a read-only-memory (r.o.m.) which stores a library of possible codes. Switching and summing of the r.f. signals requires a high performance switching network, in contrast to the remaining logic circuitry which simply provides d.c. levels except when reprogramming.

In certain applications there are however requirements for a fast reprogramming capability, necessitating consideration of both switching network and code store transient speeds.

Programmable a.m.f.s have been constructed using the 4 diode ring circuit of Fig. 3 to switch each tap. One device[4] with 90 MHz centre frequency included 7 taps at 1·24 mm pitch (400 ns delay) using discrete electronic components (glass encapsulated diodes) in printed circuitboard construction. When correlating a 7-chip Barker coded p.s.k. waveform the ratio of correlation peak to side-lobes was within 1·5 dB of the theoretical value. The insertion loss in expansion (60 dB) was however 10 dB greater than that exhibited by the fixed-coded version of the same a.m.f. An alternative switching circuit proposed by Hunsinger and Franck[5] which uses fewer components, gave a similar performance with only 5 dB additional insertion loss over a fixed coded device. Despite these encouraging results, this hard-wired circuitry is not suitable for high-performance wide-band devices (10 MHz chip rate). The small tap-to-tap spacing (310 μm) implies that discrete r.f. circuitry needs to be fanned out to overcome layout difficulties, leading to inferior performance. An alternative technology is therefore required in which the tap switches can be fabricated in a size compatible with the tap spacing.

### 2.2 Diode Convolvers

An alternative type of SAW device, the diode convolver, was recently introduced by Reeder.[6] This device has a pair of interdigital transducers and an array of regularly spaced taps with each tap connected to a diode (Fig. 4). In operation *two* input waveforms, signal and reference, are applied, with frequencies $f_1$ and $f_2$. The contra-directed surface waves generated are sampled by the taps. At each tap the non-linearity of the diode causes an output signal, at frequency $f_3 = f_1 + f_2$, proportional to the product of the amplitudes of the two surface waves. Suitable choice of $f_1$ and $f_2$ enables the harmonics to be filtered from the required signal at frequency $f_3$.

The input waveforms are assumed to have finite duration, such that the SAW wave packets produced have a spatial extent less than that of the tap array. If the signal waveform is a short r.f. pulse, the device action is

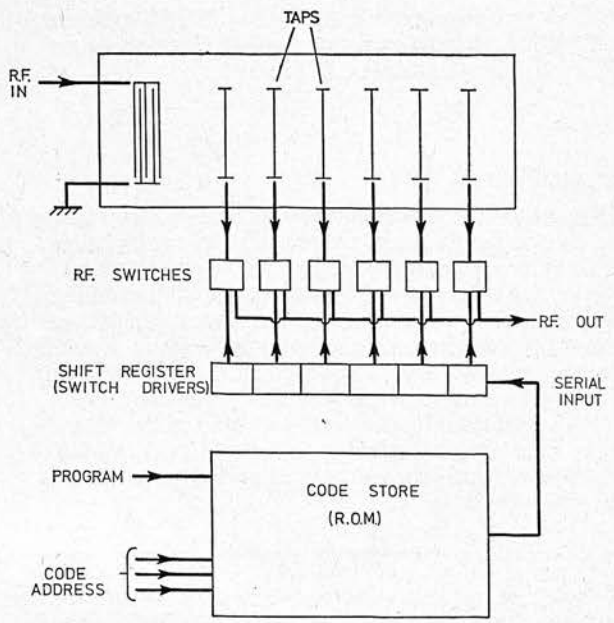


**Fig. 2.** Schematic of programmable a.m.f. with code storage and selection peripherals.

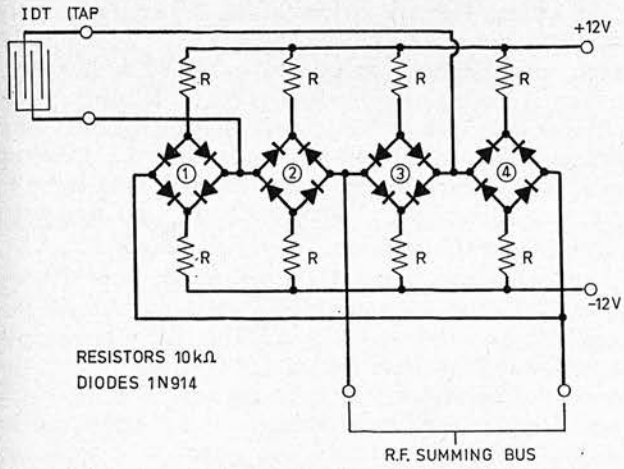


**Fig. 3.** Diode ring circuit for switching polarity of individual tap.

analogous to scanning the reference waveform by means of the signal. Thus the output, which can be regarded as the impulse response, corresponds to the reference waveform, with a time-contraction by a factor of 2 due to the relative motion of the waves. Further, the device is linear with respect to variations of the signal waveform. It thus acts much like a filter whose impulse response is determined by the reference input. To correlate a known signal waveform the reference needs to be the time-reversed waveform, and clearly a high degree of programmability is obtained since the reference can be varied at will. The bandwidth is limited by the sampling action of the taps, and in general the maximum signal bandwidth possible is $1/2T$, where $T$ is the time interval corresponding to tap spacing. However a p.s.k. waveform with a larger bandwidth can be handled provided its chip period is close to $T$.

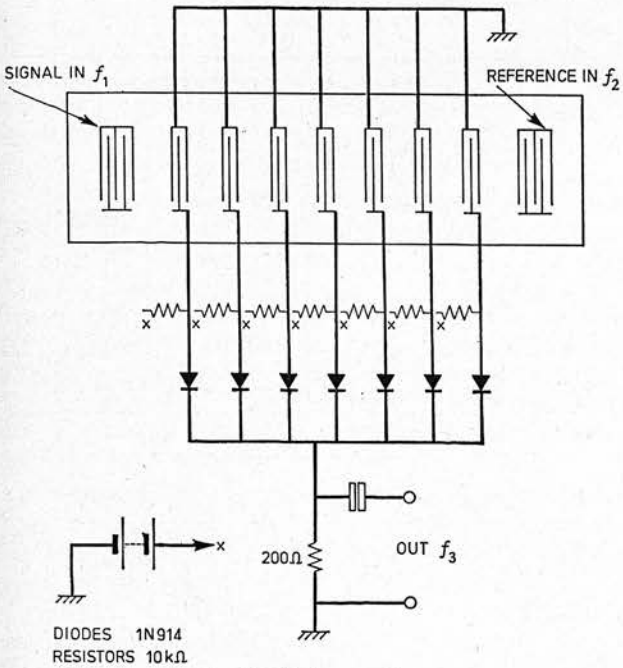


**Fig. 4.** Diode convolver.

Although Reeder[6] used a series chain of diodes, we have found that the arrangement of Fig. 4 gives better fidelity when the number of taps exceeds about ten. A d.c. bias of about 0·1 mA improves the non-linear efficiency of the diodes. Lithium niobate was used for the substrate, since its high piezoelectric coupling gives good transduction efficiency. The SAW velocity, 3485 m/s is similar to that of quartz. Figure 5 shows a result obtained with a 15-tap device with 200 ns propagation time between taps, using discrete diodes and resistors. The two input waveforms were p.s.k. coded signatures with carrier frequencies of 85 and 115 MHz, and bandwidth of 5 MHz. The output correlation waveform shown had a centre frequency of 200 MHz.

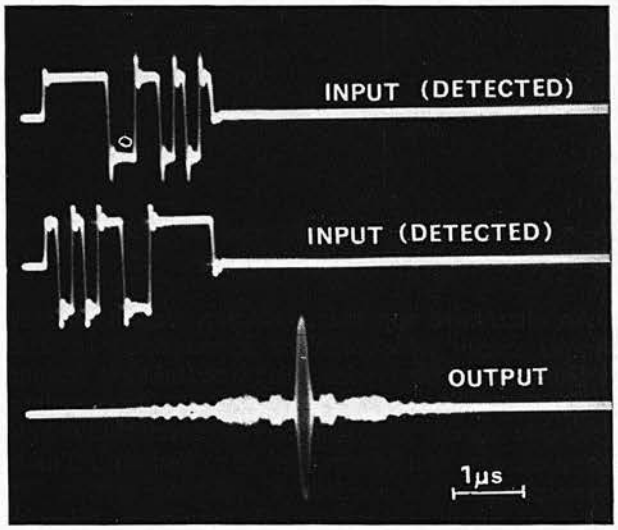


**Fig. 5.** Diode convolver performance. Input waveforms are modulated according to 13-chip Barker code and its time-reverse, and are synchronously detected for the display to show their structure. The theoretical peak-to-sidelobe ratio for the output is 22·3 dB.

For comparison with the a.m.f. we consider the use of a convolver to correlate a signal waveform whose timing is unknown. This can be done using a repetitive reference waveform[7,8] as shown in Fig. 6. The convolver system gives rise to a timing distortion which can only be removed at the expense of more complicated peripherals, although it can handle a greater variety of signal input waveforms. A much simpler system, using a single reference waveform, can be utilized when the signal timing is known.

## 3 Selection and Detail of Fabrication Techniques

### 3.1 Device Design Constraints

Sections 3.1 and 3.2 consider the typical requirements for a 127-tap device capable of handling codes at a 10 MHz chip rate, thus requiring a 310 μm tap spacing on a quartz substrate. Since discrete circuitry is excluded (Section 2.2) only integrated and hybrid circuitry are considered. In this context, the prohibitive size of the capacitors excludes the relatively simple Hunsinger–Franck circuit. Alternative circuits, for example that of Fig. 3, are more complex and unsuitable for hybrid construction, though this does not preclude integrated circuit (i.c.) construction.

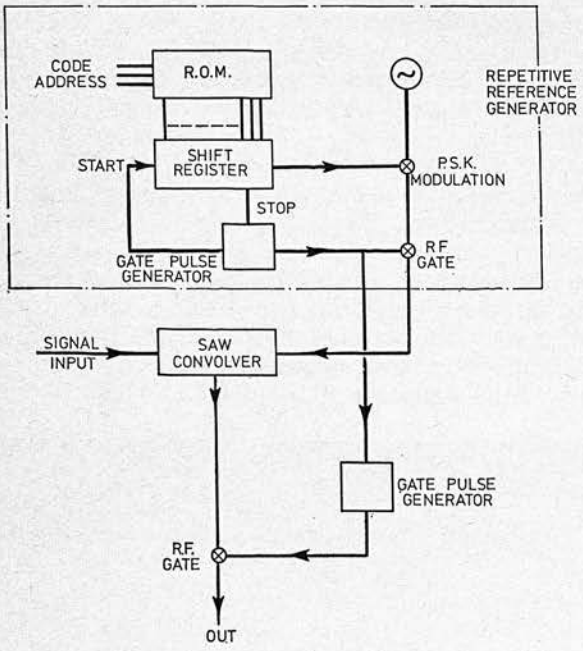


**Fig. 6.** Use of convolver to correlate arbitrary p.s.k. coded waveforms.

An alternative approach, however, leads to a much simpler circuit which can be implemented in either technology. If the tapped delay line (t.d.l.) is designed with a dual tap geometry (Fig. 7), where the taps simultaneously sample one half of the wavefront, suitable interconnexion can be arranged to output both 0 and $\pi$ phase signals to the selective switching matrix. The switching circuit is therefore only required to select the appropriate output and isolate the other one. To minimize bonding complexities and provide more space for the switching circuit, both outputs from the dual tap are taken out on the same side of the device, with half the total taps available each side. This maintains a bond-spacing equal to the tap period (310 μm) and avoids unnecessary crossovers by accommodating switching circuits down each side of the device with a 620 μm pitch. The switching circuit, designed to interface with this new t.d.l. requires only two diodes and two resistors per tap (Fig. 7).

The similarities of this new switching circuit and the diode convolver circuitry (Fig. 4) have resulted in the concept of fabricating a compatible microelectronic network for both devices. For a programmable a.m.f. with 10 MHz bandwidth the tap spacing is 310 μm, so that the 2-diode 2-resistor circuit is repeated at 620 μm intervals on both sides of the device. The simpler convolver has one diode and one resistor per tap on a 310 μm pitch, with components on one side only. Circuit fabrication is thus identical except for different device bonding requirements. The following considerations apply for the most part to both devices, though for clarity they refer specifically to the programmable a.m.f.

### 3.2 Trade-off Between Available Technologies

Two features require careful attention in the design of a programmable a.m.f. First the switching matrix must have a narrow pitch between circuits to directly interface with the tap period without any fan out. Secondly the taps, which possess capacitances of $\frac{1}{4}$ pF, must not be adversely loaded by the switching circuit if insertion loss is to be minimized. The chosen technology must have diodes which exhibit a low forward-biased impedance coupled with high reverse biased capacitive reactance to permit good switching ratios (>20 dB) and thus high fidelity operation at v.h.f.

When considering the fabrication of a high technology device it is necessary to trade off the various technologies available as shown in Table 1. This Table specifically refers to the switching matrix and does not include the code storage and selection hardware. The switching matrix which requires only diodes and resistors can be realized in a high speed, low junction capacitance (0·25 pF) semiconductor bipolar process, or even more efficiently in silicon-on-sapphire (s.o.s.) technology which utilizes vertical junction diodes to obtain 0·02 pF junction capacitance with excellent isolation between diodes and ground. The latter approach has been adopted by Hagon[9] with a s.o.s. switching matrix, m.o.s.f.e.t. shift register and holding store all fabricated on a sapphire substrate. Silicon-on-sapphire, which offers the best specification for an i.c. approach, is a new technology and unfortunately is not currently available as a production process in this country. A development process was available but the costs incurred in tailoring this process to suit our requirements would have been prohibitive. Both silicon i.c. and s.o.s. technologies can easily achieve the required narrow pitch between switching circuits irrespective of the type of circuit selected. Although either approach could be used for a 127-tap, 10 MHz chip rate device, encapsulated i.c. devices are excluded by the fan-out problem. Semiconductor chips are therefore used, each chip limited to typically 16 switching circuits to obtain high yields. This construc-

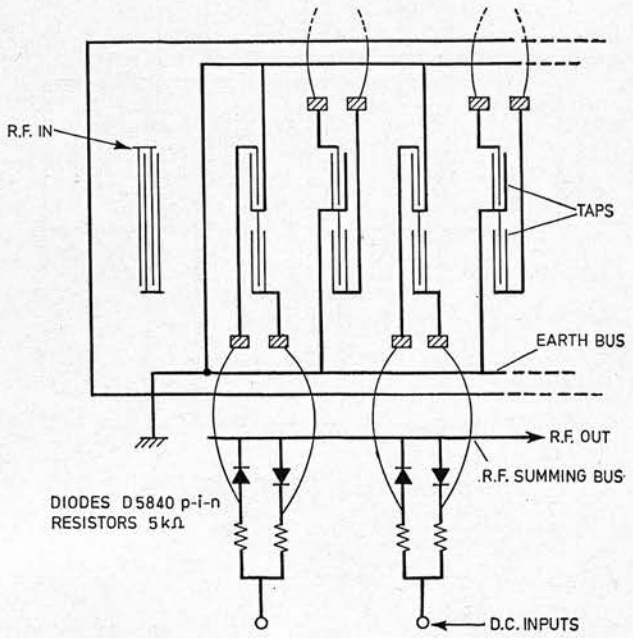


**Fig. 7.** Programmable a.m.f. incorporating a dual-tap structure.

**Table 1.** Comparison of switching-matrix technologies for two 127-tap programmable a.m.f.s

| | Silicon-on-sapphire | | Silicon i.c. | | Hybrid | |
|---|---|---|---|---|---|---|
| Diodes | 0·02 pF, 50 Ω at 1 mA | | 0·25 pF, 100 Ω at 1 mA | | 0·05 pF (p-i-n), 100 Ω at 0·5 mA | |
| Resistors | diffused | | diffused | | thin film | |
| Fabrication | few companies have technology available | | industrial production process | | simplest, and in-house | |
| | | £ | | £ | | £ |
| | masks | 750 | masks | 1000 | masks in-house | 50 |
| | process set-up | 2500 | process 1 batch | 560 | process in-house | 50 |
| Cost analysis | process 1 batch | 900 | | | diode purchase | 1560 |
| | | £4150 | | £1560 | | £1660 |
| | mask design | 16 | mask design | 16 | mask design and | |
| | mask fabrication | 12 | mask fabrication | 12 | fabrication | 3 |
| | process set-up and | | process 1st batch | 12 | thin film processing | 6 |
| Time scale (weeks) | production 1st batch | 20 | device construction | 3 | device construction | 3 |
| | evaluation | 4 | | | | |
| | device construction | 3 | | | | |
| | | 55 | | 47 | | 12 |

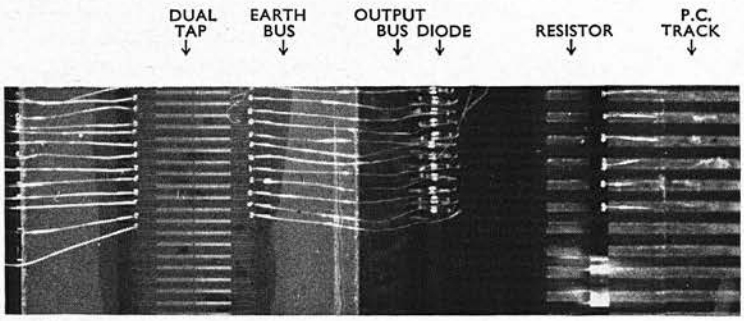


**Fig. 8.** Details of one side of the programmable a.m.f., highlighting tap structure, hybrid substrate and printed circuit tracks with interconnecting bonds.

tion still involves many wire bonds for chip-to-tap and chip-to-chip interconnexions, reducing to some extent the advantages of integrated construction.

A hybrid arrangement, with thin film resistors and beam lead diodes, offers a possible alternative to the silicon i.c. or s.o.s. approach. Beam lead p-i-n diodes can be obtained in a 0·17 mm × 0·9 mm package with 0·05 pF capacitance, and when combined with small area thin film resistors the 2-diode 2-resistor circuit meets the 620 μm period restriction of the latest a.m.f. design. Thick film resistors were considered as a possible alternative but the minimum reproducible linewidths of 600 μm excluded their use.

Although initial design studies were based on an i.c. approach including a tentative design, it was decided to use a thin film hybrid system in which all the fabrication could be performed in-house under direct control. As our requirements would be met by a small quantity of devices, the high component cost of the p-i-n diodes (£3 each) was offset by the relatively large mask making costs incurred in an i.c. approach. Thus for our requirements, the hybrid approach offers low capacitance diodes, acceptable cost, direct control and a much shorter time scale—9 weeks for a 31-tap device. In another context different considerations could conceivably make an i.c. approach more attractive.

### 3.3 Device Construction

The programmable a.m.f. consists of several separately constructed subassemblies. The hybrid microelectric circuitry was made on a 63 × 25 mm Corning 7059 glass substrate, allowing space for the SAW delay line. The latter was made on a 63 × 8 × 2·5 mm polished bar of ST-cut quartz, subsequently cemented onto the glass substrate. This assembly was then cemented on a printed circuit board carrying fan-out leads and the TTL packages which form the shift register for code selection. The r.f. parts of the device, delay line and hybrid switching matrix, were enclosed in an aluminium box which also screens the input transducer from the taps. A detail of the taps and switching circuits is shown in Fig. 8, while

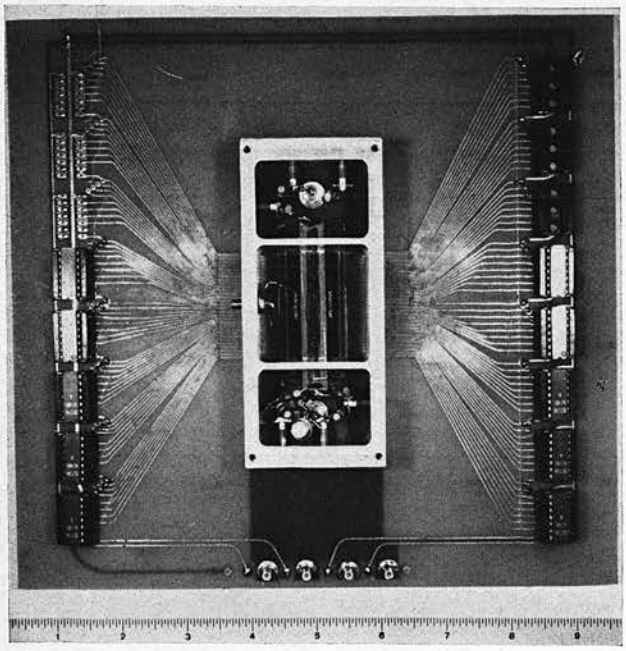

**Fig. 9.** Complete programmable a.m.f. with tunable matching networks and shift register code store.

Fig. 9 shows the whole device. The device had 127 taps and switching circuits, though only 31 were connected on the device illustrated.

The thin film resistors were fabricated using a nichrome-gold process. The 200 Ω/sq sheet resistance nichrome was evaporated onto the glass substrate then overlayed with gold. Both evaporations were performed with an electron-beam heated source. The resistive and conducting patterns were defined using a Shipley positive photoresist system combined with selective etches. The 5 kΩ resistors had a pitch of 620 μm per pair, with 60 × 1500 μm active areas and 200 μm wide bonding pads to accommodate the diodes. The resistor values varied by ±5% and improved photomasking combined with r.f. sputtering of the film is under consideration to improve film quality and composition. The Alpha D5840 beam lead p-i-n diodes, which were chosen for their very low capacitance (0·05 pF) and physical size, were bonded onto the gold overlay, bridging the gap between the resistor array and output summing bus as detailed in Fig. 7 and illustrated in the detail of Fig. 8. The bonding was performed with a pulse tip thermocompression bonder using a 'blanked-off' tool.

The SAW device was constructed by vacuum coating the polished cut quartz substrate with aluminium and then defining the interdigitated input transducer and taps using a positive resist system. The electrodes on each tap have a length of 1 mm and a linewidth of 6 μm with 1:1 mark/space ratio. Care was necessary to reproduce these long narrow lines over the large area of the device (40 × 3 mm) without any open or short circuits. Standard semiconductor photomasking techniques were used with special emphasis on tap placement. It is vital to the device performance that the placement of each tap should have an accuracy of at least ±0·5 μm without any accumulative error along the 127-tap array. Less accurate placement would cause a phase shift in the sampled signal degrading the coherence of signal summation over the entire tap array. Chrome-on-glass photomasks were used to define the SAW structure and the accuracy necessary is close to state-of-the-art for these masks.

The quartz substrate with SAW structure was positioned between the resistor diode networks and secured with an adhesive varnish. Connexion between the resistors and taps was made with gold wire, bonded between the gold and aluminium pads. A pulsed, thermocompression ball bonding technique was used as this does not require any steady-state heating of the device, but only an instantaneously pulsed heating of the bonding capillary when the preset bonding pressure is reached. This avoids any thermal degradation of the components and also allows wide freedom of choice for adhesives.

Interfacing the closely spaced thin film switches to standard encapsulated 8-stage TTL shift registers was accomplished by using a printed circuit board with 310 μm wide metal tracks having the same period as the resistors pairs (620 μm), which represents the state-of-the-art in printed circuit design. The tracks subsequently fan out to the shift register stages accommodated along the sides of the 9 in × 9 in (23 × 23 cm) board (Fig. 9). The pulsed thermocompression ball bonding system was again selected to complete the connexions between the thin film and printed circuit board. The copper tracks were gold plated in the bonding region to ensure good bond reliability. Soldering methods were discarded due to the close contact period and the possible problem of gold leaching from the thin film contacts. The remainder of the board was flow soldered both for protection and to facilitate connexion of the TTL packages. A ground plane on the printed circuit board formed the rear face of the screening box, and a web in the box screened the input transducer from the taps.

A similar construction is being used for the diode convolver, except that the printed circuit board will not be necessary. In this device it has been found that small variations of tap sensitivity, due to variations in the diode impedances and the taps themselves, can be corrected by trimming the resistors. For the thin film hybrid device the resolution (4 μm) of laser machining should yield a resistor tolerance of better than 0·5%.

## 4 Hybrid Programmable A.M.F.

### 4.1 Device Performance

To evaluate the feasibility of design, an initial sample device was constructed with 31 taps selected from the centre of the tap array. Programmable a.m.f. performance is summarized in Table 2, and compared with a fixed coded a.m.f. wired to the same 31-chip pseudo-noise code. The most significant difference is an increase in insertion loss to an individual tap from 66 to 74 dB, directly attributible to capacitive loading by the switching circuit. This accounts for the differences in signal/noise ratio and dynamic range between devices. The high fixed coded insertion loss of 66 dB over earlier devices (50 dB, see Section 2.2) can be directly attributed to the effects of the broadband matching network and

**Table 2.** Comparative performance of 31-chip fixed coded and hybrid programmable a.m.f.s

| | Fixed coded | Infinitely programmable |
|---|---|---|
| Centre frequency (MHz) | 120 | 120 |
| Code chip (bit) rate (MHz) | 10 | 10 |
| Insertion loss to a single tap (expansion) (dB) | 66 | 74 |
| Signal/noise (expansion) (dB) | >30 | >20 |
| Insertion loss to the correlation peak (dB) (pulse compression) | 36 | 44 |
| Processing gain (dB) | 15 | 15 |
| Dynamic range (dB) | 80 | 70 |
| Loop insertion loss (dB) | 102 | 118 |

dual tap geometry. The loop insertion loss quoted in Table 2 is the loss for two devices in series, one performing expansion and the other compression. The switching circuit was driven from TTL registers (see Fig. 9) with 3·5 V output swing resulting in 0·33 mW power consumption per tap for the switching matrix.

This compares very favourably with the 1 mW achieved by using an SOS switching array.[9] Trace (a) of Fig. 10 shows the impulse response for the fixed coded device. Typical tap-to-tap variation is ±2 dB. Trace (b) shows the autocorrelation of the upper waveform, obtained by using the programmable a.m.f. Here the programmable device impulse response has been coded with a time reversed version of the 31-chip code used in the fixed device.

The ratio of the amplitude of the correlation peak to the largest of the time side-lobes is 11 dB (theoretical 15·8 dB). The discrepancy is due to internal reflexions within the programmable a.m.f. mainly caused by the loading of the reversed biased diode on the off tap. This effect, which causes the time side-lobes to loose their theoretical symmetry, can be overcome by a simple modification of the switching circuit and improving the SAW tap geometry.

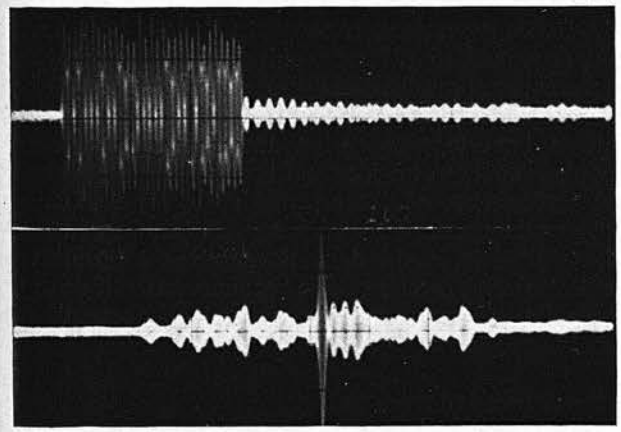

**Fig. 10.** SAW a.m.f. loop performance.

(a) Impulse response of a fixed coded a.m.f. passively generating the 31-chip maximum length p.s.k. sequence 1111100011011010100 00100101100 at 120 MHz. (b) Autocorrelation function displayed in a programmable a.m.f. coded with the same sequence receiving the 120 MHz burst signal shown in trace (a).

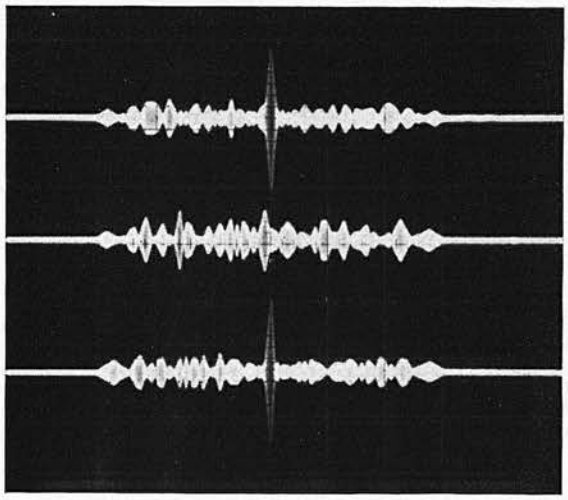


**Fig. 11.** Two-signature coding for bandspread communications. Traces (a) and (c) show the autocorrelation performance of the programmable a.m.f. to two 31-chip bi-phase coded signatures chosen as disjoint subsequences of a 127-chip maximum length sequence. These particular signatures were computer selected to exhibit low cross-correlation time sidelobes as shown in trace (b).

## 4.2 Applications

In certain multiple subscriber communication and ranging systems such as those proposed for collision avoidance surveillance,[11] user access is permitted in a truly random or uncoordinated manner. Interference between different users is avoided by allocation of a distinctive coded signature to each user. Figure 11 illustrates the performance of the programmable a.m.f. when it is coded to recognize a signature A, under conditions typical of these systems. Trace (a) shows the autocorrelation performance when receiving a signature A and trace (b) the crosscorrelation response of the same device to another signature B. The use of an envelope and threshold level detector enables a receiver to distinguish between the two signatures and decode only those signals coded with signature A. Trace (c) shows the response of the programmable a.m.f. to signature B after reprogramming the device with Code B.

Many secure communication systems[12] bandspread the baseband data by employing further modulation with a wideband binary code of very long duration prior to signal transmission. The achievement of efficient decoding in the receiver requires an identical code generator, which must be in precise time synchronization with that in the transmitter, to recover the baseband data. Synchronization of these code generators can be achieved by incorporating an infinitely programmable a.m.f. in the receiver, programmed to correlate a subsequence which will shortly occur in the transmitted code. The correlation peak provides both code recognition and accurate timing information.

**Table 3.** Comparison of potential performance for SAW and microelectronic programmable matched filters

| | Programmable a.m.f. | Diode convolver | Charge coupled a.m.f. | Microelectronic d.m.f. |
|---|---|---|---|---|
| Time—bandwidth product | fair | fair | excellent | excellent |
| Bandwidth | medium | medium | very high | high |
| Dynamic range | very good | very good | good | poor |
| Variable chip rate | no | yes | yes | yes |
| Temperature dependence | medium | low | low | low |
| Device fabrication complexity | medium | medium | medium | complex |
| Reliability | modest | high | low | low |
| Peripheral equipment | modest | complex | modest | modest |
| Total power consumption | medium | medium | low | very high |
| Cost | high | medium | very low | high |

When many subscribers are simultaneously using these systems a high co-channel interference results which renders these short code correlations (typically 127 chip) undetectable. The correlation of longer sequences with larger processing gain is often difficult due to the design, fabrication and reliability problems of a long matched filter. A programmable a.m.f., which is reprogrammable within the chip time, can however overcome this problem by correlating a code ($>1\,000$ chips) which is much longer than the device (127 tap) when coherent summation of the output in a recirculating delay line is employed.

### 4.3 Programmable Matched Filter Comparison

Several other technologies can be used to realize matched filters. The two main competitors to SAW devices are the simple digital matched filter (d.m.f.) constructed with bipolar shift registers,[13] and the truly analogue shift register realized in the new charge coupled device (c.c.d.) technology.[14]

Table 3 compares the potential performance of these devices, with the comparisons based on the 127-tap 10 MHz chip rate specification previously discussed. Both the charge coupled a.m.f. and the d.m.f. employ clocked shift register stages to achieve delay, easily permitting serial extension to handle signals with very large time bandwidth product ($>10^4$). The high clock rates of these devices also in principle permit accommodation of wideband signals ($>100$ MHz), which can have a variable chip rate. The inability to achieve variable chip rate in a programmable a.m.f. limits the overall degree of programmability available. The dynamic range of a simple d.m.f. is limited, but with 8-level quantization a 50 dB dynamic range can be obtained at the expense of high device complexity and associated loss of yield and reliability. Dynamic range of the charge coupled a.m.f. is dependent on the overall charge transfer efficiency of the device. The graceful degradation characteristics of a SAW a.m.f. are not exhibited by serial devices such as the charge coupled a.m.f. and d.m.f. which have corresponding lower reliability. Active reference generation in the convolver increases the peripheral complexity compared to the other devices which only require a simple r.o.m. code store. Charge coupled device technology requires a very low power consumption when compared to high-speed bipolar logic. Cost comparisons based on the 50 dB dynamic range device tend to highlight the complexities involved in the different technologies further accentuating the necessity to evaluate accurately the hybrid device performance against other competitive technologies.

## 5 Conclusions

This paper has described the application of hybrid microelectronic techniques to extend the capabilities of efficient programmable SAW matched filters which will further enhance the attractiveness of SAW devices for communication systems. The particular requirement of a low-capacitance, high-fidelity switching matrix has been achieved in a size compatible with the SAW device. A detailed comparison shows that the relative attractiveness of different microelectronic technologies depends in general on the particular requirements, while for our purposes the hybrid approach was clearly the optimum choice.

A future programme is planned to extend both a.m.f. and convolver to 127 taps with a 10 MHz bandwidth and compare both fixed and programmable SAW devices under identical performance conditions. It is also considered important to design and construct a charge coupled a.m.f. to an identical specification to evaluate the performance of a competing technology. Trading off insertion loss, power consumption (device and peripherals) and achievable dynamic range in these prototype devices against precise system requirements will serve to focus future work onto the area which possesses the greatest applications potential.

## 6 Acknowledgments

The authors wish to acknowledge Professor P. L. Kirby, D. Willcox, B. J. Darby and J. G. Sutherland for technical contributions, I. McGee for thin film production and to the Science Research Council and DCVD (Ministry of Defence Procurement Executive) who sponsored the authors' studies.

## References


1. Cook, C. E. and Bernfeld, M., 'Radar Signals', (Academic Press, London, 1967).
2. Stein, S. and Jones, J. J., 'Modern Communication Principles', (McGraw-Hill, New York, 1967).
3. Morgan, D. P., 'Surface acoustic wave devices and applications —1. Introductory review', *Ultrasonics*, **11,** pp. 121–131, May 1973.
4. Grant, P. M. and Collins, J. H., 'Synchronization, acquisition and data transfer utilizing a programmable SAW analogue matched filter', *Electronics Letters*, **8,** pp 299–301, 15th June 1972.
5. Hunsinger, B. J. and Franck, A. R., 'Programmable surface wave tapped delay line', *IEEE Trans. on Sonics and Ultrasonics* **SU-18,** pp. 152–4, July 1971.
6. Reeder, T. M. and Gilden, M., 'Convolution and correlation by non-linear interaction in a diode-coupled tapped delay line', *Appl. Phys. Letters*, **22,** pp. 8–10, 1973.
7. Morgan, D. P., Collins, J. H. and Sutherland, J. G., 'Asynchronous operation of SAW analog convolver', *Proc. IEEE*, **60,** pp. 1556–7, 1972. (Letters).
8. Morgan, D. P., Collins, J. H. and Sutherland, J. G., 'Asynchronous operation of a surface acoustic wave convolver', IEEE Ultrasonics Symposium, 1972, Proceedings, pp. 296–9.
9. Wrigley, C. Y., Hagon, P. J. and Seymour, R. N., 'Programmable SAW matched filters for phase-coded waveforms,' IEEE Ultrasonics Symposium 1972, Proceedings, pp. 226–8.
10. Berry, R. W., Hall, P. M. and Harris, M. T., 'Thin Film Technology', (Van Nostrand, New York, 1968).
11. Grant, P. M., Collins, J. H., Darby, B. J. and Morgan, D. P., 'Potential applications of acoustic matched filters to air traffic control', *IEEE Trans. on Microwave Theory and Techniques*, **MTT-21,** pp. 288–300, April 1973.
12. Collins, J. H. and Grant, P. M., 'The role of surface acoustic wave technology in communication systems', *Ultrasonics*, **10,** pp. 59–71, March 1972.
13. Bagley, G. C., 'Radar pulse-compression by random phase-coding', *The Radio and Electronic Engineer*, **36,** pp. 5–15, July 1968.
14. Collins, D. R., Bailey, W. H., Gosney, W. M., Buss, D. D., 'Charge-coupled device analogue matched filters', *Electronics Letters*, **8,** No. 13, pp. 328–9, 29th June 1972.


*Manuscript first received by the Institution on 14th May 1973 and in final form on 5th March 1974. (Paper No. 1592/CC 204)*

# SPREAD SPECTRUM COMMUNICATION MODEM DESIGNS EMPLOYING SURFACE ACOUSTIC WAVE ANALOGUE MATCHED FILTERS

*B J Darby and P M Grant

ABSTRACT This paper reports experimental evaluations of the performance of simple, noncoherent, prototype spread spectrum communications modulator-demodulator configurations (modems) incorporating fixed coded SAW analogue matched filters (AMF) processing aperiodic biphase modulated IF signals. Results of measurements of both false alarm and miss probability are given for an on-off keyed (OOK) modem of 5 MHz bandwidth incorporating 1, 15 and 31 tap pseudo-noise coded AMF's under conditions of band-limited noise and cochannel interference. The dependence of error rate on normalised threshold level, $\gamma$, is shown to agree with the theory of Mayher. A fully asynchronous OOK multi-subscriber random access discrete address modem using 15 tap SAW AMF's incorporating frequency and time coding with differential delays realised as integral parts of device design is detailed. Orthogonal multiple signature signaling is demonstrated in a bit synchronous binary FSK modem, by assigning the AMF's a contiguous frequency allocation.
For both modems theoretical and experimental error rate measurements are presented to show the effect of combining several short signatures within a hard decision receiver.

## Background

This paper assesses the error-rate performance of several distinct IF modems utilising surface acoustic wave (SAW) analogue matched filters[1] (AMF) designed with bandspreading and time domain encoding[2] to give digital data transfer with cochannel multiple access capability. The unique advantages of SAW devices which emerge are carrier and chip asynchronous operation combined with rapid generation of, and switching between, complex frequency and time encoded pulse patterns.

* B J Darby
University of Edinburgh
Electrical Engineering Department
King's Buildings
Mayfield Road, Edinburgh EH9 3JL
Scotland

The main theme of the paper is the application of SAW AMF's to two basic signaling techniques, namely on-off keyed (OOK) and binary frequency-shift keyed (FSK). These discussions are fundamental to the implementation of a specific multiple access concept, namely random access discrete address (RADA). The OOK RADA modem demonstrates both the inherent hardware reduction and the ability to significantly increase the complexity of coding formats with SAW devices.

## Spread Spectrum Modulation

Spread spectrum coding is achieved through the multiplication of a narrow bandwidth, $B_d$, data bit modulated IF carrier, by a distinct wideband signal which spreads the intelligence over a large chip bandwidth, $B_s > B_d$. The wideband modulation can be classified under three headings[2]:

(1) direct pseudo-noise (PN) ;
(2) frequency-hopping (FH); and
(3) time-hopping (TH)

Specific combinations of the properties of these permit the optimum trade for any desired system between:

Cochannel multiple access; channel utilisation; low detectibility by unauthorised users; jamming immunity; multipath resolution; and range and velocity measurement.

## Error Rate Considerations for OOK and Binary FSK Signaling

Several important bandspread links use OOK techniques to perform detection and synchronisation of PN and FH signals[3]; generation and detection in RADA[4] and detection and accurate timing of received signals for navigation and ranging[5] applications.

In each case, link operation necessitates the asynchronous detection of a burst of bandspread signal. This involves *noncoherent (envelope) demodulation*. The analysis of error probabilities for OOK reception[6] assumes that:

(1) sampling of the matched filter output envelope occurs at the instant t = T when the output SNR is maximised;
(2) the signal sample is compared with a predetermined threshold and the decision rule applied, "If the output envelope exceeds the threshold level, accept 'signal transmitted', otherwise accept the 'no signal' hypothesis".

Due to interference and noise, two types of decision error occur. A false alarm when detection results and nothing was transmitted. A false rest when a signal was sent but not detected. The probabilities of making these errors will be denoted by $P_F$ and $P_M$ respectively. Mayher[7] has derived expressions for conditional decision error probabilities with large $B_sT$, OOK signals. This paper applies Mayher's equations to the worst case situation of cochannel interference; when

$$P_F = \exp \frac{-\gamma^2 B_s T}{\left[\frac{I}{S} + \frac{N}{S}\right]} \tag{1}$$

and,

$$P_M = 1 - Q\left[\left[\frac{2B_sT}{\frac{I}{S}+\frac{N}{S}}\right]^{\frac{1}{2}}, \gamma\left[\frac{2B_sT}{\frac{I}{S}+\frac{N}{S}}\right]^{\frac{1}{2}}\right] \tag{2}$$

where the Q-function[8] is defined by:

$$Q(\alpha,\beta) = \int_{\beta}^{\infty} x \exp\left[-\tfrac{1}{2}(x^2 + \alpha^2)\right] I_0(\alpha x).\, dx \tag{3}$$

and $\gamma$ is the ratio of threshold level to AMF peak output, N the noise power, I the interference power, S the signal power and $I_0$ the modified zero order Bessel function.

The primary disadvantage of OOK signaling results from the necessity to maintain the threshold at the optimum level[6]. As this level is a function of SNR, fixed thresholds cannot reliably discriminate between signal and noise in channels subject to deep fade.

In contrast binary FSK signaling[6], employs two distinguishable waveforms with a comparison of the receiver AMF output envelopes at the sampling instant. Minimum error probability for equally energetic and equiprobable Mark and Space signals is achieved with zero threshold level. Total error probability ($P_e$) for a noncoherent *orthogonal* binary FSK modem is given by[9]

$$P_e = \tfrac{1}{2} \exp\left[-\tfrac{1}{2}\rho_o\right] \qquad (4)$$

where $\rho_o = B_s T \left(\frac{S}{N}\right)$ is the AMF output SNR at the sampling instant in the filter which received the signal.

## Measurement Technique

Figure 1 details the experimental configuration adopted[10] to evaluate a non-coherent spread spectrum OOK modem in a gain stable channel employing a back-to-back test. The modulator-demodulator functions are accomplished by a conjugate pair arrangement of SAW AMF's (A,A*). The peripheral equipment, shown allows direct measurement of the error rates $P_F$ and $P_M$. These evaluations are executed under controlled signal-to-noise conditions for specific decision thresholds. This permits comparison with Mayher's theory[7].

Passive spread spectrum modulation of the baseband OOK signal is achieved by impulsing the expansion AMF, A, to generate its characteristic PSK waveform. The counter reference clock is used both to trigger the impulse generator and to reference the second counter, automatically compensating for any variations in clock rate. The expanded signal is amplified prior to spread spectrum demodulation in the conjugate AMF, (A*).

Bandlimited noise was generated by cascading amplifiers and filtering. The independent measurement of both $P_F$ and $P_M$ necessitates the generation of two sampling pulses to separate the noise induced outputs and detected correlation peaks. Strictly, since each sampling pulse coincides with a correlation peak *only one conditional* error rate, $P_M$, is measured. The $P_F$ measured is *unconditional* as occurs in synchronisation search conditions.

This modem was evaluated with several AMF's with differing centre frequencies and characteristic PN waveforms. Figure 2 highlights the improvement in processing gain when the time duration of the coded waveform is increased at constant signal bandwidth. Figure 3 shows $P_M$ as a function of $\gamma$, versus input SNR with $B_s T = 31$. In the following section similar curves are presented for 15 chip m-sequence coded AMF's and their evaluation discussed in the context of an OOK RADA modem. Comparisons of large $B_s T$ (>10) device performances in both noise and interference limited channels illustrates that similar processing gain is obtainable.

## Random Access Discrete Address Communications Modem

RADA systems, contrary to some other multiplexing techniques which employ address preambles, impress on the data a unique spread spectrum modulation exclusively to address transmissions to the intended receiver. Specifically quantised pulse positions modulated (QPPM), pulse code modulation (PCM), or other digital traffic is further modulated bit by bit by one of an alphabet of frequency-time coded pulse patterns. This permits uncoordinated access of many subscribers to the same wideband channel[4]. OOK and binary FSK signaling techniques are both applicable to RADA systems.

Experiments were conducted on a simple OOK RADA communications modem employing two characteristic waveforms in the address, Figure 4. Two similar AMF's to those utilised in the binary FSK modem were employed. Suitable design of AMF geometry[10] permitted compensating delays to be incorporated as shown in Figure 4. Cross-talk signals were further minimised by time-reversed coding AMF's A and B. In addition cross-talk at the sampling instant was eliminated by the temporal separation of the RADA waveforms.

In the transmitter a *single* 5 nsec duration, 10 volt peak impulse from an avalanche mode circuit was used to generate the complete IF address waveform, illustrating the simplicity of SAW device and peripheral hardware when compared with that described by Blasbalg[11]. After matched filter processing in the receiver and envelope demodulation the

correlation peaks were detected individually. The resulting baseband pulses were combined logically in a coincidence gate (hard decision) to regenerate the transmitted data.

The performance of the modem was determined when bandlimited noise was applied to the receiver input using the synchronous measurement procedure. This experiment demonstrated the operation of the hard decision receiver logic. Comprehensive evaluation of the RADA receiver was not carried out as this involves the synthesis of many RADA system signals.

The total error rate for *this* RADA modem can be derived as:

$$P_E = \tfrac{1}{2} P_F^2 + \tfrac{1}{2}(2P_M) \qquad (5)$$

where $P_E$ and $P_M$ are given by equations 1, 2. Thus, in terms of $P_F$, the hard decision logic effectively doubles the processing gain. This is illustrated by the curves of Figure 5. Included are theoretical $P_F$ characteristics for a single AMF with $B_sT = 15$, and effective $B_sT = 30$ for the modem. The effective false rest probability, $2P_M$, is twice that obtained from a single AMF. Note that the experimental and theoretical $P_M$ curves for the modem are closely aligned. For all SNR the combined error rate $P_E$ is predominantly due to false rests, indicating that the $\gamma$= -5 dB level was too high. A reduction in $\gamma$ will decrease $P_M$ while still maintaining an acceptably low $P_F$, improving overall error rate, $P_E$.

## Binary Frequency Shift Keyed Modem

Binary FSK signaling employs a pair of distinguishable waveforms, (Mark, Space) to denote the two message states (1,0). Receiver performance is dependent on both the SNR and mutual correlation of the two waveforms. Optimum performance for noncoherent reception is achieved with orthogonal waveforms which have zero cross correlation at the sampling instant. Experimental verification has been achieved with an AMF with centre frequency $f_o$ receiving microelectronically generated 15 chip m-sequence coded pulses modulating an rf carrier at $f_o$, $f_o+B_s$ and $f_o+2B_s$. The time domain response of the AMF exhibits orthogonality for the offset carriers. Maximum cross-talk, when $t \neq T$ is -10 dB for an adjacent band. In comparison the autocorrelation time-sidelobe levels were -12 dB. Cross-talk signals were reduced to -14 dB by time reversing the adjacent channel code, or to a -16 dB level by separating Mark and Space carriers by $2B_s$. Low cross-talk levels are desirable in synchronisation search since false alarms increase acquisition times.

An experimental bit synchronous binary modem, Figure 6, was constructed using AMF's matched to the 15 chip m-sequence. Carriers of 127.3 MHz (Mark) and 132.3 MHz (Space) were modulated at a 5 MHz chip rate to achieve orthogonality. The baseband encoder is implemented with a clock synchronised data stream by the logic circuit shown. On positive clock transitions binary ones are routed through the upper AND gate and trigger and impulser resulting in a Mark transmission. Similarly, binary zeros are routed through the lower AND gate to transmit Space signals. Signals are summed at IF, prior to transmission. On reception the two conjugate AMF outputs, are envelope demodulated prior to subtraction in the differential video amplifier. Positive excursions of the complementary bipolar outputs, signify reception of the Mark and Space signals. With zero threshold level, the dual comparators make random decisions except at the sampling instant when Mark and Space signals are easily identified. Reliable asynchronous operation is achieved at high output SNR, by raising the threshold level, which removes the random fluctuations of the comparator output. Separate Mark and Space decisions are obtained and used to preset and clear the flip flop to regenerate the data unambiguously. This mode of operation would be utilised for synchronisation search procedures when a reduced dynamic range can be tolerated.

Modem performance has been evaluated at zero decision threshold with the same basic peripheral equipment detailed earlier. Error rate measurements were made only with the addition of bandlimited noise to the channel, by summing the independently monitored equal error rates of Mark and Space signals emerging from the flip flop. The resulting $P_E$ is shown together with the theoretical curve, in Figure 7.

## Conclusions

This paper has examined the performance under laboratory conditions of moderate time-bandwidth product SAW AMF's to prototype IF spread spectrum digital communication modems employing OOK and binary FSK signaling techniques. Close to theoretical error rate performance has been achieved. Laboratory experiments on a simple OOK RADA modem demonstrated the unique advantages of SAW AMF's in the rapid synthesis, switching between, and detection of frequency and time encoded pulse patterns with minimal hardware. This RADA modem exhibited predictable error rate performance in the presence of bandlimited noise at the receiver input.

RADA techniques offer uncoordinated multiple access capability. They are particularly significant for mobile communications over geographical areas where low activity factors of subscribers exist, for example terminal area air-traffic control[5]. Achievement and detailed error rate assessment requires larger address alphabets and larger time-bandwidth product (>15) SAW AMF's than were utilised in the above experiments. Deployment of binary FSK signaling would remove the OOK requirement to maintain accurate receiver thresholds. This is advantageous for practical channels subject to deep fade.


## Acknowledgements

The authors would like to thank J H Collins for technical contributions, R D Lambert and R R Halstead for device fabrication, I M Crosby for modem construction, and acknowledge the British Science Research Council who supported this work.


## References


1. S T Costanza et al, IEE Trans MTT-17, pp 1042-1043, Nov 1969.
2. C R Cahn, AGARD Lecture Series No 58, Ref 5, 1973.
3. B J Hunsinger, IEE Conf Proc No 109, Aviemore 1973, pp 309-318.
4. M Magnuski, "Communications Systems Engineering Handbook", Ch 18 ,1953.
5. P M Grant et al, IEEE Trans MTT-21, pp 288-300, 1973.
6. S Stein et al, "Modern Communication Principles", 1967.
7. R J Mayher, IEEE EMC Symposium Record, pp 230-7, 1967.
8. C W Helstrom, "Statistical Theory of Signal Detection", p 153, 1960.
9. A H Nuttall, IRE Trans IT-8, pp 305-314, 1962.
10. B J Darby et al, IEE Conf Proc No 109, Aviemore 1973, pp 319-328.
11. H Blasbalg et al, IEEE International Convention Record, pp 192-216, 1964.


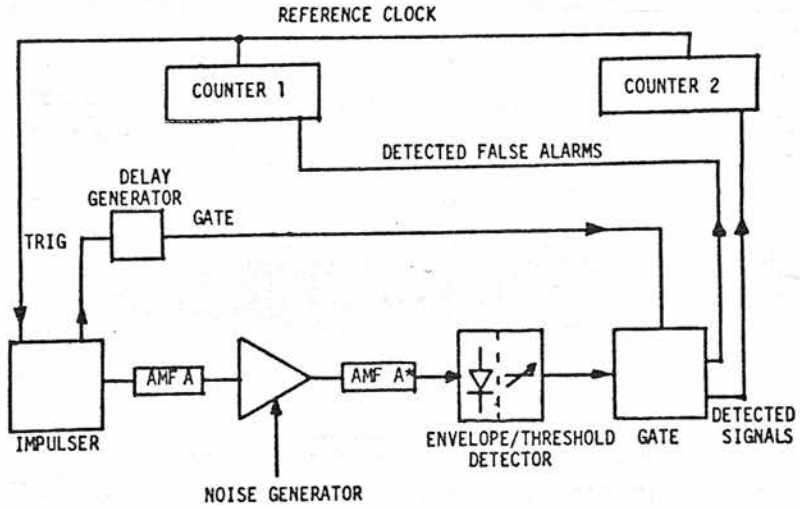


FIGURE 1 EXPERIMENTAL CONFIGURATION FOR MEASUREMENT $P_F$ AND $P_M$

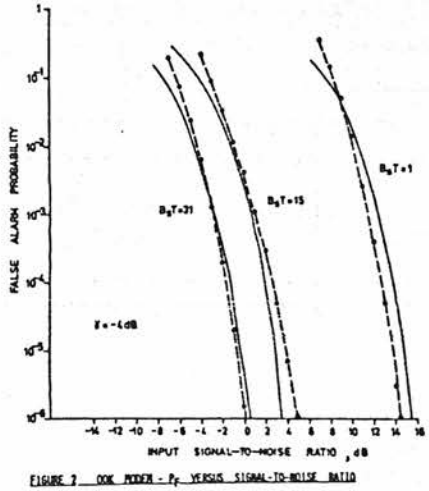


FIGURE 2 OOK MODEM - $P_F$ VERSUS SIGNAL-TO-NOISE RATIO

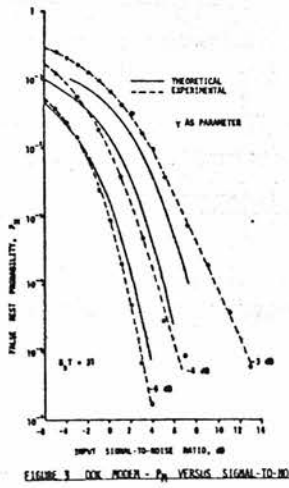


FIGURE 3 OOK MODEM - $P_M$ VERSUS SIGNAL-TO-NOISE RATIO AT FIXED K

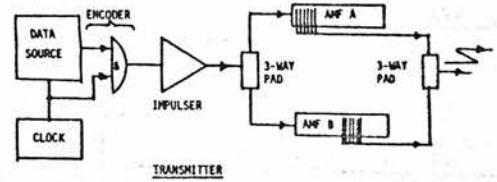


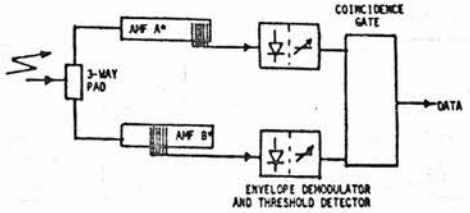


FIGURE 4 RADA MODEM BLOCK DIAGRAM

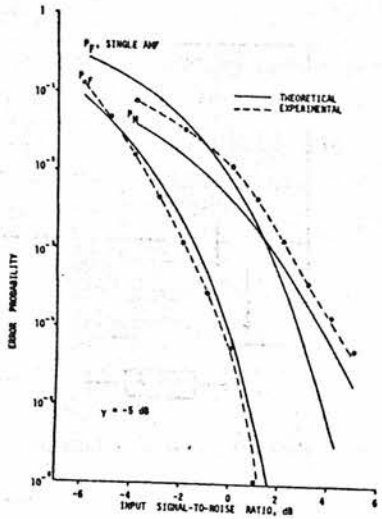


FIGURE 5 RADA MODEM PERFORMANCE

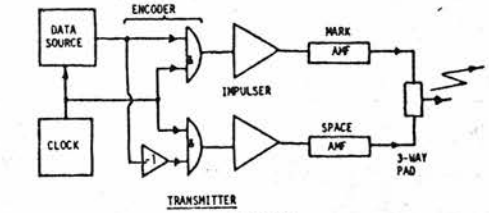


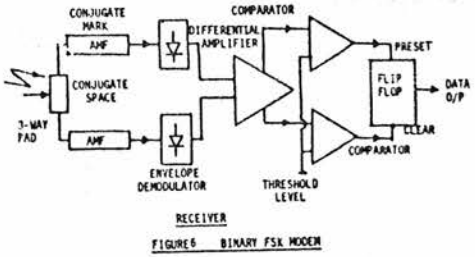


FIGURE 6 BINARY FSK MODEM

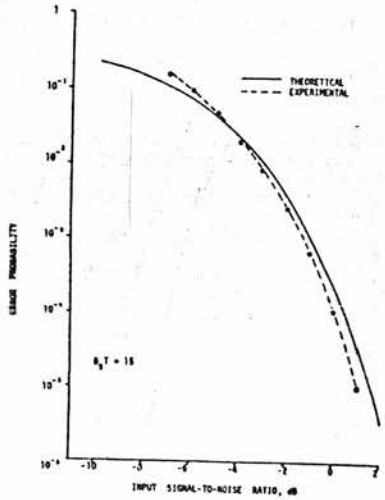


FIGURE 7 BINARY FSK MODEM PERFORMANCE